The Signaling Pathway of Aldosterone in Distal Nephron and its Influences on Sodium Reabsorption

Jianghui Hou

Doctor of Philosophy
The University of Edinburgh
2003

DECLARATION

I declare that this thesis and the work presented here are entirely the result of my own independent investigation. Where I have received assistance this is indicated in the text or acknowledgement on the following page. The work has not been submitted for any other degree or professional qualification except as specified.

ACKNOWLEDGEMENTS

I would like to thank my supervisors Dr Roger Brown and Prof Jonathan Seckl, for the continual guidance and encouragement that they have given me over the past three years. In particular, I would like to thank Roger for being such an excellent supervisor and for helping me in my research.

I acknowledge the animal work conducted at the local animal biomedical research unit by staff holding appropriate small animal handling personal licence (including June Noble, Dr Helen Speirs, Dr Chris Kenyon and others) under existing project licence held by Prof JR Seckl; and approved by the local ethical committee being in accordance with the UK Home Office Animal Act 1986. I have only assisted these personnel in procedures that do not require any licence.

I would like to thank all the staff in the Molecular Endocrinology Laboratory for all the help that they have given me and for generating such an enjoyable place to work.

I would like to thank Dr Rory Duncan (Dept of Biomedical Sciences) for kindly providing an antibody against the Golgi apparatus and for valuable advice on microscopic imaging during my research.

I would like to thank Prof David Porteous (Dept of Medical Genetics) for kindly allowing me to use the FACS facilities in his department.

Table of Contents

Publications from this thesis

Papers

Hou J, Speirs HJL, Seckl JR, and Brown RW. Sgk1 gene expression in kidney and its regulation by aldosterone: spatio-temporal heterogeneity and quantitative analysis. *J Am Soc Nephrol* 13: 1190–1198, 2002.

Hou J, Chapman KE, Seckl JR and Brown RW. Trafficking of the Epithelial Sodium Channel (ENaC) in Mouse Collecting Duct Cells and Influences of Epithelial Polarity and Hormones. (submitted)

Abstracts

Hou J, Chapman KE, Seckl JR and Brown RW. Trafficking of the Epithelial Sodium Channel (ENaC) in Mouse Collecting Duct Cells. 35th American Society of Nephrology (ASN) Annual Meeting 2002.

Hou J, Speirs HJL, Seckl JR, and Brown RW. Sgk1 gene expression in kidney and its regulation by aldosterone. 34th American Society of Nephrology (ASN) Annual Meeting 2001.

Speirs HJL, Hou J and Brown RW. Aldosterone Excess Downregulates a Glutathione S-Transferase Isoform Predominantly Expressed in Sodium Transporting Epithelia. 34th American Society of Nephrology (ASN) Annual Meeting 2001.

Abstract

Regulation of sodium reabsorption in kidney is crucial for maintenance of whole body fluid homeostasis. The Na^+ transport induced by aldosterone, either *in vivo* or *in vitro*, is sensitive to the K^+-sparing diuretic amiloride, which blocks the epithelial Na^+ channel (ENaC). ENaC comprises three homologous subunits (α, β and γ). Each subunit is composed of two transmembrane domains, an extracellular loop and short N- and C-termini. The major renal site of aldosterone action is in the distal nephron, including the second half of distal convoluted tubules, the connecting tubules, the cortical and medullary collecting ducts. Two phases are distinguished in its regulation of sodium transport: an early phase starting after a lag period of 20 to 60 minutes, during which the pre-existing channels are activated; and the late phase (>3h) is when *de novo* synthesis of ENaC and its translocation to the plasma membrane take place.

Aldosterone influences expression of a broad pool of genes, the protein products of which transduce the actions of aldosterone in the nucleus out to the plasma membrane where its final effector ENaC is located. The serine-threonine kinase sgk1 was recently identified as a gene rapidly induced by aldosterone, resulting in increased sodium transport *in vitro*. To carefully localize and quantify the renal sgk1 expression response to aldosterone, I have performed *in situ* hybridization on kidneys of mice having aldosterone excess over a range of doses and durations. In control and adrenalectomized animals, the glomeruli and inner medullary collecting ducts are the major sites of sgk1 expression, which is maintained independent of aldosterone. Sgk1 upregulation induced by aldosterone excess exhibits spatial-temporal heterogeneity. Both acute (3 hours) and chronic (6 days) aldosterone excess stimulates sgk1 expression in the distal nephron, i.e. from the distal convoluted tubules through to the outer medullary collecting ducts. Treatments for 6 days with low sodium diet [0.03% (I)] and aldosterone infusions [50μg/kg/day (II), 150μg/kg/day (III) and 750μg/kg/day (IV)] generate elevation of circulating aldosterone. Across these treatments (I-IV), the circulating level correlates with the progressive induction of sgk1 expression, with highly stimulated tubules first appearing in cortex (I) and continuing downward (II) until there is a strong stimulation throughout outer medulla (III-IV). Interestingly,

chronic but not acute aldosterone excess causes a slight increase of sgk1 expression in glomerulus (30%-50%, $p<0.01$), and a dramatic down-regulation in the initial portion of inner medulla, which could result from diminished interstitial osmolarity. Relative quantification (*vs* control) of sgk1 upregulation in individual tubules reveals: (1) a 1.8-fold increase of sgk1 mRNA at 3 hours (150μg/kg injection); (2) a dose-dependence of chronic upregulation reaching a ceiling of 8-fold elevation.

In addition to sgk1, I have screened through 21 novel candidate genes (including 29 isoforms in total) by *in situ* hybridization and reported the identification of U12b, a glutathione S-transferase isoform, as being downregulated by aldosterone.

To elucidate the molecular events underpinning ENaC translocation to and from the plasma membrane and their hormonal regulation (including corticosteroids and vasopressin), I have generated stable mouse collecting duct cell (M-1) lines that express an N-terminally fused EGFP-ENaCβ subunit. The cell lines grow normally, express easily visualized quantities of the EGFP fused ENaC subunit and form confluent epithelia with high transepithelial resistance when grown on semi-permeable filters. Imaging by confocal microscopy revealed that ENaC was confined to the endoplasmic reticulum (ER) in unpolarized M-1 cells. Activation of the vasopressin pathway results in ENaC exodus from the ER into intracellular vesicles and this stimulated ENaC trafficking does not involve the endocytic vesicle pathway. When cells are fully polarized, ENaC largely exits the ER and the Golgi apparatus. Corticosteroids (≥100nM dexamethasone) profoundly alter the trafficking of ENaC proteins in polarized M-1 cells by promoting ENaC translocation to the apical membrane. Collectively, polarization, corticosteroids and vasopressin modulate the trafficking of ENaC in distinctive manners such that vasopressin or polarization fosters ENaC trafficking from ER to intracellular vesicles, whereas corticosteroids play a role further downstream in the cascade of ENaC trafficking events by increasing delivery of ENaC to the apical membrane.

In unpolarized distal nephron M-1 cells, I have found that sgk1 has no effects on ENaC intracellular trafficking. In addition, sgk1 itself is localized to intracellular

compartment distinct from ENaC. To elucidate the role of sgk1 in modulating ENaC conductance, I have generated M-1 cell lines stably express sgk1 whose gene expression level is tightly controlled by the tetracycline-inducible system. In these cell lines, sgk1 gene has no 'leaky' expression and its expression induction is highly responsive to tetracycline (10-fold induction at $\leq$10ng/ml versus 10μg/ml). This model can become available and widely accessible to determine whether upregulation of sgk1 by tetracycline influences ENaC-mediated sodium reabsorption in parallel to that by corticosteroids.

Outcomes of my PhD project have contributed to our understanding the signaling pathway of aldosterone and its influences on sodium transport in the distal nephron. It has also shed light on the roles of sgk1 in kidney and the trafficking of transmembrane proteins involved in ion transport such as ENaC in unpolarized and polarized epithelial cells; and how these processes are regulated by hormones and genes whose products mediate the transduction of hormonal signals to altered trafficking events.

Abbreviations

11β-HSD2	11β-hydroxysteroid dehydrogenase type 2
ACTH	adrenocorticotropic hormone
ADH	antidiuretic hormone
AI	angiotensin I
AII	angiotensin II
AIP	aldosterone induced protein
AME	apparent mineralocorticoid excess
ASDN	aldosterone sensitive distal nephron
ATP	adenosine triphosphate
bp	base pair
cAMP	cyclic adenosine monophosphate
Cap1	channel activating protease 1
CCD	cortical collecting duct
CD	collecting duct
cDNA	complementary deoxyribonucleic acid
CIP	corticosteroid induced protein
CMV	cytomegalovirus
CNT	connecting tubule
CRH	corticotropin-releasing hormone
C-terminal	carboxyl terminal
dATP	2'-deoxyadenosine-5'-triphosphate
dCTP	2'-deoxycytidine-5'-triphosphate
dGTP	2'-deoxyguanosine-5'-triphosphate
dTTP	2'-deoxythymidine-5'-triphosphate
DCT	distal convoluted tubules
DEPC	diethyl pyrocarbonate
dH_2O	distilled water
DNA	deoxyribonucleic acid
DTT	dithiothreitol
ECF	extracellular fluid

EDTA	ethylenediaminetetracetic acid
EGFP	enhanced green fluorescence protein
EYFP	enhanced yellow fluorescence protein
ENaC	epithelial sodium channel
Endo-H	endoglycosidase H
ER	endoplasmic reticulum
FACS	fluorescence activated cell scanning
FITC	fluorescein isothiocyanate
GFR	glomerulus filtration rate
GILZ	glucocorticoid-induced leucine zipper protein
GR	glucocorticoid receptor
GRA	glucocorticoid-remediable aldosteronism
GRE	glucocorticoid response element
HEPES	N-2-hydroxyethylpiperazine N-2-ethansulphonic acid
IGF	insulin-like growth factor
iMCD	inner medullary collecting duct
kDa	kilodalton
LSCM	laser scanning confocal microscopy
MAPK	mitogen activated protein kinase
MDCK	Madin-Darby canine kidney
MR	mineralocorticoid receptor
mRNA	messenger ribonucleic acid
NDRG2	N-Myc downstream regulated gene 2
Nedd4	neuronal precursor cells expressed developmentally down-regulated 4
N-terminal	amino terminal
oMCD	outer medullary collecting duct
PAS	periodic acid-schiff
PCR	polymerase chain reaction
PBS	phosphate buffered saline
PDK1	3-phophoinositide-dependent protein kinase 1
PEPCK	phosph*oenol*pyruvate carboxykinase

PHAI	pseudohypoaldosteronism type I
PKA	protein kinase A
PKB	protein kinase B
PKC	protein kinase C
PI3K	phosphatidylinositol 3-kinase
PNGaseF	peptide N-glycosidase-F
PVDF	polyvinylidene difluoride
RNase	ribonuclease
RT-PCR	reverse-transcriptase polymerase chain reaction
SDS	sodium dodecyl sulphate
Sgk	serum glucocorticoid kinase
SNAP	soluble N-ethylmaleimide-sensitive-factor attachment protein
SNARE	SNAP receptor
SRE	steroid-responsive element
TEMED	N'N'N'N'-tetramethylethylenediamine
TGF	tubular-glomerular feedback
Tris	tris(hydroxymethyl)aminoethane
Triton X-100	octyl phenoxy polyethoxyethanol
UV	ultraviolet
WGA	wheat germ agglutinin

List of figures

Chapter 1: Introduction

Chapter 2 Materials and Methods

Chapter 3: Sgk1 Gene Expression in Kidney and Its Regulation by Aldosterone: Spatio-Temporal Heterogeneity and Quantitative Analysis

Chapter 4: Identification and Characterization of Aldosterone Induced/Repressed Genes

Chapter 5: Trafficking of the Epithelial Sodium Channel (ENaC) in Mouse Collecting Duct Cells and Influences of Epithelial Polarity and Hormones

Chapter 6: Generation of a cell model to control sgk1's expression and mimic corticosteroids' effects *in vivo*

List of tables

Chapter 3: Sgk1 Gene Expression in Kidney and Its Regulation by Aldosterone: Spatio-Temporal Heterogeneity and Quantitative Analysis

Chapter 4: Identification and Characterization of Aldosterone Induced Genes

CHAPTER 1 INTRODUCTION

1.1 THE ROLE OF KIDNEY IN CONTROL OF EXTRACELLULAR FLUID VOLUME

1.1.1 Control of Extracellular Fluid Volume

Extracellular fluid (ECF) volume is maintained within narrow ranges in normal humans, despite day-to-day variations in the dietary intake of salt and water over a wide range (Halperin ML et al 1986). Plasma volume, in turn determined by the total ECF volume and the partitioning of this volume between extravascular and intravascular compartments according to the dictates of the Starling relationship, also remains remarkably constant despite alterations in dietary salt intake. The relationship of ECF volume and, in particular, the volume of the plasma compartment to overall vascular capacitance determines fundamental indices of cardiovascular performance such as mean arterial blood pressure and left ventricular filling volume.

In a given steady state, total daily Na^+ intake and excretion are equal. Acute deviations from a pre-existing normal steady state, consequent to an alteration in Na^+ intake or extrarenal excretion, result in an adjustment in renal Na^+ excretion. This adjustment in renal Na^+ excretion occurs as a result of a new total body Na^+ content and ECF volume, and aims to restore the body fluid balance back within the normal limits. The establishment of a new steady-state level of Na^+ excretion reflects a new total body Na^+ content and ECF volume. Alternatively, an alteration in the capacitance of the extracellular compartment affecting circulatory filling can also result in an adjustment in renal sodium excretion, which thereby can restore normal circulatory hemodynamics (Bonventre JV et al 1982; Guyton 1990, 1991; Hall JE et al 1986(a)).

It is clear that the operation of such a system for Na^+ homeostasis requires 1) sensors that detect changes in ECF volume relative to vascular and interstitial capacitance and 2) effectors that ultimately modify the rate of Na^+ excretion by the kidney to meet the demands of volume homeostasis. Adjustments in effector mechanisms occur in

response to perceived alterations in sensory input, with the aim of optimizing circulatory performance. Derangements in either sensor or effector mechanisms therefore can lead to disordered Na^+ balance and disruption of optimal circulatory homeostasis (Figure 1.1).

1.1.1.1 Sensors for Fluid Homeostasis

Afferent sensors for fluid homeostasis comprise the cardiopulmonary and arterial baroreceptors as well as central nervous system, renal and hepatic sensors (Goetz KL et al 1970; Paintal AS et al 1973; Linden RJ 1979; Gross R et al 1980; Beers ET et al. 1986; Skott O et al 1987; Passo SS et al 1973). Each compartment can be viewed as reflecting a unique characteristic of overall circulatory function, such as cardiac filling, cardiac output and renal perfusion. Sensors within each compartment monitor a physical parameter (e.g., stretch, tension) that serves as an index of circulatory function within that compartment. Signals emanating from afferent sites engage efferent mechanisms that affect compensatory changes in renal Na^+ excretion. Volume expansion results in an integrated sequence of reflex and hormonal responses that enhance the renal excretion of salt and water. Conversely, the reflex response to volume contraction is renal conservation of salt and water.

1.1.1.2 Effectors for Fluid Homeostasis

Efferent effectors for fluid homeostasis comprise adjustments in the glomerular filtration rate (GFR) and changes in the factors that affect reabsorption of filtered electrolytes and water. These encompass not only the physical factors common to reabsorption from all capillary beds (including capillary permeabilities, hydrostatic and osmotic gradients contributing to the net peritubular capillary Starling forces), but also those unique to the nephron governing transepithelial transport via both paracellular and transcellular routes. Regulation of GFR, transepithelial and capillary reabsorption in response to afferent stimuli is incompletely understood but utilizes efferent signaling via nerves and hormones (that include the renin-angiotensin-aldosterone system, vasopressin, natriuretic peptides and endothelins) (Rector FCJ et

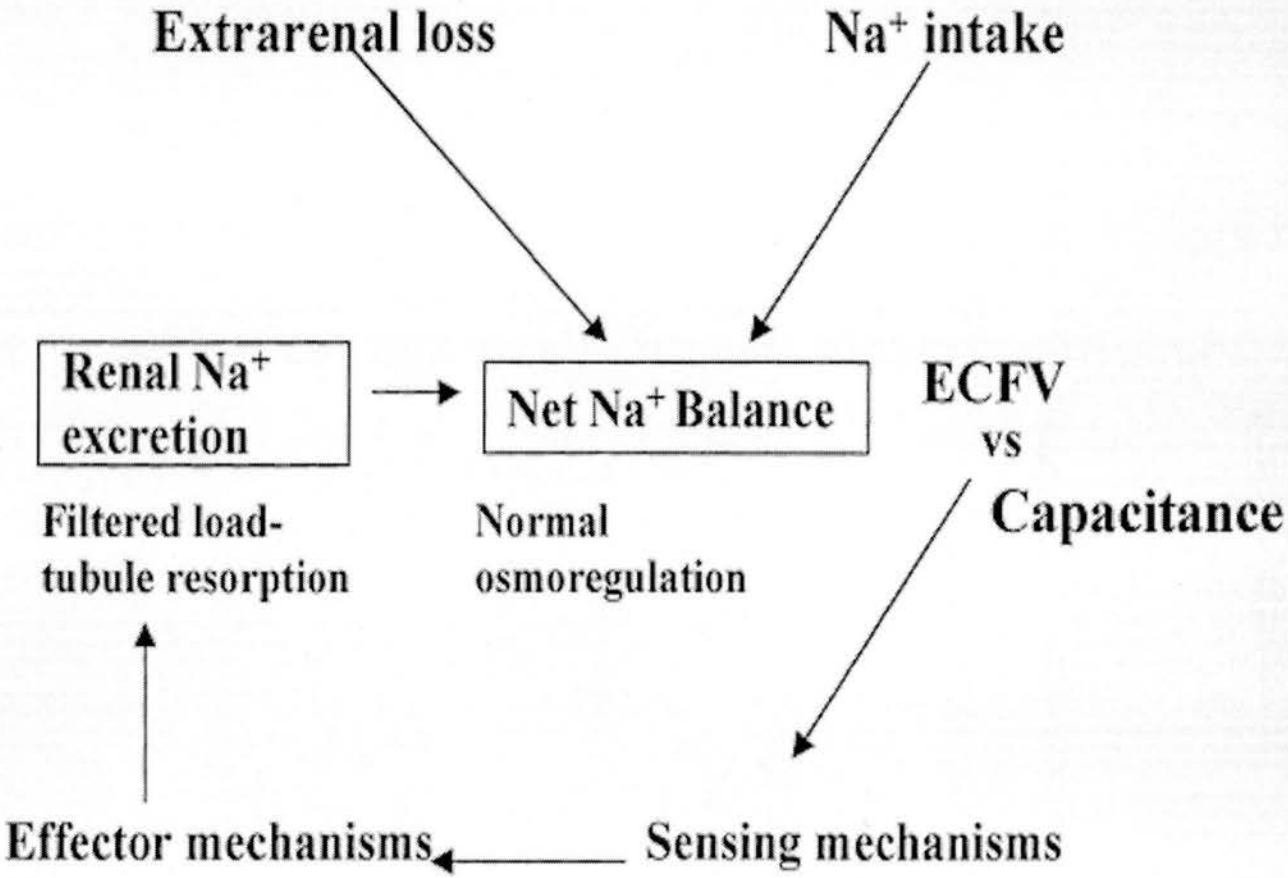

Figure 1.1 Overall scheme for body Na^+ balance and partitioning of extracellular fluid volume. In the setting of normal osmoregulation, extracellular Na^+ content is the primary determinant of extracellular fluid volume. Overall Na^+ homeostasis depends on the balance between loss and intake. Renal Na^+ excretion, in turn, is determined by the balance between filtered load and tubule reabsorption. This latter balance is modulated under the influence of effector mechanisms, which, in turn, are responsive to sensing mechanisms that monitor the relationship of the extracellular fluid volume to capacitance. ECFV = extracellular fluid volume.

al 1996; Burg MB et al 1968; Bank N et al 1984; Guyton 1990, 1991; Ardaillou R et al 1997; Reif MC et al 1986).

1.1.2 Renin-Angiotensin-Aldosterone System

The renin-angiotensin-aldosterone system plays a pivotal role in the regulation of ECF volume and Na^+ homeostasis. This system is activated in situations that compromise extracellular volume homeostasis, such as reduced ECF and circulatory volumes, low sodium intake, hypotension, and an increase in sympathetic nerve activity. The kidney is both an important source of several components of the renin-angiotensin system and a target organ for their actions. The juxtaglomerular cells are the major site of renin synthesis and release. Angiotensinogen is produced primarily from the liver and less from the kidney and the adipose tissue. Angiotensin-converting enzyme, which cleaves angiotensin I (AI) to AII, is found in large amounts in the lung, but is also found in the brush border of proximal convoluted tubules of the kidney and in endothelial cells of many organs, including the kidney. AI is rapidly converted to AII in the lungs and other extrarenal tissues, as well as in the kidney (Figure 1.2). AII exerts multiple direct intrarenal influences, including renal vasoconstriction, stimulation of tubular epithelial Na^+ reabsorption, augmentation of tubular-glomerular feedback (TGF) sensitivity, and modulation of pressure-natriuresis (Ardaillou R et al 1997; Blantz RC et al 1976; Chou SY et al 1990; Hall JE 1986(b); Schuster VL et al 1984; Olsen ME et al 1985). Importantly, AII stimulates the synthesis of aldosterone that has major effects in augmentation of long-term renal sodium reabsorption.

1.2 THE ROLE OF THE ALDOSTERONE PATHWAY IN THE MAINTENANCE OF SODIUM HOMEOSTASIS

1.2.1 Synthesis of Aldosterone

Aldosterone is a steroid synthesized in the zona glomerulosa region of the adrenal cortex, and, because it is not stored, regulators of aldosterone secretion act by controlling various steps of aldosterone synthesis. The adrenal production of

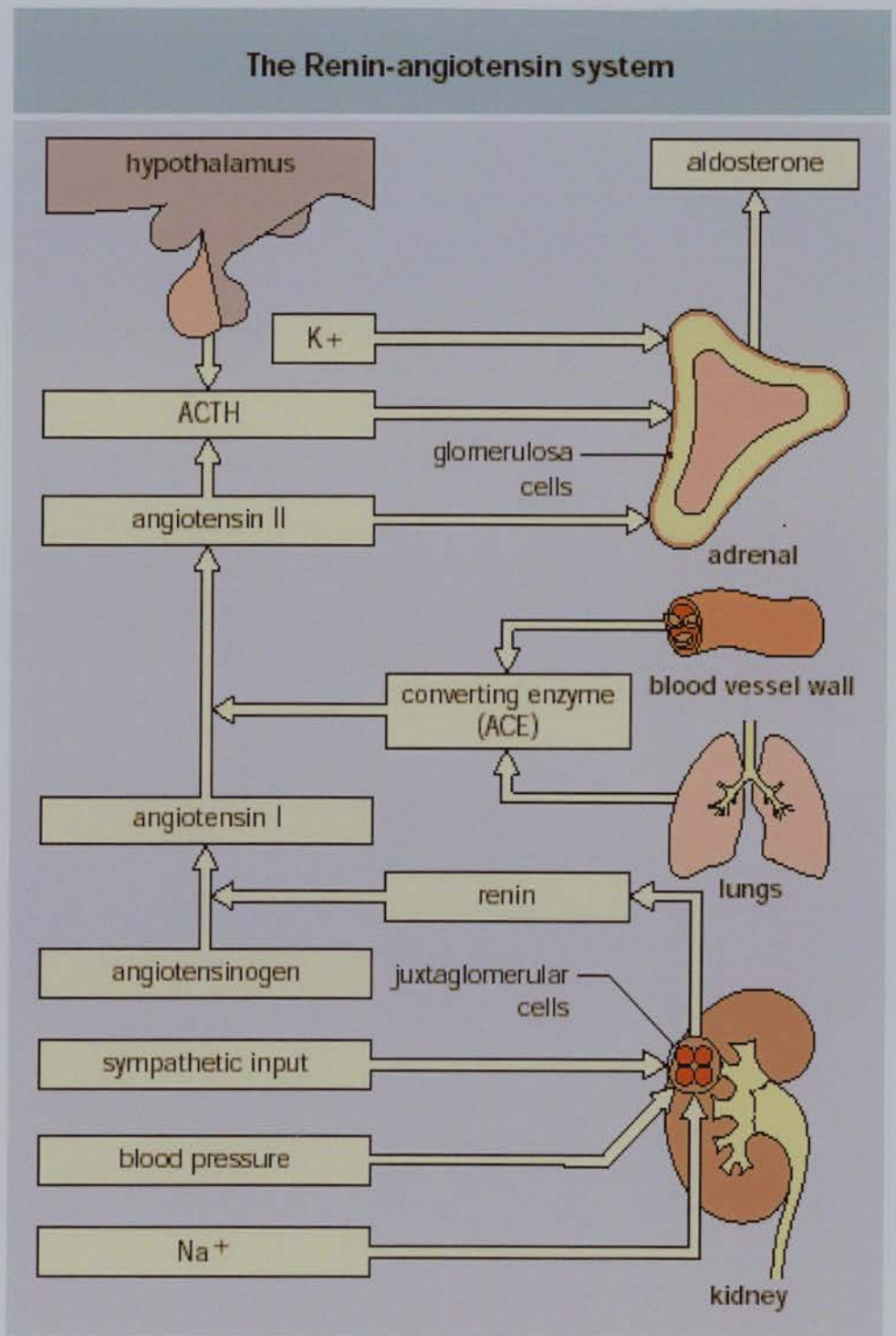

Figure 1.2. The Renin-Angiotensin-Aldosterone System

aldosterone is catalyzed by a synthetic pathway largely of enzymes from the cytochrome P450 family (CYPs). Angiotensin II is the principal circulating effector of increased aldosterone secretion. It acts by stimulating the G protein-PKC cascade, leading to an influx of extracellular calcium (Quinn SJ and Wiliams GH 1988). These events increase the conversion of corticosterone to aldosterone (catalyzed via the enzyme CYP11B2 or aldosterone synthase) in the aldosterone systhesis pathway (McKenna TJ et al. 1978; Kramer RE et al. 1980; Quinn SJ and Wiliams GH 1988) (Figure 1.3). In addition to angiotensin II, elevated potassium also has powerful stimulatory influences, whilst other factors play a more minor role in aldosterone secretion (such as short-term stimulation by ACTH and repression by dopamine) (Figure 1.2).

1.2.2 Physiology of Aldosterone Action

The most important and conserved functions of aldosterone are to promote sodium reabsorption and to promote potassium secretion across certain 'tight' epithelia, that is, epithelia that display a high transepithelial electrical resistance and an amiloride-sensitive, electrogenic sodium transport. In mammals, such epithelia are found in the distal part of the nephron and the intestine, and the ducts of exocrine glands (salivary, mammary and sweat glands). Using receptor localization techniques, the aldosterone sensitive distal nephron (ASDN) has been reported as including the late distal convoluted tubules (DCT) and connecting tubules (CNT) through to the cortical collecting duct (CCD), and to a lesser extent the outer medullary collecting duct (oMCD) (Doucet A et al 1981; Farman N 1992) (Figure 1.4).

Aldosterone action is best understood in collecting ducts (CD), which are composed of two cell types: principal cells and intercalated cells (further subdivided into α and β cell types). Principal cells reabsorb Na^+ and H_2O, secrete K^+ and express the amiloride sensitive epithelial sodium channel (ENaC) and the Na^+/K^+-ATPase. Intercalated cells either secrete H^+ (α type) or reabsorb HCO_3^- (β type) and thus are important in regulating acid-base balance. Aldosterone diffuses freely across the plasma membrane of cells and binds to its receptor. The steroid-receptor complex is

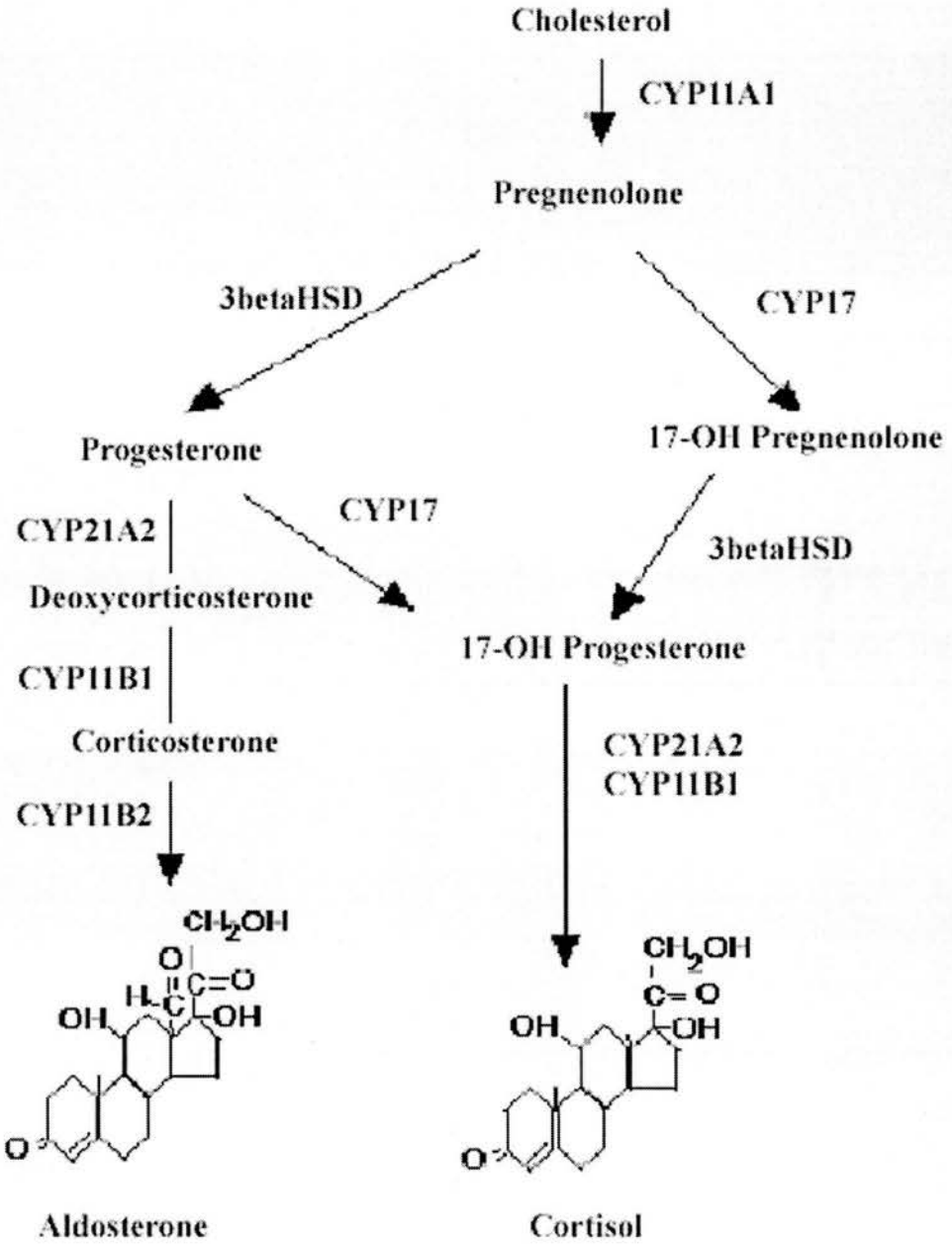

Figure 1.3. Corticosteroid biosynthesis pathways in adrenal cortex. CYP, cytochrome P450 enzyme family; 3 beta HSD, 3β-hydroxysteroid dehydrogenase.

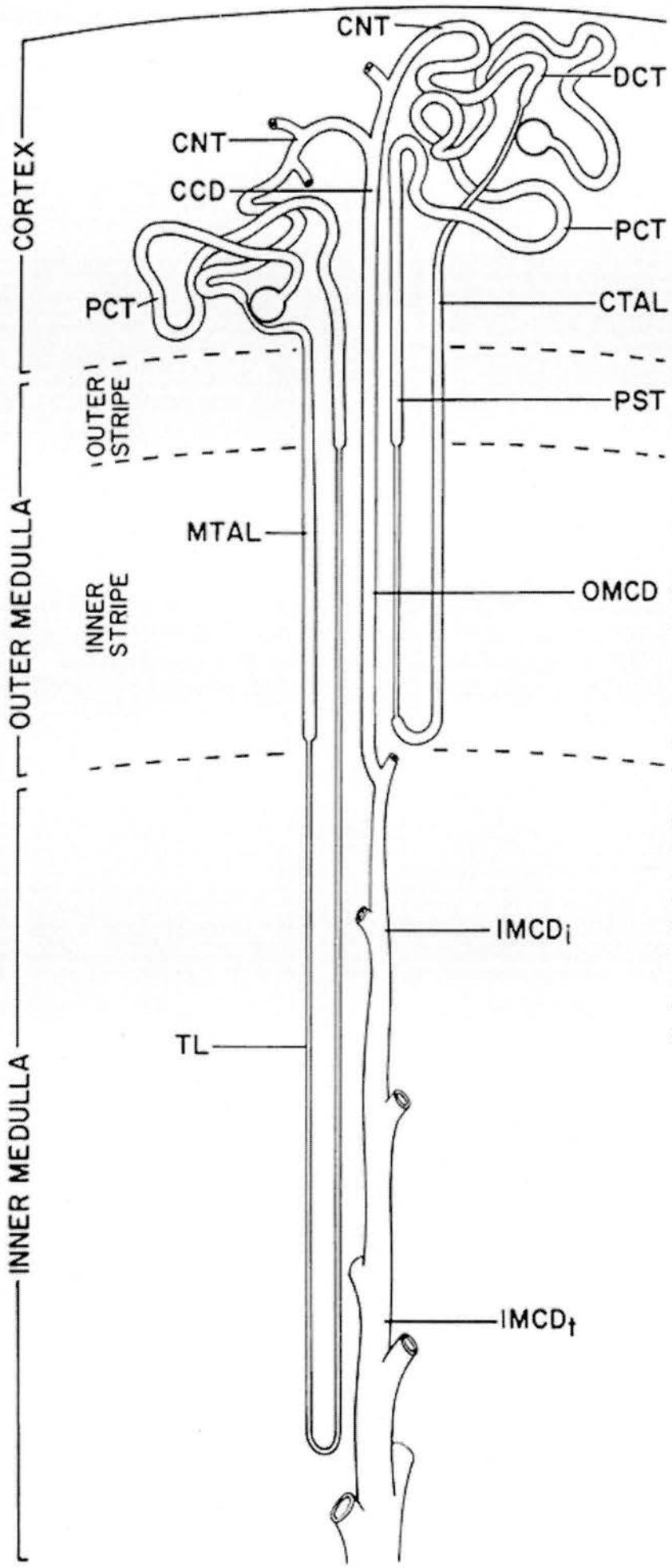

Figure 1.4. Diagram illustrating superficial and juxtamedullary nephron. PCT: proximal convoluted tubule; PST: proximal straight tubule; TL: thin limb of loop of Henle; MTAL: medullary thick ascending limb; CTAL: cortical thick ascending limb; DCT: distal convoluted tubule; CNT: connecting segment; CCD: cortical collecting duct; OMCD: outer medullary collecting duct; IMCDi: initial inner medullary collecting duct; IMCDt: terminal inner medullary collecting duct.

transported into the nucleus and binds to specific steroid-responsive elements (SRE) within the promoters of a number of genes. The interaction of the steroid-receptor complex with the transcription machinery leads to an increase in transcription and to the accumulation of corresponding mRNA, which are, in turn, translated into proteins, a key subset of which mediate Na reabsorption and K secretion (Farman N et al 2001; Fuller PJ et al 2000; Funder JW 1997) (Figure 1.5).

1.2.3 Temporal Phases of Aldosterone Action

The genomic actions of aldosterone are traditionally divided into an early and late phase (Verrey F et al 1995, 1999, 2000). The early phase is predicted to respond to acute changes in salt and water balance to allow for more rapid responses to movements away from homeostasis. The early phase of aldosterone action is most often demarcated as the period where Na transport is increased without an accompanying increase in the expression levels of the transporter proteins involved in this action. This phase directly follows the 10-20 min latent period required for changes in gene expression and proceeds for 2–4 h. The late phase, then, is classified as that following this period and is when the *de novo* synthesis of transporter proteins takes place, such as ENaC and the Na^+/K^+-ATPase (Feraille E et al 2001; Verrey F et al 1995, 1999, 2000). Moreover, a prolonged phase developing over days and even weeks is often regarded as the *very late* phase when tubular hypertrophy is observed.

1.2.3.1 Early actions of aldosterone.

The initial actions of aldosterone with respect to increasing Na reabsorption and K secretion are mediated by stimulating the existing transporter proteins. There are ultimately only two such ways aldosterone can enhance transport: 1) by increasing the open probability of apical ion channels and the activity of the basolateral Na^+/K^+-ATPase and 2) by increasing the number of ion channels and Na^+/K^+-ATPase in the cell membrane. There is considerable evidence regarding both mechanisms of aldosterone action in ASDN (Dijkink L et al 1999; Frindt G et al 2001; Garty H et al 1983; Hager H et al 2001; Helman SI et al 1998; Kemendy AE et al 1992; Kleyman

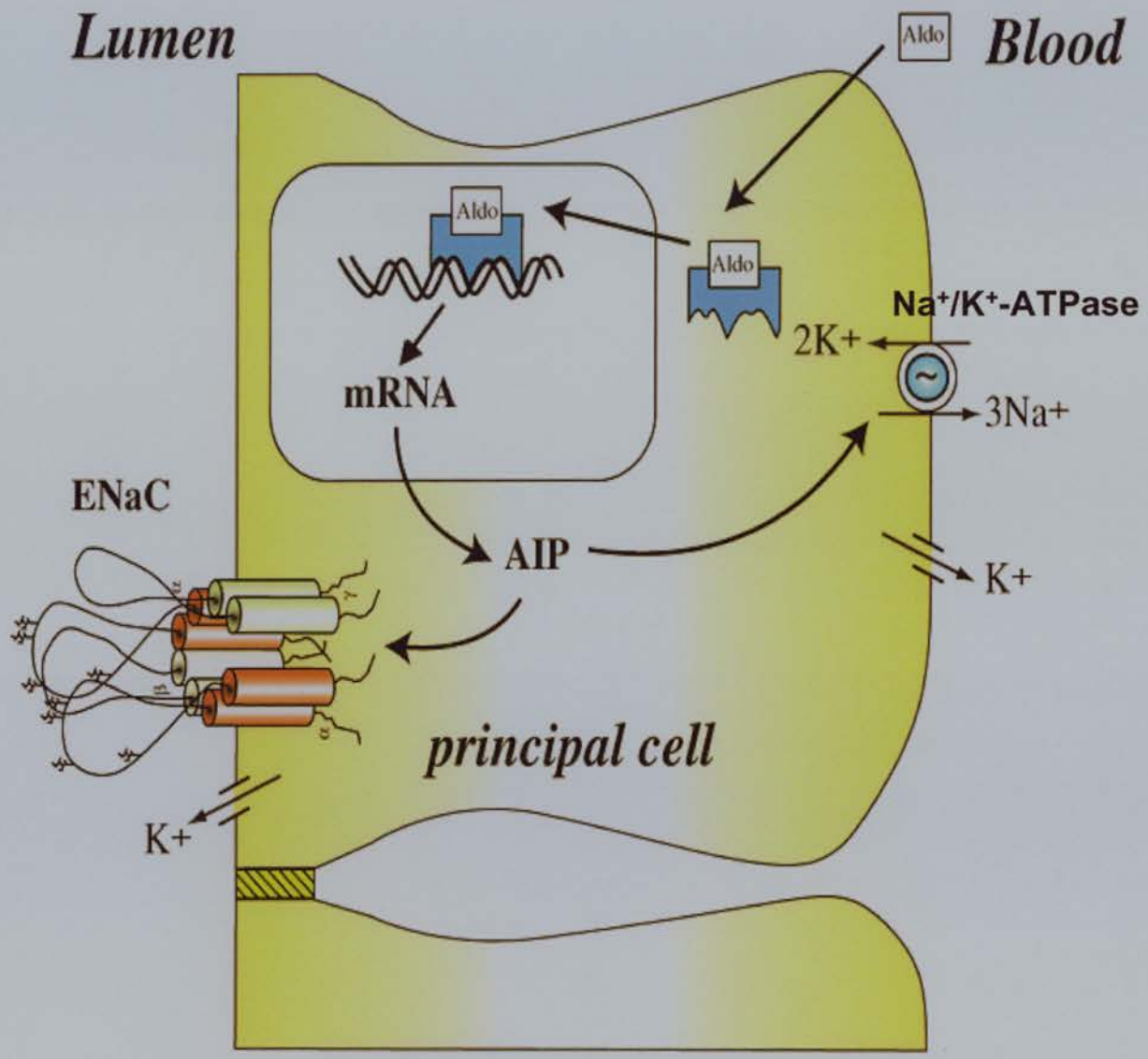

Figure 1.5. Aldosterone action in distal nephron cells. Aldo: aldosterone; AIP: aldosterone induced proteins; ENaC: epithelial sodium channel.

TR et al 1992, 2001; Weisz OA et al 2000).

1.2.3.2 Late actions of aldosterone.

During the late phase of aldosterone action, there is a clear increase in the amount of ENaC protein within the cell, as well as at the apical membrane (Weisz OA et al 2000; Loffing J et al 2000; Masilamani S et al 1999). Aldosterone induces expression of the genes encoding the α subunit of ENaC (Asher C et al 1996; Escoubet B et al 1997)and the α1- and β1-subunits of the Na^+/K^+-ATPase (Kolla V et al 1999, 2000; Blot-Chabaud M et al 2001). In addition to upregulation in these transporter proteins, enzymes essential to energy metabolism also increase in response to aldosterone (Feraille E et al 2001; Verrey F et al 1995, 2000). All three actions (i.e. energy metabolism, protein synthesis and protein trafficking) combine to program cells for prolonged ion transport.

1.2.4 Maintenance of sodium balance by pressure natriuresis during aldosterone escape

Excessive secretion of mineralocorticoids, or infusion of mineralocorticoids such as aldosterone causes sodium and water retention and gradual elevation of arterial pressure. Such sodium and water retention lasts for a few days depending on sodium intake and the severity of hormone excess, and is followed by an 'escape' in which sodium excretion returns towards normal despite continual mineralocorticoid excess. A classic experiment performed by JE Hall and AC Guyton indicates the essential role of pressure natriuresis in regulating sodium balance during mineralocorticoid escape (Hall JE et al. 1986a). In control animals, sodium excretion decreased transiently but returned towards normal on the second day of aldosterone infusion. After 7 days the cumulative sodium balance and arterial pressure was only slightly elevated. In contrast, when renal perfusion pressure was servocontrolled (kept constant and separated from the increase of systemic pressure) during infusion, sodium excretion remained suppressed and cumulative sodium balance continued to increase throughout the 7 days of treatment. It is clear that sodium transport in distal nephron

persists to increase during such an event (Tomita K et al. 1985). The site of compensatory reduction in sodium reabsorption allowing this 'escape' is not entirely clear but seems to involve tubules of the more proximal nephron and contribution by adjusting the rates of glomerular filtration (Wright FS et al. 1969; Kohan DE et al. 1980).

1.2.5 Components of the Aldosterone Pathway and its Molecular Mechanism

1.2.5.1 Corticosteroid Receptors

Aldosterone, as a mineralocorticoid, is a high affinity ligand for the mineralocorticoid receptor (MR) and it has considerably weaker affinity for the related glucocorticoid receptor (GR), a receptor activated almost exclusively by the 100-1000 higher level of glucocorticoids (Fuller PJ et al 2000; Funder JW 1997). It is clear that the potent glucocorticoid inactivating enzyme (11β-hydroxysteroid dehydrogenase type 2) confers aldosterone specificity in many aldosterone target tissues such as the distal nephron (Funder et al 1988, Brown RW et al 1996(a,b)).

MR and GR translocate to the nucleus in a ligand-dependent manner, form homodimers and function as transcription factors through interaction with genomic DNA at a steroid response element (SRE; consensus sequence AGAACAnnnTGTTCT). Two distinct molecular mechanisms are widely accepted to define the actions of corticosteroid receptors (MR and GR) on gene expression: 1) the classic mechanisms involving *trans*-activation and *trans*-repression via interaction with cognate DNA-binding sites, such as SRE and 2) mechanisms of transcription interference and synergy mediated by protein-protein interactions between corticosteroid receptors and other *trans*-acting factors.

1.2.5.1.1 Transactivation

The *cis*-acting elements responsive to corticosteroid receptors for many corticosteriod-induced genes have now been identified. A corticosteroid-sensitive gene encodes serum and glucocorticoid-inducible kinase (Chen S et al 1999; Maiyar AC et al 1997; Webster MK et al 1993, 1993(a)). The promotor region of the human *sgk1* gene contains a classic but imperfect pentadecameric *cis*-acting SRE (AGGA-CAgaaTGTTCT; Maiyar AC et al 1997; Webster MK et al 1993a). In mammary epithelia, this element is *trans*-activated in response to dexamethasone signaling (Webster MK et al 1993(a); Maiyar AC et al 1997). Indirect evidence from numerous epithelia, including the renal distal nephron and distal colon, indicates that this *cis*-element is also responsive to aldosterone via MR (Bhargava A et al 2001; Brennan FE et al 2000; Chen S et al 1999; Loffing J et al 2001; Shigaev A et al 2000). That glucocorticoids and aldosterone via GR and MR *trans*-activate *sgk1* in distinct tissues possibly through a common SRE suggests that both types of steroid may initiate a cellular response mediated by a common signaling pathway or one that contains many common signaling elements. Thus GR and MR likely have, at least partially, overlapping functions in epithelia expressing both receptors. Functional redundancy or promiscuity is supported, nevertheless, by findings showing that aldosterone via MR and glucocorticoids via GR induce expression of many of the same genes and that the widely expressed GR is sometimes capable of complementing MR dysfunction or eliciting a mineralocorticoid response, especially in *in vitro* propagated cell lines (see below 1.2.5.1.4) (Kunzelmann K et al 1999; Chen SY et al 1998; Ferrari P et al 2000; Funder JW 1997; Holmes MC et al 2001; Lifton RP et al 2001; Rogerson FM et al 2000). A corticosteroid-sensitive gene also encodes the α-subunit of ENaC (Dagenais A et al 2001; Mick VE et al 2001). A classic but slightly imperfect SRE (AGAACAgaaTGTCCT) was recently identified as sufficient and necessary for *trans*-activation of the human and rat α-ENaC promotors in renal, lung, salivary, and colonic epithelial cell lines (Lin HH et al 1999; Mick VE et al 2001; Sayegh R et al 1999; Wang HC et al 2000; Zentner MD et al 2001). This *cis*-acting element is responsive to MR and GR, with no overt specificity for either glucocorticoids or aldosterone.

1.2.5.1.2 Transrepression

Glucocorticoids via GR repress expression of a host of genes. Recent studies also have identified several aldosterone-repressed genes and proteins (Laverty G et al 2001; Robert-Nicoud M et al 2001; Spindler B et al 1997). Compared with induction, less is known about the molecular mechanisms of direct gene repression in response to corticosteroids. The term "negative"-SRE (nSRE) is used sometime to define the *cis*-acting element that directly mediates *trans*-repression in response to glucocorticoid signaling via GR. GR interacts directly with the 5'-ATTTTTGTCAATGGACAAGTCATAAGAA-3' nSRE sequence in the promotor region of the corticotropin-releasing hormone (CRH) gene to *trans*-repress cAMP activated expression of CRH (Malkoski SP et al 1996, 1997). The nSRE in the gene encoding proopiomelanocortin (POMC; 5'-GGAAGGTCACGTCCA-3') has also been identified (Charron J et al 1986; Drouin J et al 1989, 1993). The effects of MR on these nSREs have not been studied, and thus it remains to be determined whether MR is capable of modulating expression via these sorts of nSREs. The recent identification of a number of putative aldosterone-repressed genes and proteins (Laverty G et al 2001; Robert-Nicoud M et al 2001; Spindler B et al 1997) points to possible candidates worthy of further investigation in this regard.

1.2.5.1.3 Protein-protein interactions during MR and GR modulation of gene expression

The β-casein gene is induced by GR independently of an SRE (Stoecklin E et al 1997). The mechanism of action here entails GR "tethering" through a protein-protein interaction to a transcription factor itself binding the promoter called Stat-5 (signal transducer and activator of transcription-5). Induction of β-casein in response to glucocorticoids, then, is actually dependent on formation of GR/Stat-5 complexes that bind to Stat-5 response elements. GR forms an equivalent type of complex with the transcription factor Oct-2 (organic cation transporter-2) (Prefontaine GG et al 1998) and has also been reported to associate with Stat-3 (Zhang Z et al 1997). It is not known whether MR also binds these and/or other such tethering factors, and thus such

a mechanism of action involving transcription synergy for MR is purely speculative at this time. If MR has limited interaction with these tethering factors or interacts with distinct ones, this mechanism might then distinguish between GR and MR responses. Ample results demonstrate that GR negatively influences the actions of activator protein (AP)-1 and nuclear factor (NF)-κB on transcription via direct protein-protein interactions (Karin M et al 1998, 2001). The functional consequence of protein-protein interactions involving GR *in vivo* have been clarified by the use of a transgenic mouse model containing mutant GR incapable of forming dimers (GR^{dim}), which thus cannot bind and *trans*-activate at SREs (Heck S et al 1994; Karin M. 1998). Also, *trans*-repression of POMC and prolactin via nSRE is compromised in $GR^{dim/dim}$ mice, but these mice retain the ability for ligand-activated GR to interfere via protein-protein interactions with transcription initiated by other *trans*-acting factors (Reichardt HM et al 1998). Indeed, the ability of activated GR via AP-1 to interfere with *trans*-activation of genes encoding collagenase and gelatinase is retained in $GR^{dim/dim}$ mice. The ability of GR to interfere with NF-κB activity also is retained in $GR^{dim/dim}$ mice. It is presently unclear whether MR has such an ability to mediate some of its cellular actions via protein-protein interactions involved in transcription interference and/or synergy. In addition, Maiyar AC et al (1997) recently identified a novel mechanism of reciprocal interference between GR and the p53 protein. Induction of *sgk1* by GR signaling is abrogated by simultaneous activation of p53. p53 interferes with GR via protein-protein interactions by preventing its interaction with its cognate SRE.

1.2.5.1.4 Promiscuity vs Specificity of physiological response to mineralocorticoids and glucocorticoids

Because MR and GR are homologous, and because they have overlapping functions in epithelia expressing both receptors, it is sensible to ask whether they might be redundant. Knocking out the GR resulted in mice that died a few hours after birth (Cole TJ et al 1995). They exhibited profound impairment of lung maturation and lack of activation of genes of key gluconeogenic enzymes. The phenotype of MR-knockout mice was different (Berger S et al 1998): during the first few days of the

postnatal period, there was a progressive syndrome of sodium and water loss, with weight loss, hyperkalemia, and hyponatremia (reflecting human pseudohypoaldosteronism), leading to death. Interestingly, the MR knockout mice can be rescued by sodium chloride injections but not glucocorticoids (Bleich M et al 1999). These experiments clearly show that each of these receptors has, at least some, specific functions that cannot be fulfilled by the remaining receptor *in vivo*.

Nevertheless, there are well established cell culture and *in vitro* systems where upregulation of epithelial sodium reabsorption is strongly driven by corticosteroids (glucocorticoids or mineralocorticoids) acting via GR, such as in *Xenopus* A6 renal cells, frog skin and toad bladder (May A et al 1997; Schmidt TJ et al 1993); and in cultured mammalian collecting duct cells (including rat, rabbit and mouse) (Laplace JR et al 1992; Naray-Fejes-Toth A et al 1990, 2000), as the expression of MR in cultured cells or *in vitro* is largely reduced or silenced.

Thus, in study of the signaling pathway of aldosterone, I have used experimental models involving aldosterone stimulation of sodium reabsorption *in vivo* in mouse kidney; and a validated cell culture model (mouse collecting duct M-1 cells: Stoos BA et al 1991) involving glucocorticoid stimulation of sodium reabsorption *in vitro*.

1.2.5.1.5 Non-genomic aldosterone action

According to the traditional model, aldosterone binds to intracellular receptors and subsequently modulates transcription and protein synthesis, thus triggering genomic events. In addition, very rapid effects (developing over seconds or minutes) of aldosterone mainly affecting intracellular signaling are widely regarded as being incompatible with the genomic model. These effects involve a surge of intracellular Ca^{2+} release and production of inositol-1,4,5-trisphosphate (IP3) and diacylglycerol (DAG) in collecting duct cells, vascular smooth muscle cells and aortic endothelial cells (Wehling M et al 1991; Estrada M et al 2000; Harvey BJ et al 2000). These rapid, non-genomic aldosterone actions are independent of actinomycin D (transcription inhibitor), cycloheximide (translation inhibitor) (Wehling M et al 1991) and classic

MR (Haseroth K et al 1999), thus likely to be transmitted via specific but unidentified membrane receptors. Nevertheless, the actions of aldosterone on electrolyte transport are mediated via MR (blocked by MR antagonist) and requiring new gene expression (blocked by actinomycin D or cycloheximide). Thus there is little doubt that the sodium retaining effects of aldosterone occur via the nuclear receptor MR involving classic genomic events.

1.2.5.2 11β-HSD2

Despite the fact that the circulating level of aldosterone is normally 100- to 1,000-fold less than that of glucocorticoids, MR in kidney is selectively occupied by aldosterone. This apparent contradiction can be explained by the presence of a glucocorticoid-converting enzyme, 11β-hydroxysteroid dehydrogenase type 2 (11β-HSD2). This enzyme catalyzes the conversion of the active 11-hydroxycorticosteroids (cortisol and corticosterone) to 11-oxo-corticosteroids (cortisone and 11-dehydrocorticosterone respectively), which have a much lower affinity for the corticosteroid receptors and are thus effectively inactive (Funder JW et al 1988; Brown RW et al 1996(a,b)). The renal cellular distribution of 11β-HSD2 essentially parallels that of the MR (Albiston AL et al. 1994).

1.2.5.3 Aldosterone Induced Proteins (AIP)

Aldosterone influences expression of a broad pool of genes, the protein products of which participate in aldosterone signaling and alter ion transport in the plasma membrane of distal nephron, where its final effectors (ENaC and Na^+/K^+-ATPase) are located (Verrey F 2000; Pearce D 2001). A number of aldosterone induced genes have been identified in kidney or renal cell lines, which include sgk1, Ki-ras, GILZ, NDRG2, ENaC and Na^+/K^+-ATPase (*discussed next in detail*).

1.2.5.3.1 *Sgk1*

REGULATION Of the recently identified aldosterone-induced genes, sgk1 has attracted the most attention. This gene was identified originally in fibroblasts and mammary epithelia as an immediate-early gene induced by glucocorticoids at the level of transcription independently of *de novo* protein synthesis (Webster MK et al 1993, 1993(a)). Subsequent work by Chen S et al (1999) and Naray-Fejes-Toth A et al (2000) identified sgk1 as a primary aldosterone-induced gene in amphibian and mammalian renal epithelia. This transcript also is strongly induced by corticosteroids throughout the gastrointestinal tract but not the lungs (Shigaev A et al 2000; Brennan FE et al 2000). The sgk1 transcript is also commonly expressed in many nonepithelial tissues in a corticosteroid-insensitive manner, suggesting that sgk1 expression has very different regulation and may be constitutive (Chen S et al 1999; Webster MK et al 1993). Corticosteroids, through both GR and MR, increase sgk1 levels within 10-30 min of treatment, with levels peaking after 1-2 h and returning to pretreatment values soon afterward. Induction by aldosterone of Sgk1 protein in renal epithelia follows a similar time course, with protein levels increasing within 10-30 min, peaking by 6 h, and returning to pre-treatment levels by 24 h (Chen S et al 1999). Sgk1 itself is a phosphoprotein, with phosphorylation at threonine-256 and serine-422 by PDK-1 being required for Sgk1 activity. Aldosterone increases both absolute and phospho-Sgk1 levels in renal A6 cells (Wang J et al 2001). The lipid/protein kinase PI3K is upstream of PDK-1 in the PI3K signaling cascade and is required for activation of PDK-1 and Sgk1 by insulin, insulin-like growth factor (IGF)-1, and other stimuli (Park J et al 1999). Thus Sgk1 is a constituent of the PI3K signaling cascade positioned downstream of PDK-1 in parallel with PKB/Akt (Kobayashi T et al 1999; Vanhaesebroeck B et al 2000). In renal A6 epithelia, inhibition of PI3K attenuates aldosterone-induced increases in Na transport and in the active (phosphorylated) but not absolute levels of Sgk1 (Wang J et al 2001). This maneuver also blocks activation of Sgk1 and Na transport by insulin in the same cells. Sgk1 localizes to both the cytosol and nucleus and has proposed roles in preventing apoptosis and promoting cell proliferation in mammary tumor cells (Alliston TN et al 2000; Buse P et al 1999; Gonzalez-Robayna IJ et al 1999; Mikosz CA et al 2001; Park J et al 1999). It is

unclear how such an action could ultimately lead to increased transport if it were manifest in sodium transporting epithelia.

FUNCTION Sgk1 is a serine/threonine kinase that shares much homology with protein kinase B (PKB)/Akt kinases and phosphorylates at a consensus sequence (RXRXXS/T; optimal site KKRNRRLSVA) similar to that targeted by PKB/Akt, protein kinase C, and p90 ribosomal protein S6 kinase (Park J et al 1999; Kobayashi T et al 1999(a)). Several laboratories have shown that overexpression of Sgk1 with ENaC in the heterologous *X. laevis* oocyte expression system leads to increase of the channel conductance (Chen S et al 1999; De La Rosa DA et al 1999; Loffing J et al 2001; Naray-Fejes-Toth A et al 1999; Shigaev A et al 2000; Wagner CA et al 2001). Wulff P et al (2002) generated a knockout mouse model of sgk1. $Sgk1^{-/-}$ mice show no gross functional abnormalities and have normal Na and K metabolism when maintained on a normal diet. Nevertheless these animals showed inappropriate Na wasting when stressed with a low-Na diet. These studies suggest that sgk1 plays a pivotal role in linking aldosterone to the hormone driven Na reabsorption. In *Xenopus* oocytes, sgk1 increases the number of co-expressed ENaC in the plasma membrane independently of overt effects on the gating kinetics of this channel (De La Rosa DA et al 1999; Loffing J et al 2001; Wagner CA et al 2001). Initial thoughts about the mechanism of action of Sgk1 included the notion that it directly interacted and phosphorylated ENaC to dynamically regulate ENaC insertion into and/or retrieval from the apical membrane. Indeed, Sgk1 physically interacts with the COOH termini of both α- and β-ENaC, when the latter proteins are expressed as glutathione S-transferase fusion proteins (Wang J et al 2001). However, attempts to phosphorylate native as well as in vitro transcribed/translated ENaC with active, purified, recombinant Sgk1 have been unsuccessful to date (Chigaev A et al 2001; Stockand JD et al 2001). Because introduction of mutations to ENaC that results in loss of ENaC retrieval from the membrane to the lysosome and/or proteosome does not abrogate Sgk1 actions on the channel in oocytes (Chigaev A et al 2001; De La Rosa DA et al 1999; Shigaev A et al 2000), it is more likely that this kinase regulates ENaC insertion.

SUBSTRATE The substrates of Sgk1 and those that physically interact with Sgk1 largely remain unspecified. Zhang et al. (Zhang BH et al 2001) recently identified B-Raf as a substrate of Sgk1. In addition to B-Raf, the Forkhead family member FKHRL1, a proapoptotic transcription factor, is targeted by Sgk1 (Brunet A et al 2001). A role for regulation of FKHRL1 by Sgk1 during a mineralocorticoid response is presently unclear. The ubiquitin ligase NEDD4 directly interacts with the COOH termini of ENaC subunits at the PY motif and targets this channel for degradation (Staub O et al 1997, 2000). Debonneville C et al (2001) recently showed that Sgk1 directly interacted with NEDD4–2 to inhibit the latter protein's function and its binding to ENaC, which was independently reported by Snyder PM et al (2002). However, conflicting data show that mutations or deletions within ENaC COOH termini that destroy the NEDD4-binding site do not interfere with Sgk1 activation of these channels in oocytes (De La Rosa DA et al 1999; Loffing J et al 2001; Wagner CA et al 2001). Resolution of this apparent controversy is paramount to understanding Sgk1 actions on ENaC.

ISOFORMS OF SGK The recent development of $Sgk1^{-/-}$ mice has confirmed that SGK1 is a physiologically important mediator of aldosterone effects on renal sodium handling (Wulff P et al 2002). However, the Sgk knockout mouse has far less severe sodium wasting (only occurring when challenged with low-sodium diet) than the MR knockout (Berger S et al 1998), suggesting that other factors also mediate MR regulation of sodium transport. These factors may include two other forms of Sgk (Sgk2 and Sgk3), both of which are expressed in the kidney (Kobayashi T et al 1999(b); Liu D et al 2000; Dai F et al 1999). However, preliminary studies have failed to show responsiveness of Sgk2 and Sgk3 to corticosteroids (Kobayashi T et al 1999(b)). One recent study has found that Sgk2 and Sgk3 both stimulate ENaC mediated Na^+ current in *Xenopus* oocytes (Friedrich B et al 2003). Hence, it seems likely that Sgk2 and/or Sgk3 are implicated in either basal or hormone-regulated Na transport in the kidney. Whether either is a mediator of aldosterone action remains to be determined.

A diagram summarizing the role of Sgk1 in the pathway of aldosterone is shown in Figure 1.6.

1.2.5.3.2 Ki-RasA

REGULATION Spindler B et al (1997) identified Ki-ras A splice variant as an aldosterone-induced transcript. Aldosterone induces Ki-RasA during the early phase of action, with levels rising as early as 30 min after treatment. There are four homologous Ras proteins: Ha-Ras, N-Ras, Ki-RasA, and Ki-RasB. The latter two result from splice variants encoded by a common gene (Bar-Sagi D. 2001). Induction of Ki-rasA is a primary action of aldosterone that is independent of de novo protein synthesis. Previously, it has been shown that both the Ha-ras and Ki-ras genes were induced by glucocorticoids (Neades R et al 1991; Pethe V et al 1999; Strawhecker JM et al 1989). Controversy surrounded the importance of Ki-RasA in aldosterone signaling. Ki-rasA does not appear common to all epithelia capable of a mineralocorticoid response. Aldosterone via MR preferentially increases the Ki-RasA transcript and protein levels in amphibian distal nephron (Spindler B et al 1999) and via GR in amphibian renal A6 cells (Spindler B et al 1997; Stockand JD et al 1999). In contrast to these findings, Robert-Nicoud and colleagues (Robert-Nicoud M et al 2001), using serial analysis of gene expression (SAGE), were unable to identify Ki-Ras as being induced by aldosterone in a collecting duct cell line. Similarly no evidence of upregulation of Ki-Ras mRNA in kidney was seen by acute or chronic (6 days) aldosterone excess treatment of mice when sgk1 exhibited striking upregulation under the same experimental conditions (Christy C et al 2000). Others have also found similar negative results *in vivo* in mice (Verrey F: personal communication). Unlike Sgk1, the candidacy of Ki-ras as an important intermediary in aldosterone pathway in mammalian kidney remains in doubt.

FUNCTION Mastroberardino L et al (1998) showed in the heterologous *X. laevis* oocyte expression system that overexpression of constitutively active Ki-RasA with ENaC has conflicting actions on the ion channel, both stabilizing the open probability and decreasing the number of channels in the plasma membrane. The

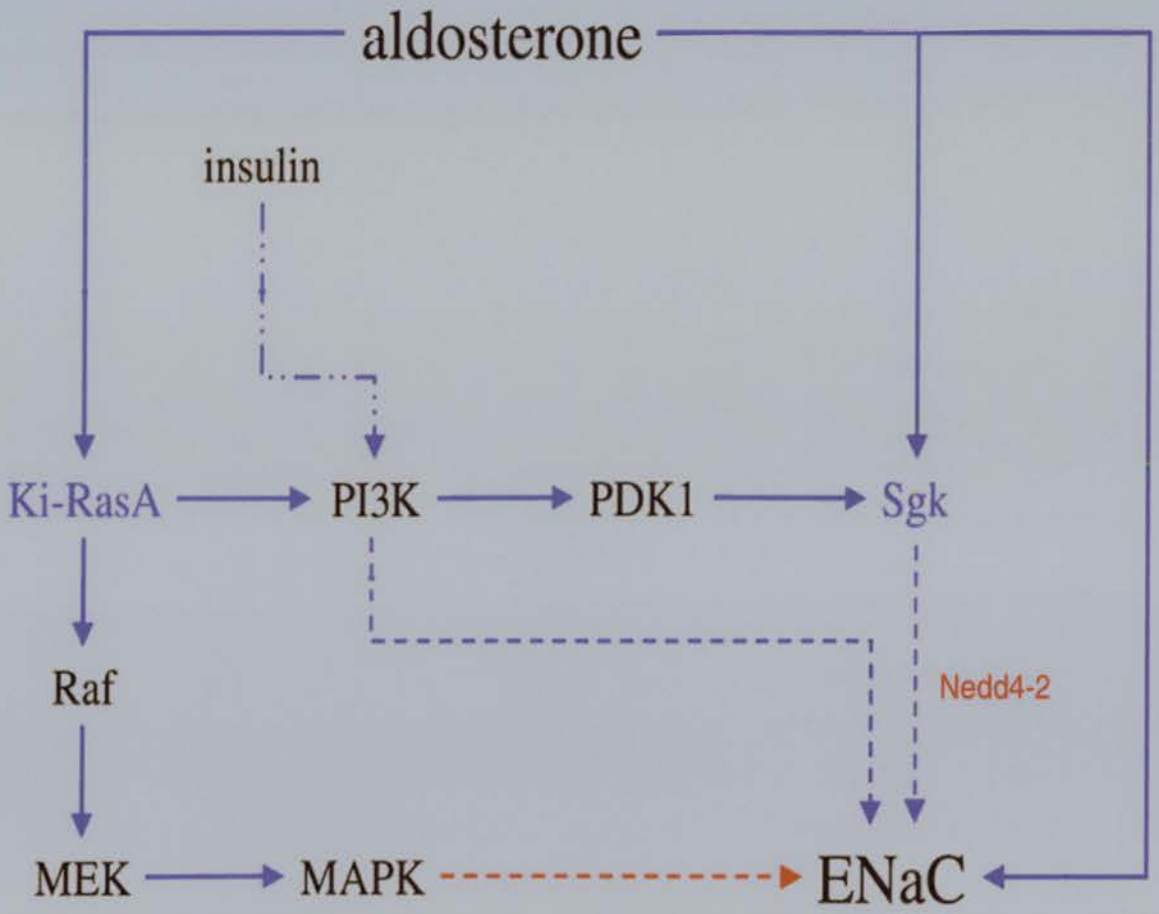

Figure 1.6. Aldosterone pathway in distal nephron. PI3K, phosphatidylinositol 3-kinase; PDK1, 3-phophoinositide-dependent protein kinase 1; MEK, mitogen extracellular kinase kinase kinase; MAPK, mitogen activated protein kinase; sgk, serum and glucocorticoid-induced kinase; ENaC, epithelial sodium channel; Nedd4-2: ubiquitin protein ligase 4-2.

effect on channel number resulted from nonspecific actions of activated Ki-RasA on induction of oocyte maturation. Stockand JD et al (1999) demonstrated that induction of Ki-RasA during the early phase is necessary and sufficient for some part of aldosterone's action on Na transport in polarized renal A6 epithelial cells. Indirect evidence from several other studies (Becchetti A et al 2000; Stockand JD et al 2001(a)) suggests that Ras must be in close proximity to ENaC. Alternatively, Ras could signal to ENaC through effector proteins that are also localized to the plasma membrane. For example, Ras signaling is known to activate PI3K in numerous cell types (Foschi M et al 1997; Rommel C et al 1999; Yan J et al 1998) and PI3K activates Sgk1 *in vitro* (Park et al 1999), which clearly affect ENaC conductance. During chronic activation of Ras and its downstream effector cascades, specifically the MAPK cascade, ENaC expression levels are ultimately decreased in both native epithelia and heterologous systems (Lin HH et al 1999; Mastroberardino L et al 1998; Wang HC et al 2000; Zentner MD et al 1998).

A diagram summarizing the role of Ki-RasA in the pathway of aldosterone is shown in Figure 1.6.

1.2.5.3.3 GILZ

Robert-Nicoud et al. (Robert-Nicoud M et al 2001) have identified the glucocorticoid-induced leucine zipper protein (GILZ) as an aldosterone-induced gene in an immortalized mouse collecting duct cell line (mpkCCD). GILZ transcript levels were increased by aldosterone within 30 min, indicating that it is an early response event. GILZ belongs to the transforming growth factor-β-stimulated clone 22 (TSC-22)/DSIP-immunoreactive leucine zipper protein family, thought to be transcription factors. How GILZ could affect ENaC conductance remains unclear.

1.2.5.3.4 NDRG2

Boulkroun S et al (2002) have identified an early response cDNA highly homologous to human and murine NDRG2 (N-Myc downstream regulated gene 2), using a

subtractive hybridization technique on isolated renal cortical collecting ducts from rats injected with a physiological dose of aldosterone. NDRG2 mRNA was expressed in classical aldosterone target epithelia (including the kidney) and localized in the collecting duct, the site of aldosterone-regulated sodium absorption. NDRG2 mRNA was increased within 45 min by aldosterone in the kidney and distal colon. In the RCCD2 collecting duct cell line, NDRG2 gene expression was increased as early as 15 min by aldosterone (1nM-10nM) but was not responsive to the glucocorticoid dexamethasone. The function of NDRG2 and its role in sodium reabsorption remain unclear.

1.2.5.3.5 ENaC

The regulation of ENaC mRNAs by aldosterone shows tissue-specificity in kidney and colon. In the distal nephron, aldosterone increases the ENaC α subunit mRNA without affecting the mRNAs encoding the β and γ subunits. In contrast, in colon it is the β and γ subunit mRNAs that are upregulated by aldosterone, whereas the α subunit is expressed constitutively (Asher C et al. 1996; Escoubet B et al. 1997; Renard S et al. 1995). In the *Xenopus* A6 cell line, aldosterone specifically increases protein levels of the ENaC α subunit 60 min after treatment. A few hours later, the synthesis of the β subunit increases as well, but not that of the γ subunit (May A et al. 1997; Spindler B et al. 1997).

The discussion of ENaC and its structure, function and trafficking is elaborated in more detail in the following chapter.

1.2.5.3.6 Na^+/K^+-ATPase

The Na^+/K^+-ATPase belongs to the family of P-type ATPases including Ca^{2+}-ATPases of the endoplasmic reticulum and H^+/K^+-ATPases of the plasma membrane. Na^+/K^+-ATPase exchanges three intracellular Na^+ for two extracellular K^+ per cycle and hydrolyzes ATP. In aldosterone target epithelia, Na^+/K^+-ATPase consists of the α1 and β1 subunits (Burgener-Kairouz P et al. 1994). The Na^+/K^+-ATPase α1 and β1

subunit genes have been shown to be regulated by aldosterone in A6 epithelia. The increase in β1 subunit mRNA starts to be measurable after 1 hour of aldosterone treatment and that of α1 after approximately 3 hours (Spindler B et al. 1997; Verrey F et al. 1989). In animals, long-term treatment with aldosterone produces a large increase in the number of Na^+/K^+-ATPase subunits and a parallel increase in the basolateral surface area (El Mernissi G et al. 1983; Garg LC et al. 1981; Hayburst RA et al. 1988; Wade JB et al. 1990; Welling PA et al. 1993). Na^+/K^+-ATPase activity in basolateral membrane is also upregulated in distal nephron epithelia in less than 1 hour of aldosterone treatment (Mujais SK et al 1984; Rayson BM et al 1984). This appears largely relating to enhanced recruitment of existing Na^+/K^+-ATPase from an intracellular pool rather than *de novo* protein synthesis. The mechanism of this upregulation is not well understood but likely involves the influences of aldosterone induced proteins and/or the effects of apical entry of sodium and electro-osmotic changes it elicits (Blot-Chabaud M et al 1990; Coutry N et al 1994).

1.2.6 The Pivotal Importance of Aldosterone Pathway in Control of Blood Pressure and Clinic Relevance

The identification of genes related to blood pressure variation has contributed enormously to defining primary physiologic mechanisms underpinning this trait, thereby helping elucidate pathogenic pathways and targets for therapeutic intervention. The genetic approach has investigated rare Mendelian forms of blood pressure variation in which mutations in single genes impart large effects on blood pressure; and the subsequent genetic engineering to generate transgenic or knockout mouse models to mirror the human disorders. So far, genetic studies have identified mutations in more than 10 genes that cause Mendelian forms of hyper- and/or hypotension. Out of these genes related to hypertension, more than half are involved in the aldosterone pathway.

1.2.6.1 Genes Involved in Aldosterone Synthesis

1.2.6.1.1 Glucocorticoid-Remediable Aldosteronism

Glucocorticoid-remediable aldosteronism (GRA) is an autosomal dominant trait featuring early onset of hypertension with normal or elevated aldosterone levels despite suppressed plasma renin activity (Sutherland et al., 1966). GRA is caused by a gene duplication arising by unequal crossing over between two closely related genes involved in adrenal steroid biosynthesis. The two genes encode aldosterone synthase and steroid 11β-hydroxylase, an enzyme involved in cortisol biosynthesis whose expression is regulated by adrenocorticotropic hormone (ACTH) (Lifton et al., 1992a, 1992b). The resulting chimeric gene has the promoter of 11β-hydroxylase and the coding region of aldosterone synthase. Thus the aldosterone synthase activity is ectopically expressed under control of ACTH rather than agiotensin II, the normal aldosterone regulator. As a consequence, aldosterone synthesis becomes linked to cortisol synthesis that is normally ~1,000 fold higher, and maintenance of normal cortisol levels results in constitutively excessive aldosterone secretion and hypertension.

1.2.6.1.2 Defective Aldosterone Synthesis

Conversely, mutations resulting in loss of aldosterone synthase activity lead to impaired aldosterone biosynthesis. Individuals bearing two defective gene copies of aldosterone synthase have a mirror image of the GRA phenotype, with severely impaired renal salt retention in the distal nephron and hypotension (Mitsuuchi et al., 1992; Pascoe et al., 1992).

1.2.6.2 MR

1.2.6.2.1 Hypertension Exacerbated in Pregnancy

A mutation in the ligand binding domain of the mineralocorticoid receptor (MRS810L) causes an autosomal dominant form of hypertension that is markedly accelerated in pregnancy (Geller et al., 2000). Compounds that normally bind, but do not activate MR are all potent agonists of the mutant receptor. This includes steroids lacking 21-hydroxyl groups, such as progesterone, and clinically used antagonists of MR, such as spironolactone. Since progesterone levels rise 100-fold during pregnancy, this observation suggested that patients harboring MR-L810 might develop severe hypertension in pregnancy. Indeed, all pregnancies among patients harboring this mutation have been complicated by dramatic acceleration of hypertension associated with complete suppression of the renin-angiotensin system (Geller et al., 2000).

1.2.6.2.2 Autosomal Dominant PHA1

Pseudohypoaldosteronism type I (PHAI) features severe neonatal salt wasting with hypotension despite markedly elevated aldosterone levels. Patients with the dominant form have heterozygous loss-of-function mutations in MR, with a variety of premature termination and frameshift mutations identified in affected kindreds (Geller et al., 1998). This partial loss of MR function impairs maximal salt reabsorption. These findings indicate that two normal copies of MR are required for normal salt homeostasis in the neonatal period. However, upon assumption of a normal salt-rich diet, these patients typically become entirely asymptomatic and show no obvious phenotypic consequence (Geller et al., 1998).

1.2.6.3 11β-HSD2

1.2.6.3.1 Syndrome of Apparent Mineralocorticoid Excess (AME)

This autosomal recessive disease features early onset hypertension with hypokalemia and metabolic alkalosis accompanied by suppressed plasma renin activity and the virtual absence of circulating aldosterone. Affected individuals showed impaired conversion of cortisol to cortisone due to absence of the enzyme 11β-hydroxysteroid dehydrogenase type 2 (11βHSD-2; Ulick et al., 1979). The homozygous loss-of-function mutations of 11βHSD-2 in AME patients allow cortisol to activate MR, resulting in hypertension mediated by increased ENaC activity (Mune et al., 1995).

1.2.6.4 ENaC

1.2.6.4.1 Autosomal Recessive PHAI

Loss-of-function mutations in any of the three different ENaC subunits cause the autosomal recessive form of PHAI (Chang et al., 1996; Strautnieks et al., 1996). Like dominant PHAI, the recessive form features severe salt wasting and hypotension in the neonatal period despite high levels of aldosterone. In addition to these effects on renal salt handling, mutations in ENaC impair the clearance of fluid from the surface epithelium of the lung in humans and mice. Indeed, mice with targeted knock-out of ENaC subunits have the PHAI phenotype and, in addition, have respiratory failure due to impaired clearance of lung water (Hummler et al., 1996; Barker et al., 1998).

1.2.6.4.2 Liddle Syndrome

Liddle syndrome is characterized by autosomal dominant phenotype of early onset hypertension associated with suppressed plasma renin activity, and low plasma aldosterone levels. This disease is caused by mutations in either the β or the γ subunit of ENaC that truncate their cytoplasmic C termini (Shimkets et al., 1994; Hansson et al., 1995a), or missense mutations in a segment in the C terminus of the β or the γ

subunit, bearing a PPPXY amino acid motif (Hansson et al., 1995b; Inoue et al., 1998). These deletions or mutations yield an increase in the number of functional channels at the cell surface (Snyder et al., 1995; Schild et al., 1996). Two lines of evidence have suggested mechanisms for the reduced clearance of mutant ENaC from the cell surface. Inhibition of endocytosis via clathrin-coated pits induces an increase in Na current by markedly prolonging the half life of ENaC at the cell surface (Shimkets et al., 1997). In parallel, two WW domain–containing proteins, Nedd4-1 (Staub et al., 1996) and Nedd4-2 (Kamynina et al., 2001) have been identified that specifically interact with the PPPXY sequence of ENaC subunits. These proteins have ubiquitin ligase domains and target ENaC for degradation by ubiquitination. Expression of modified forms of *Xenopus* Nedd4 (Abriel et al., 1999) or mammalian Nedd4-2 (Kamynina et al., 2001), containing the WW domain without the ubiquitin ligase domain, also prolongs the half-life of wild-type ENaC by impairing the retrieval of ENaC for degradation.

1.2.7 Research Models for Studying Aldosterone Action *in vitro* and *in vivo*

1.2.7.1 In vitro cell culture

Cell culture systems have been very useful in characterizing the aldosterone response *in vitro*. Handler *et al* (1979) established cell lines from the *Xenopus laevis* kidney (A6). This epithelial cell line has been frequently used to characterize the response of sodium reabsorption to corticosteroids via GR (little or no MR is expressed in this cell line) both qualitatively and quantitatively. A mouse cortical collecting duct (CCD) cell line (M-1), reported in Stoos BA et al (1991), requires dexamethasone, a synthetic glucocorticoid, to establish a transepithelial Na transport but is not directly sensitive to aldosterone. A rat CCD cell line was established by Blot-Chabaud et al (1996). Nevertheless, it does not appear to respond to aldosterone either. A novel mouse CCD cell line (mpkCCD) generated by Bens et al (1999) displays a high level of sodium transport that can be upregulated by high aldosterone concentrations. However, whilst M-1 cells are available via national tissue culture collection facilities, mpkCCD cells

are not yet.

1.2.7.2 Normal (wild-type) and genetically modified animals

The effects of aldosterone on ion transport have been extensively studied *in vivo* in a variety of animal species, including rats, rabbits, mouse, dogs and humans. Plasma level of aldosterone in these animals can be varied by aldosterone injections, aldosterone infusion or by a range of other means such as changing the Na or K intake. These research models are very useful in elucidating the overall physiological response to aldosterone. The feasibility of generating genetically modified animals has enabled study of the effects of specific molecular components of the aldosterone pathway *in vivo*. Eight mouse models relevant to aldosterone action and the control of blood pressure are summarized below.

1.2.7.2.1 $MR^{-/-}$ mice and $GR^{-/-}$ mice

Mice in which the MR was knocked out developed severe symptoms of pseudohypoaldosteronism with failure to thrive, weight loss, severe Na and water loss, and a highly stimulated renin-angiotensin system (Berger S et al. 1998). These mice develop normally in utero but die 8-12 days after birth from pseudohypoaldosteronism. Although the amiloride-sensitive Na^+ reabsorption was reduced, the mRNA level of ENaC and Na^+/K^+-ATPase was not changed in the kidney, indicating even the maintenance of basal levels of Na reabsorption sufficient to allow survival was apparently not achieved by such MR independent transcriptional control of the amount of ENaC and Na^+/K^+-ATPase. Mice rescued by a subcutaneous injection of sodium chloride during the critical phase survive and develop normally, compensating a persisting loss of salt by an increased uptake and a chronically upregulated renin-angiotensin system (Bleich M et al. 1999). Daily injections of the glucocorticoid betamethasone from day 5 after birth prolonged the survival of $MR^{-/-}$ mice, but failed to completely replace the MR function. Knocking out GR *in vivo* resulted in perinatal death due to respiratory failure and severely retarded lung maturation. ENaC mRNA was markedly downregulated in lung in these

$GR^{-/-}$ mice (Cole TJ et al. 1995).

1.2.7.2.2 11β-HSD2$^{-/-}$

Apparent mineralocorticoid excess is characterized by the lack of 11β-HSD2, an enzyme which prevents glucocorticoids from occupying and activating co-localized mineralocorticoid receptors. As expected, 11β-HSD2 null mice display hypertension, hypokalaemia and show striking hypertrophy and hyperplasia of the distal nephron (Kotelevtsev Y et al. 1999).

1.2.7.2.3 Genetically engineered mouse models to study ENaC function

A series of ENaC subunit-defective mice and a mouse model expressing a hyperactive channel corresponding to that found in Liddle's syndroms have been generated over the past few years (Hummler E et al. 1996-1997; Barker et al. 1998. McDonald F et al. 1999; Pradervand S et al. 1999(a,b)). A major conclusion of these studies is that all three ENaC subunits are necessary for normal neonatal lung liquid clearance and also for the function of the kidney ASDN.

Knocking-out the mouse αENaC gene locus ($\alpha ENaC^{-/-}$) led to respiratory complications and neonatal death, thus indicating the crucial role of αENaC in lung liquid clearance at birth. The amiloride-sensitive electrogenic Na transport in airway epithelia was abolished (Hummler E et al. 1996). Expressing the αENaC subunit in the αENaC knockout mice under the control of cytomegalovirus promoter rescued the αENaC knockout mice from this fatal neonatal lung disorder (Hummler E et al. 1997). Although these rescued mice had sufficient basal Na reabsorption to clear the liquid in lung and survived the early neonatal period, they developed a phenotype similar to the pseudohypoaldosteronism type I (PHA-I) with renal salt-wasting despite high plasma aldosterone levels.

Disruption of the beta subunit of ENaC in mice resulted in similar salt wasting, hyperkalemia and neonatal death associated with a pseudohypoaldosteronism

phenotype (McDonald F et al. 1999). Mice bearing a mutation in the mouse βENaC gene locus ($\beta ENaC^{m/m}$) had βENaC protein deficiency (Pradervand S et al. 1999a). On a regular salt diet (0.3% Na), these $\beta ENaC^{m/m}$ mice exhibited a mild PHA-I phenotype but developed an acute PHA-I when challenged with a low salt (0.01% Na) diet.

Knock-out of the γENaC subunit in mice resulted in early death (36h after birth) of animals probably due to disturbed circulatory and electrolyte balance, relating to renal salt wasting PHA-I phenotype (Barker PM et al. 1998).

An interesting 'ENaC dosage' experiment was performed by replacing the carboxy-terminus of the wild-type β subunit with that of a 'Liddle mutation'. These mice developed a salt-sensitive hypertension with hypokalaemic alkalosis typical of Liddle's syndrome (Pradervand S et al. 1999b).

1.3 THE EPITHELIAL SODIUM CHANNEL (ENAC)

A major breakthrough in understanding sodium regulation in distal nephron came with the cloning of the subunits of the amiloride-sensitive epithelial sodium channel (ENaC) (Canessa CM et al 1993, 1994). ENaC is expressed primarily in polarized epithelia in the distal nephron, lung, distal colon, and other organs (Garty H et al 1997).

1.3.1 Structure

ENaC is composed of three related subunits, α, β and γ (Canessa CM et al 1993, 1994; Lingueglia E et al 1993; McDonald FJ et al 1994, 1995; Voilley N et al 1995), arranged in a stoichiometry of 2α:1β:1γ (Firsov D et al 1998; Kosari F et al 1998). Expression of all three ENaC subunits is needed for full channel activity, although expression of the α-subunit alone or αβ- or αγ-subunit combinations leads to the generation of small currents as well (Canessa CM et al 1993, 1994; Firsov D et al 1996). Every subunit consists of two transmembrane domains (M1, M2), a long extracellular loop and the intracellular N/C-termini (Figure 1.7). The C-termini of all

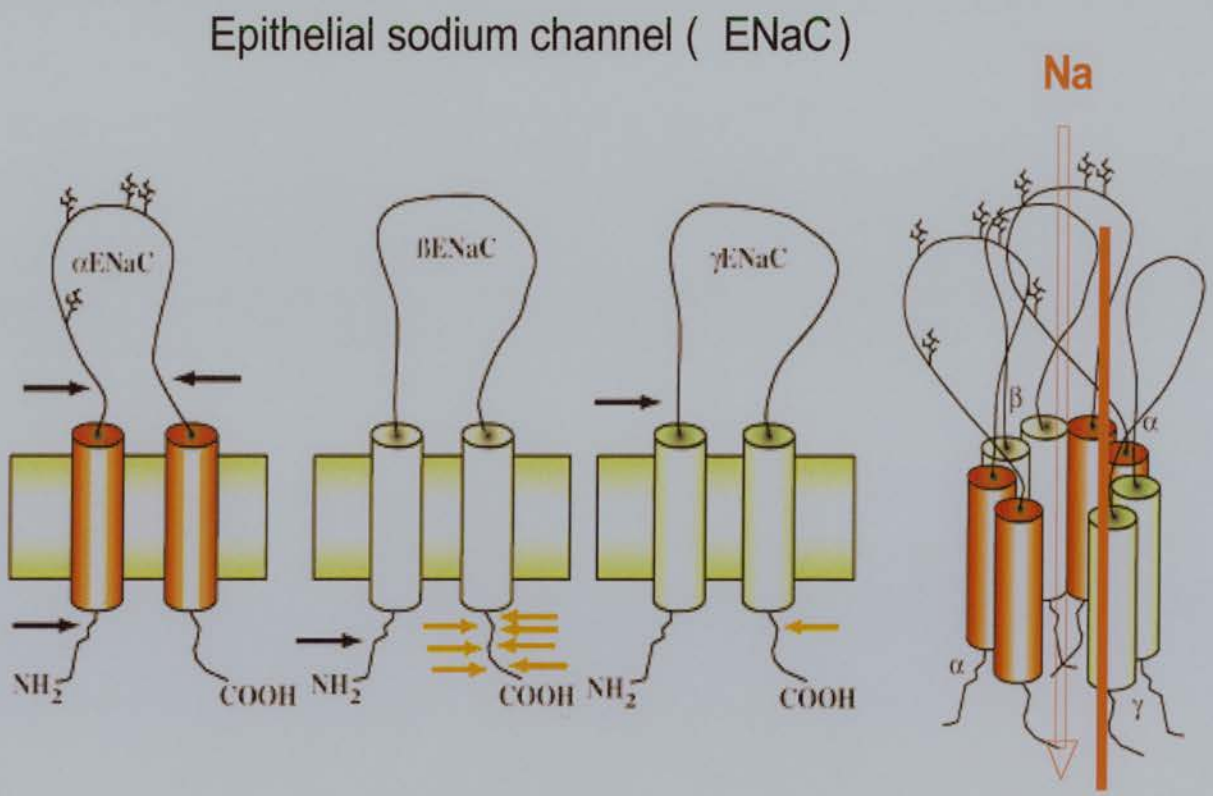

Figure 1.7. Structure and stoichiometry of ENaC.

subunits contain two proline-rich consensus sequences PY (PPPnY) (Schild L et al. 1996). Premature truncation of the C-terminus in either β or γ subunit results in both an increased channel open probability (P_o) and decreased channel retrieval rate from the apical membrane (Schild L et al. 1995; Snyder PM et al. 1995). The deletion of β or γ N-terminals dramatically alteres single channel values of mean open/close time (τ) and reduces ENaC-mediated sodium conductance. The N-terminal of α subunit (1-109) contains two distinct motifs. Truncation of amino acids 2-67 increases the number of active channels in the apical membrane whereas deletion of the entire N-terminal abolishes ENaC sodium currents (Chalfant ML et al. 1999). The large extracellular loop of about 500 amino acids includes the amiloride-binding sites, several glycosylation sites and a cysteine-rich domain, using which subunits are connected by disulfide bonds (Snyder PM et al.1994).

1.3.2 Topology

Hydropathy plot analysis indicates that all ENaC subunits have two hydrophobic regions separated by a large (~500 amino acids) hydrophilic loop. Three independent studies have determined the membrane topology of the rat αENaC subunit (Synder PM et al 1994; Canessa CM et al 1994(a); Renard SE et al 1994). *In vitro* translation of αENaC produced a 73kDa protein and an additional 93kDa protein corresponding to the glycosylated form. The αENaC subunit contains eight potential sites for N-linked glycosylation, among which mutation of six sites (Asn 190-538) abolished the glycosylation of αENaC, suggesting the six sites are localized to the extracellular side of the plasma membrane. To localize the N or C-terminus with respect to the plasma membrane, Synder et al (1994) placed a Flag epitope at the terminus and determined the sensitivity of the epitope to proteinase K. Both the N and C-terminal epitopes were not protected from the protease digestion, indicating that they are oriented on the intracellular side of the plasma membrane. Topological analysis of the β and γ subunits have not been reported so far, but it is likely to be the same as αENaC. The fact that >60% of the amino acids in αENaC face the extracellular domain is somewhat surprising. Such a structure might be thought to be important for interaction with large molecules that cannot diffuse close enough to the membrane

surface. This is not likely to be the case for Na ion. The N-terminus of ENaC subunits plays a role in subunit-subunit interactions (Adams et al 1997) whereas the C-terminus functions in the regulation of ENaC, at least in part by mediating the ubiquitination of ENaC and its endocytosis.

1.3.3 ENaC Trafficking to Cell Surface

In recent years, several groups have focused their studies on characterizing ENaC processing and trafficking, primarily in A6 cells and in cells that express ENaC heterologously [e.g. *X. laevis* oocytes, COS cells, HEK-293 cells, and Madin-Darby canine kidney (MDCK) epithelial cells]. In general, it appears that ENaC processing is inefficient, with ~1% of channels synthesized in the endoplasmic reticulum (ER) making it to the cell surface when they are expressed in *X. laevis* oocytes (Valentijn JA et al 1998) and an estimated ~20% in A6 cells, which express *X. laevis* ENaC (xENaC) endogenously (Weisz OA et al 2000). Moreover, the presence of ENaC at the cell surface is almost undetectable in renal tight epithelia that are not stimulated by aldosterone. Thus virtually no channel activity is observed in cortical collecting ducts from rats with low plasma aldosterone levels (Pacha J et al 1993), and ENaC subunits cannot be detected at the apical membrane of the distal nephron by immunohistochemistry under similar conditions (Loffing J et al 2000, 2001; Masilamani S et al 1999). An important determinant of the efficiency of ENaC maturation is the assembly of its subunits in the ER. ENaC assembly likely occurs very early during its processing in the ER, as suggested by co-immunoprecipitation experiments that demonstrate association of ENaC subunits in both glycosylated and unglycosylated forms (Adams CM et al 1997). Although biochemical (Adams CM et al 1997; Cheng C et al 1998; Firsov D et al 1996) and functional (Canessa CM et al 1994; Ishikawa T et al 1998) data have demonstrated that the expression of the α-subunit alone, or a combination of αβ- or αγ-subunits, can lead to the appearance of functional channels at the cell surface, the efficiency of maturation of such "partial" channels is extremely low. This coincides with enhanced ubiquitination and proteasomal degradation of ENaC subunits when expressed individually (Staub O et al 1997; Valentijn JA et al 1998). Moreover, although ectopic expression of the α-

subunit leads to exclusive lactacystin-sensitive (proteasomal) degradation, expression of all three ENaC subunits results in the appearance of an ENaC pool that is sensitive to lysosomal inhibitors (Staub O et al 1997).

1.3.4 Glycosylation

A useful tool in studying maturation and trafficking of transmembrane proteins from the ER to the Golgi is to trace their Asn (N)-linked glycosylation pattern. In the ER, transmembrane proteins acquire core glycosylation, which is sensitive to peptide N-glycosidase-F (PNGaseF). This core glycosylation is then trimmed at the ER and, on transport to the Golgi apparatus, is replaced with complex glycosylation that is resistant to endoglycosidase H (Endo-H). The Endo-H-resistant pool is often used as a marker to follow the mature transmembrane protein. However, one of the major difficulties in studying ENaC trafficking and maturation is the apparent lack of a detectable Endo-H-resistant pool of this channel (Canessa CM et al 1994(a); Renard S et al 1994; Snyder PM et al 1994; Valentijn JA et al 1998; Hanwell D et al 2002). The lack of a detectable Endo-H-resistant pool of cellular ENaC has suggested that either this channel does not acquire complex glycosylation or that the very small fraction of ENaC that actually translocates to the cell surface has complex glycosylation but is below the detection limits. Hanwell D et al (2002) have demonstrated that the surface pool of ENaC is glycosylated in a pattern similar to that for the ER pool and exhibits PNGaseF and Endo-H sensitivity, suggestive that an immature pattern of glycosylation persists in ENaC during its trafficking to the cell surface. The role of glycosylation of transmembrane proteins has received great attention, and it appears that in some cases it is involved in apical targeting, whereas in others it does not appear to be so (Yeaman C et al 1999). The role of ENaC glycosylation in ENaC trafficking is presently obscure. All three ENaC subunits possess numerous potential N-linked glycosylation sites at their ectodomains (Canessa CM et al 1994(a)). Mutating some or all of the glycosylation sites does not seem to affect channel activity (Canessa CM et al 1994(a); Snyder PM et al 1994), suggesting that sugar modification of ENaC does not affect proper trafficking to and insertion of the channel in the plasma membrane.

1.3.5 Solubility in Nonionic Detergent

Recent work in COS and HEK-293 cells heterologously expressing ENaC has shown that the channel is transformed during its processing from a nonionic detergent (Triton X-100)-soluble form in the ER to a Triton X-100-insoluble form during trafficking to the cell surface (Prince LS et al 1998, 1999). The acquisition of such nonionic detergent insolubility is often proposed to be mediated by an association with 'lipid rafts'. Lipid rafts are cholesterol- and sphingolipid-rich microdomains within membranes often associated with (mainly apical) targeting of proteins sequestered in such rafts (Simons K et al 1997). However a recent study shows that ENaC expressed in MDCK cells is not associated with lipid rafts (Hanwell D et al 2002). Thus, it appears that ENaC is not utilizing lipid rafts to traffic to the cell surface, at least in such cells.

1.3.6 ENaC Association with Cytoskeleton

Several reports have proposed interactions between ENaC and cytoskeletal proteins, including α-spectrin (Rotin D et al 1994; Zuckerman JB et al 1999) and actin (Berdiev BK et al 1996; Jovov B et al 1999). Although it appears likely that cytoskeletal interactions are involved in stabilizing ENaC at the cell surface and possibly in regulating its activity, it is not known what precise role such interaction may play.

1.3.7 Endocytosis of ENaC

Nedd4, a ubiquitin protein ligase, plays a key role in endocytosis of ENaC. The binding of Nedd4 with the PY domains of ENaC β and γ subunits facilitates the ubiquitination at lysine residues of ENaC α and γ N-terminals (Staub O et al. 1996, 1997). Degradation of ubiquitinated proteins is carried out by 26S proteasomes or lysosomes. As for ENaC degradation, the unassembled subunits are targeted to the 26S proteasome whereas the assembled αβγ complex is directed to the lysosome by clathrin-mediated endocytosis (Staub O et al. 1997). The half-life of (heterologously

expressed) ENaC at the cell surface of *X. laevis* oocytes was reported to be ~2-3.5 h (Shimkets RA et al 1997; Staub O et al 1997). In mammalian MDCK cells, this value is lower ~1-2 h (Hanwell D et al 2002), which is reasonable considering the higher temperature in which these cells are grown relative to that for *X. laevis* oocytes. A recent study using A6 cells has proposed a much longer half-life of xENaC and suggested that cell surface stability of α- and γ-ENaC (at least 24 h) is much greater than that of β-ENaC (6 h) (Weisz OA et al 2000). The turnover of ENaC is inhibited in the context of β- or γ-ENaC subunit bearing Liddle's syndrome mutations in the PY domain that abrogate the Nedd4 binding, resulting in several-fold increased half-life of the channel in the plasma membrane (Firsov D et al 1996; Schild L et al 1996; Shimkets RA et al 1997; Snyder PM et al 1995).

1.3.8 Regulatory Hormones

1.3.8.1 Aldosterone

Patch-clamp experiments in rat renal cortical collecting ducts (CCD) have indicated that variations in plasma aldosterone levels, induced by changes in dietary salt intake, modify the abundance of active ENaC in the apical plasma membrane (Pacha J et al 1993). No apical channel activity can be detected in animals that had low plasma aldosterone and were fed a high-salt diet, whereas increasing plasma aldosterone levels by restriction of Na intake dramatically increases the number of functional apical channels. The physiological relevance of this regulation has been quantitatively assessed recently by measurements of amiloride-sensitive Na currents recorded in CCD cells of rats that were subjected to short-term salt deprivation and also had their urinary Na excretion measured (Frindt G et al 2001). This study has shown that the increase in ENaC current in response to a two- to threefold increase in plasma aldosterone levels can account for reduced Na excretion under these conditions. *In situ* immunohistochemical studies in mouse kidney have clearly showed that changes in plasma levels of aldosterone affect the intracellular distribution of ENaC subunits (Loffing J et al 2000; Masilamani S et al 1999). An increase in plasma aldosterone level associated with dietary salt restriction causes a large increase in abundance of α-

ENaC and a redistribution of ENaC subunits from the cytoplasm to the apical membrane. The stimulation of α-ENaC expression and its shift from a cytoplasmic to an apical membrane pool in the distal nephron can be observed as early as 2 h after aldosterone injection (Loffing J et al 2001). The molecular and cellular mechanisms underlying these effects remain to be elucidated. Besides the increase in α-ENaC mRNA levels, aldosterone induces or represses the synthesis of many other transcripts in principal cells of the distal nephron (Chapter aldosterone-induced proteins). These aldosterone-induced proteins are likely to play an important role in ENaC regulation.

1.3.8.2 Vasopressin

Vasopressin (antidiuretic hormone; ADH) increases ENaC conductivity in a variety of sodium-transporting epithelia (Ausiello DA et al. 1987; Schafer JA and Hawk CT. 1992; Eaton D et al. 1995). The effect of AVP is mediated via AVP binding to its V2 receptors, leading to the stimulation of adenylate cyclase and a concomitant increase in the level of intracellular cAMP. A number of observations suggest that such a cAMP stimulated pathway acts by translocating ENaC from a cytoplasmic pool into the apical membrane (Erlij D et al 1999; Kleyman TR et al 1994; Blazer-Yost BL et al 2001). Stimulation of ENaC expression at the cell surface by vasopressin seems different from that of aldosterone because the effects of the two hormones are synergistic (Breyer MD and Ando Y 1994).

1.3.8.3 Insulin

Insulin evokes a ~50% upregulation of amiloride-sensitive sodium transport across frog skin (Civan MM et al. 1988, 1989), toad bladder (Blazer-Yost B et al. 1988, 1989) and A6 cells (Erlij D et al. 1994; Marunaka Y et al. 1992; Record R et al. 1998). In frog skin, the increase in Na conductance was accompanied by a parallel increase in the apical electrical capacitance, suggesting that the hormone promotes an exocytic delivery of channels to the apical membrane (Civan MM et al. 1988, 1989). On the other hand, studies in A6 cells using patch clamping have shown effects of insulin on channel open probability but not on the number of channels per patch (Marunaka Y et

al. 1992). The precise mechanism mediating the insulin response is yet to be elucidated though phosphatidylinositol 3-kinase activation was required for insulin-stimulated sodium transport in A6 cells (Record R et al. 1998).

1.3.9 Regulatory Proteins

A few proteins have been shown to interact with ENaC and regulate its activity. Among them, sgk1, cap1 and syntaxin 3 increase ENaC mediated sodium transport whereas Nedd4 and syntaxin 1A reverse the process. These appear to act by very different mechanisms (*discussed next in detail*).

1.3.9.1 Kinases

Although it is well known that cAMP activates amiloride-sensitive sodium transport in rat and *Xenopus* renal epithelia (Ausiello DA et al. 1987; Schafer JA and Hawk CT 1992; Eaton D et al. 1995), disparate observations were reported on the stimulation of ENaC by cAMP or PKA (protein kinase A) when the channel was incorporated into artificial lipid bilayers or coexpressed in *Xenopus* oocytes (Lester DS et al. 1988; Awayda MS et al. 1996). PKC (protein kinase C) was shown to cause a direct reduction of channel open probability in the oocyte expression system (Awayda MS et al. 1996; Oh YS et al. 1997). Both PKA and PKC increase the phosphorylation of the β and γ subunits of ENaC in *Xenopus* oocytes (Shimkets RA et al. 1998). A recently identified serine/threonine kinase, sgk1 (Chen SY et al. 1999) stimulates ENaC translocation to the cell membrane of *Xenopus* oocytes (De la Rosa D et al. 1999). Pearce and colleagues have demonstrated its *in vitro* binding to the C-termini of ENaC α or β subunits (Wang J et al. 2001). Nevertheless, the phosphorylation of ENaC β and γ C-terminals was not mediated via sgk1 (Wang J et al. 2001), although stimulation of ENaC did require sgk1 kinase activity (Loffing J et al. 2001).

1.3.9.2 Proteases

In *Xenopus* oocytes injected with ENaC cRNA, addition of exogenous trypsin or

chymotrypsin to media (Chraibi A et al. 1998), or expression of the protease CAP-1 (channel activating protease, Vallet V et al. 1997), increases the conductivity of ENaC. Incubation with serine protease inhibitor-aprotinin abolishes this effect, suggesting the involvement of a proteolytic pathway (Vallet V et al. 1997). Careful studies using the cell-attached patch-clamp mode indicate that the protease effect is a 'local' phenomenon, i.e. a mechanism that involves protein(s) which are bound or adjacent to the channel within the $1um^2$ of membrane area included in a pipette patch and that does not include signal transduction through second messengers remotely from such cell patches (Chraibi A et al. 1998). The inhibitory effect of aprotinin and subsequent restoration by protease were also observed in mammalian cells (Nakhoul N et al. 1998), suggesting the presence of a conserved proteolytic pathway regulating ENaC conductance. No evidence has yet been found supporting the direct cleavage of ENaC subunits.

1.3.9.3 SNARE

The specificity of docking and fusion of vesicles with plasma or organelle membranes is mediated by specialized membrane proteins present in vesicles and target membranes, named v-SNARE or t-SNARE respectively (McNew JA et al. 2000; Parlati F et al. 2000). The interaction between v and t-SNAREs requires SNAPs (soluble N-ethylmaleimide-sensitive-factor attachment protein). In kidney cells, syntaxin 1A (t-SNARE) is localized to the basolateral membrane and co-precipitates with ENaC γ subunits. When co-expressed with ENaC in *Xenopus* oocytes, syntaxin 1A inhibits ENaC conductance (Qi J et al. 1999). In contrast, syntaxin 3 (t-SNARE) stimulates ENaC mediated Na transport in *Xenopus* oocytes and is localized to the apical membrane of renal cells (Saxena S et al. 1999).

1.3.9.4 Nedd4 isoforms

Nedd4, originally cloned as a gene that is developmentally down-regulated in mouse brain (Kumar S et al 1992), represents the prototype for a larger protein family, the emerging Nedd4/ Nedd4-like family of ubiquitin-protein ligases (Rotin D et al 2000;

Harvey KF and Kumar S 1999). Members of the Nedd4/Nedd4-like family possess a similar molecular organization: two to four WW (protein-protein interaction) domains, a C-terminal HECT (homologous to E6-AP-carboxy-terminal ubiquitin-protein ligase) domain and many having an N-terminal C2 (Ca^{2+} dependent lipid binding) domain. Two isoforms of Nedd4 have been identified in mice (Kamynina E et al 2001). Whereas mNedd4-1 contains a C2 domain, three WW domains and a HECT domain, mNedd4-2 contains four WW domains and a HECT domain, yet lacks a C2 domain. In *Xenopus*, one isoform has been cloned (Staub O et al 1996), containing a C2 domain, four WW domains and a HECT domain and showing higher homology to mNedd4-2. The third and fourth WW domains of xNedd4 and mNedd4-2 are protein-protein interaction modules that bind the proline-rich PY motif (xPPxY) in the C-terminus of β- or γ-subunit of ENaC (Staub O et al 1996; Kamynina E et al 2001). Several recent reports have demonstrated that xNedd4 or mNedd4-2 is a repressor of ENaC that regulates the endocytosis of channels from the cell surface (Abriel H et al 1999; Farr TJ et al 2000; Staub O et al 1997; Harvey KF et al 1999; Kamynina E et al 2001). This function of Nedd4 requires the presence of intact PY motifs, to which the Nedd4-WW domains bind. Snyder et al (1995) and Schild et al (1996) have demonstrated that mutations of the prolines and tyrosine of the PY motif lead to elevation of ENaC activity. Moreover, repression by Nedd4 also required its HECT domain to be active, indicating that ENaC ubiquitination is involved (Abriel H et al 1999). Ubiquitination of ENaC was previously demonstrated to regulate its cell surface stability, and mutation (to arginine) of key conserved lysine residues (where ubiquitination occurs) located at the NH_2 termini of α- and γ-ENaC leads to both impaired channel ubiquitination and increased stability of the channel at the plasma membrane (Staub O et al 1997).

1.4 Research Aims

1, to examine sgk1 gene expression in kidney and its regulation by aldosterone (e.g. dose response, cellular localization and time course);

2, to identify and characterize other novel aldosterone induced genes in the kidney;

3, to characterize corticosteroid modulation of ENaC trafficking in mouse collecting duct cells (e.g. dissecting the subcellular events underpinning ENaC trafficking and its hormonal regulation);

4, to elucidate the role of sgk1 in modulating ENaC conductance and to generate a cell model in which the expression of sgk1 can be tightly regulated by the tetracycline inducible system. This model can become available and widely accessible to determine whether upregulation of sgk1 by tetracycline influences ENaC-mediated sodium reabsorption in parallel to that by corticosteroids.

CHAPTER 2 MATERIALS AND METHODS

2.1 Material

2.1.1 Chemicals

All chemicals were obtained from BDH Chemicals Ltd (Magna Park, Lutterworth, Leicestershire LE17 4XN) or Sigma Chemicals Ltd (Fancy Road Poole, Dorset, BH17 7NH) unless otherwise stated.

Agarose	Invitrogen (Renfrew Road, Paisley PA3 4EF)
Bactotryptone	Beckton Dickinson (Towns Road, Oxford OX4 3LY)
Caesium Chloride	Invitrogen (Renfrew Road, Paisley PA3 4EF)
D19 developer	H.A. West Ltd (41 Watson Cresent, Edinburgh EH11 1ES)
Ethanol	Hayman Ltd (70 Eastways Industrial Witham, Essex CM8 3YE)
G418 (geneticin)	Invitrogen (Renfrew Road, Paisley PA3 4EF)
Hygromycin B	BD Clontech (1020 East Meadow Circle, Palo Alto, CA, USA)
Nucleotide triphosphates	Amersham Pharmacia Biotech UK Ltd (Little Chalfont, Bucks HP7 9NA)
Proteinase K	Boehringer Mannheim UK (Bell Lane, Lewes BNY 1LG)
Puromycin	BD Clontech (1020 East Meadow Circle, Palo Alto, CA, USA)
Tetracycline	BD Clontech (1020 East Meadow Circle, Palo Alto, CA, USA)
Yeast extract	Beckton Dickinson (Towns Road, Oxford OX4 3LY)
Yeast tRNA	Invitrogen (Renfrew Road, Paisley PA3 4EF)

2.1.2 Radiochemicals

All radiochemicals were supplied by Amersham Pharmacia Biotech UK Ltd (Little Chalfont, Bucks HP7 9NA).

Compound	Specific Activity
[^{35}S]-UTP	800Ci/mmol
[^{32}P]-dCTP	3000Ci/mmol

2.1.3 Fluorescent Reagents

All fluorescent dyes or antibodies were purchased by Molecular Probes (Leiden, Netherland).

Compound	Absorptance(nm)	Emission(nm)
AlexFluor 633-transferrin (#T23362)	633	647
AlexFluor 660 tagged goat anti-mouse secondary antibody (#A21054)	640	660
MitoTracker (#M22426)	640	662
rhodamine-B hexyl ester (#R648)	556	578
rhodamine-conjugated wheat germ agglutinin (#W849)	555	580

2.1.4 Enzymes

All restriction enzymes (except stated), DNaseI, *Taq* DNA polymerase, T7 DNA polymerase, T4 DNA polymerase, AMV reverse transcriptase and T4 DNA ligase were supplied by Promega Ltd (Chilworth Research Center, Southampton SO16 7NS).

AgeI restriction enzyme	New England Biolabs Ltd (73 Knowl Piece, Hertfordshire SG4 0TY)
BsrGI restriction enzyme	New England Biolabs Ltd (73 Knowl Piece, Hertfordshire SG4 0TY)
Pfu DNA polymerase	Statagene Ltd (North Torrey Pines Road, La Jolla, CA, US)
RNase A	Sigma Chemicals (Fancy Road Poole, Dorset, BH17)

2.1.5 Plasmids

pGEM-Teasy	Promega (Chilworth Research Center, Southampton SO16 7NS)
pEGFP-C2	BD Clontech (1020 East Meadow Circle, Palo Alto, CA, USA)
pEYFP-C1	BD Clontech
pHcRed-C1	BD Clontech
pTet-Off	BD Clontech
pTRE2hyg	BD Clontech

2.1.6 Antibodies

Anti-GFP	BD Clontech (1020 East Meadow Circle, Palo Alto, CA, USA)
Anti-GM130 (Anti Golgi antibody)	Gift of Dr Rory Duncan (Dept of Biomedical Sciences, University of Edinburgh)
Goat anti-mouse secondary Antibody conjugated to horseradish peroxidase	Roche Molecular Biochemcials (Sandhofer Strasse 116, D 68305 Mannheim, Germany)

2.1.7 Cell Culture Reagents

All media and additives for maintenance of cell lines were supplied by Invitrogen (Renfrew Road, Paisley PA3 4EF).

Dulbecco's Modified Eagle Medium (DMEM)
Nutrient Mixture F-12
Dulbecco's PBS
Fetal Bovine Serum
L-glutamine (200mM)

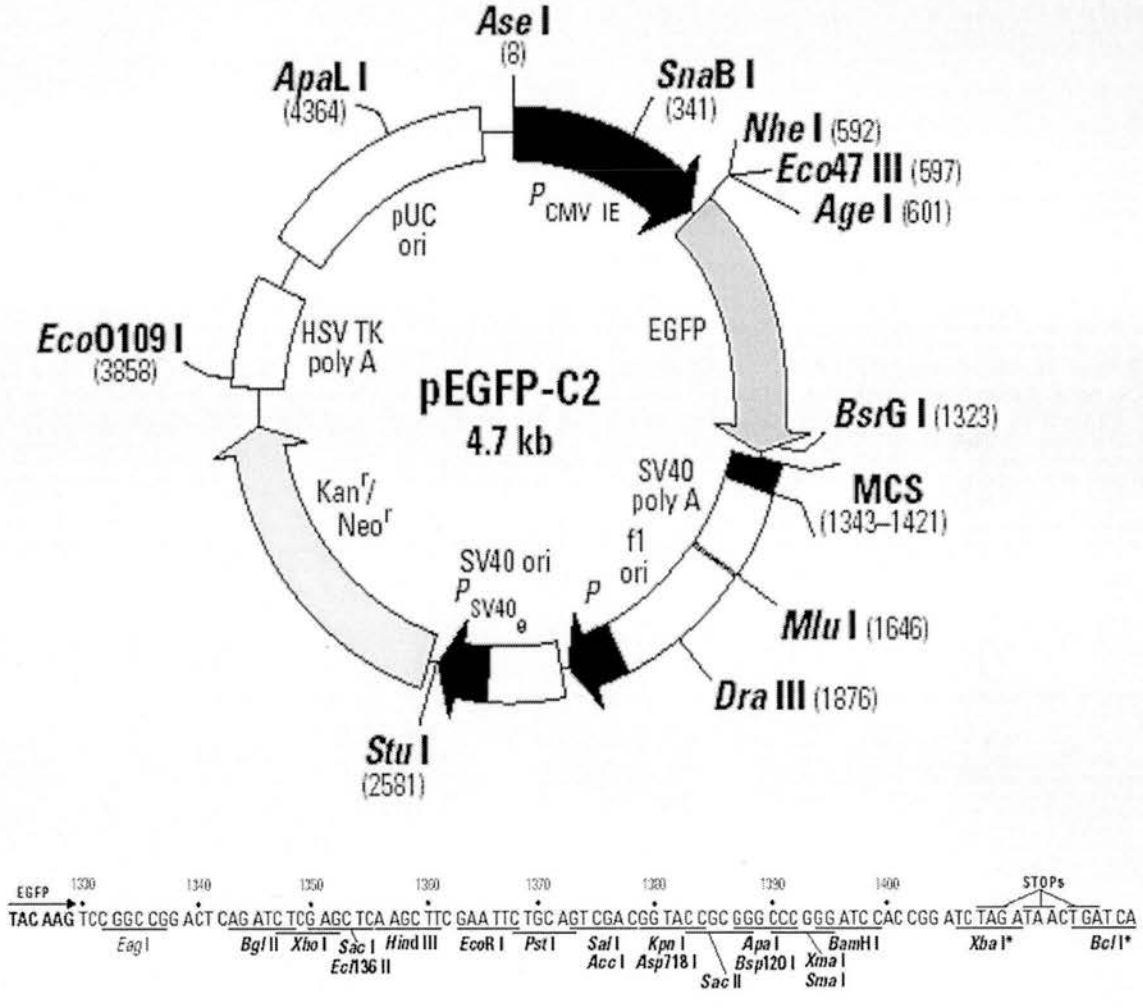

Figure 2.1. Map of the plasmid pEGFP-C2.

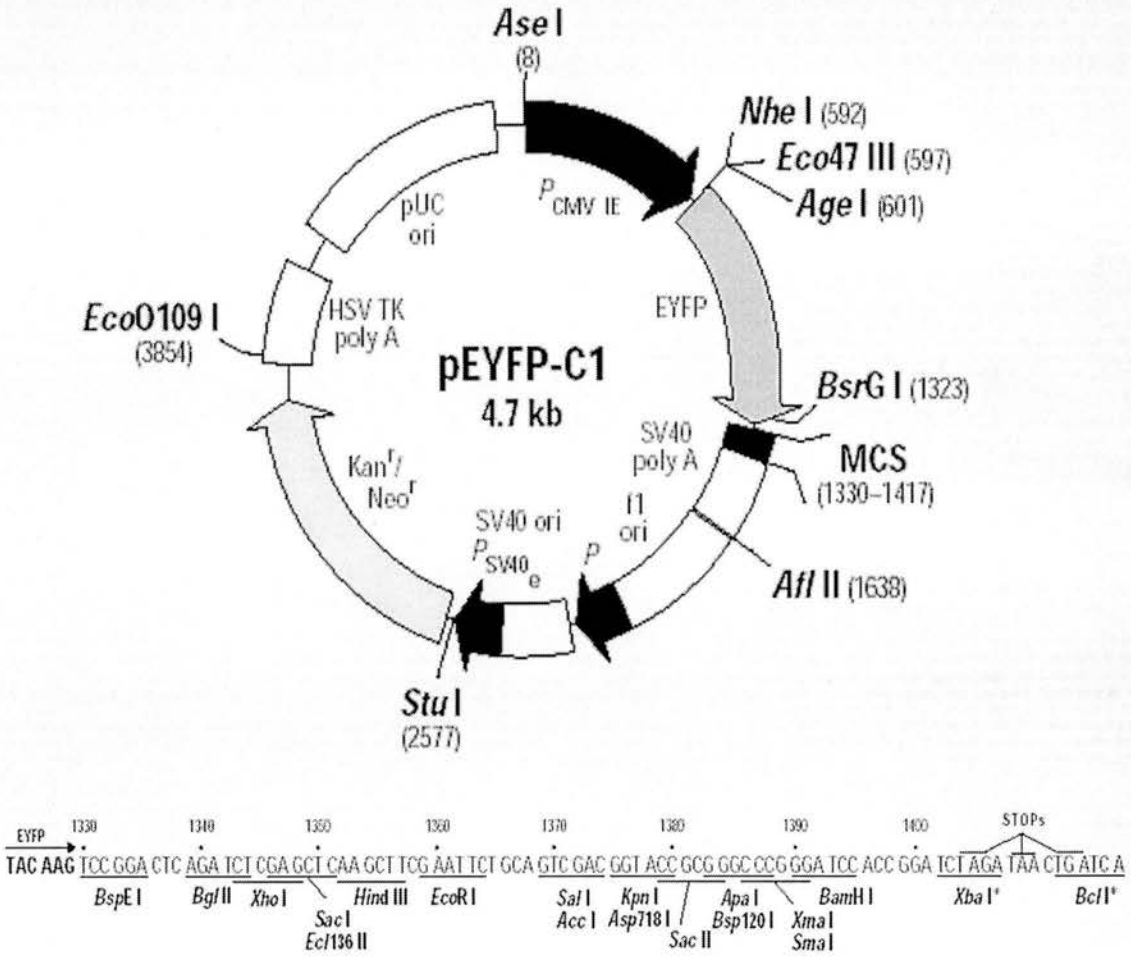

Figure 2.2. Map of the plasmid pEYFP-C1.

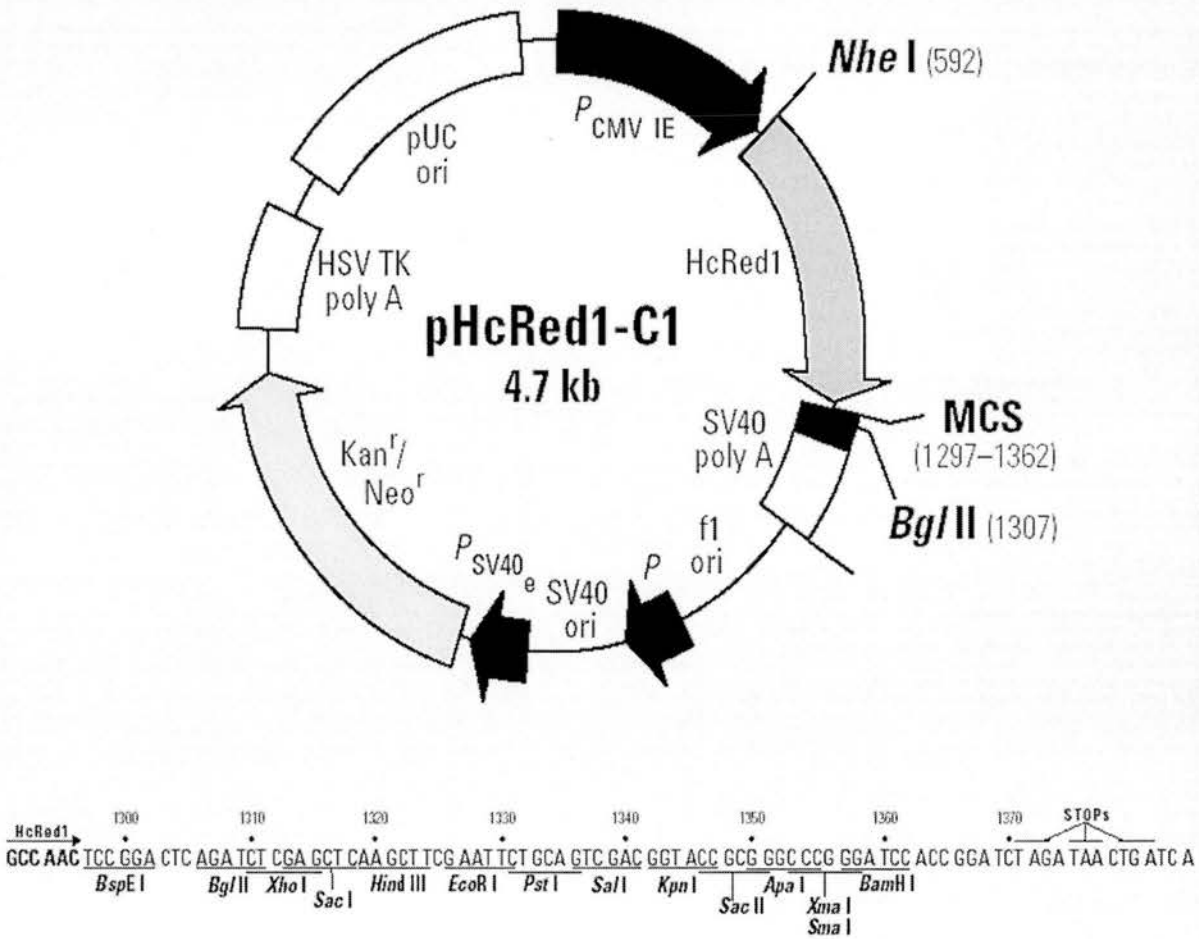

Figure 2.3. Map of the plasmid pHcRed1-C1.

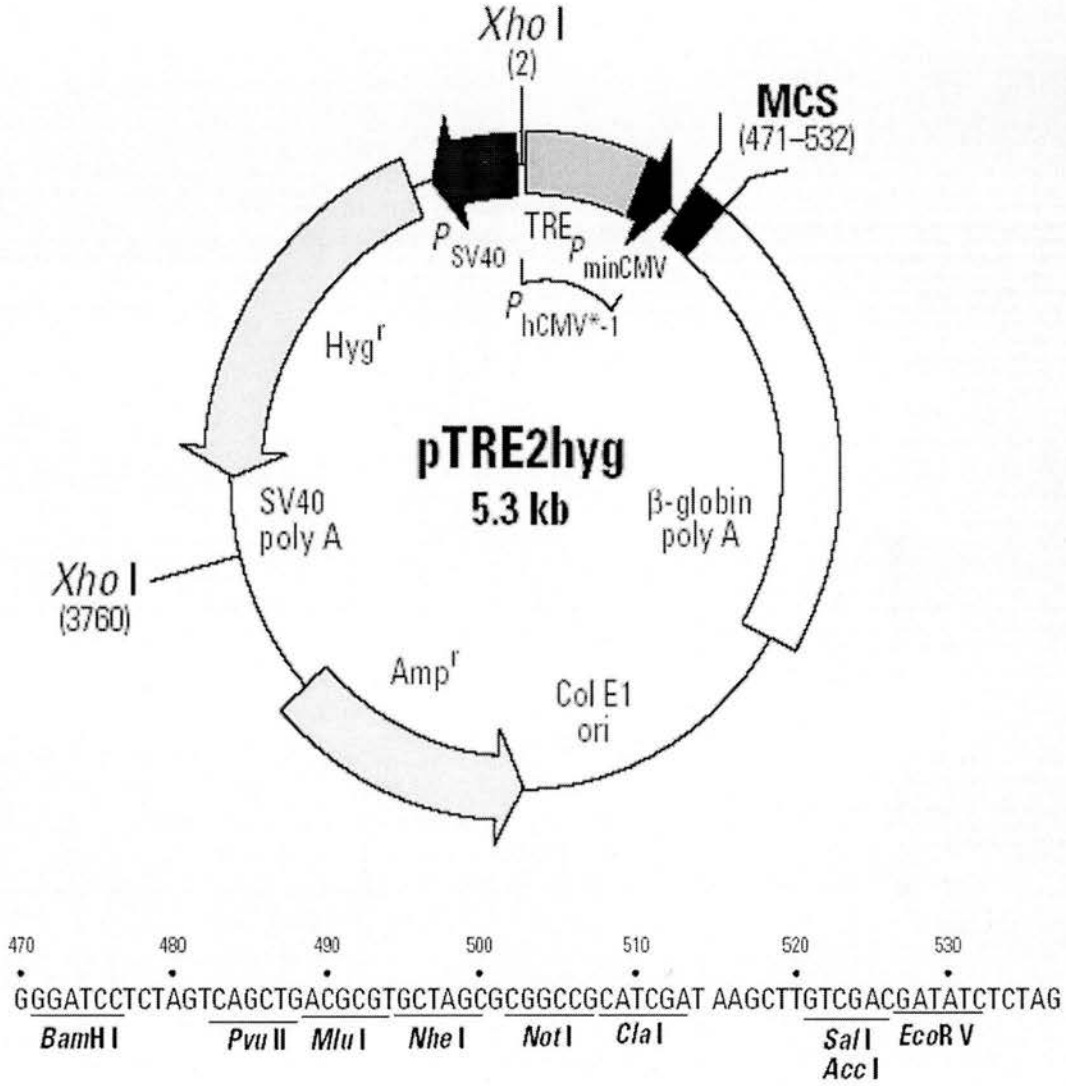

Figure 2.4. Map of the plasmid pTRE2hyg.

Penicillin/Streptomycin (10000U/ml; 10000μg/ml)
Trypsin/EDTA (10x)

2.1.8 Cells and Animals

2.1.8.1 Bacteria strains for cloning

The *E.coli* strain HB101 was supplied by Promega Ltd (Chilworth Research Center, Southampton SO16 7NS).

2.1.8.2 Cell lines

The mouse collecting duct M-1 cell line was purchased from the European Cell Line Collection.

2.1.8.3 Animals

Animals were supplied by Charles River Ltd (Margate Kent, UK)

2.1.9 Miscellaneous

BioRad protein assay solution	BioRad Laboratories Ltd. UK
CELLQuest software	Becton Dickinson (2350 Qume Drive, San Jose, CA, US)
Cryostat	Bright Instruments Ltd. UK (Maylands Avenue, Hemel Hampstead HP2 7TD)
DNA size markers	Invitrogen (Renfrew Road, Paisley PA3 4EF)
Dried skimmed milk powder	Marvel (Premier Beverages, Stafford SR20 0QJ)
ECL (peroxidase-based chemiluminescent detection method)	Amersham Pharmacia Biotech UK Ltd (Little Chalfont, Bucks HP7 9NA)

FACS (fluorescence activated cell scanning) system	Becton Dickinson (2350 Qume Drive, San Jose, CA, US)
Horizon 58 electrophoresis tank	Invitrogen (Renfrew Road, Paisley PA3 4EF)
^{125}I-RIA kit	DPC (Los Angeles, CA, US)
Lens tissue	Whatman Labsales Ltd. UK
β-Max Hyperfilms	Amersham Pharmacia Biotech UK Ltd (Little Chalfont, Bucks HP7 9NA)
Microscope slide	BDH [Merck Ltd.] UK
NICK column (Sephadex G50)	Amersham Pharmacia Biotech UK (Little Chalfont, Bucks HP7 9NA)
Oligonucleotides	Invitrogen (Renfrew Road, Paisley PA3 4EF)
Pico-fluor 40 scintillant fluid	Amersham Pharmacia Biotech UK Ltd (Little Chalfont, Bucks HP7 9NA)
Qiagen DNA recovery kit	Qiagen UK (Boundary Court, Gatwick Road, West Sussex RH10 9AX, UK)
Radioactive microscale standards (#RPA504, RPA511)	Amersham Pharmacia Biotech UK Ltd (Little Chalfont, Bucks HP7 9NA)
Razorblades	BDH (Magna Park, Lutterworth, Leicestershire LE17 4XN)
Transwell (#3470) *[6.5-mm diameter, 0.4-μm pore size]*	Corning Costa (10 Valley Center, Gordon Road, Bucks HP13 6EQ)
TRIzol reagent	Invitrogen (Renfrew Road, Paisley PA3 4EF)
Zeiss Axioskop Microscope	Carl Zeiss UK (Woodfield Road, Herts AL7 1LU)
Zeiss Axioskop Microscope silver-grain counting software (KS300-v3)	Carl Zeiss UK
Zeiss epifluorescence microscope	Carl Zeiss UK
Zeiss confocal LSM microscope	Carl Zeiss UK

Zeiss LSM Image Brower (v3.1)	Carl Zeiss UK

2.1.10 General Buffers

Unless stated, the distilled water was used to prepare all buffers. All buffers were sterilized in an autoclave except those marked with *.

Alkaline SDS solution*	0.2M NaOH, 1% SDS
DEPC water	0.5ml DEPC was added to 500ml water and kept at room temperature for 1h before autoclaving
DNA loading buffer*	0.25% (w/v) bromophenol blue, 0.25% (w/v)
xylene	cyanol, 30% glycerol
0.5M EDTA (pH8.0)	800ml water was added to 186.1g EDTA. pH was adjusted to 8.0 with NaOH and the volume adjusted to 1000ml
Formamide loading buffer*	34.03% bromophenol blue, 0.03% xylene cyanol, 20mM EDTA in deionized formamide
GTE (lysis buffer)	50mM glucose, 25mM Tris-HCl (pH 8.0), 10mM EDTA
MOPS electrophoresis buffer (10x)	0.2M MOPS (pH7), 20mM sodium acetate, 10mM EDTA
SDS lysis buffer	150mM NaCl, 50 mM Tris, pH 7.4, 1% SDS, 0.5mM phenylmethylsulfonyl fluoride
SDS running buffer (10x)	0.25M Tris, 2.5M Glycine, 1% SDS
1M Tris-HCl (pH8.0)	121.1g Tris was added to 800ml water. pH was adjusted to 8.0 with concentrated HCl and the volume to 1000ml with water
5M potassium acetate	245.6g potassium acetate was dissolved in 300ml water. The volume was adjusted to 500ml by adding 57.5ml glacial acetic acid and

	142.5ml water
TBE (10x)	108g Tris, 55g boric acid, 20ml 0.5M EDTA were made to 1000ml water
TE (10x)	10mM Tris-HCl (pH8.0), 1mM EDTA
2M sodium acetate (pH4.0)	272g sodium acetate was dissolved in 800ml water. pH was adjusted to 4.0 with glacial acetic acid and the volume to 1000ml

2.1.11 Molecular Biology Buffers

Restriction buffer A	90mM Tris-HCl, 10mM $MgCl_2$, 50mM NaCl, 1mM DTT (pH7.5)
Restriction buffer B	6mM Tris-HCl, 6mM $MgCl_2$, 150mM NaCl, 1mM DTT (pH7.9)
Restriction buffer C	10mM Tris-HCl, 10mM $MgCl_2$, 150mM KCl 1mM DTT (pH7.4)
Restriction buffer D	6mM Tris-HCl, 6mM $MgCl_2$, 100mM NaCl, 1mM DTT (pH7.5)
Restriction buffer (Multi-Core)	500mM NaCl, 500mM Tris-HCl, 110mM MgCl2, 60mM β-mercaptoethanol, 1mg/ml bovine serum albumin (pH8.0)
Transcription optimized buffer	40mM Tris-HCl (pH7.9), 6mM $MgCl_2$, 2mM spermidine, 10mM NaCl
T4 DNA ligase buffer	30mM Tris-HCl (pH7.8), 10mM $MgCl_2$, 10mM DTT, 1mM ATP
Reverse transcription buffer	10mM Tris-HCl (pH8.8), 50mM KCl, 0.1% Triton X-100

2.2 Methods

2.2.1 Gel Electrophoresis

2.2.1.1 Agarose gels

Agarose gels were prepared by adding solid agarose to 1xTBE at 0.8-2% (w/v) followed by boiling in a microwave oven. Up to 50μg/ml of ethidium bromide was added to the gel mixture. Once set the gel was submerged in 1xTBE in a Horizon 58 electrophoresis tank and electrophoresed at 100-200V. DNA was visualized on a UV transilluminator at 254nm. To purify DNA fragments, the low melting point (LMP) agarose was used instead and allowed to set in the cold room. DNA was visualized on the UV transilluminator at 365nm to prevent UV damage to DNA.

2.2.1.2 Denaturing polyacrylamide gel electrophoresis

A standard glass-plate sandwich of electrophoresis apparatus was assembled according to the manufacturer's instructions. The 10% separating gel solution was prepared by mixing 5ml 30% acrylamide, 3.75ml Tris-SDS (pH8.8) with 6.25ml H_20 and 50μl 10% (w/v) ammonium persulfate and 10μl TEMED. The gel solution was applied to the sandwich using a Pasteur pipet and covered with a layer of H_2O. After polymerization (30-60min) at room temperature, H_2O was poured off and replaced with the stacking gel containing a mixture of 0.65ml 30% acrylamide, 1.25ml Tris-SDS (pH6.8), 3ml H_2O, 25μl 10% ammomium persulfate and 5μl TEMED. An electrophoresis lane comb was inserted. Once set the gel sandwich was attached to buffer chambers according to manufacturer's instructions. These chambers were filled with 1x SDS electrophoresis running buffer and the gels were run at 10mA of constant current until the tracking dye reached the bottom of the gel.

2.2.2 *Preparation of Total RNA*

Total RNA was prepared from homogenized tissue using TRIzol as instructed by the manufacturer. The concentration of RNA was measured as 40 x A_{260} x dilution factor/1000 (μg/μl). The purity of RNA was checked by A_{260}/A_{280}. RNA samples displaying A_{260}/A_{280} values in the range of 1.7 to 2.0 can be regarded as highly pure. The integrity and size distribution of total RNA was checked by formaldehyde-denaturing agarose gel electrophoresis in MOPS solution and ethidium bromide staining.

2.2.3 *Reverse Transcription (RT)*

A 20μl RT reaction contained the following: 2.6-2.9μg template RNA, 1μl oligo(dT) primer (5' GGAATTCTTTTTTTTTTTTTTTT 3'), 200U AMV reverse transcriptase, 1x first strand buffer, 10mM DTT, 0.5mM dNTPs (dATP, dGTP, dCTP, dTTP) and H_2O. The RNA template and the oligo(dT) primer were denatured together for 10 minutes at 65°C and snap-cooled on ice. This step removed secondary structures from the template enabling template:primer complex formation. The RT reaction was carried out at 42°C for 70 minutes. 1μl of RT product was used as a template for subsequent PCR amplification.

2.2.4 *Polymerase Chain Reaction (PCR)*

A 50μl PCR reaction consisted of the following: 0.5μM primers, 0.2 mM dNTPs (dATP, dGTP, dCTP, dTTP), 1x DNA polymerase buffer, 2.5U DNA polymerase, template DNA and H_2O. The PCR programs follows: *A.* 95°C denaturation 2 minute (1 cycle); 95°C denaturation 30 seconds, T°C annealing 30 seconds, 72°C elongation 2 minutes (30 cycles); 72°C elongation 10 minutes. The annealing temperature was adjusted according to the primers used. PCR with the Pfu DNA polymerase was used in preference to that with the Taq DNA polymerase when PCR required high fidelity amplification and involved amplification of large (>1.5kb) products. For subsequent *in situ* hybridization, flanking T3 and T7 phage polymerase consensus sites were

included at the 5' end of PCR primers and the nested PCR was performed as described previously (McDonald P et al 2000). 15µl of PCR product was run on an ethidium bromide stained 1% agarose gel until sufficient separation of bands was observed. 1kb molecular weight markers were used.

2.2.5 Cloning of DNA

2.2.5.1 DNA digestion/ligation

Plasmid DNA or PCR product was digested using 5-15U of restriction endonuclease in 1x appropriate restriction buffer in a final volume of 10-40µl at 37°C for 2-5 hours. DNA fragments (approximately 50ng) were ligated to vectors (approximately 100ng) using 1-5U of T4 DNA ligase in 1x ligase buffer in a final volume of 10µl at 14°C overnight.

2.2.5.2 Preparation of competent E.coli

For general cloning procedures, the *recA* HB101 strain was used. Transformation-competent cells were prepared by inoculating in 1ml of Luria Broth (LB) a single colony of HB101 and incubating in a rotator at 37°C overnight. 50ml of LB was then inoculated with this 1ml culture and incubated at 37°C in a shaking bed for 2h so that the cells were in the late log phase of proliferation. The culture was centrifuged in the Beckman J2 centrifuge at 7000rpm for 5min and the pellet was resuspended in 20ml of cold 0.1M $CaCl_2$. Cells were kept for 10min on ice and centrifuged again at 7000rpm for 5 min and resuspended in 2ml of cold $CaCl_2$.

2.2.5.3 Transformation

To transform the competent HB101 cells, 200µl of cells were placed in a pre-chilled 1.5ml eppendorf tube on ice. 200-500ng of DNA was added to the cells and kept on ice for 15min. The cells were then heat shocked for 1min at 42°C and kept on ice for a few minutes to recover. The entire content of the tube was then plated on a LB agar

plate and incubated at 37°C overnight.

2.2.5.4 Minipreps

Following transformation, single transformant colonies were picked and used to seed 2ml of LB containing 100μg/ml ampicillin. After overnight incubation at 37 °C, cultures were transferred into 1.5ml eppendorf tubes and centrifuged at 13,000rpm for 1min and the pellet was resuspended in 100μl GTE Lysis buffer. Next 200μl fresh 0.2M NaOH/1%SDS was added followed by 150μl 5M potassium acetate (pH4.8). The tubes were then centrifuged at 13,000rpm for 5min and the supernatant was transferred to fresh eppendorf tubes and washed with 500μl phenol/chloroform/isoamyl alcohol (25:24:1) and centrifuged. The supernatant was precipitated with 1ml ethanol.

2.2.5.5 CsCl density gradient centrifugation

Single colonies of transformants containing the required plasmid were used to inoculate 2ml LB containing 100μg/ml ampicillin and grown for 8h at 37°C. The culture was transferred to 500ml LB containing ampicillin and grown overnight at 37°C with shaking. Cells were pelleted at 6000rpm for 5min and the pellet was resuspended in 12 GTE lysis buffer, followed by 24ml of fresh 0.2M NaOH/1%SDS and 16ml cold 5M potassium acetate. After centrifugation, the supernatant was filtered through gauze and DNA was precipitated with 32ml isopropanol. The pellet was air-dried and resuspended in 2.2ml TE buffer to which 3g CsCl and 100μl ethidium bromide (10mg/ml) were added. The DNA solution was transferred into a 3ml Beckman Quickseal tube, sealed and centrifuged for 4h at 100,000rpm. The plasmid DNA band (formed in the middle of the tube) was removed using a syringe and remixed with 1g CsCl and 1ml TE buffer and re-centrifuged as before. Plasmid DNA was extracted using isopropanol until no ethidium bromide color was observed. Plasmid DNA was then dialyzed against 2L TE at 4°C.

2.2.5.6 *Construction of expression vector*

The full-length cDNA encoding the mouse ENaCβ subunit (20-2318bp, #AF112186) was cloned from mouse kidney cDNA by polymerase chain reaction (PCR) using the high-fidelity *Pfu* DNA polymerase. The expression vector for the EGFP-ENaCβ was generated by cloning the ENaCβ PCR product into the *BglII/SalI* sites of pEGFP-C2. The full-length cDNA encoding the mouse sgk1 (33-1675bp, #AF205855) was cloned from mouse kidney cDNA by PCR using the *Pfu* DNA polymerase. The expression vector for HcRed-sgk1 was generated by cloning the sgk1 PCR product into the *BglII/SalI* sites of HcRed-C1. The coding region of HcRed was replaced with EYFP using *AgeI/BglII* to generate the expression vector EYFP-sgk1. In addition, the region encoding the fusion protein EYFP-sgk1 was digested with *NheI/SalI* and subcloned into the vector pTRE2hyg to generate the expression vector TRE-EYFP-sgk1 for the usage in the tetracycline inducible system. The cloned ENaCβ subunit and sgk1 inserts in the initial plasmids were sequenced fully confirming the absence of any PCR mutation errors.

2.2.6 *Cell Culture*

Mouse cortical collecting duct M-1 cells were grown at 37°C in a modified DMEM/F-12 (1:1) supplemented with 100 U/ml penicillin, 100 mg/ml streptomycin, and 10% fetal bovine serum (FBS: stripped twice with charcoal to remove endogenous steroids) in a humidified incubator gassed with 5% CO_2. For experiments with unpolarized M-1 cells, the cells were sparsely seeded onto glass coverslips and incubated overnight (i.e., 16-18 h). For experiments with polarized M-1 cells, the cells were cultured on 6.5-mm diameter, 0.4-μm pore size Transwell polycarbonate filters (Corning Costa #3470) for at least 10 days to achieve high transepithelial resistance (>1,000 $\Omega \cdot cm^2$). Potential difference and transepithelial resistance were measured with Millicell-ERS.

2.2.7 Transfection

Cells were seeded on 60mm dishes at the density of $5x10^5$ cells/ml 24h before transfection. All solutions used were equilibrated to room temperature prior to use. For each construct, 300µl solution was set up containing 37µl 2M $CaCl_2$, 5µg DNA and mixed with 300µl 2x HEPES-buffered saline with slow agitation and incubated at room temperature for 20min. After brief vortexing, the DNA solution was added slowly to the dishes of cells with agitation. 24h after transfection the medium in the dish was changed and replaced with 3ml fresh medium.

2.2.8 Making of Stable Cell Lines

2.2.8.1 Titrating G418, Hygromycin, and Puromycin (Killing Curves)

Prior to using G418, hygromycin or puromycin to establish stable and double-stable cell lines, it is important to titrate your selection agent stocks to determine the optimal concentration for selection with the particular host cell line being tested. Around 2 x 10^5 cells were plated in each of six 10-cm tissue culture dishes containing 10 ml of the appropriate complete medium plus varying amounts (0, 50, 100, 200, 400, 800 µg/ml) of hygromycin or G418. Cells were incubated for 10–14 days, replacing the selective medium every four days. For selecting stable transformants, the lowest concentration of drug is used that begins to give massive cell death in ~5 days and kills all the cells within two weeks.

2.2.8.2 Transfection and selection of stable cell lines

Cells were transfected with EGFP-ENaCβ construct at the density of $5x10^5$ cells/ml. 48 h after transfection, cells were trypsinized and seeded to medium in 10 plates containing 500µg/ml G418. After 2-4 weeks, isolated colonies began to appear. Large and healthy colonies were selected using the cloning cylinders and transferred to individual wells in a 24-well plate. 30-50 individual clones were screened for expression of EGFP-ENaCβ.

2.2.8.3 *Making of the tetracycline inducible cell lines*

The making of tetracycline inducible cell lines involved two rounds of transfection and selection of stable clones. On the first round, M-1 cells were seeded onto plastic Petri dishes and grown to 20% confluence. The CaPO4 method was used to transfect the construct pTet-Off. After transfection, the cells were grown in the presence of a toxic concentration of puromycin (1μg/ml), resistance to which is encoded by the pTet-Off vector. When individual clones had grown to colonies of 100–200 cells, they were isolated using cloning cylinders. The next step was to perform transient transfection assays with TRE-EYFP-sgk1 to identify clones that showed high transcription induction level. Cells of each clone were split into 2 single well of a 6-well plate and transfected with 2μg TRE-EYFP-sgk1 as before. Tetracycline (1μg/ml) was added to one of the two wells and incubated for 24 hr. +/–EYFP-sgk1 expression was screened for by fluorescence microscopy. The clones with the highest fold-induction (highest expression with lowest background, >20 fold) were selected for propagation (named *Tet* cell line). The next step was to transfect the stable Tet cell line with the TRE-EYFP-sgk1 construct. The goal was to generate a cell line that gave low background and high expression of EYFP-sgk1. Cells were transfected with the construct TRE-EYFP-sgk1 and grown in the appropriate complete medium, 1μg/ml tetracycline and 300μg/ml hygromycin (resistance to which is encoded by the pTRE2hyg vector). After 2-4 weeks, hygromycin resistant clones started to appear. Large and healthy clones were selected and tested for the expression and induction of EYFP-sgk1.

2.2.9 *Western Blot Analysis*

M-1 cell homogenates were prepared from confluent cell monolayers and pelleted by centrifugation (1,000 *g*). The pellet was solubilized in the sodium dodecyl sulfate (SDS) lysis buffer. The homogenate was centrifuged in a microcentrifuge and its supernatant was separated by 8% polyacrylamide gel electrophoresis. After electrophoresis, the separated proteins were electrophoretically transferred to a polyvinylidene difluoride (PVDF)-blotting membrane and the membrane was blocked

with 5% milk to prevent nonspecific binding and probed with an anti-GFP antibody (1:1,000 dilution), followed by binding of a secondary goat anti-mouse horseradish peroxidase IgG (1:5,000 dilution). The specific binding was detected using a peroxidase-based chemiluminescent detection method (ECL) according to the manufacturer's instructions.

2.2.10 Fluorescence Activated Cell Scanning (FACS)

For each M-1 cell population, 1,000 cells were subjected to FACS analysis to quantify their fluorescence intensity at the EG(Y)FP emission wavelength band <560nm (known as FL-1 or green channel) *vs* that at 560-640nm (known as FL-2 or red channel) as an index of non-specific emission. Data analysis was carried out using the CELLQuest software.

2.2.11 Staining of Cell Organelles and Plasma Membrane

Endoplasmic reticulum was labeled for 10 min at room temperature with the rhodamine-B hexyl ester (Molecular Porbes #R648) at 0.5μg/ml; mitochondrion with MitoTracker (#M22426) at 2μM; Golgi apparatus with an anti-GM130 antibody [a mouse anti-GM130 antibody from Dr Rory Duncan detected with an AlexFluor 660 tagged goat anti-mouse secondary antibody (#A21054)]; and endosomes with AlexFluor 630-transferrin (#T23362) at 10μM. Previous studies show at high concentrations (0.5-1μg/ml) the rhodamine-B hexyl ester specifically stains the endoplasmic reticulum of fixed cells (Terasaki and Reese 1992; Yang L et al. 1997). The apical membranes were labeled on ice with rhodamine-conjugated wheat germ agglutinin (WGA, #W849) at 2μg/ml. The Transwell filters or coverslips bearing the stained M-1 cells were then mounted onto a microscopic slide for visualization.

2.2.12 Fluorescence Microscopy.

Conventional fluorescence images were captured by a CCD camera attached to a Zeiss 210 Axio-epifluorescence microscope using the fluorescein isothiocyanate

(FITC) filter set and a 100x Plan-Neofluar objective (Numerical Aperture NA 1.4 oil). Laser scanning confocal microscopy (LSCM) was performed with the Zeiss 510 confocal imaging system equipped with a Plan-Neofluar 40x (NA 1.3 oil) objective and the rhodamine and FITC filter sets. For the dual imaging of EGFP and rhodamine, fluorescent images were collected by exciting the fluorophores at 488 nm (EGFP) and 543 nm (rhodamine) with argon and HeNe lasers respectively. Emissions from EGFP and rhodamine were detected with the band-pass FITC filter set of 500-550 nm and the long-pass rhodamine filter set of 560nm, respectively. A sequential scanning program was used to collect *z*-optical sections (i.e. in the transverse plane) at 0.16 μm intervals. An overlay of collected 2D images at each depth was performed to allow a *z* dimension stack yielding a 3D reconstruction then sectionable in alternative planes (Zeiss LSM Image Browser version 3.1). Reconstructed images oriented with coordinates (*xy* 0°, *yz* 0°, *xz* 90°) were used to visualize the epithelial monolayer in sagittal section.

2.2.13 Animal Treatments

The animal work was conducted at the local animal biomedical research unit by staff holding appropriate small animal handling personal license (including June Noble, Dr Helen Speirs, Dr Chris Kenyon and others) and was approved by the local ethical committee being in accordance with the UK Home Office Animal Act 1986 under existing project license held by Prof JR Seckl. I have only assisted these personnel in procedures that do not require any license. Eight-week-old male C57BL/6J mice (23.5 to 25 g) were segregated into ten groups (each n=6) and caged in pairs within their own group (Table 3.1). All mice had free access to normal diet (0.3% sodium) and water (with saline additionally available to adrenalectomized mice). The bilateral adrenalectomy operations were performed under gaseous anesthesia. Animals were sacrificed by terminal anesthesia. ALZET 1007D osmotic mini-pumps (preloaded with treatments or vehicle) were implanted subcutaneously in groups of mice having aldosterone infusions with various doses (50μg/kg per d, 150μg/kg per d, and 750μg/kg per d) for 6 or 21 d. To investigate the acute effects of aldosterone, injections of 150μg/kg aldosterone were given to mice 3 h before sacrifice.

Additionally, one group of mice was kept on 0.03% low sodium diet for 6 d inducing a degree of secondary hyperaldosteronism.

2.2.14 Plasma Aldosterone Assay

Experiments performed by others yielded mouse blood samples that were taken by cardiac puncture rapidly after initiation of terminal anesthesia. Samples were then centrifuged at 4°C for 10 min. Plasma was separated and stored at -20°C. Aldosterone was assayed using a ^{125}I-RIA kit according to the manufacturer's instructions. The polypropylene tubes coated with antibodies to aldosterone were filled with 200μl calibrators (containing a series of known amounts of aldosterone) or 200μl samples, followed by adding 1ml aldosterone labeled with ^{125}I and incubation at room temperature for 18 hours. The tubes were then decanted thoroughly and counted to reveal ^{125}I irradiation in a gamma counter. A single calibration curve provides the basis for determining aldosterone concentrations in the samples.

2.2.15 In Situ Hybridization

On the basis of the nucleotide sequence of a gene, primers were designed to amplify a fragment encompassing a region (normally 150-500nt long) that had no significant homology to other sequences. Flanking T3 and T7 phage polymerase consensus sites were introduced by nested PCR as described previously (McDonald P et al 2000). Single-stranded [^{35}S]UTP-labeled RNA probes were generated using the required RNA phage polymerases (T7 for antisense and T3 for sense probes). For each mouse, sagittal cryostat sections (10 μm) were cut from intact kidney, which included cortex and outer and inner medulla. Sections were thaw-mounted onto 3-amino propyltriethoxysilane-coated slides and stored at -80°C. 4% paraformaldehyde was used for fixation, followed by acetylation and prehybridization at 50°C for 2 h. Hybridization with 4×10^6 c.p.m [^{35}S]UTP-labeled RNA probe per slide was performed at 50°C for 14 to 16 h and then followed by RNaseA treatment and washes with a maximum stringency of 0.1xSSC at 60°C. This follows well-established methodology that reflects findings that show that these conditions create the high

subsaturation/saturation riboprobe concentrations that provide specific radiolabeled probe hybridization that reflects the amount of target RNA present. When quantitatively detected (films with co-exposed microscale calibration standards, dipped emulsion autoradiography and image analysis) this then allows relative quantitation for gene expression between slides processed together. After washes, slides were dehydrated and placed against β-Max Hyperfilms. Three to five days of exposure gave a satisfactory range of autoradiographs in the linear range of the films as judged by coincident exposure of the film to radioactive microscale standards for this purpose (calibrated for moderate β-emitters [^{14}C, ^{35}S] in thin tissue slices; Amersham International #RPA504, RPA511). All slides were then dipped in photographic emulsion and exposed in a light tight box for 2 to 3 wk before being developed. This optimal time was determined by the optimal exposure for the film autoradiographs. In preliminary work, we emulsion-dipped slides with attached microscales (such as above) and found a wide linear range (correlation, r=0.98), relating grain-count density *versus* radioactivity. For all the dipped slides, grain-count densities did not exceed this linear range. Selected sections were then counterstained with the periodic acid-Schiff (PAS) method. The sample slides were first treated with KOH solution (0.5% KOH in 70% aqueous ethanol) for 20 mins, followed by treatment in 1% periodic acid (aqueous) for 5mins and in the Schiff solution (Sigma #S5133) for 10mins.

2.2.16 Quantitative Image Analysis

Autoradiographic films were scanned on a high-resolution flatbed scanner. Developed emulsion-dipped slides were analyzed on a Zeiss Axioskop Microscope with the KS300 (v3) silver-grain counting software. Steps to minimize background tissue hybridization included the employment of a postfixing acetylation procedure to block the positively charged ammonium groups on tissue and a posthybridization RNase A treatment to cleave unhybridized single-stranded RNA molecules. Thus, the tissue background for antisense probes was considered as the nonspecific binding to tissue RNA by probes with equal GC percentage, and so equal to the hybridization level on sense control sections. When silver grains were counted in high magnification fields,

the tissue background was normalized for each slide as follows. The background grain density of tissue and glass on the sense control slide were measured separately. The ratio between such paired background measurements was calculated for the slide. The tissue background for an antisense slide was thus estimated by multiplying its glass background by this ratio. Quantification was done by counting the number of silver grains over areas under high-power magnification (×400) using automated image analysis software (Zeiss KS 300) calibrated to accurately count silver grains over a wide range of grain densities).

2.2.17 Statistical Analyses

The *Statistica* software package (v5) was used to analyze data. For experiments involving multiple groups, the significance of differences between groups was tested by ANOVA. When the all-effects F value was significant ($P < 0.05$), *post hoc* analysis of differences between individual groups was made with the Neuman-Keuls test. For graphical presentation, values were expressed as mean ± SE (standard error). For two-variable correlation studies (involving generation of standard curves), the linear regression analysis was performed to fit a line in a two-variable space defined by the equation $Y=a+b*X$, so that the squared deviations of the observed points from this line are minimized (*least squares estimation*).

CHAPTER 3

SGK1 GENE EXPRESSION IN KIDNEY AND ITS REGULATION BY ALDOSTERONE: SPATIO-TEMPORAL HETEROGENEITY AND QUANTITATIVE ANALYSIS

3.1 Summary

The serine-threonine kinase sgk1 was recently identified as a gene rapidly induced by mineralocorticoids, resulting in increased sodium transport *in vitro*. To carefully localize and quantify the renal sgk1 expression response to aldosterone, I have performed *in situ* hybridization on kidneys of mice having aldosterone excess over a range of doses and durations. In control and adrenalectomized animals, the glomeruli and inner medullary collecting ducts are the major sites of sgk1 expression, which is maintained independent of aldosterone. Sgk1 upregulation induced by aldosterone excess exhibits spatial-temporal heterogeneity. Both acute (3 hours) and chronic (6 days) aldosterone excess stimulates sgk1 expression in the distal nephron, i.e. from the distal convoluted tubules through to the outer medullary collecting ducts. Treatments for 6 days with low sodium diet [0.03% (I)] and aldosterone infusions [50μg/kg/day (II), 150μg/kg/day (III) and 750μg/kg/day (IV)] have generated elevation of circulating aldosterone. Across these treatments (I-IV), the circulating aldosterone level correlates with the progressive induction of sgk1 expression, with highly stimulated tubules first appearing in cortex (I) and continuing downward (II) until there was a strong stimulation throughout outer medulla (III-IV). Interestingly, chronic but not acute aldosterone excess causes a slight increase of sgk1 expression in glomerulus (30%-50%, $p<0.01$), and a dramatic down-regulation in the initial portion of inner medulla, which could result from diminished interstitial osmolarity. Relative quantification (*vs* control) of sgk1 upregulation in individual tubules reveals: (1) a 1.8-fold increase of sgk1 mRNA at 3 hours (150μg/kg injection); (2) a dose-dependence of chronic upregulation reaching a ceiling of 8-fold elevation.

3.2 Introduction

Regulation of sodium reabsorption in the kidney is crucial for maintenance of whole body fluid homeostasis. The Na^+ transport induced by aldosterone, either *in vivo* or *in vitro*, is sensitive to the K^+-sparing diuretic amiloride, which is a potent blocker of the epithelial Na^+ channel (ENaC) (Rossier BC 1997; Horisberger JD 1998). The major site of aldosterone action is in the distal nephron from late distal convoluted tubules (DCT) through to cortical collecting ducts (CCD) and outer medullary collecting ducts (oMCD) (Doucet A et al. 1981; Farman N 1992). Two phases are distinguished in regulation by aldosterone of sodium transport: an early phase starting after a lag period of 20 to 60 minutes, during which the pre-existing channels and Na^+/K^+-ATPase pumps are activated, and a late phase (>2.5 hours), which involves increasing contribution from newly synthesized channel and pump proteins (Verrey F 2000).

In the A6 *Xenopus* cell line, which is a good model of mammalian distal nephron, efforts have been made to elucidate the pathway of aldosterone action, leading to the finding of an early-response gene, sgk1 (serum/glucocorticoid kinase), the transcription of which is rapidly (<3 hours) stimulated by aldosterone excess (Chen SY et al. 1999). Intriguingly, sgk1 was shown to significantly elevate ENaC-mediated sodium transport via increasing the surface expression of ENaC subunits in *Xenopus* oocytes (Alvarez de la Rosa D et al. 1999), which is in keeping with evidence suggesting sgk1 may facilitate a similar increased apical translocation of ENaC in distal nephron *in vivo* (Loffing J et al. 2000, 2001; Masilamani S et al. 1999). Other stimuli such as insulin, glucocorticoids and cell volume change were documented to regulate sgk1 (Perrotti N et al. 2001; Wang J et al. 2001; Webster MK et al. 1993a; Waldegger S et al. 1997). These *in vitro* findings identify sgk1 as a key gene in hormonal regulation of sodium transport in cells of distal nephron. It thus becomes of great interest to determine the distribution of sgk1 in intact kidney and study its hormonal regulation *in vivo*.

Previous animal studies have focused on the short-term (0.5hr-4hr) effect of aldosterone on sgk1 expression (Chen SY et al. 1999; Brennan FE and Fuller PJ 2000;

Bhargava A et al. 2001). Here I aim to elucidate, firstly, whether regulation of sgk1 expression is consistent with its playing a role in transduction of aldosterone-driven sodium reabsorption in distal nephron in both short term (acute) and chronic hyperaldosteronism. Secondly, I look for evidence of other potential regulators of and roles for sgk1 in kidney. In particular, sgk1 expression may exhibit an aldosterone dose dependence in such a way that a plateau or a peak occurs at a dose beyond which there is no further induction or even a fall off in the degree of sgk1 induction. This would be of particular interest as it may identify a response moderating aldosterone-sgk1 driven sodium retention and imply that 'escape' from aldosterone-induced Na retention is contributed to by such a mechanism (i.e. the reaching of the ceiling of sgk1 expression translates to the peaking of sodium reabsorption induced by sgk1 and its related pathway). Finally, these detailed studies on a wide range of aldosterone-related treatments will allow a clearer view of sgk1 expression and regulation along the nephron and will help to guide future studies. To address these issues, I performed *in situ* hybridization using radiolabelled riboprobes, autoradiographic films and silver grain counting, which are well established as means of relative quantitation of expression level (Wilkinson DG 1998). This approach allows comparison of sgk1 mRNA expression levels in renal regions and nephron segments.

3.3 Methods

(The materials and common molecular biology methods are described in CHAPTER 2)

3.3.1 Animal Treatments

The animal work was conducted at the local animal biomedical research unit by staff holding appropriate small animal handling personal license (including June Noble, Dr Helen Speirs, Dr Chris Kenyon and others) and was approved by the local ethical committee being in accordance with the UK Home Office Animal Act 1986 under existing project license held by Prof JR Seckl. I have only assisted these personnel in procedures that do not require any license. Eight-week-old male C57BL/6J mice (23.5 to 25 g) were segregated into ten groups (each n=6) and caged in pairs within their own group (Table 3.1). All mice had free access to normal diet (0.3% sodium) and

water (with saline additionally available to adrenalectomized mice). The bilateral adrenalectomy operations were performed under gaseous anesthesia. Animals were sacrificed by terminal anesthesia. ALZET 1007D osmotic mini-pumps (preloaded with treatments or vehicle) were implanted subcutaneously in groups of mice having aldosterone infusions with various doses (50μg/kg per d, 150μg/kg per d, and 750μg/kg per d) for 6 or 21 d. To investigate the acute effects of aldosterone, injections of 150μg/kg aldosterone were given to mice 3 h before sacrifice. Additionally, one group of mice was kept on 0.03% low sodium diet for 6 d inducing a degree of secondary hyperaldosteronism. Table 3.1 gives details of these groups.

3.3.2 Quantitative Image Analyses

In situ hybridization was performed upon sections (10μm) of mouse kidney using single-stranded antisense [^{35}S]-UTP labeled RNA probes that encompassed a region of sgk1 cDNA sequence (spanning base pairs 1091-1336, #AF205855) showing no significant homology to other known sequences. Autoradiographic films were scanned on a high-resolution flatbed scanner. Developed emulsion-dipped slides were analyzed on a Zeiss Axioskop Microscope (Carl Zeiss) with the KS300 (v3) silver-grain counting software. Steps to minimize background tissue hybridization included the employment of a post-fixing acetylation procedure to block the positively charged ammonium groups on the tissue surface and a post-hybridization RNase A treatment to cleave unhybridized single-stranded RNA molecules. Thus, with use of these methods the tissue background for antisense probes was low and considered as nonspecific binding being no greater than the hybridization level on sense control sections. When silver grains were counted in high magnification fields, the tissue background was normalized for each slide as follows. The background grain density of tissue and glass on the sense control slide were measured separately. The ratio between such paired background measurements was calculated for the slide. The tissue background for an antisense slide was thus estimated by multiplying its glass background by this ratio. Quantification was done by counting the number of silver grains over areas under high-power magnification (×400). Grain-counting involved determining the grain density over glomeruli and tubules that highly expressed sgk1.

Table 3.1. Experimental groups

Group name	Group description	Infusion methods	Drug-delivery rate	Lasting time
Adx	Adrenalectomy	Vehicle[a] mini-pump	-	6 days
Con	Control	Vehicle mini-pump	-	6 days
Aldo50	Aldosterone	Aldosterone/Vehicle Mini-pump	50ug/kg per day	6 days
Aldo150	Aldosterone	Aldosterone/Vehicle Mini-pump	150ug/kg per day	6 days
Aldo750	Aldosterone	Aldosterone/Vehicle Mini-pump	750ug/kg per day	6 days
Aldo21d	Aldosterone	Aldosterone/Vehicle Mini-pump	150ug/kg per day	21 days
ConInj	Control	Saline injection	-	3 hours
AldoInj	Aldosterone	Aldosterone injection	150 ug/kg	3 hours
Spiron	Aldosterone & pre-treatment with Spironolactone	Aldosterone injection & pre-treatment with Spironolactone/Vehicle mini-pump	150ug/kg aldosterone/ 20mg/kg per day spironolactone	3 hours of aldosterone & 6 days of spironolactone
LowSalt	0.03% sodium diet	Vehicle mini-pump	-	6 days

[a] vehicle: 0.9% saline, 2% (v/v) ethanol

Identification of glomeruli was straightforward for all groups. Identification of tubules in both cortex and outer medulla involved comparing highly expressing tubules in animals with aldosterone excess and those in controls, where tubular expression merged with "background" levels. Although there was some variation across non-glomerular cortex (mean ± SE grain density, 0.0869 ± 0.0106 counts/μm^2), this did not clearly correspond to tubule outlines and was present over a wider cortical area in control and treatment groups than the highly expressing tubules readily identifiable in treatment groups. The best valid solution to estimate control tubular grain counts was to measure this grain density over a larger area, (full-field [×400] view of medulla or non-glomerular cortex) rather than individual tubules. This control expression level was used for comparison with animals with aldosterone excess. I followed a protocol for random selection of regions, glomeruli, and tubules, which involved aligning the field of view over renal cortex at such low power that the viewer was unable to see local renal structure or grain density. The view was then zoomed to ×100 to ×200, and glomeruli or tubules in the central field of view were those designated to be subjected to grain counting at ×400. The process was repeated, counting ten glomeruli or tubules (with grain-density elevated allowing them to be demarcated against background) out of eight sampled fields in each region (for cortex and medullary regions separately). Sampling cortical or medullary regions was carried out in the same fashion for each kidney section. When it came to control sections, five full-field (×400) views were counted (minus glomeruli in cortex, five rather than eight because of their larger area). Rarely, part of the section with poor morphology was excluded from subsequent statistical analyses. For each mouse, the mean density of each such renal component assessed (glomeruli and cortical and medullary tubules or areas) was then calculated.

3.4 Results

3.4.1 Renal expression profile of sgk1

Examination of control and adrenalectomized animals revealed that sgk1 mRNA had a discrete distribution in kidney, with a punctate appearance in cortex, little expression

in outer medulla and high abundance in inner medulla (Figure 3.1A). This expression profile was not dependent on circulating corticosteroids, as it was maintained in adrenalectomized animals (aldosterone <400±<100pmol/l, corticosterone <55nmol/l). The cortical expression of sgk1 was primarily confined to glomeruli (Figure 3.1B). Its expression in glomeruli was uniform and centrally distributed (Figure 3.1E), so ruling out the possibility that the glomerular visceral or parietal epithelium was the expression site. This is consistent with the data from human kidney (Lang F et al. 2000), suggesting sgk1 expression in the glomerular mesangium. In inner medulla, as the papilla was approached, nearly all tubular cells strongly expressed sgk1 (Figure 3.1C-D). This characteristic indicates the inner medullary collecting ducts to be the expression location, because the number of thin limbs of Henle's loop diminishes towards the papilla.

3.4.2 Chronic effects of aldosterone and dosage response

A range of 6-day treatments with sodium depletion [(I) 0.03% sodium diet] and aldosterone infusions [(II-IV) 50μg/kg/day, 150μg/kg/day and 750μg/kg/day] resulted in sustained elevation of circulating aldosterone levels: (I) 1234±124pmol/l, (II) 4660±120pmol/l, (III) 15485±471pmol/l and (IV) 53569±3198pmol/l. In view of the fact that severe sodium deficiency has been reported to increase aldosterone secretion 20-25 fold in sheep or human (Laragh JH et al. 1960; Mills JN 1962), the two higher-dose infusions (III-IV) mimicked these physiologically extreme conditions of aldosterone excess (25-fold and 75-fold elevation of plasma level *vs* 699±56pmol/l of controls). Correlated with the elevation of circulating aldosterone across these animal groups, there was a change in the pattern of sgk1 expression, with highly stimulated tubules first appearing in cortex (I, Figure 3.2-A and a) and continuing distally along the nephron (II, Figure 3.2-B, b and c) until there was a strong stimulation throughout outer medulla (III-IV, Figure 3.2-C and d). Silver-grain counting of individual tubules showed a dose-dependent upregulation of sgk1 in both cortex and outer medulla (Figure 3.3). The mild excess of aldosterone in sodium-depleted animals (I) induced a 4.7-fold increase of sgk1 expression (compared to that in kidneys of untreated control mice), which was confined to cortical tubules. Such cortical induction reached the

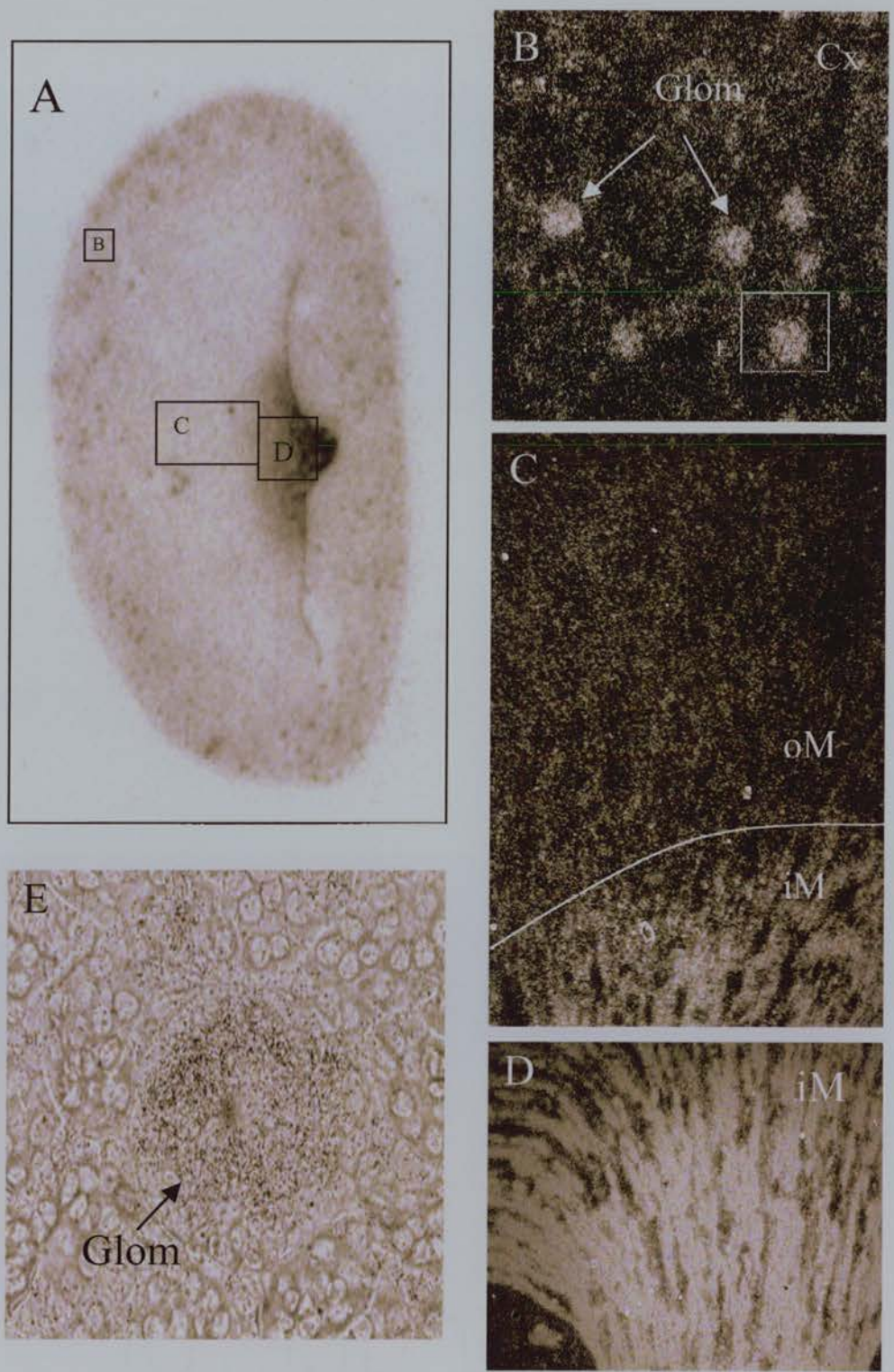

Figure 3.1. Sgk1 expression profile in kidney. Autoradiograph (A: expression black) and photomicrographs (B through D: dark-field, expression white; E: bright-field, expression visible silver grains) showing sgk1 expression in detail in the kidney of a normal (control) mouse. The boxes in the autoradiograph in panel A show the sites of capture of the photomicrographs on the corresponding kidney section slide (B: x100, cortex; C and D: x50, medulla). A single glomerulus was visualized in panel E at 400 magnification. Note the abundant expression in glomeruli and inner medulla. Glom, glomerulus; Cx, cortex; oM, outer medulla; iM, inner medulla.

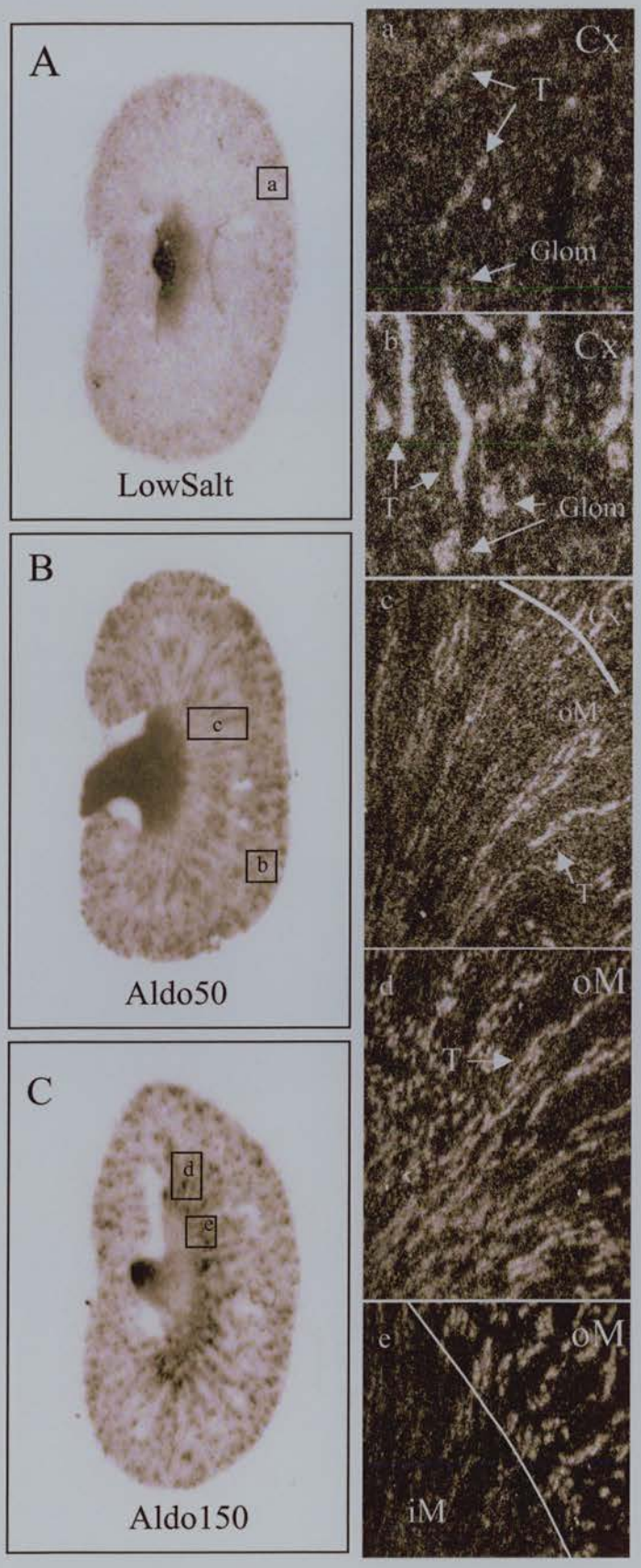

Figure 3.2. Chronic effects of aldosterone on sgk1 expression. Autoradiographs (A through C: expression black) and photomicrographs (a through e: dark-field, expression white) showing sgk1 expression in kidneys of animals treated with aldosterone excess (Magnifications: 100 in a and b; 50 in c through e). The sites of capture of the photomicrographs on the kidney sections are indicated on the corresponding autoradiographs. Note the highly stimulated tubules traversing from cortex to outer medulla. T, stimulated tubules.

ceiling (8-fold) in animals infused with aldosterone (II-IV). In outer medulla, sgk1 stimulation (6.4-fold) was first observed in animals with moderate aldosterone excess (II). The ceiling of 8-fold increase was reached at groups with more severe aldosterone excess (III-IV). Moreover, in animals treated with 150μg/kg aldosterone for 21 days, sgk1 stimulation persisted and its pattern and extent remained similar to that at 6 days (Figure 3.3). Finally, water intake of animals was substantially increased by the high-dose aldosterone infusions (2-fold in the 150μg/kg/day groups and 3-fold in the 750μg/kg/day group *vs* control).

3.4.3 Acute effects of aldosterone

In mice injected with 150μg/kg aldosterone 3 hours before sacrifice, highly stimulated tubules were visualized in cortex and outer medulla (Figure 3.4). The rapid sgk1 induction caused by injection was completely abolished in animals pre-treated with spironolactone (MR antagonist) (Figure 3.4), suggesting mediation via mineralocorticoid receptors (MR). Silver-grain counting to examine the acute effects of aldosterone revealed a 1.8-fold upregulation of sgk1 in cortical tubules and 1.4-fold in outer medullary tubules, lower than that elicited by the chronic treatments, eg 6 days and 21 days (Figure 3.5). Nevertheless I cannot rule out the possibility that a peak of sgk1 stimulation may have occurred before 3 hours, considering the short half-life of circulating aldosterone (20 minutes) (Tait JF et al. 1961) and sgk1 mRNA (30 minutes) (Webster MK et al. 1993b). Furthermore, other studies showed that sgk1 stimulation peaked in rat kidney within 1-2 hours following aldosterone injection (Brennan FE and Fuller PJ 2000; Bhargava A et al. 2001).

3.4.4 Aldosterone induction of sgk1 expression is in distal nephron

Examination of emulsion-dipped slides revealed both acute and chronic aldosterone treatments induced sgk1 expression in a minority of cortical tubules. The Periodic Acid Schiff counterstaining method stains the brush border of proximal tubules with pink colour. Sgk1 stimulation was visualized in tubules lacking this border (Figure 3.6, A-B and D-E), indicative of more distal tubules, which in cortex were distributed

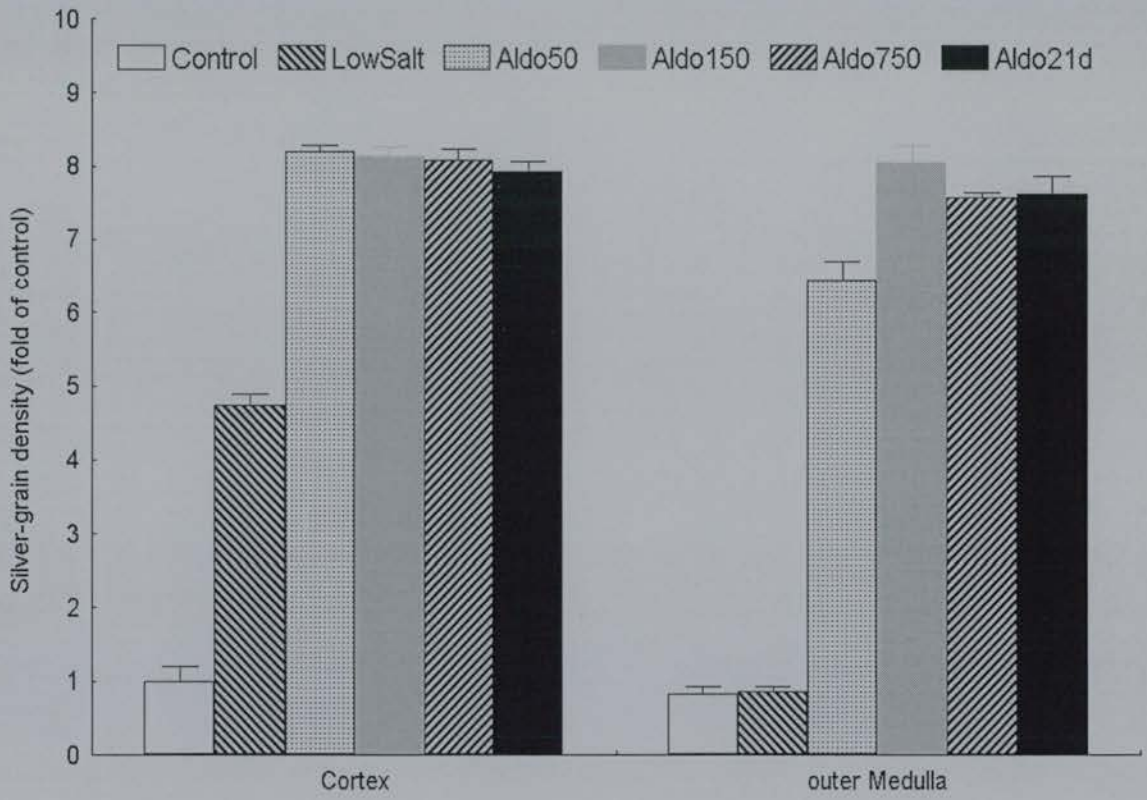

Figure 3.3. Quantification of sgk1 expression in response to chronic aldosterone excess. Mice were treated for 6 d with sodium depletion, low-dose (50μg/kg) and high-dose (150 to 750μg/kg) aldosterone infusions or for 21 d with 150μg/kg infusion. Sodium depletion induced a 4.7-fold increase of sgk1 mRNA level in cortical tubules ($P<0.01$ *versus* control). The 50μg/kg infusion stimulated sgk1 by 8.2-fold in cortex and 6.4-fold in outer medulla. Sgk1 stimulation by high-dose infusions for 6 or 21 d reached a ceiling of upregulation (eightfold elevation) in cortex and outer medulla. The mean grain density in cortical tubules of control animals was designated as one unit.

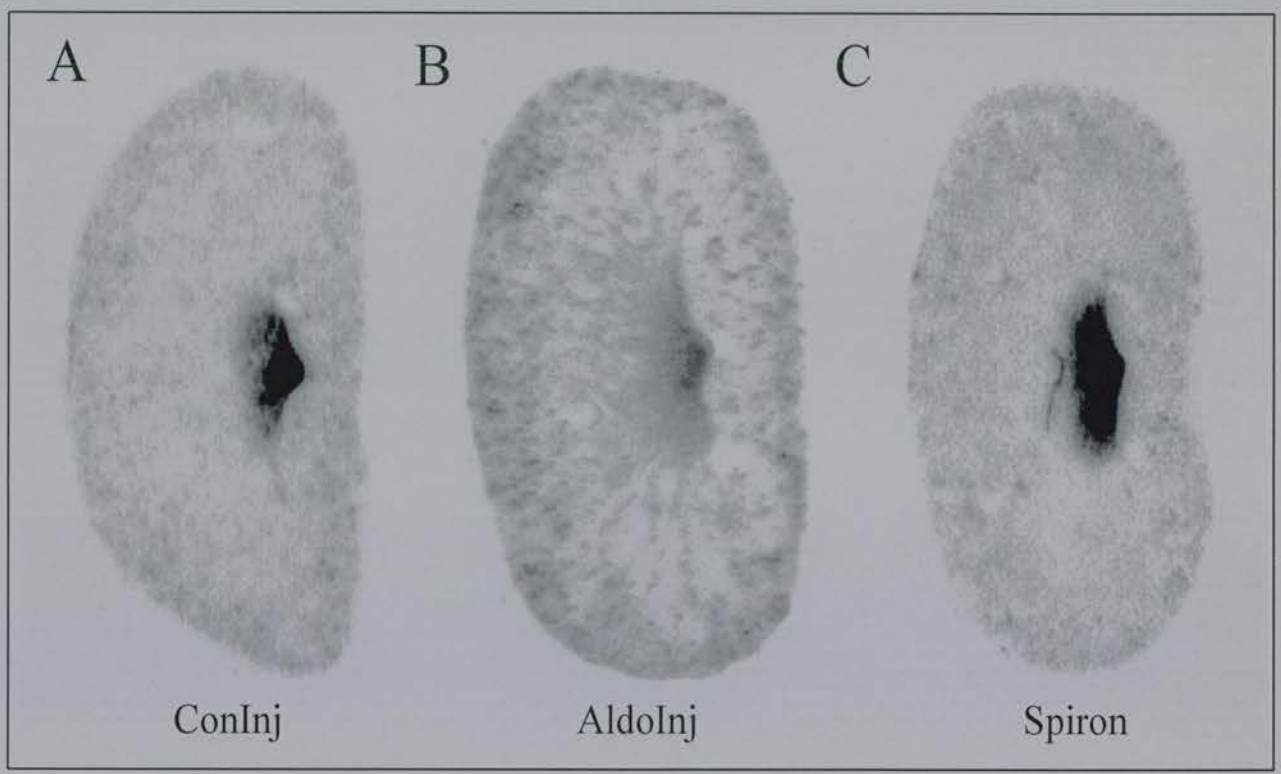

Figure 3.4. Acute effects of aldosterone on sgk1 expression. Autoradiographs (expression black) showing comparison of sgk1 expression among control (A), animals injected with 150μg/kg aldosterone 3 h before sacrifice (B), and those pretreated with spironolactone (MR antagonist) (C).

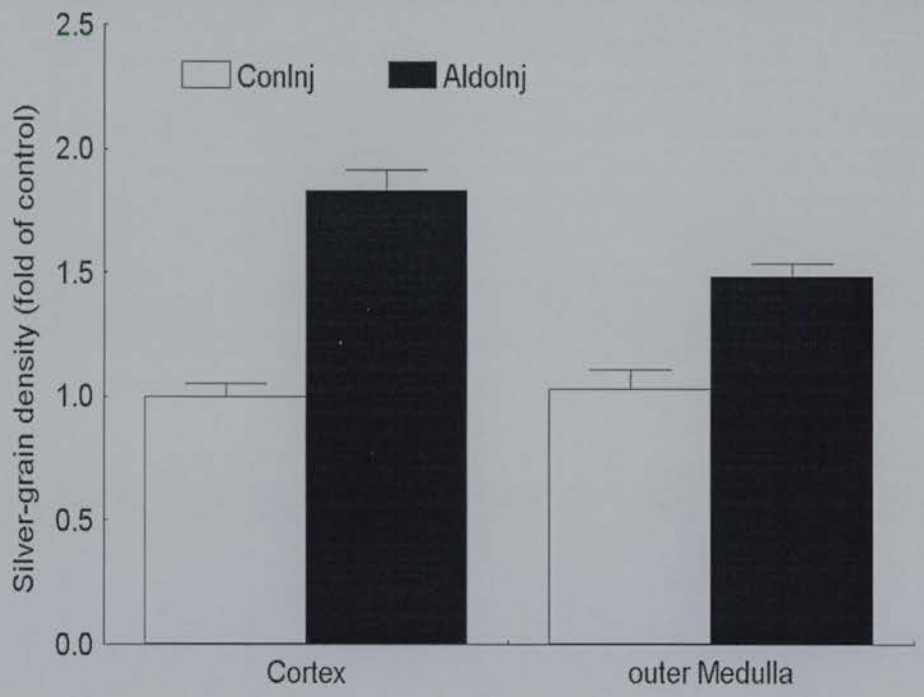

Figure 3.5. Quantification of sgk1 expression in response to acute aldosterone excess. Aldosterone-induced upregulation of sgk1 mRNA by 1.8-fold in cortex and 1.4-fold in outer medulla ($P<0.01$ *versus* control). The mean grain density in cortical tubules of control animals was designated as one unit.

widely across cortical labyrinths as well as in cortical medullary rays; in fact from distal convoluted tubules (DCT) to cortical collecting ducts (CCD). Moreover, tubules at the glomerular vascular pole exhibited sgk1 induction (Figure 3.6, C and F), suggesting involvement of the early portion of DCT. However to characterize the DCT distribution definitively would require additional studies. Sgk1 stimulation could be seen in long single tubules extending in continuity from cortex through outer medulla to enter inner medulla without a major change in diameter (Figure 3.2, c-e). This pattern was fully consistent with the cortical and outer medullary collecting ducts being sites of upregulation of sgk1 expression.

3.4.5 Distinct regulation by aldosterone in glomeruli and inner medullary collecting ducts

It was somewhat unanticipated that sgk1 mRNA abundance was raised (30-50%) by chronic (50μg/kg/day) but not acute aldosterone excess in glomeruli (Figure 3.7), a site not regarded as a classical MR responsive target. A similar upregulation was also detected in animals with higher doses of aldosterone infusion but not in those with sodium depletion. *Interestingly*, the abundant sgk1 expression in inner medulla was downregulated in its initial portion by chronic and severe aldosterone excess (150 or 750μg/kg/day for 6 or 21 days). The degree of this effect showed some individual variation within treatment groups and was more striking at 21 days. As illustrated in Figure 3.2 C and e, the outer-inner medulla junction was easy to identify on the autoradiograph, where the outer medullary collecting ducts with high sgk1 expression were adjoining the inner medulla with much repressed expression.

3.5 Discussion

The expression of sgk1 mRNA and its regulation by aldosterone were studied in detail. In kidney of control mice, I found an abundant expression of sgk1 in glomeruli and inner medullary collecting ducts, which was substantially maintained independent of corticosteroids and thus persisted in adrenalectomized animals. Both acute and chronic aldosterone infusions induced sgk1 expression in distal tubules through to

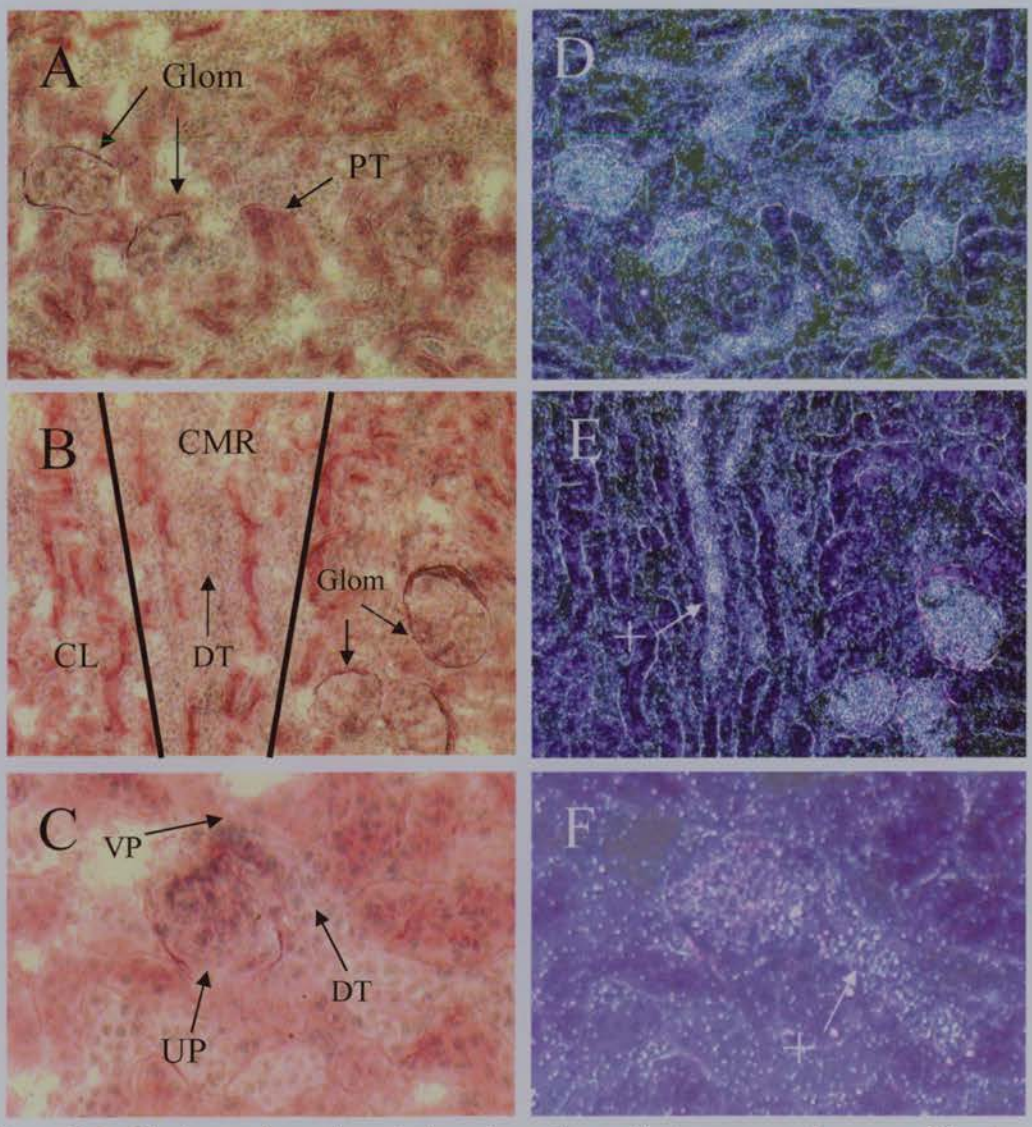

Figure 3.6. Histology of renal cortical sections from aldosterone-treated groups. The images (magnification, 100) of panels A through C were taken by phase-contrast microscopy, and D through F are their respective counterparts under dark-field view. The cortical labyrinth (CL) is illustrated on panel A. Panel B shows a region where a cortical medullary ray (CMR) protrudes into cortical labyrinth. Periodic acid-Schiff (PAS) stains the brush border of proximal tubules (PT). In dark-field view (D through F), the counterstaining caused the image to have a dark green (negative) or dark purple (positive) background, on top of which silver grains are visible. In cortex (both CL and CMR), the tubules in which upregulation of sgk1 by aldosterone is seen are PAS-stained negative, indicating they are tubules of the distal nephron. Glomerulus and surrounding structures are illustrated in panels C and F. The distal tubule approximating to the vascular pole of glomerulus exhibited sgk1 induction, suggesting the possible involvement of the early portion of distal convoluted tubules. Glom, glomerulus; VP, vascular pole; UP, urine pole; +, high expression.

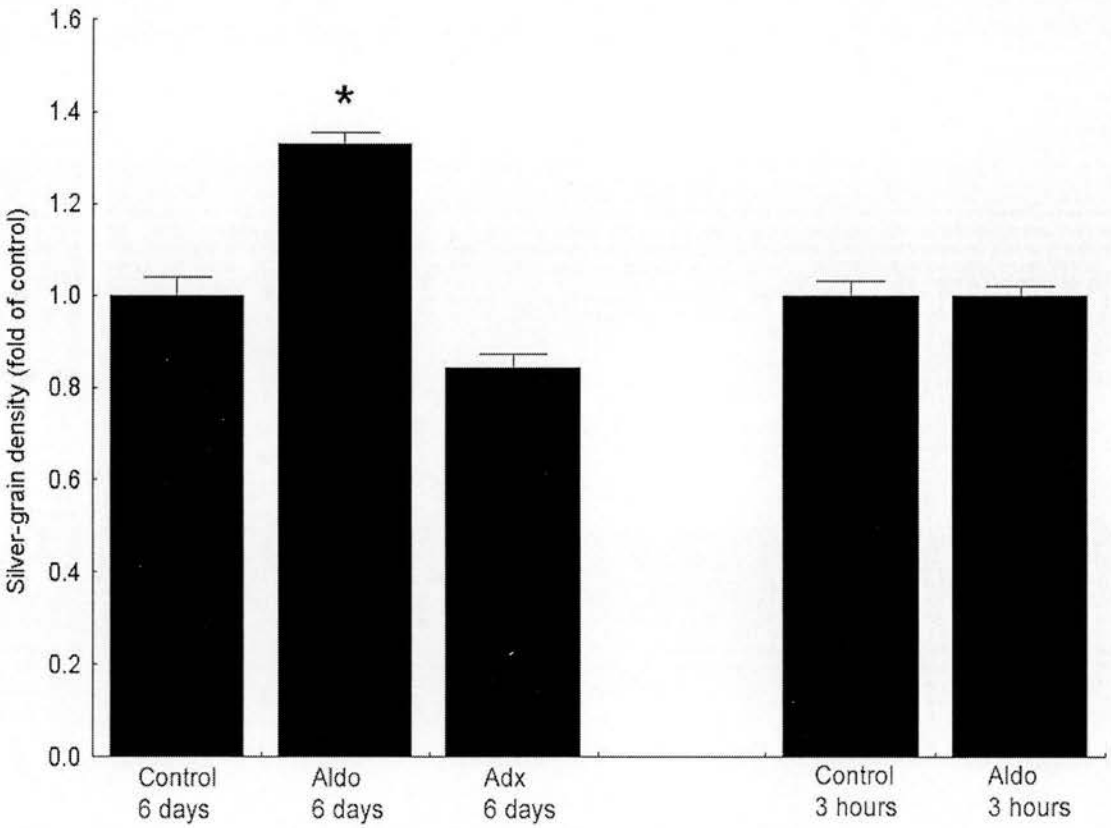

Figure 3.7. Quantification of sgk1 expression in glomerulus. Silver grain counting revealed a slight increase (30 to 50%) of sgk1 expression induced by chronic (6 d) but not acute (3 h) aldosterone excess (* $P < 0.01$ *versus* control).

outer medullary collecting ducts. These regions have the potential to mediate amiloride-sensitive sodium transport, as they include the major sites of ENaC action. Although sgk1 was shown to increase the surface expression of ENaC subunits in *Xenopus* oocytes (Alvarez de la Rosa D et al. 1999), a recent report suggested that ENaC translocation to the apical membrane was limited to the proximal portion of the distal nephron, i.e. from distal convoluted tubules to connecting tubules, in response to rapid aldosterone infusion (2-4 hours) in rats (Loffing J et al. 2001). Both our findings (mRNA) and reports of other groups (protein) showed that acute induction of sgk1 expression was localized to the entire aldosterone sensitive distal nephron (ASDN: i.e. from distal convoluted tubules to outer medullary collecting ducts). An axially heterogeneous mechanism can be proposed to control the activation of sgk1 (eg by phosphorylation), and thereby restrict ENaC translocation to the more proximal portion of the distal nephron. Beyond previous findings, our work shows an axial heterogeneity of prolonged upregulation of sgk1 mRNA, which correlates with the plasma level of aldosterone. It appeared that mild aldosterone excess (0.03% sodium diet) induced sgk1 in the cortical portion of ASDN whereas moderate (50μg/kg infusion) and more severe (150μg/kg and 750μg/kg infusions) excess affected the entire ASDN. Two recent studies, in mouse (Loffing J et al. 2000) and rat (Masilamani S et al. 1999), have reported that treatments with chronic aldosterone excess (Masilamani S et al. 1999) or dietary sodium restriction (Loffing J et al. 2000) are associated with ENaC translocation to the apical membrane of distal nephron. Dietary sodium restriction in mice caused ENaC to shift from cytoplasm to the apical membrane in cells confined to the cortical segments of ASDN (Loffing J et al. 2000). This could be interpreted as potentially due to the aldosterone-induced accumulation of sgk1, which promotes ENaC trafficking into the apical membrane.

The studies described in this chapter are the first to assess sgk1 regulation using *in situ* hybridization in mouse as well as the first to carefully quantify the relative degree of its induction in different parts of the nephron (distal tubules, glomeruli and inner medulla) using silver-grain counting. Previous work has examined aldosterone regulation of sgk1 mRNA levels in renal cell lines (Chen SY et al. 1999; Naray-Fejes-Toth A et al. 1999), the whole kidney (Brennan FE and Fuller PJ 2000; Bhargava A et

al. 2001) or dissected renal components (Loffing J et al. 2001; Shigaev A et al. 2000) by northern blotting or RT-PCR, as well as demonstrated the accumulation of sgk1 protein in response to hormone excess by immunohistochemistry (Chen SY et al. 1999; Loffing J et al. 2001). As the current work examines the effects of a wider range of treatments (Table 3.1) this allows a clearer view of the way aldosterone affects sgk1 expression across the nephron. In the present study, up to 8-fold increase of sgk1 mRNA was found in individual renal tubules in response to chronic aldosterone excess and 1.8-fold to acute excess. The upregulation of sgk1 mRNA exhibited dose dependence over a range of circulating aldosterone (2 to 75-fold elevation). The fact that the induction of sgk1 exhibited a ceiling (8-fold elevation) in animals with severe aldosterone excess suggests that the aldosterone-sgk1-ENaC pathway responses reach saturation at this level. It is possible that this relates to saturation of available MR sites.

The mediator that upregulated sgk1 in glomeruli remains unclear. It is possible that at high doses, aldosterone will to some degree bind to GR (glucocorticoid receptors) and subsequently induce sgk1 expression (Yan K et al. 1999; Escoubet B et al. 1996). However circulating physiological glucocorticoid levels (MacDonald P et al. 2000) supply a better GR ligand at even higher levels than the raised plasma aldosterone in our aldosterone excess groups, especially the 50μg/kg/d group which nonetheless exhibits this glomerular sgk1 upregulation. Moreover adrenalectomy does not abolish glomerular sgk1 expression indicating other non-corticosteroid pathways are involved. As elevated mesangial sgk1 in diabetic nephrons has been thought to follow altered GFR (Lang F et al. 2000) it may be that glomerular haemodynamic changes during chronic aldosterone excess initiate the mesangial sgk1 upregulation.

The axial osmolality gradient in the renal medulla is made up of gradients of several individual solutes, including NaCl and urea. In antidiuresis, progressive increases in tissue NaCl and urea concentration and osmolality are observed along the corticomedullary axis from the cortex to the papilla. In contrast, the gradients are markedly attenuated during water diuresis (Hai MA et al. 1969). I propose an osmotic theory to explain the high abundance of sgk1 expression in inner medullary collecting

ducts, although I cannot rule out the possibility of sgk1 expression additionally in interstitial cells. Evidence from other research supports this proposal and it seems that the extracellular hypertonicity or cell shrinkage can stimulate sgk1 expression *in vitro* (Waldegger S et al. 1997). Thus, a certain osmotic threshold sufficient to induce sgk1 may be reached at the outer-inner medullary junction. The unexpected down-regulation of sgk1 in inner medulla induced by severe aldosterone excess indicates the engagement of regulatory mechanisms other than MR mediation. Possibly the osmotic gradient was partially washed out by the increased water intake (2-fold in the 150μg/kg/day groups and 3-fold in the 750μg/kg/day group *vs* control), which was elicited by longer-term and more severe aldosterone excess. Hence, in such a partial "wash-out", the osmotic gradient including the threshold at which sgk1 was stimulated would move further distally towards papilla so this may explain the reduction of sgk1 expression in the initial part of inner medulla. Although further investigation is required, as there is an individual variation in fluid intake within chronic and severe aldosterone excess groups, it may account for the corresponding variation in the degree to which inner medullary sgk1 expression is downregulated under these circumstances. The action of sgk1 in inner medulla is unclear but it could be involved in controlling cell volume in face of high interstitial osmolarity towards the papilla. Additionally it could be involved in regulating sodium reabsorption in inner medullary collecting ducts. In the latter case, a reduction in sgk1 expression with prolonged aldosterone infusion might contribute to facilitating natriuresis in 'escape' from the sodium retention induced by aldosterone.

CHAPTER 4

IDENTIFICATION AND CHARACTERIZATION OF ALDOSTERONE INDUCED GENES

4.1 Summary

The signaling pathway of aldosterone plays a key role in maintenance of the extracellular fluid homeostasis. Largely unknown to date are the genes whose expression is regulated by aldosterone. In this study, I have screened through 21 candidate genes (including 29 isoforms in total) by *in situ* hybridization and reported the identification of U12b, a glutathione S-transferase isoform, as being downregulated by aldosterone.

4.2 Introduction

Aldosterone influences expression of a broad pool of genes, the protein products of which transduce the actions of aldosterone in the nucleus out to the plasma membrane, where its final effectors (ENaC and Na^+/K^+-ATPase) are located (Verrey F 2000; Pearce D 2001). The next aim of my PhD studies was to identify and characterize the genes that are transcriptionally regulated by aldosterone in the distal nephron. The strategy to achieve these aims involved: 1, systematically screening a large pool of candidate genes including those playing a pivotal role in the aldosterone pathway (MR and 11β-HSD2); those discovered by others and shown to be regulated by aldosterone (such as sgk1 and K-Ras) and those generated in the host laboratory. In our group (Brown RW unpublished data), a source of candidate genes was generated by comparing whole-kidney mRNA (transcriptome) from mice treated with and without chronic aldosterone infusion (50μg/kg/day for 6 days). By this strategy, genes directly regulated by the aldosterone-MR pathway (AIPs) in the distal nephron should be isolated, as well as those responsible for aldosterone 'escape' throughout the nephron (Chapter 1.2.4).

4.3 Screening Strategy

As reported in Chapter 3, *in situ* hybridization clearly showed sgk upregulation by aldosterone. Such regulation was further quantified by the silver-grain counting, which assured the authenticity of differences between groups. By using the same groups as in the previous sgk studies, candidate genes were screened. Initially, one or two mice chosen from each of the groups treated with adrenalectomy (Adx), control (Con) and aldosterone (Aldo) infusion (50μg/kg for 6 days) were compared. If the results were encouraging, a full-scale comparison with n=6 in these groups was undertaken by *in situ* hybridization.

4.4 Results

I have screened through 21 genes in total (including 29 isoforms), involving one mouse from each of the groups Adx, Con and Aldo. The data are summarized in Table 4.1-2. Autoradiography images of the renal profile of the genes screened are shown in Figure 4.1-2. Among these genes, four (MR, 11β-HSD2, Ki-RasA, and u12b) were selected for further study on the basis of prior knowledge or possible changes in the initial work. This involved groups of 6 mice from each treatment (Adx, Con and Aldo).

MR and 11β-HSD2 mRNAs showed similar expression profiles, with hybridization signals detected over long single tubular structures extending in continuity from the cortex through the outer medulla and ending at the outer-inner medullary junction. This pattern is fully consistent with localization to the cortical and outer medullary collecting ducts. Ki-RasA mRNA had a more uniform distribution throughout the cortex and outer medulla. Interestingly, Ki-RasA was not expressed in inner medulla. Nevertheless, the hormonal regulation studies did not show any significant regulation of MR, 11β-HSD2, and Ki-RasA mRNAs in any renal subregion (Figure 4.3).

Image analysis showed u12b mRNA expression was significantly regulated by aldosterone. U12b is an isoform of the mu class of glutathione S-transferase (GST-

Table 4.1 Screening results

Name	Database match	Screening results/Aldosterone effect
U1	Yes	No significant difference
U2A	Yes	No significant difference
U2B	Yes	No significant difference
U3	No	No significant difference
U4	Yes	No significant difference
U5A	Yes	No significant difference
U5B	Yes	No significant difference
U6	No	No significant difference
U7A	No	No significant difference
U7B	No	No significant difference
U8	Yes	No significant difference
U9	Yes	No significant difference
U10	Yes	No significant difference
U11	No	No significant difference
U12	Yes	No significant difference
U12A	Yes	No significant difference
U12B	Yes	Downregulation in inner medulla
U12F	Yes	No significant difference
U13	No	No significant difference
U14	Yes	No significant difference
U15	Yes	No significant difference
U16	No	No significant difference
D1	No	No significant difference
D2	No	No significant difference
D4A	No	No significant difference
D4B	No	No significant difference
MR	Yes	No significant difference
11β-HSD2	Yes	No significant difference
Ki-RasA	Yes	No significant difference

Table 4.2 Renal distribution

Name	Cortex	Outer Medulla	Inner Medulla	Comments on expression pattern
U1	low	low	low	Regional difference not apparently identified
U2A	low	high (OS)/ low (IS)	low	Clear difference among cortex, OS/IS of outer medulla and inner medulla
U2B	low	high (OS)/ low (IS)	low	Clear difference among cortex, OS/IS of outer medulla and inner medulla
U3	high	not expressed	not expressed	Expressed only in cortex
U4	high	low (OS)/high (IS)	not expressed	Clear difference among cortex, OS/IS of outer medulla and inner medulla
U5A	not expressed	not expressed (OS)/ high (IS)	low	High expression in IS of outer medulla
U5B	low	not expressed (OS)/ high (IS)	high	Clear difference among cortex, OS/IS of outer medulla and inner medulla
U6	high	low	not expressed	Clear difference among cortex, outer medulla and inner medulla
U7A	low	low (OS)/high (IS)	low	Clear difference among cortex, OS/IS of outer medulla and inner medulla
U7B	low	low (OS)/high (IS)	low	Clear difference among cortex, OS/IS of outer medulla and inner medulla
U8	low	low	low	Regional difference not apparently identified
U9	low	low	low	Regional difference not apparently identified
U10	low	high	high	Clear difference between cortex and medulla
U11	low	low	not expressed	Clear difference between cortex and medulla
U12	low	high (OS)/ low (IS)	low	Clear difference among cortex, OS/IS of outer medulla and inner medulla
U12A	low	high (OS)/ low (IS)	low	Clear difference among cortex, OS/IS of outer medulla and inner medulla
U12B	low	low	high	Clear difference between cortex and medulla
U12F	low	low	low	Regional difference not apparently identified
U13	low	high (OS)/ low (IS)	low	Clear difference among cortex, OS/IS of outer medulla and inner medulla
U14	low	high (OS)/ low (IS)	not expressed	Clear difference among cortex, OS/IS of outer medulla and inner medulla
U15	low	high (OS)/ low (IS)	low	Clear difference among cortex, OS/IS of outer medulla and inner medulla
U16	low	low	low	Regional difference not apparently identified
D1	low	low	low	Regional difference not apparently identified
D2	low	low	low	Regional difference not apparently identified
D4A	low	low	low	Regional difference not apparently identified
D4B	low	low	low	Regional difference not apparently identified
MR	high	high	not expressed	Clear difference between cortex and medulla
11β-HSD2	high	high	not expressed	Clear difference between cortex and medulla
Ki-RasA	high	high	not expressed	Clear difference between cortex and medulla

‡ OS: Outer stripe of outer medulla; IS: Inner stripe of outer medulla.

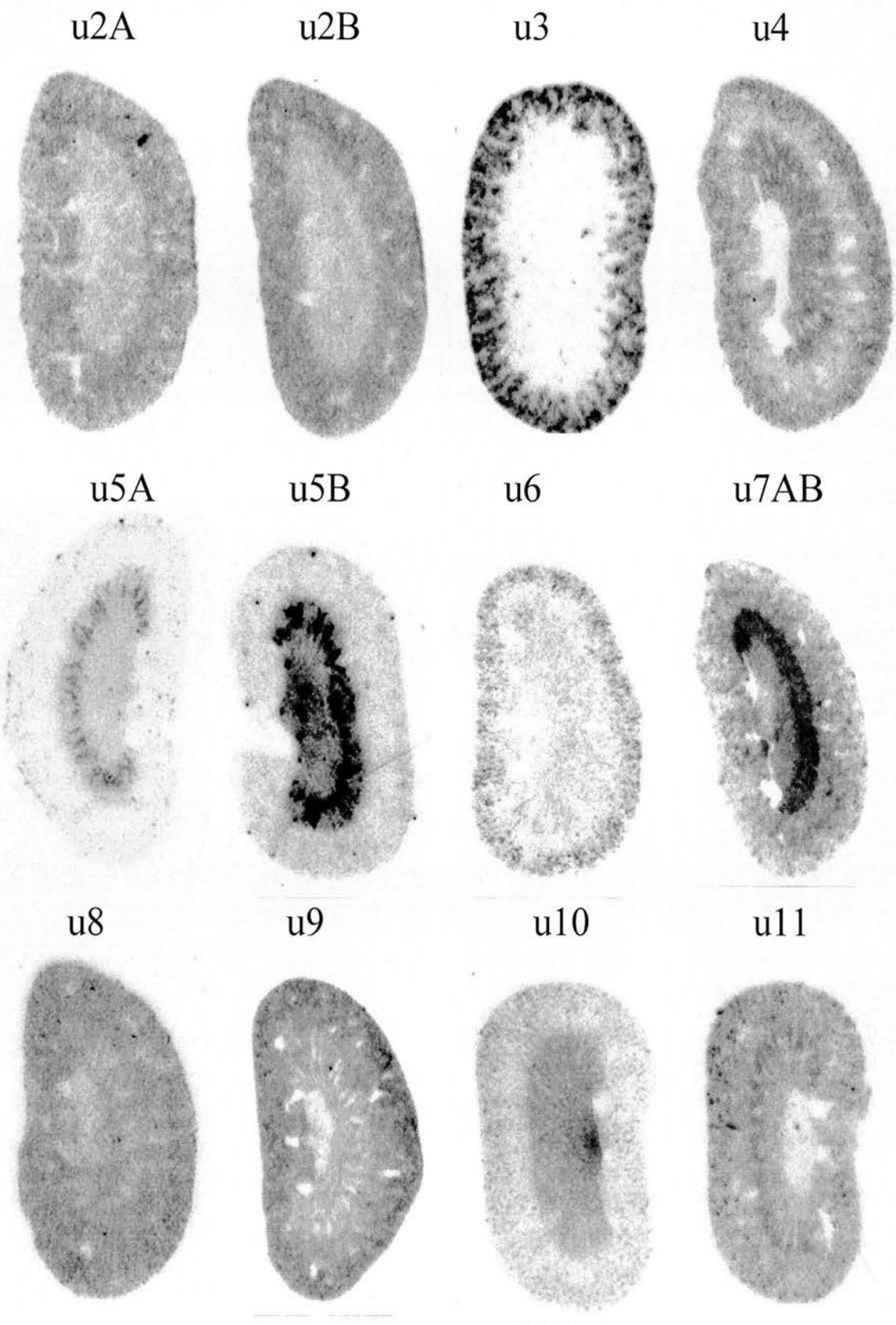

Figure 4.1. Autoradiography images of the renal profile of the genes screened through.

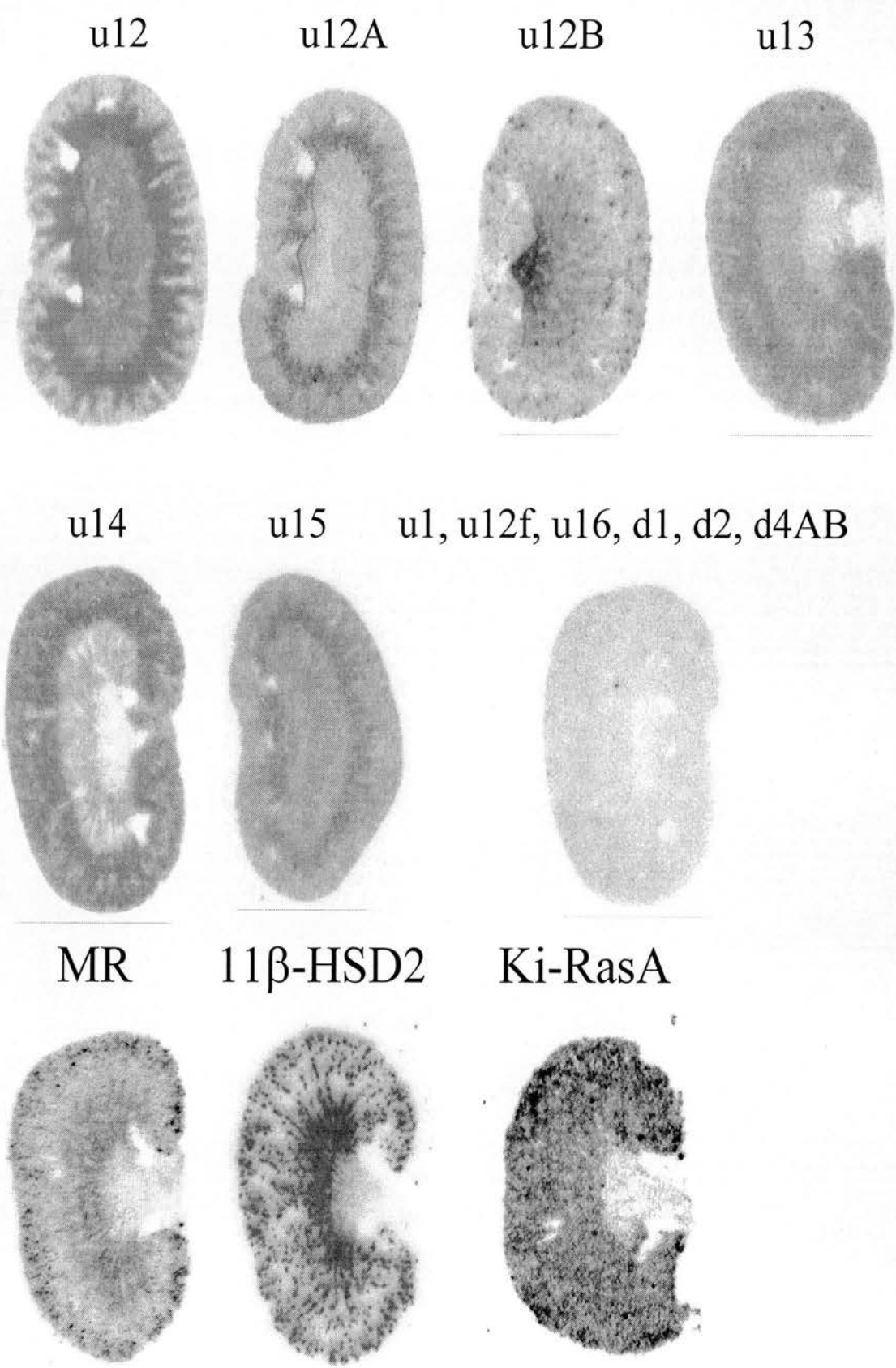

Figure 4.2. Autoradiography images of the renal profile of the genes screened through.

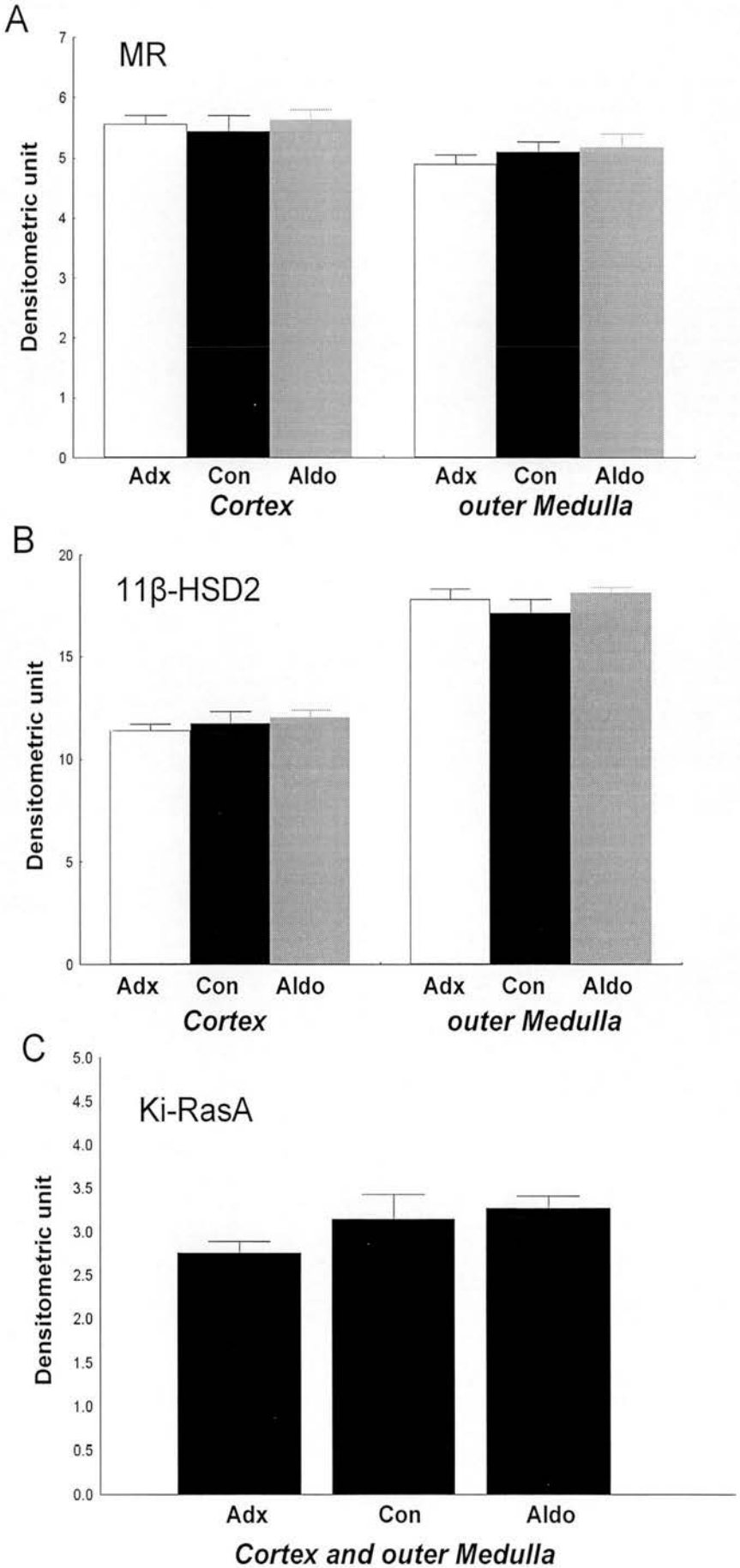

Figure 4.3. Regional densitometric analysis of mRNA expression of MR (A), 11β-HSD2 (B) and Ki-RasA (C). No significant regulation of MR, 11β-HSD2 and Ki-RasA mRNAs was found in any renal subregion (n=6, $p>0.1$).

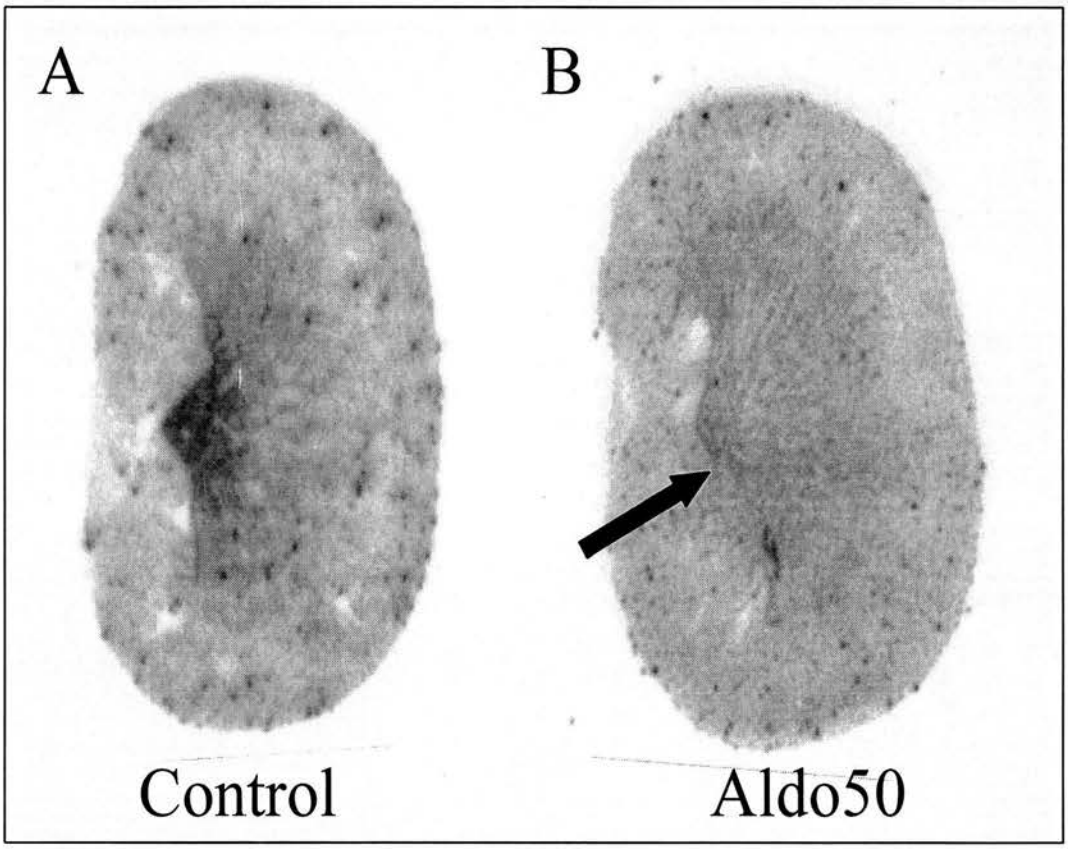

Figure 4.4. Aldosterone effects on u12b expression. Autoradiographs (expression black) showing comparison of u12b expression between control (A) and animals infused with 50μg/kg aldosterone for 6 d (B). Note the downregulation of u12b in inner medulla (arrow).

mu2) (Brown RW unpublished data). GST-mu2 was expressed from cortex to medulla, with prominent expression in inner medullary collecting ducts converging towards the papilla. Chronic aldosterone excess reduced the expression of GST-mu2 mRNA in inner medulla (Figure 4.4), but not in other subregions of the kidney. This gene was further investigated by Speirs HJL and Hou J et al (2001), with the work encompassed by this thesis.

4.5 Discussion

As reported in Chapter 3, *in situ* hybridization clearly showed sgk to be upregulated by aldosterone. Furthermore, the localization of gene expression and regulation was easily spotted with the aid of microscopic analysis. The expression level was quantified using silver-grain counting, which assured the authenticity of differences between groups. By this approach, I have screened through other candidate genes including MR, 11β-HSD2, Ki-RasA and those discovered previously in the host lab.

MR and 11β-HSD2 are two key genes involved in the signaling pathway of aldosterone. A tantalizing hypothesis is that aldosterone may modulate the expression level of MR and/or 11β-HSD2 to form an auto-feedback mechanism to amplify or reduce its effects in mineralocorticoid-sensitive cells. It has long been known that GR, a close homologue of MR, is regulated by glucocorticoids themselves in various tissues (Kalinyak JE et al 1987; Rosewicz S et al 1988). However, my *in situ* hybridization studies have largely ruled out significant autoregulation of MR and/or 11β-HSD2 mRNAs by aldosterone in any kidney subregion. This is consistent with other reports that in vivo changes in aldosterone status showed no effects on 11β-HSD2 activity, 11β-HSD2 transcripts or MR transcripts in the kidney (Alfaidy N et al 1995; Farman N and Bocchi B 2000). The advantage of in situ hybridization approach is that it allows anatomical regions to be identified and subtle region-specific effects to be defined. None was found for MR or 11β-HSD2 mRNAs. A disadvantage is the semi-quantitative nature of the technique, but here all sections from all 3 treatment groups were hybridized to the same probe in a single experiment. Thus comparisons between groups should be valid giving some confidence in the intergroup and

interregional comparisons made. Finally, this study examined mRNA not protein, but the major mode of action of corticosteroids is upon gene expression at a transcriptional level, underlining my basic motivation to employ this approach.

Ki-RasA was identified as an aldosterone-induced transcript in *Xenopus* renal A6 cells (Spindler B et al 1997; Stockand JD et al 1999). In a mammalian collecting duct cell line, however, Ki-RasA gene expression was found to be unchanged by aldosterone (Robert-Nicoud M et al 2001). My studies also showed no significant change in the mRNA level of Ki-RasA in response to aldosterone *in vivo* in mouse, and thus supported the view that, unlike Sgk1, the candidacy of Ki-RasA as an important intermediary gene in the aldosterone pathway in mammalian kidney remains in doubt.

My study was the first to identify u12b, a glutathione S-transferase (GST) isoform mu-2, as being downregulated by aldosterone in the kidney. GSTs are soluble cytosolic proteins that can be grouped into eight classes: alpha, kappa, mu, omega, pi, sigma, theta and zeta, based on amino acid sequence homologies and subunit assembly (Sheehan D et al 2001). GSTs play an important role in the cellular detoxification of electrophilic xenobiotics and can also act as antioxidants (Wilce MCJ, Parker MW 1994). It is intriguing to notice that the downregulation of GST-mu2 by aldosterone occurs only in inner medullary collecting ducts, where MR expression is absent (Figure 4.2-3). This suggests that regulation of GST-mu2 by aldosterone is due to a secondary effect of aldosterone. The mechanism underpinning GST-mu2 downregulation in inner medulla is probably the same as proposed in Chapter 3.5 to explain the downregulation of sgk1 in inner medulla in response to severe and chronic aldosterone excess. The axial osmolality gradient in renal medulla, washed out by increased water intake (due to aldosterone excess), may have caused the downregulation of GST-mu2 as well as sgk1. Previous studies have shown that stress (including extracellular hypertonicity or cell shrinkage) can stimulate sgk1 expression *in vitro* (Waldegger S et al. 1997). Further studies to investigate whether GST-mu2 expression responds to stress (such as cell volume change) are potentially interesting. Recently, it has been found that GSTs modulate the signaling pathway of JNK and apoptosis signal-regulating kinase, both of which are stress activated

signaling pathways (Adler V et al 1999; Cho SG et al 2001).

Although some of the other candidates had a substantial expression in kidney, no significant difference was observed comparing the group given aldosterone treatment with controls in the initial phase of screening. Future studies may include a larger number of individuals (n>6) and *in situ* hybridization to examine for even more subtle changes in expression; or may require a more sensitive approach, such as real-time PCR analysis of microdissected nephron segments. The latter might be crucial to identification of aldosterone-induced genes in the microdissected distal nephron, as the distal nephron cells constitute less than 20% of the cell population of the kidney. An alternative may be to examine the regulation of some of the candidate genes in cultured distal nephron cells, for example the mouse M-1 cells.

CHAPTER 5

TRAFFICKING OF THE EPITHELIAL SODIUM CHANNEL (ENAC) IN MOUSE COLLECTING DUCT CELLS AND INFLUENCES OF EPITHELIAL POLARITY AND HORMONES

5.1 Summary

Regulation of the epithelial sodium channel (ENaC) trafficking in cells of the distal nephron is of major importance in control of sodium reabsorption and blood pressure. The molecular events underpinning ENaC trafficking to and from the plasma membrane and their hormonal regulation are poorly understood. To start elucidating these pathways I have generated stable mouse collecting duct cell (M-1) lines that express an N-terminally fused EGFP-ENaCβ subunit. The cell lines grow normally, express easily visualized quantities of the EGFP fused ENaC subunit and form confluent epithelia with high transepithelial resistance when grown on semi-permeable filters. Imaging by confocal microscopy revealed that ENaC was confined to the endoplasmic reticulum (ER) in unpolarized M-1 cells. Activation of the vasopressin pathway (forskolin) results in ENaC exodus out of the ER and entering intracellular vesicles and this stimulated ENaC trafficking does not involve the endocytic vesicle pathway. When cells are fully polarized, ENaC largely exits the ER and the Golgi apparatus. Corticosteroids (≥100nM dexamethasone) profoundly alter the trafficking of ENaC proteins in polarized M-1 cells by promoting ENaC translocation to the apical membrane. Collectively, polarization, corticosteroids and forskolin modulate the trafficking of ENaC in distinctive manners such that forskolin or polarization fosters ENaC trafficking from ER to intracellular vesicles, whereas corticosteroids play a role further downstream in the cascade of ENaC trafficking events by increasing delivery of ENaC to the apical membrane.

5.2 Introduction

Regulation of sodium reabsorption in kidney is crucial for maintenance of whole body fluid homeostasis (Guyton and Hall 2000). The epithelial sodium channel (ENaC) in the apical membrane of aldosterone responsive cells of the distal nephron mediates entry of Na^+ into these cells, which exits in exchange for K^+ at the basolateral side via the Na^+/K^+-ATPase (Rossier BC 1997; Horisberger JD 1998). ENaC comprises three homologous subunits (α, β and γ), arranged in a stoichiometry of 2α:1β:1γ (Firsov et al. 1996, 1998). Each subunit is composed of two transmembrane domains, an extracellular loop and short N- and C-termini (Canessa et al. 1993, 1994). Maximal surface expression of the channel complex is reached when all three ENaC subunits are expressed in *X. laevis* oocytes, even though expression of α alone and αβ or αγ two-subunit combinations can lead to appearance of a minute (<1%, 5% and 5% respectively) quantity of 'partially functional' channel proteins on the plasma membrane (Canessa et al. 1994; Firsov et al. 1996; Konstas A and Korbmacher C. 2003).

It is widely accepted that ENaC processing and maturation are inefficient, such that around 1% of channels synthesized in the endoplasmic reticulum (ER) actually translocate to the cell surface when they are expressed in *X. laevis* oocytes (Valentijin JA et al. 1998) and an estimated 20% in *X. laevis* A6 cells (Weisz OA et al. 2000). An important determinant of the efficiency of ENaC maturation is the assembly of its subunits in the ER. ENaC assembly likely occurs very early during its processing in the ER, as suggested by studies on ENaC glycosylation (Adams CM et al. 1997).

Epithelial cells display an additional layer of complexity in that they are polarized and possess two distinct plasma membrane domains, apical and basolateral. This plasma membrane polarity is established and maintained by protein sorting and specific vesicle trafficking in exo- and endocytic pathways. Largely unknown to date are the molecular pathways mediating the trafficking of ENaC to the apical surface of polarized renal epithelia, although evidence implicating the SNARE (soluble *N*-ethylmaleimide-sensitive factor attachment protein receptor) (Qi J et al. 1999; Saxena

S et al. 1999) and the lipid 'raft' pathways has been reported (Prince LS et al 1998, 1999).

Corticosteroids are the primary hormones responsible for maintaining sodium reabsorption in the distal nephron of kidney. The early phase of corticosteroid action is often demarcated as the period when the pre-existing ENaC channels in the plasma membrane are activated; and the late phase (>3h) is when *de novo* synthesis of ENaC and its translocation to the plasma membrane take place (Verrey F et al 2000). Arginine-vasopressin (AVP) evokes an increase in ENaC conductance in models of the distal nephron that develops over a period of 5-20 min and that is synergistic to the effect of corticosteroids (Breyer MD and Ando Y 1994). The effect of AVP is mediated via AVP binding to its V2 receptors, leading to the stimulation of adenylate cyclase and a concomitant increase in the level of intracellular cAMP. Nevertheless controversy surrounds the precise mechanism underpinning the AVP effect, though some concur that AVP promotes an exocytic delivery of ENaC to the apical membrane (Kleyman et al 1994; Marunaka and Eaton 1991; Snyder PM. 2000).

Previously studies on characterizing ENaC processing and trafficking were conducted primarily in non-epithelia [e.g. *X. laevis* oocytes] (Valentijin JA et al. 1998; Shimkets RA et al 1997) or epithelia with less resemblance to the mammalian distal nephron [e.g., COS cells, HEK-293 cells (Prince LS et al 1998, 1999), Madin-Darby canine kidney (MDCK) epithelial cells (Hanwell D et al. 2002) or *X. laevis* A6 cells (Weisz OA et al. 2000)]. As these are not cells of mammalian distal nephron origin they have shortcomings in modeling the high resistance mammalian epithelia normally expressing ENaC. In this study, I have generated mouse collecting duct cell lines (M-1) that stably express the ENaCβ subunit fused to the enhanced green fluorescent protein (EGFP). Using this I have firstly determined the subcellular localization of EGFP-ENaC in M-1 cells by confocal microscopy. Secondly, I have examined the trafficking of channel proteins in response to stimulation of the hormonal pathways (including corticosteroids and AVP). Finally, I have studied changes in ENaC subcellular localization and its response to hormonal stimulation in M-1 cells and how this alters depending upon the state of cell polarity.

5.3 Methods

(The materials and common molecular biology methods are described in CHAPTER 2)

5.3.1 Staining of cell organelles and plasma membrane

Endoplasmic reticulum was labeled for 10 min at room temperature with the rhodamine-B hexyl ester (#R648, Molecular Probes) at 0.5μg/ml; mitochondrion with MitoTracker (#M22426) at 2μM; Golgi apparatus with an anti-GM130 antibody [a mouse anti-GM130 antibody (gift of Dr Rory Duncan) detected with an AlexFluor 660 tagged goat anti-mouse secondary antibody (#A21054)]; and endosomes with AlexFluor 630-transferrin at 10μM (#T23362). Previous studies show at high concentrations (0.5-1μg/ml) the rhodamine-B hexyl ester specifically stains the endoplasmic reticulum of fixed cells (Terasaki and Reese 1992; Yang L et al. 1997). The apical membranes were labeled on ice with rhodamine-conjugated wheat germ agglutinin (#W849) at 2μg/ml. The Transwell filters or coverslips bearing the stained M-1 cells were then mounted onto a glass slide for microscopic visualization.

5.3.2 Fluorescence microscopy.

Conventional fluorescence images were captured by a CCD camera attached to a Zeiss 210 Axio-epifluorescence microscope using the fluorescein isothiocyanate (FITC) filter set and a 100x Plan-Neofluar objective (Numerical Aperture NA 1.4 oil). Laser scanning confocal microscopy (LSCM) was performed with the Zeiss 510 confocal imaging system equipped with a Plan-Neofluar 40x (NA 1.3 oil) objective and the rhodamine and FITC filter sets. For the dual imaging of EGFP and rhodamine, fluorescent images were collected by exciting the fluorophores at 488 nm (EGFP) and 543 nm (rhodamine) with argon and HeNe lasers respectively. Emissions from EGFP and rhodamine were detected with the band-pass FITC filter set of 500-550 nm and the long-pass rhodamine filter set of 560nm, respectively. A sequential scanning program was used to collect *z*-optical sections (i.e. in the transverse plane) at 0.16 μm intervals. An overlay of collected 2D images at each depth was performed to allow a *z* dimension stack yielding a 3D reconstruction then sectionable in alternative planes

(Zeiss LSM Image Brower version 3.1). Reconstructed images oriented with coordinates (*xy* 0°, *yz* 0°, *xz* 90°) were used to visualize the epithelial monolayer in the sagittal plane.

5.4 Results

5.4.1 Characterization of the transgenic cell lines

The full-length mouse ENaCβ subunit cDNA was cloned and ligated to the carboxy terminus of EGFP cDNA to generate a chimeric protein (Figure 5.1A). Expression of the EGFP-ENaCβ construct was driven by the cytomegalovirus promoter. Previous studies show that the PY motif at the carboxy terminus of the ENaCβ subunit is involved in the endocytosis of the channel proteins. To avoid potential disruption of ENaC trafficking, I therefore fused the EGFP to the amino terminus of the ENaCβ gene. In addition, Chalfant ML et al (1999) reported that fusion of EGFP to the amino terminus of the ENaCβ protein had no effect upon the ENaC-mediated sodium transport when the chimeric ENaCβ protein was compared to unmodified ENaCβ in co-expression studies with the other two subunits in *X. laevis* oocytes. Thereafter, M-1 cells were transfected with the EGFP-ENaCβ construct and among the 30 lines selected, I analyzed two lines expressing easily-visualized quantities of EGFP-ENaCβ proteins. Comparable to the parent M-1 cells, both cell lines exhibited high transepithelial resistance (>1,000 $\Omega \cdot cm^2$) when fully polarized. To verify that the EGFP-ENaCβ was expressed in the clonal cell lines, I analyzed the EGFP fusion protein product by western blotting. A distinct band with a molecular weight of ~110kDa (GFP: 40kDa and ENaCβ 70kDa) was detected on the PVDF membrane probed with an anti-GFP antibody (Figure 5.1B). The parental M-1 cells did not contain a similar epitope. By FACS analysis, I found both cell lines were highly pure in that 87% of cells of the cell line EGFP-ENaC1 expressed the GFP fusion protein; and that 95% of EGFP-ENaC2 (Figure 5.1C).

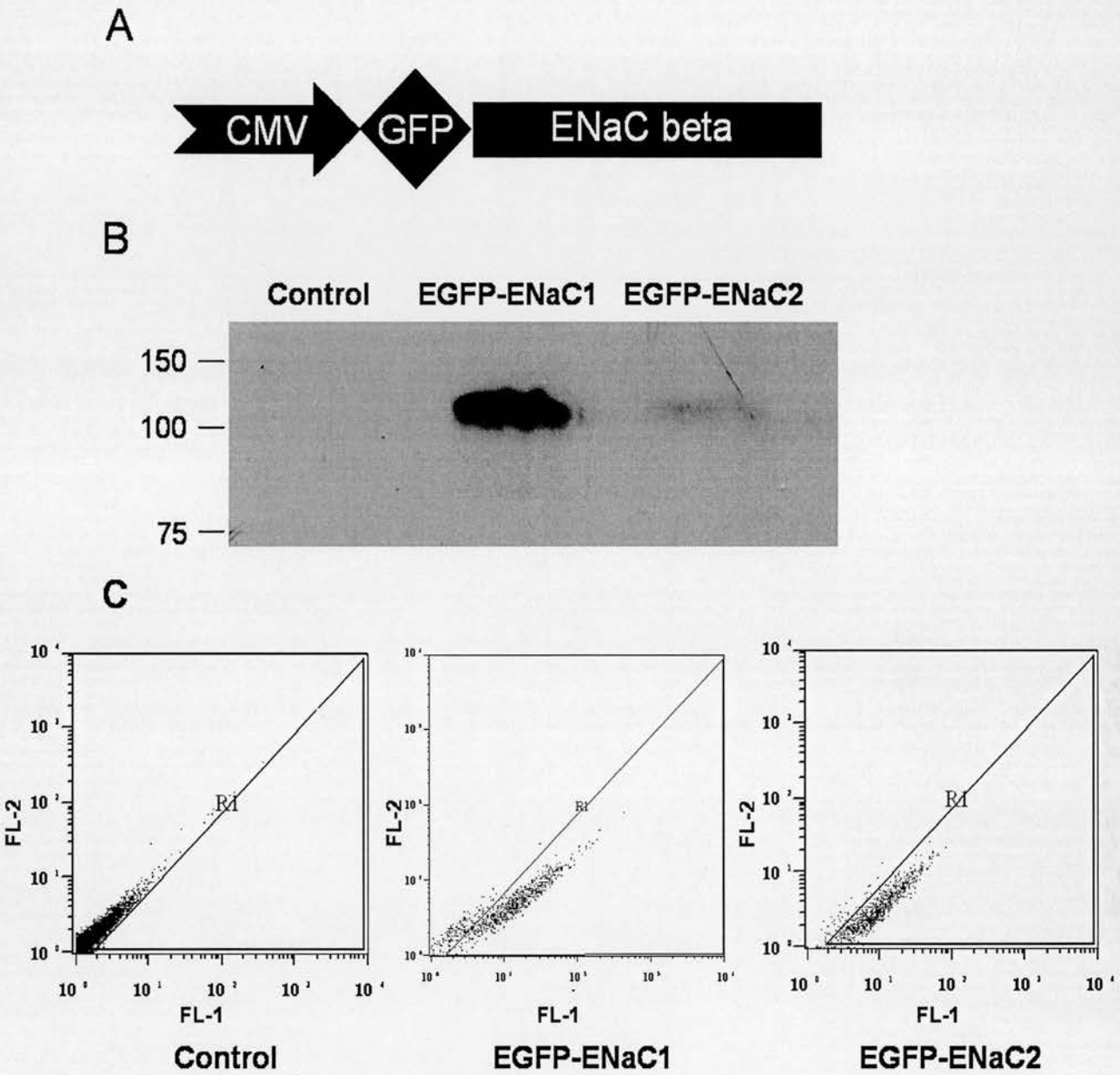

Figure 5.1. Characterization of stable M-1 cell lines expressing EGFP-ENaC β proteins. A: schematic of the expression vector plasmid. CMV, cytomegalovirus promoter; EGFP: enhanced green fluorescence protein; ENaC β: epithelial sodium channel beta subunit. B: Western blotting analysis of the EGFP-ENaCβ stable cell lines. The position of the molecular weight standards (in kDa) is shown at left. A distinct band with the molecular weight of ~110kDa was found in the stable cell lines (EGFP-ENaC 1 and 2) but not in the control (parental M-1 cells). C: FACS analysis of EGFP-ENaCβ stable cell lines. The fluorescence intensity graphs show dots representing cells from each cell line with their FL-1 (green channel) values *vs* FL-2 (red channel) values. Those that do not express GFP fusion proteins (control) are found along the diagonal of this graph (*i.e. where values in FL-1 equals those in FL-2*). Those that express EGFP fusion proteins have FL1>FL2 and are shifted below the diagonal towards the horizontal axis (in red).

5.4.2 ENaC is confined to the endoplasmic reticulum in unpolarized M-1 cells

To determine the localization of the ENaC fusion protein in unpolarized cells, I sparsely seeded cells onto glass coverslips and incubated them overnight (i.e., 16-18 h). Examination of the fluorescence micrograph (Figure 5.2) of the M-1 cells revealed that the channel proteins had a cytoplasmic distribution, with a fine reticular network all over the cytoplasm and around the nuclear envelope. This subcellular distribution of channel proteins was fully consistent with their localization being in the endoplasmic reticulum (ER). Some cells displayed one or more large vacuolar compartments that excluded the accumulation of EGFP-ENaCβ (Figure 5.2). Early studies have shown similar structures in MDCK cells having prolonged inhibition of epithelial polarity and that this compartment bore some structural resemblance to the plasma membrane (Vega-Salas et al. 1987). To confirm the chimeric ENaC protein is localized to ER, I examined the green fluorescence pattern of EGFP-ENaC counter-staining with various established organelle and membrane markers. The ER membrane was specifically stained with the red fluorescent dye rhodamine-B hexyl ester, the mitochondrion membrane with the far-red dye MitoTracker and the plasma membrane with the wheat germ agglutinin (WGA) conjugated to a red fluorophore. Merging the fluorescence channel of rhodamine-B hexyl ester (Figure 5.3 A1, red) with EGFP-ENaC (Figure 5.3 A2, green) demonstrated the co-localization of the ENaC proteins with ER, as shown in yellow on Figure 5.3 A3. Corresponding studies ruled out the possibility that ENaC resided in the mitochondrion (Figure 5.3 B1-3). WGA labeled the plasma membrane and delineated its boundary (Figure 5.3 C1). As illustrated in Figure 5.3 C2-3, the EGFP-ENaCβ fusion proteins were localized to the ER rather than the cell membrane. To determine the corticosteroid effects on ENaC trafficking in M-1 cells, I gave cells 24-h treatments with a range of doses of dexamethasone (Dex: 10nM, 100nM and 1μM). As a control group, cells were cultured in the presence of 100nM Dex plus an excess amount of glucocorticoid antagonist (RU486 10μM). Each treatment group comprised three independent experiments. I found the restricted ER localization of ENaC persisted in all of the Dex treatment groups as well as the control group.

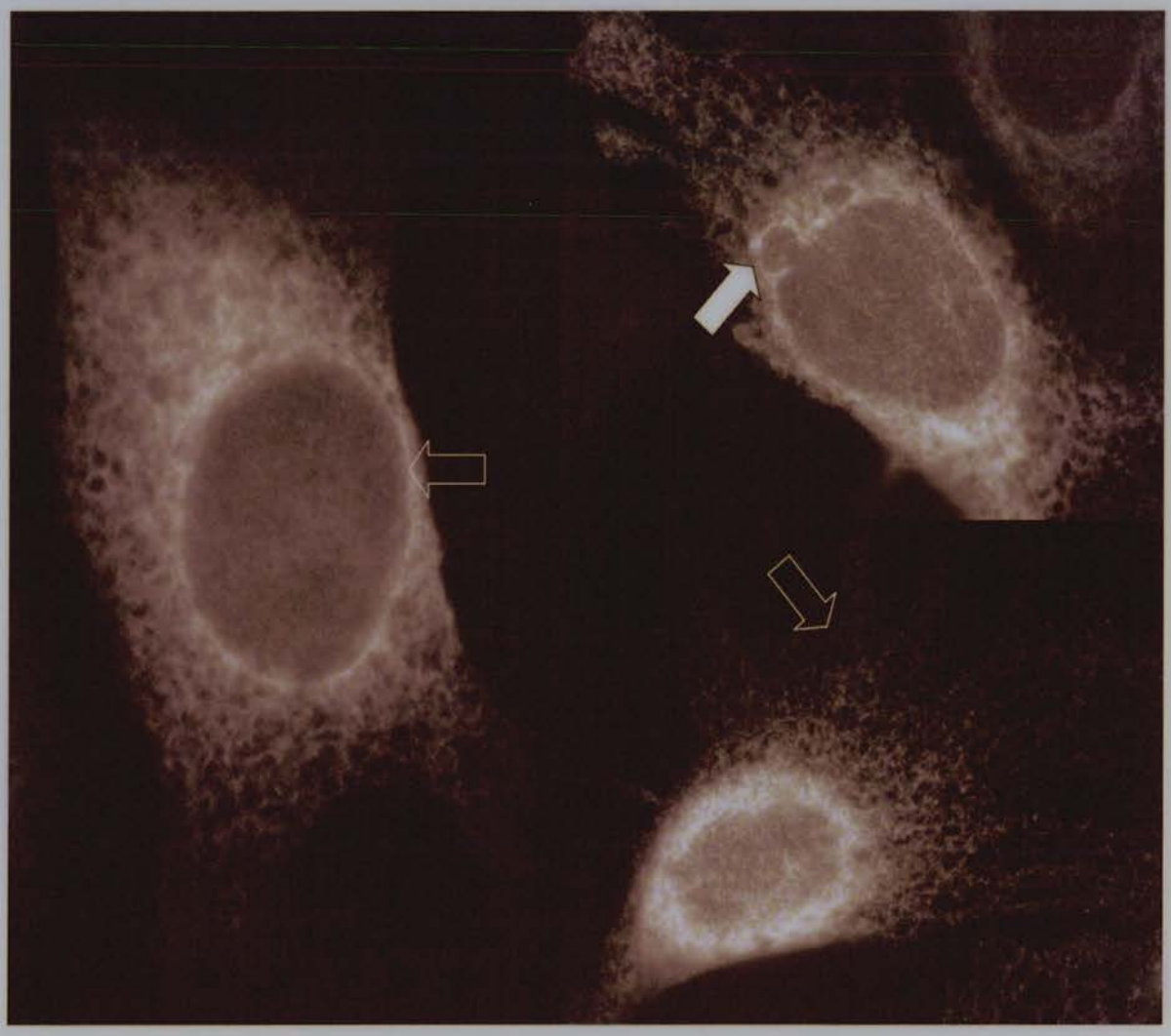

Figure 5.2. Fluorescence images of the M-1 cells stably expressing EGFP-ENaCβ subunit. Cells were grown on coverslips, fixed and mounted as described under Methods . Fluorescence images were captured by the Zeiss Axio-epifluorescence microscope (x100, NA1.4). Note the EGFP chimeric proteins are located in the nuclear envelope and cytoplasmic structures with the appearance of a fine reticular network (white unfilled arrow) whilst the large vacuolar compartments excluded the accumulation of EGFP-ENaCβ (white filled arrows).

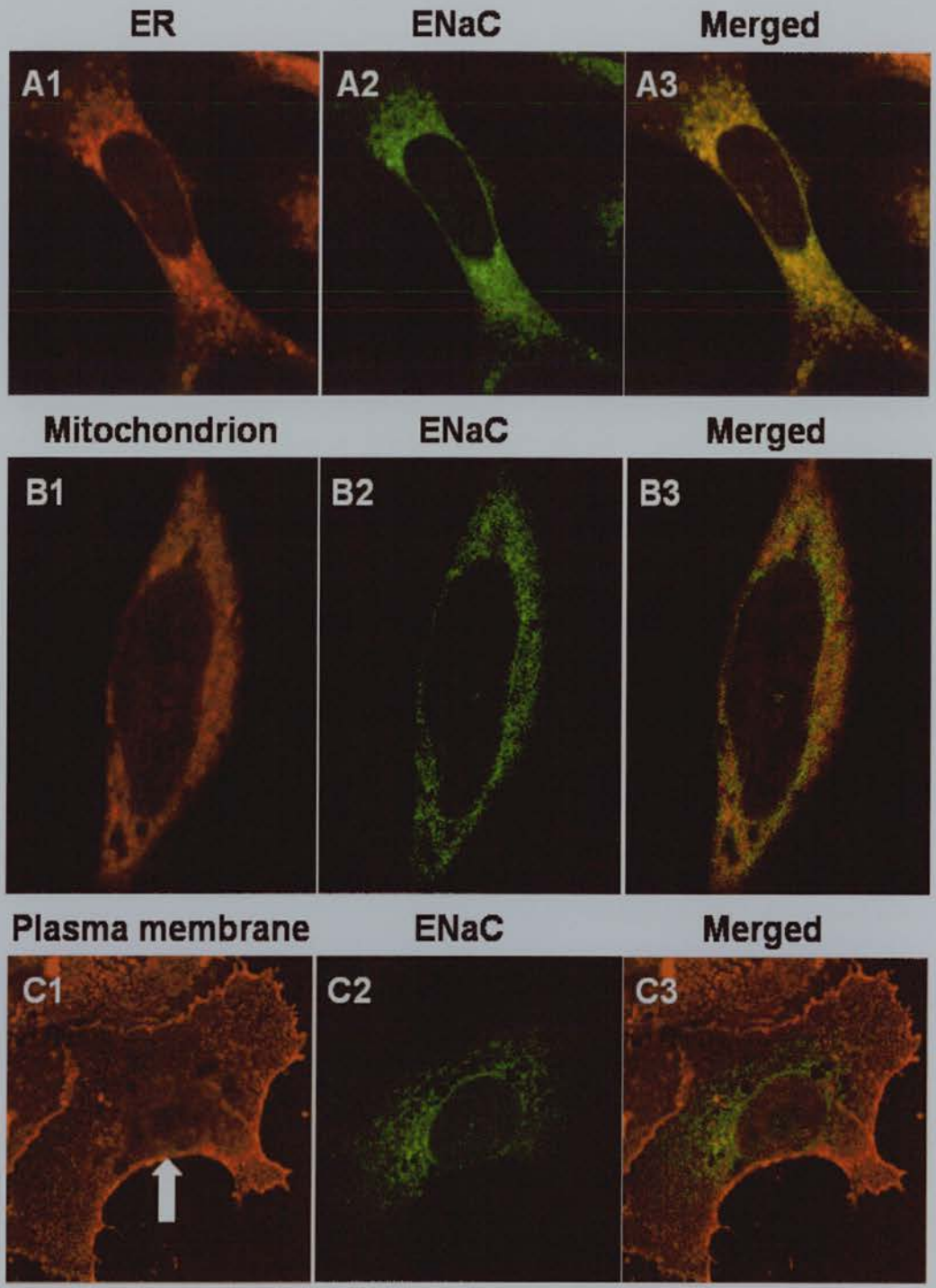

Figure 5.3. Comparison of the EGFP-ENaCβ subcellular localization to the ER, the mitochondrion and the plasma membrane. The M-1 cells were grown on coverslips and the fluorescence images of M-1 cells were captured by confocal microscopy (x40, NA1.3). The cell shown in panel A1 was stained with the ER marker and A2 showed the localization of EGFP-ENaC in this cell. Note the extensive co-localization between ENaC and ER in A3 (yellow or orange) after A1 was merged with A2. The labeling of mitochrondrion and plasma membrane is shown in B1 and C1 respectively. B2 and C2 reveal the ENaC subcellular localization. The merged images in B3 and C3 show adjacent red and green indicating a lack of co-localization.

5.4.3 Activation of the AVP pathway results in ENaC exodus out of the ER and this stimulated ENaC trafficking does not involve the endocytic vesicle pathway.

To activate the AVP pathway, I exposed the unpolarized M-1 cells to a downstream activator of this pathway (50μM forskolin: a direct activator of adenylate cyclase) for 30 min. The chimeric EGFP-ENaC proteins accumulated in small punctate structures suggestive of intracellular vesicles (Figure 5.4A). Counter-staining the ER showed a clear segregation of ENaC localization separate from the ER (Figure 5.4 B1-3). To test whether ENaC trafficking occurs via endosomes upon exiting the ER, I labeled both internalized and recycling endosomes with a transferrin red fluorophore conjugate (Ghosh RN et al. 1994). As shown in Figure 5.4 C1-3, I found that ENaC largely resided in a structure distinct from the endosomes, though there was some incidental overlap towards the cell periphery. Thus the population of vesicles to which ENaC traffics from ER upon foskolin treatment is not within the endosomal pathway and hence rather appears within an exocytic pathway with potential to deliver the cargo protein (ENaC) to the plasma membrane.

5.4.4 ENaC exits the ER and the Golgi apparatus when cells are fully polarized

To determine the localization of the ENaC fusion protein in polarized cells, I cultured cells on Transwell polycarbonate filters for at least 10 days until high transepithelial resistance (>1,000 $\Omega \cdot cm^2$) was reached. After the M-1 cells were polarized, endoplasmic reticulum (ER) and Golgi apparatus were labeled with rhodamine-B hexyl ester and an antibody against the Golgi membranes respectively. Merging the channel of ER fluorescence (Figure 5.5 A1) with that of the EGFP fusion protein (Figure 5.5 A2) indicated that ENaC was not co-localized to this organelle (Figure 5.5 A3). The staining of the Golgi apparatus manifested as tubular structures close to the periphery of the nucleus (Figure 5.5 B1). Image analysis revealed some co-localization between ENaC and the Golgi apparatus (Figure 5.5 B3). Nevertheless, the majority of ENaC proteins appeared to be excluded from the ER and the Golgi apparatus in polarized cells and thus in some alternative cytoplasmic compartments,

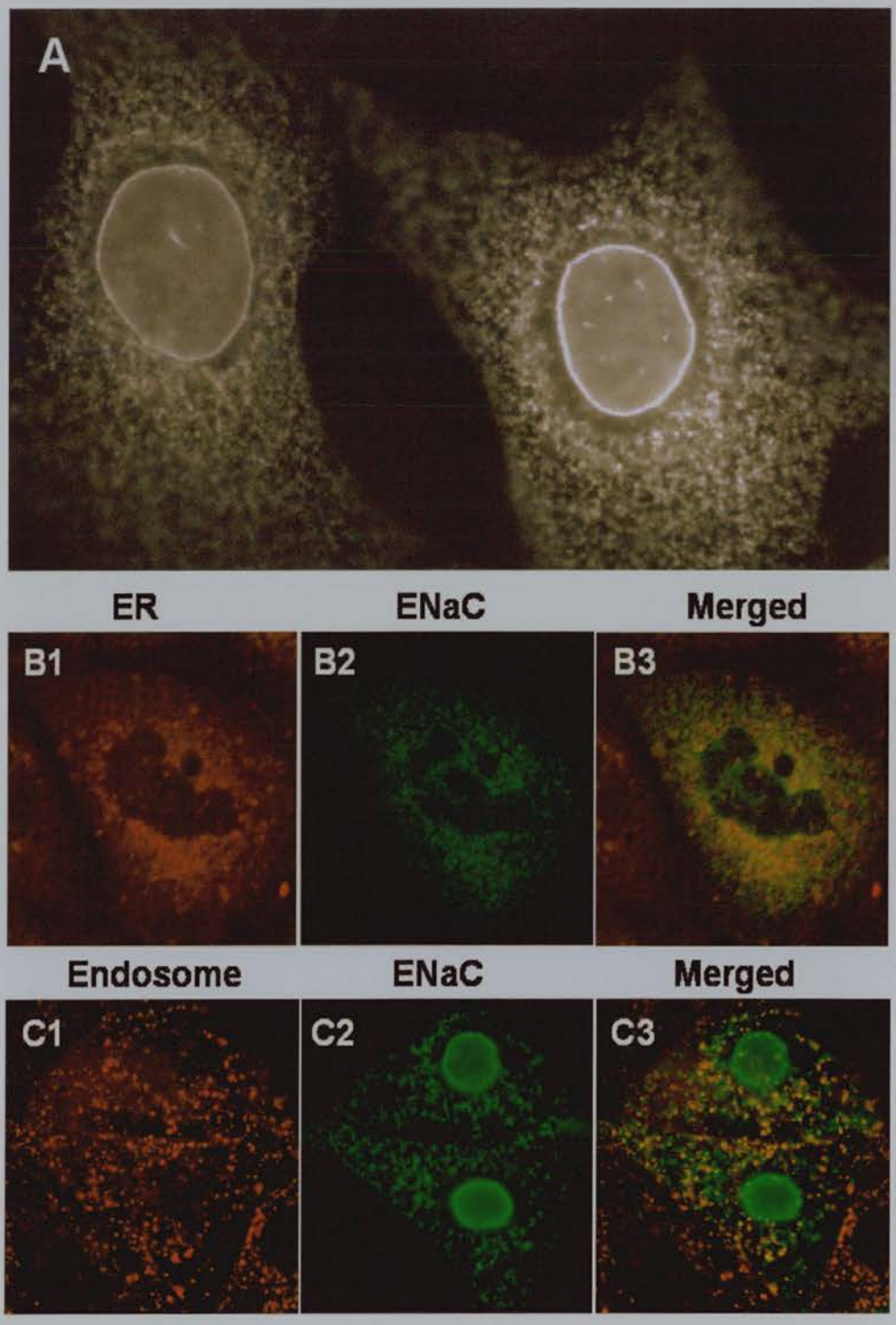

Figure 5.4. Forskolin effect on ENaC trafficking. Unpolarized M-1 cells were exposed to 50uM forskolin (a downstream activator of the vasopressin pathway). The fluorescence image of M-1 cells (A) was captured by the Zeiss Axio-epifluorescence microscope (x100, NA 1.4); and images (B-C) by the Zeiss 510 confocal microscope (x40, NA 1.3). B1 shows the staining with the ER marker; C1 shows a marker for endosomes. B2 and C2 show the EGFP-ENaC localization in these cells. The merged images were placed in the panel B3 (B1+B2) and C3 (C1+C2). Note the separation of ENaC localization from the ER in B3 and its separation from endosomes in C3.

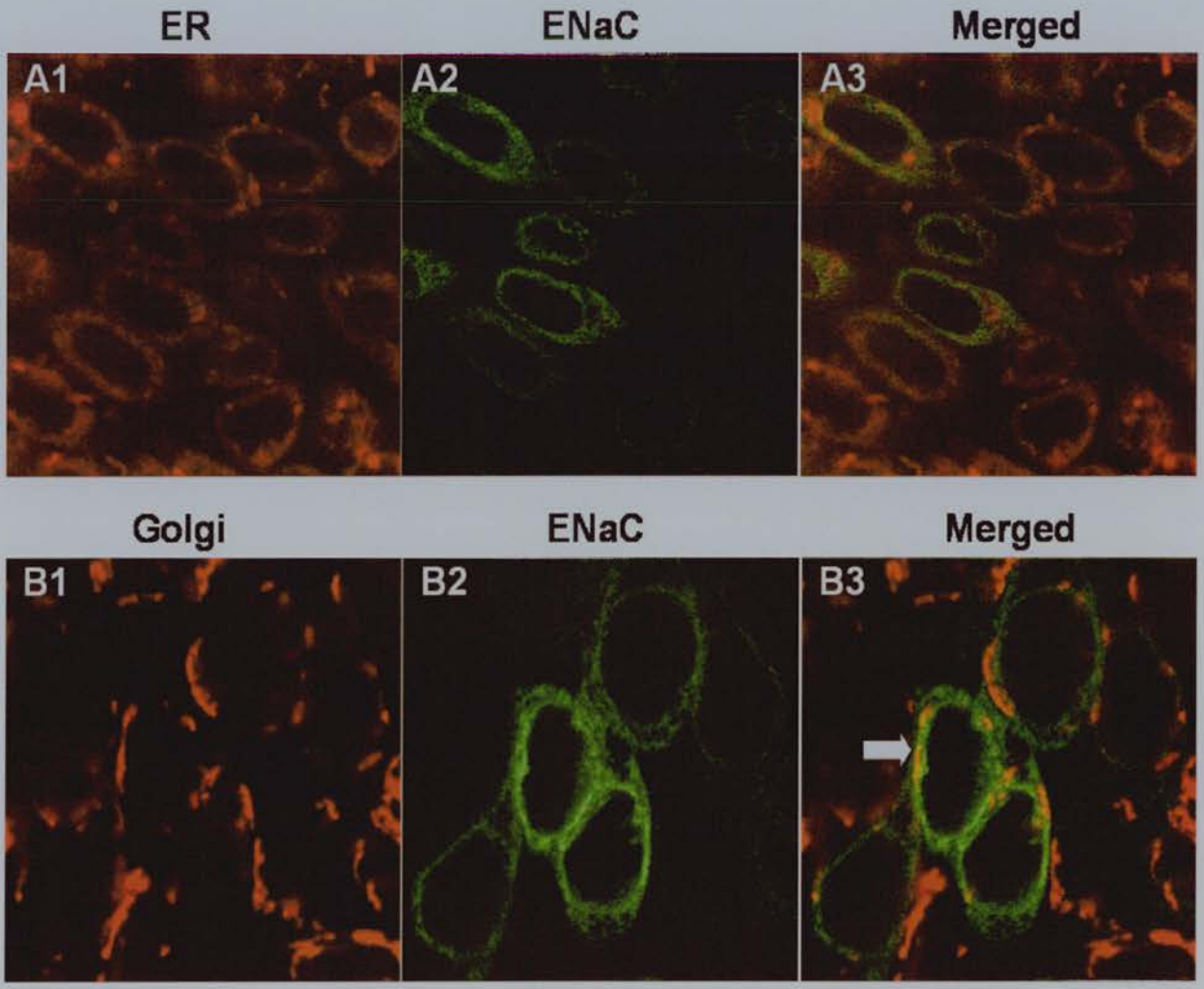

Figure 5.5. Comparison of the EGFP-ENaCβ subcellular localization to the ER and the Golgi apparatus in polarized M-1 epithelia. The fluorescence images of cell monolayers were captured by confocal microscopy. The cells were labeled with the ER marker (A1) or with the anti-Golgi antibody (B1). A2 and B2 reveal the ENaC subcellular localization. The merged images were placed in the panel A3 (A1+A2) and B3 (B1+B2). Note some co-localization of ENaC to the Golgi apparatus (B3).

presumably involving intracellular vesicles.

5.4.5 Corticosteroids promote ENaC translocation to the apical membrane of polarized M-1 cells

Next I labeled the apical membrane of polarized M-1 cells with WGA. To evaluate the distribution of ENaC throughout the entire volume of the cells as a monolayer, I acquired serial transverse optical sections from the top (apical) to the bottom (basal) of the cells by confocal microscopy and generated 3D stack reconstruction of these optical sections to allow a sagittal (side) view of the monolayer. In the control group (10μM RU486 and 100nM Dex), I found little or no ENaC localization to the apical membrane but high abundance of ENaC proteins in cytoplasm, especially the subapical region (Figure 5.6 A1-3 and a1-3). In contrast, stimulation with Dex resulted in translocation of ENaC proteins to the apical membrane of M-1 cells (Figure 5.6 B1-3 and c1-3). The effect was observed at concentrations of Dex as low as 10nM and became more pronounced at 100nM and 1μM. With or without the hormonal stimulation, the GFP fusion protein was not localized to the lateral membrane of M-1 cells (Figure 5.6 b1-3 and d1-3). In addition, I found ENaC distribution on the apical surface of M-1 cells and the apical surface itself labeled with WGA had a reticulated fluorescence pattern (Figure 5.6 c1-3). It is well established that this pattern is caused by increased optical path lengths through the microvilli and microridges compared with the flat areas on the apical membrane (Colarusso and Spring, 2002). The microvilli and microridges cause diffraction errors that make the apical plasma membrane one of the most difficult area of cells to study precise localization by the sagittal reconstruction. To provide a clearer view of the sagittal section of a monolayer, I rapidly froze the monolayer and performed the sagittal sectioning of the monolayer with a cryostat to produce 10μm-thick sections. These sections were thereafter visualized by confocal microscopy. Consistent with my previous data supplied by analyzing the stack of optical sections, I observed segregation of ENaC from the apical membrane in the control group as exemplified by measuring the apical to basal fluorescence intensity profile (Figure 5.7A). In contrast, the intensity profile of the Dex treatment group (100nM) showed a high

Figure 5.6. Corticosteroid effects on ENaC trafficking. Confocal optical sections of polarized M-1 cell monolayers in the sagittal plane (A-B: 1-3) and in the transverse plane (a-d: 1-3) show a predominantly subapical ENaC localization shifting apically into the plasma membrane in response to dexamethasone treatment (100nM). The apical and lateral membranes of cells were labeled with the membrane marker WGA (A-B1 and a-d1). A-B2 and a-d2 reveal the ENaC subcellular localization. The merged images were placed in the panel A-B3 and a-d3. Note the abundance of ENaC proteins in the subapical region (A3) and the apical translocation of ENaC (B3). Panels a1-3 and c1-3 show a transverse optical section through the top of the cells (at the level depicted by the line a and c); b1-3 and d1-3 through the middle (line b and d).

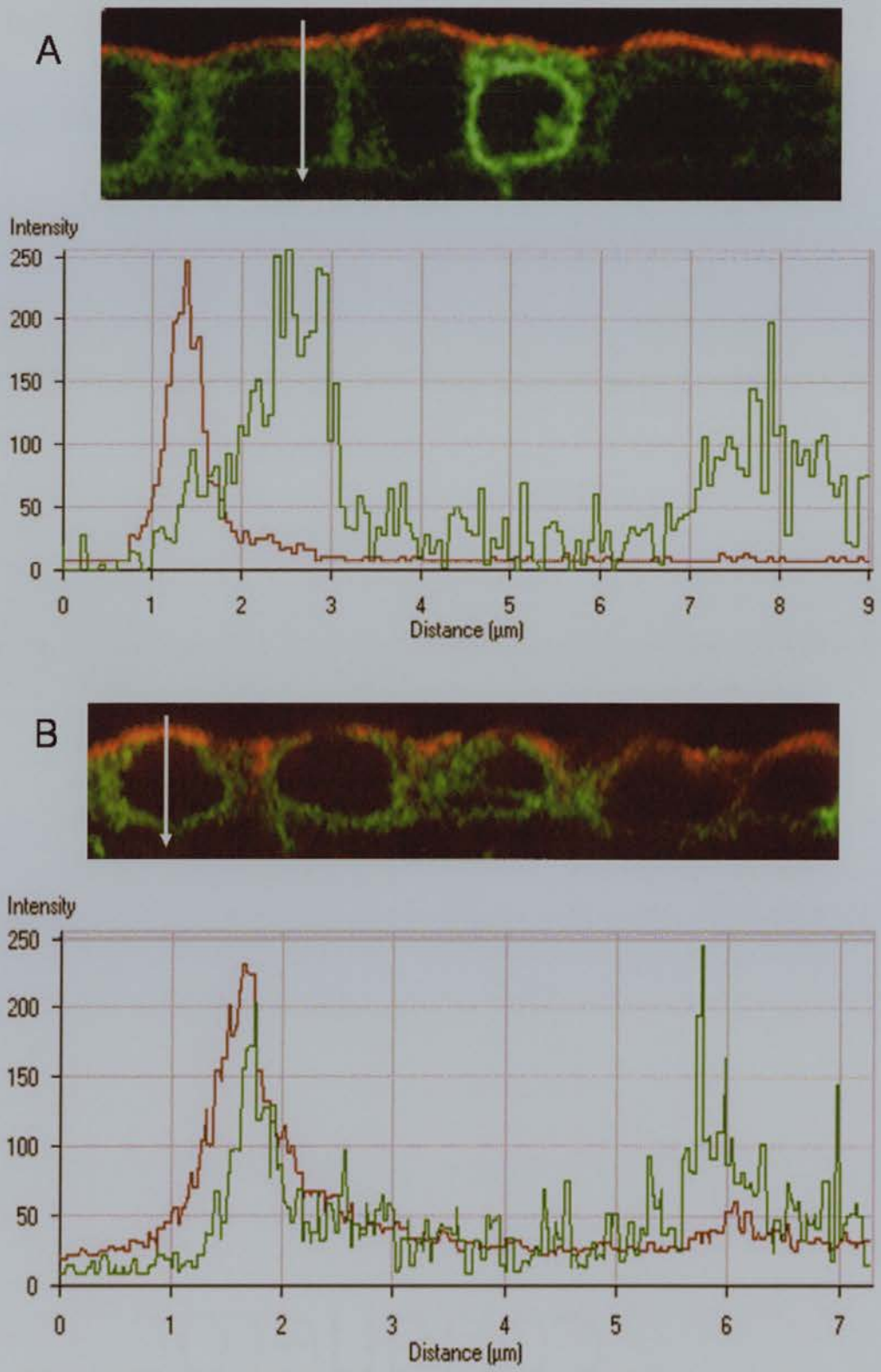

Figure 5.7. Apical movement of ENaC in M-1 cell monolayers sagittally sectioned to allow a clearer and more direct view from side (c.f. sagittal reconstruction images in Figure 5.6). Confocal microscopy images show the sagittal view of localization of the EGFP-ENaC proteins (green) and the apical membrane (red) in cell monolayers from the control group (A) and the Dex treatment group (B). The two-color fluorescence intensity profiles across the monolayer in A and B are shown underneath the images. The white arrow indicates where the representative intensity profiles were obtained. Note the shift of EGFP-ENaC to overlapping with the apical membrane in response to dexamethasone treatments.

degree of overlap between ENaC and the apical membrane (Figure 5.7B).

5.5 Discussion

Understanding the process of ENaC trafficking and its hormonal regulation is of fundamental importance. ENaC has three homologous subunits (α, β and γ) and forms a complex in a stoichiometry of 2α:1β:1γ (Firsov et al. 1996, 1998). ENaC assembly likely occurs in the ER (Adams CM et al. 1997) and the maximal surface expression of the channel complex is reached only when all three ENaC subunits are expressed in *X. laevis* oocytes (Canessa et al. 1994; Firsov et al. 1996). This indicates that if one subunit is labeled with the enhanced green fluorescence protein (EGFP) and expressed ectopically in the M-1 cells (that express all three subunits endogenously), it will replace some of the same subunit endogenously expressed and contribute to forming the three-subunit complex with the other two subunits and serve as a molecular tracer of the channel complex. Potentially each of the three subunits is a candidate with which to tag EGFP. One earlier study has reported ENaC subcellular localization and its trafficking in A6 cells by tagging EGFP to either α or β subunit and obtained similar findings (Blazer-Yost BL et al. 2001). As part of my research aim is to determine corticosteroids' influences on ENaC trafficking, it seems sensible to avoid choosing the α subunit of ENaC as a candidate because the endogenous ENaCα is itself transcriptionally upregulated by corticosteroids in the distal nephron cells (Asher C et al. 1996; Escoubet B et al. 1997; MacDonald P et al. 2000) and the constitutively expressed EGFP-ENaCα may obscure the stimulation of ENaCα by corticosteroids and its contribution to ENaC trafficking. Moreover, corticosteroids induce a shift in molecular weight of ENaCγ from 85 kDa to 70 kDa, due to the proteolytic clipping of the extracellular loop (Masilamani S et al. 1999). To avoid the post-translational modification of EGFP tagged ENaCγ, I have decided to use the β subunit and generated the mouse collecting duct M-1 cell lines stably expressing EGFP-tagged ENaCβ subunits.

I found ENaC fusion proteins had a distribution restricted to the endoplasmic reticulum (ER) in these mammalian collecting duct cells as single unpolarized cells.

This is consistent with previous studies conducted in *Xenopus* oocytes showing that ENaC maturation is inefficient (Valentijin JA et al. 1998). Treatments for 24-h with doses of dexamethasone ranging from 10nM to 1μM had no effect on the translocation of ENaC proteins in unpolarized M-1 cells. It is possible that the action of corticosteroids on ENaC depends upon the activation of proteins in the pathway contributing to the epithelial polarization. Recent studies have shown potential cell signaling molecules localized to the tight junction of cells or the regions of cell-cell contact, including the small GTPase Ras and the p85 regulatory subunit of phosphatidyl-inositol (PI) 3-kinase (Woo PL et al. 1999). Both Ras (Spindler B et al 1997, 1999) and PI3 kinase (Blazer-Yost BL et al 1998, 1999) are engaged in the transduction of corticosteroid-driven sodium re-absorption in the distal nephron.

When cells were polarized, the EGFP-ENaC proteins exited the ER and the Golgi apparatus and accumulated in punctate structures (presumably in intracellular vesicles) in cytoplasm. Numerous studies have confirmed that there exists a cytoplasmic pool of ENaC proteins (Morris RG et al. 1998; Hager H et al. 2001). Although I noticed some co-localization of ENaC to the Golgi apparatus, it only represented a minority of the chimeric ENaC proteins. This stands in contrast to other reports that ENaC is extensively co-localized to the Golgi apparatus in the MDCK cells (a cell line with a more proximal nephron ancestry) (Hanwell D et al. 2002). In addition, the exodus of EGFP-ENaC out of the ER was virtually complete, indicating incorporation of EGFP-ENaC into an efficient endogenous cell trafficking pathway.

Corticosteroids exert a profound impact upon the trafficking of ENaC proteins. Though one early study analyzed ENaC trafficking in A6 cells by labeling ENaC in the apical membrane with an anti-idiotypic antibody and showed that aldosterone failed to alter the apical surface expression of ENaC (Kleyman TR et al. 1992), my report is more consistent with more recent *in vitro* studies (Alvarez de la Rosa DA et al. 2002) and *in vivo* studies (Loffing J et al. 2000, 2001; Masilamani S et al. 1999) showing that translocation of ENaC proteins to the apical membrane follows treatments elevating the corticosteroid concentration. Furthermore, my study is the first one so far showing unequivocal imaging evidence of ENaC translocation to the

apical membrane induced by corticosteroids by counter-staining the cell membrane. Previous studies visualizing ENaC membrane expression lacked simultaneous counter-staining of cell membrane (Loffing J et al. 2000, 2001; Masilamani S et al. 1999; Blazer-Yost BL et al. 2001). Both my findings and reports of other groups showed that the accumulation of ENaC proteins did not occur on the basolateral membrane in response to corticosteroid stimulation (Loffing J et al. 2000, 2001).

Previous studies have indicated that AVP (that signals downstream pathways via cAMP) or forskolin (a direct activator of adenylate cyclase) stimulates the translocation of ENaC to the apical surface. Kleyman et al (1994) addressed the effect of AVP to promote ENaC trafficking to the apical membrane of A6 cells by labeling ENaC with an anti-idiotypic antibody. Blazer-Yost BL et al (2001) used A6 cell lines to express *Xenopus* ENaC subunits tagged to GFP. She demonstrated that forskolin treatment produced an acute increase in the fluorescence labeled ENaC in the apical membrane. My study is the first to dissect the subcellular events underpinning the ENaC trafficking response to forskolin stimulation. I found that forskolin fostered the exodus of ENaC out of the endoplasmic reticulum and entering intracellular vesicles. These vesicles where ENaC resided were distinct from those involved in the endocytic pathway as shown by the lack of their co-localization with transferrin-labeled vesicles. This suggests that forskolin stimulates the exocytic transport of ENaC, which is consistent with these earlier studies.

In conclusion, this study is the first to investigate the intracellular trafficking of ENaC proteins in mouse collecting duct M-1 cells as well as the first to generate M-1 cell lines stably expressing EGFP-fused ENaC proteins. Previous work has examined ENaC trafficking in the *Xenopus* A6 cells, *Xenopus* oocytes, HEK-293 cells, COS cells and MDCK cells that either endogenously or ectopically (usually transiently) expressed ENaC. While these studies have contributed to our understanding of channel trafficking, it is difficult to use such surrogate systems to study channel trafficking when its endogenous regulators in mammalian distal nephron are largely unknown and may be absent in other distinctly related cell types. As the current work was conducted in cells derived from the mammalian distal nephron, it allows a clearer

view of ENaC trafficking and its regulation by hormones. Additionally, M-1 cells are a well-established model for assessing the hormonal stimulation of sodium transport (Stoos BA et al. 1991; Helms MN et al. 2003; Letz B et al. 1995; Chalfant ML et al. 1996; Nakhoul NL et al. 1998). Furthermore, this study gives novel insights by determining the effect of epithelial polarization upon the intracellular localization of ENaC proteins. ENaC localization is conspicuously dependent upon the state of polarization. Not only does this suggest that the pathway involved in the cell polarization may cross-talk with that regulating ENaC trafficking, but also it contrasts with the view that trafficking of ENaC proteins may be governed by a universal mechanism common to diverse cell types: from the non-epithelia (the *Xenopus* oocytes), less differentiated renal cells (the HEK-293 cells) and fully differentiated renal epithelial cells (the collecting duct cells) alike. Finally, polarization seems to be a key factor in hormonal modulation of ENaC trafficking and appears to be a prerequisite for corticosteroid induced apical trafficking of ENaC. I hypothesize a pathway of ENaC trafficking and its response to corticosteroids. Firstly, an early corticosteroid-independent stage may occur prior to polarization with ENaC exodus from the ER to vesicles, forming a potentially mobile intracellular pool of ENaC. Once cells become fully polarized, a second corticosteroid-dependent stage may then follow in which corticosteroids promote ENaC translocation to the apical membrane. The genes underpinning the first stage are largely unknown but the individual molecular steps comprising the second stage have attracted much attention and clearly involve corticosteroid induced proteins (CIPs). For example, sgk1, a kinase induced in distal nephron by corticosteroids (Hou J et al. 2002) may be a key factor that modulates the apical targeting of ENaC (Alvarez de la Rosa D et al. 1999).

CHAPTER 6

THE ROLE OF SGK1 IN MODULATING ENAC CONDUCTANCE AND TRAFFICKING AND GENERATION OF A CELL MODEL TO CONTROL SGK1 EXPRESSION

6.1 Summary

The serine-threonine kinase sgk1 was recently identified as a gene rapidly induced by corticosteroids, resulting in increased sodium transport. In unpolarized distal nephron M-1 cells, I have found that sgk1 has no effects on ENaC intracellular trafficking. In addition, sgk1 itself is localized to the intracellular compartment distinct from ENaC. To elucidate the role of sgk1 in modulating ENaC conductance, I have generated M-1 cell lines stably transfected with sgk1 whose gene expression level is tightly controlled by the tetracycline-inducible system. In these cell lines, sgk1 gene has no 'leaky' expression and its gene induction is highly responsive to tetracycline (10-fold induction at ≤10ng/ml versus 10μg/ml). This model can become available and widely accessible to determine whether upregulation of sgk1 by tetracycline influences ENaC-mediated sodium reabsorption in parallel to that by corticosteroids.

6.2 Introduction

The serum and glucocorticoid kinase 1 (sgk1) was first identified as an aldosterone induced protein *in vitro* in amphibian (Chen SY et al. 1999) and mammalian cell lines (Naray-Fejes-Toth A et al. 1999) and later *in vivo* in rat (Brennan FE and Fuller PJ. 2000; Bhargava A et al. 2001) and mouse kidneys (Hou J et al. 2002). When co-injected with ENaC subunits into *Xenopus* oocytes, sgk1 significantly elevates the ENaC-mediated sodium transport and the surface expression of ENaC subunits (Chen SY et al. 1999; Alvarez de la Rosa D et al. 1999). Over-expression of sgk1 in *Xenopus* A6 cell line (Faletti CJ et al. 2002; Alvarez de la Rosa D and Canessa CM. 2003) and mouse M-1 cell lines (Helms MN et al. 2002) increases the basal level of sodium transport by 2-5 fold. These studies suggest that sgk1 may be a critical component in

the pathway of aldosterone to the hormone driven sodium reabsorption.

How sgk1 modulates ENaC conductance and its surface expression is largely elusive. Initial thoughts about the mechanism of sgk1's action included the notion that it directly interacted with ENaC to dynamically regulate ENaC insertion into and/or retrieval from the apical membrane. Indeed, Sgk1 physically interacts with the COOH termini of both α- and β-ENaC, when the latter proteins are expressed as glutathione S-transferase fusion proteins (Wang J et al 2001). Snyder and colleagues (Snyder PM et al 2002) recently showed that sgk1 phosphorylated the ubiquitin ligase NEDD4–2 to inhibit the latter's function and its binding to ENaC, which was independently confirmed by Debonneville and colleagues (Debonneville C et al 2001). The reduced binding of NEDD4-2 to ENaC leads to a subsequent decrease in the rate of ENaC endocytosis from the cell surface and thus prolongs the half-life of ENaC. This view of sgk1's suppressing ENaC endocytosis is further complicated by the fact that sgk1's homologue in *S. cerevisiae* (Ypk1) is required for both receptor-mediated and fluid-phase endocytosis (DeHart A et al. 2002).

Previous studies of determining sgk1's effects on ENaC conductance and protein trafficking were mostly conducted in *Xenopus* oocyte expression system. In this study, I aim to first answer whether sgk1 alters ENaC subcellular localization in distal nephron M-1 cells. Second, I aim to answer whether sgk1 co-localizes with ENaC in M-1 cells. Finally, I aim to generate a cell model in which the expression of sgk1 can be tightly regulated by the tetracycline inducible system. This model can become available and widely accessible to determine whether upregulation of sgk1 by tetracycline influences ENaC-mediated sodium reabsorption in parallel to that by corticosteroids.

6.3 Results

6.3.1 ENaC is confined to the endoplasmic reticulum when co-transfected with sgk1 in unpolarized M-1 cells

In Chapter 5.4.2, I have shown ENaC is confined to the endoplasmic reticulum in unpolarized M-1 cells. To determine sgk1's effects on the localization of ENaC protein in unpolarized M-1 cells, I sparsely seeded cells onto glass coverslips and co-transfected cells with EGFP-ENaCβ and sgk1 at the molar ratio of 1:1, 1:2 and 2:1 48h prior to fixation. As shown in Figure 6.1A, sgk1 co-transfection with EGFP-ENaCβ did not alter the intracellular localization of ENaC. ENaC had a cytoplasmic reticular distribution suggestive of the endoplasmic reticulum (ER). Counterstaining the ER membrane with the rhodamine-B hexyl ester revealed the localization of ENaC in the ER (Figure 6.1a-c).

6.3.2 Sgk1 and ENaC are localized to distinct intracellular compartments

To determine whether sgk1 co-localizes with ENaC in unpolarized M-1 cells, I co-transfected cells with EGFP fused ENaCβ and HcRed (red fluorescence protein) fused sgk1. Merging the channel of EGFP fluorescence (Figure 6.2 A1) with the HcRed fluorescence (Figure 6.2 A2) indicated that sgk1 was localized largely to some intracellular compartment distinct from that of ENaC (i.e. the ER), probably in cytosol (Figure 6.2 A3).

6.3.3 Generation of tetracycline-inducible expression of sgk1 in M-1 cells

The tetracycline-inducible (Tet) system (Gossen M and Bujard H. 1992) was used to regulate the expression level of sgk1 in M-1 cells (Figure 6.3). The first critical component of the Tet system is the regulatory protein (named tetracycline transactivator or tTA encoded by pTet-Off), a 37-kDa fusion protein made of the *E.coli* DNA binding protein (TetR) and the Herpes simplex virus VP16 activation domain. The second component is the response plasmid (TRE-EYFP-sgk1) that

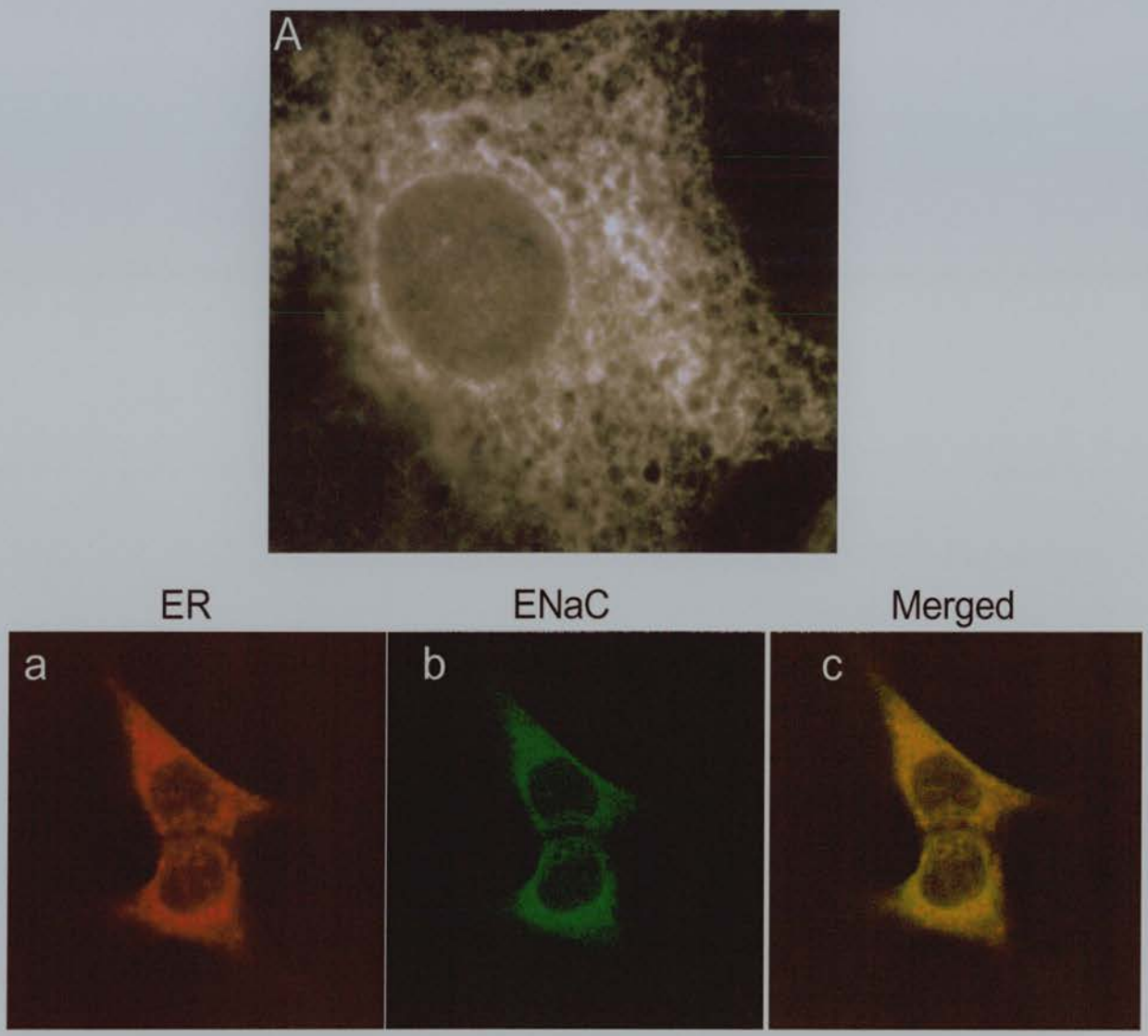

Figure 6.1. Sgk1 effect on ENaC trafficking in unpolarized M-1 cells. Unpolarized M-1 cells were co-transfected with EGFP-ENaCβ and sgk1. The fluorescence image of M-1 cells (A) was captured by the Zeiss Axio-epifluorescence microscope (x100, NA 1.4); and images (a-c) by the Zeiss 510 confocal microscope (x40, NA 1.3). Panel a shows the staining with the ER marker; b the localization of ENaC and the merged image was placed in the panel c. Note the confinement of ENaC in ER in the presence of sgk1 expression.

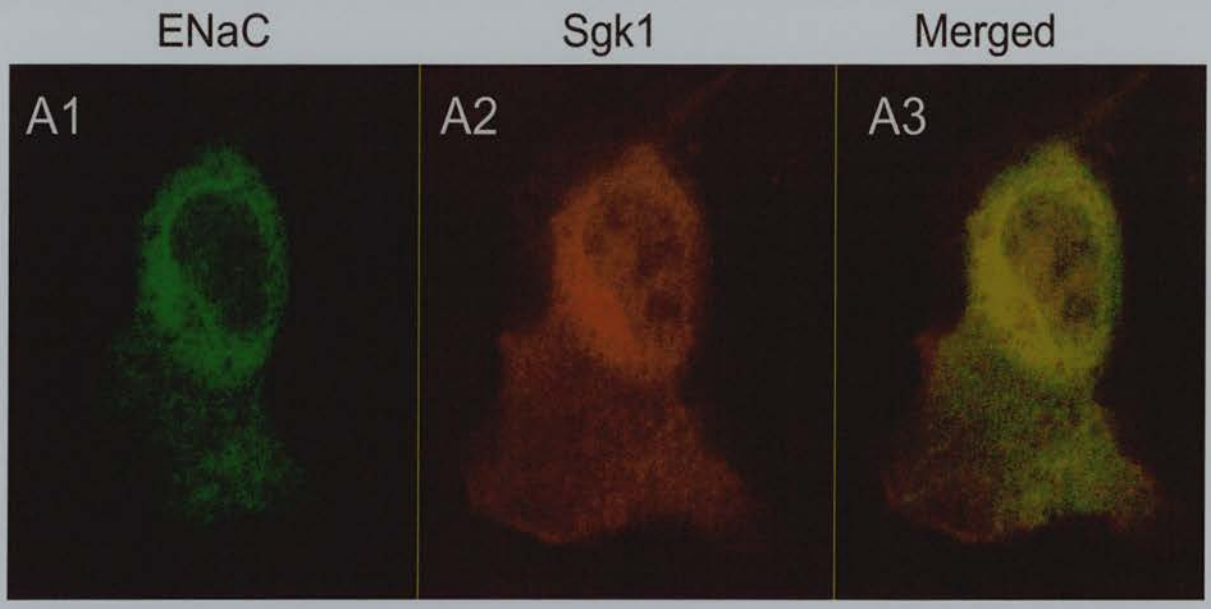

Figure 6.2. Studies of the intracellular localization of ENaC and Sgk1. Unpolarized M-1 cells were co-transfected with EGFP-ENaCβ and HcRed-sgk1. The fluorescence images (A1-3) were captured by the Zeiss 510 confocal microscope (x40, NA 1.3). Panel A1 shows the localization of ENaC; A2 the localization of sgk1 and the merged image was placed in the panel A3. Note the lack of co-localization between ENaC and sgk1.

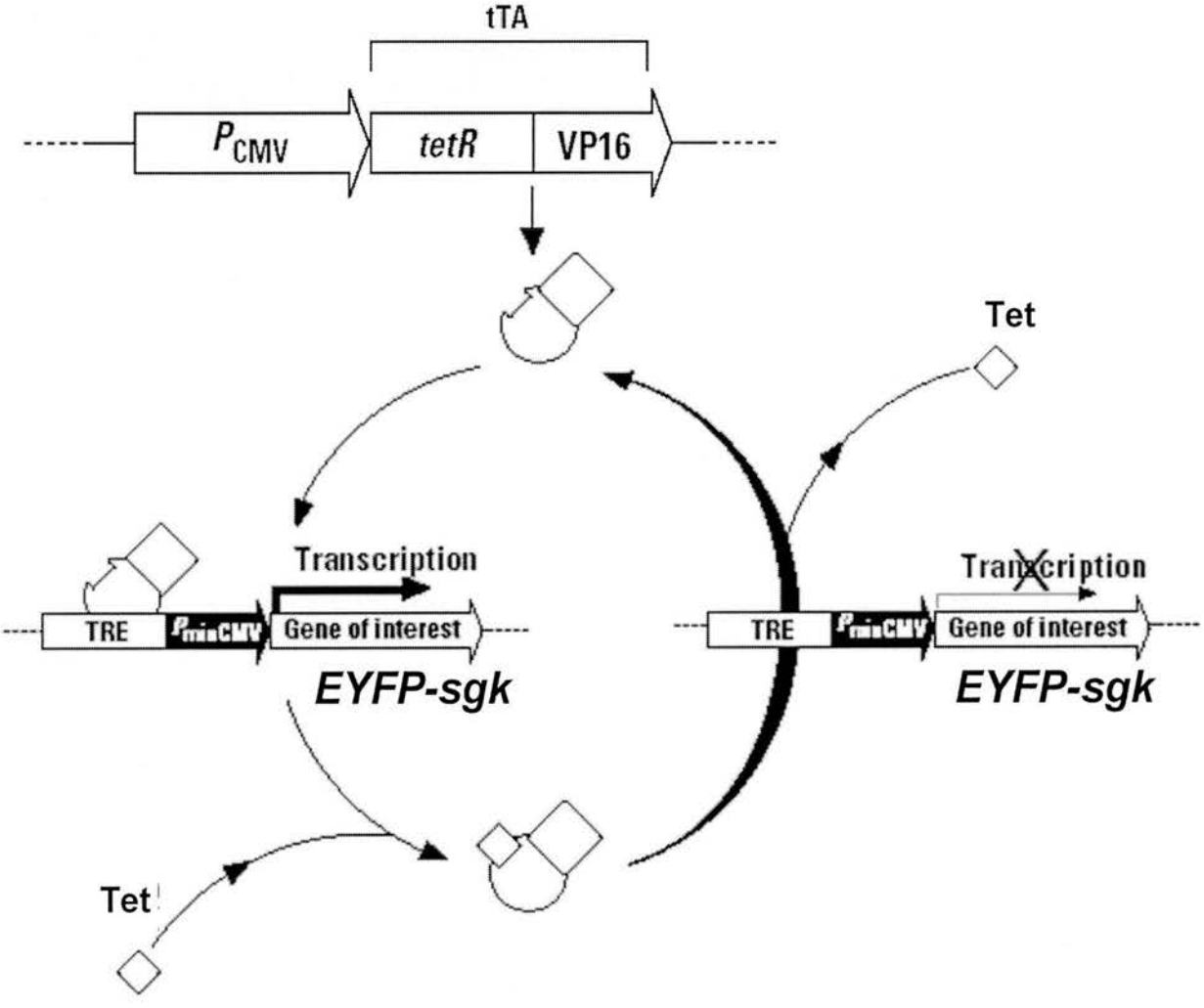

Figure 6.3 Schematic of the expression vector plasmid and the mechanism of tetracycline-inducible system. PCMV, cytomegalovirus immediate early promoter; PminCMV, minimal cytomegalovirus promoter; TRE, tetracycline responsive element; tTA: tetracycline transactivator; EYFP: enhanced yello fluorescence protein; SGK: serum and glucocorticoid kinase; Tet: tetracycline.

expresses enhanced yellow fluorescence protein (EYFP) fused sgk1 under control of the tetracycline-response element, or TRE. TRE consists of seven direct repeats of a 42-bp Tet operator sequence (TetO), and is located just upstream of the minimal CMV promoter that lacks the strong enhancer elements normally associated with the CMV immediate early promoter. Because these enhancer elements are missing, there is no 'leaky' expression of EYFP-sgk1 from TRE. tTA stimulates the transcription of EYFP-sgk1 by binding to TetO in the absence of tetracycline. Addition of tetracycline prevents the binding of tTA to TetO and thus silences gene expression. The making of tetracycline inducible cell lines involved two rounds of transfection and selection of stable clones. On the first round, M-1 cells were transfected with the construct pTet-Off that expressed tTA from the CMV immediate early promoter. Out of 30 cell lines selected, one was chosen with the highest fold-induction of transient EYFP-sgk1 expression and thus named tTA-M-1. Next round, tTA-M-1 cells were transfected with the construct TRE-EYFP-sgk1 and grown in the presence of 1μg/ml tetracycline. Among the 50 cell lines screened through, I analyzed two cell lines showing highest fold-induction of stable EYFP-sgk1 expression and focused on one cell line in the following experiments.

6.3.4 Characterization of the transgenic cell lines.

To verify that EYFP-sgk1 gene was expressed in the clonal cell lines and tightly regulated by tetracycline, I analyzed the EYFP fusion protein product by western blotting. When medium was depleted with tetracycline (ON status), a distinct band with a molecular weight of ~80kDa was detected on the PVDF membrane probed with an anti-EYFP antibody (Figure 6.4). The 24-h treatment with 1μg/ml tetracycline (OFF status) effectively silenced EYFP-sgk1's expression. The parental M-1 cells did not contain a similar epitope. Examination of the fluorescence micrograph (Figure 6.5A) of the M-1 cells revealed that the sgk1 fusion gene had no 'leaky' expression and was highly stimulated upon removal of tetracycline. At high magnification the fluorescence imaging of sgk1 fusion proteins showed a diffuse cytoplasmic pattern lacking the appearance on nuclear envelope and a reticular structure (Figure 6.5B), suggestive of their localization being cytosolic. Next, I gave cells 24-h treatments

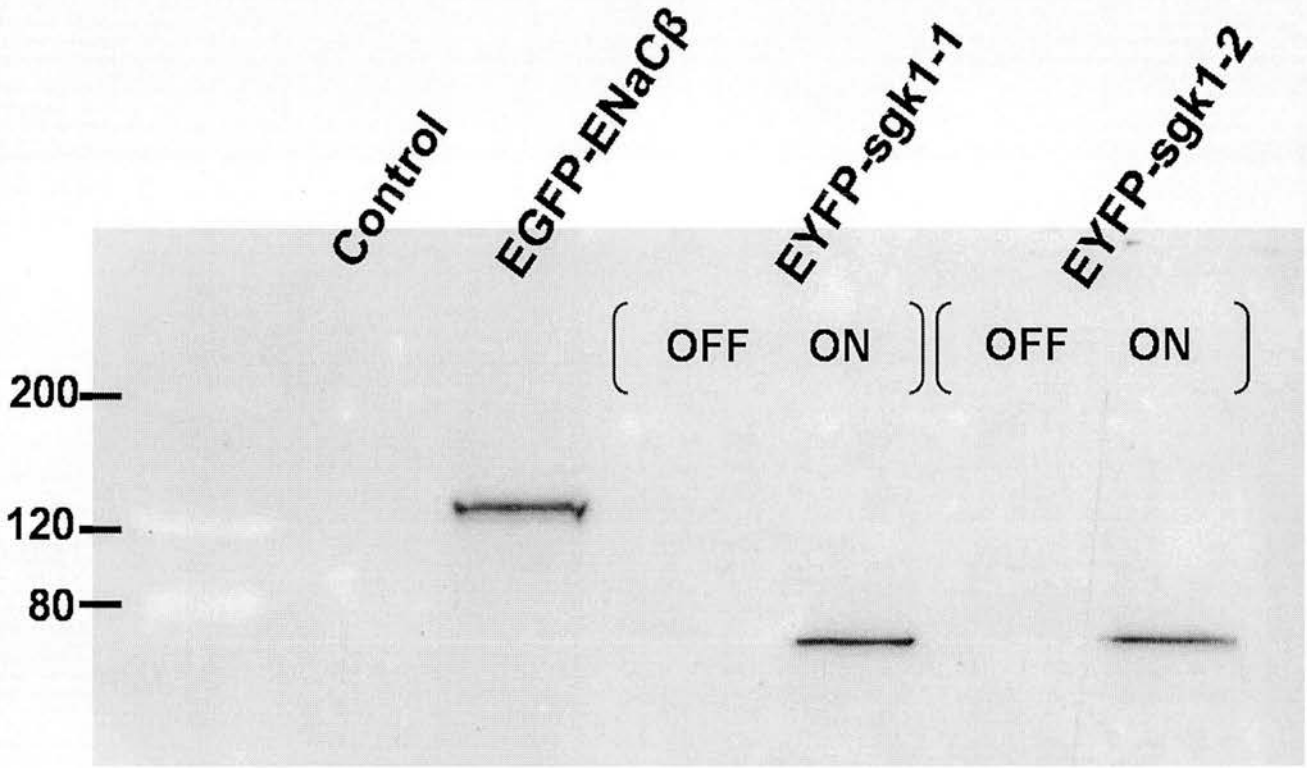

Figure 6.4. Western blotting analysis of the EYFP-sgk1 stable cell lines. The position of the molecular weight standards (in kDa) was shown at left. When medium was depleted with tetracycline (ON status), a distinct band with the molecular weight of ~80kDa was found in the stable cell lines (EYFP-sgk1-1 and -2) but not in the control (parental M-1 cells). The 24-h treatment with 1μg/ml tetracycline (OFF status) effectively silenced EYFP-sgk1's expression. The expression of EGFP-ENaCβ was used as a positive control.

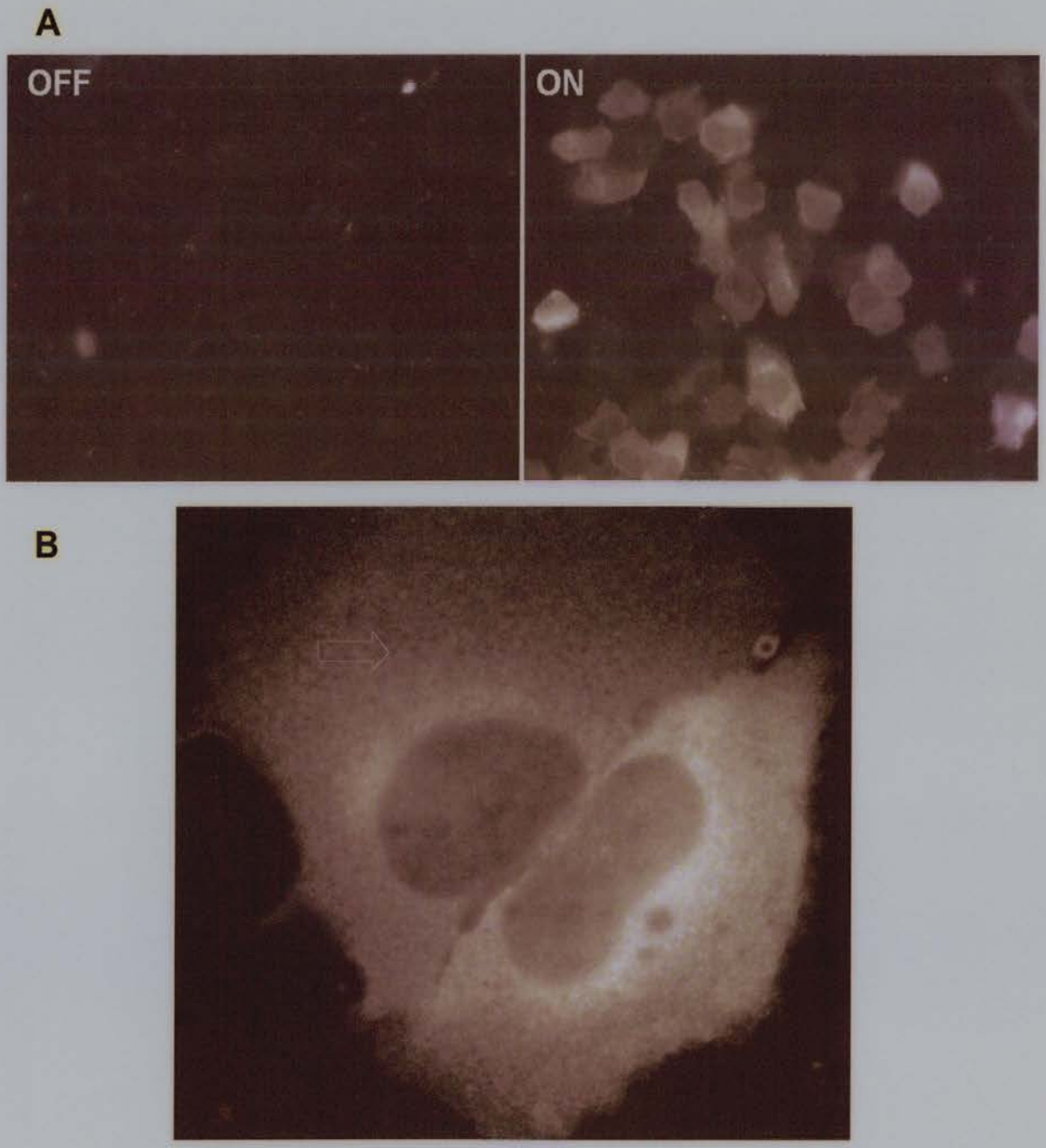

Figure 6.5. Fluorescence images of the M-1 cells expressing EYFP-sgk1 proteins. Cells were grown on coverslips, fixed and mounted as described under Methods . Fluorescence images were captured by the Zeiss Axio-epifluorescence microscope (A: x16, NA 0.5; B: x100, NA1.4). Note the sgk1 fusion proteins have a diffuse cytoplasmic distribution (B: arrow).

with a range of doses of tetracycline (Tet: 10μg/ml, 1μg/ml, 100ng/ml, 10ng/ml and 1ng/ml and 0). The analysis by FACS revealed that the expression level of EYFP-sgk1 was dependent upon the dose of tetracycline (removal of tetracycline) in two ways: (1) the percentage of EYFP expressing cells increased, even though the heterogeneity of EYFP fluorescence level existed in this cell line (Figure 6.6); (2) the absolute EYFP fluorescence level increased, showing a maximum of 10-fold induction at the tetracycline concentration of ≤1ng/ml ($p<0.001$ *versus* 10μg/ml) (Figure 6.7). In addition, the cell line exhibited high transepithelial resistance (>1,000 $\Omega \cdot cm^2$) when fully polarized after 7-10 days. Tetracycline-induced sgk1 expression had no effect on transepithelial resistance (1.715±0.127kΩ at 0 tetracycline compared to 2.370±0.28kΩ at 10μg/ml tetracycline, p=0.260, n=6).

6.4 Discussion

The mechanism of sgk1's influences on ENaC conductance has been elusive so far. Previous attempts to elucidate sgk1's function have been mostly carried out in *Xenopus* oocytes. In oocytes, sgk1 increases the number of ENaC in the plasma membrane independently of overt effects on the gating kinetics of this channel (De La Rosa DA et al 1999; Loffing J et al 2001; Wagner CA et al 2001). In contrast, I have found sgk1 has no effects on ENaC intracellular trafficking in unpolarized distal nephron M-1 cells. This is consistent with my previous findings and hypothesis (Chapter 5) that polarization is a prerequisite for corticosteroid induced membrane trafficking of ENaC and furthermore indicates that polarization may have to be fulfilled so that sgk1 functions to link corticosteroids to stimulated ENaC trafficking.

Though sgk1 has been shown to physically interact with ENaC α and β subunits *in vitro* (Wang J et al 2001), my findings suggest that in distal nephron cells sgk1 and ENaC β are actually localized to distinct intracellular compartments. It is possible that the physical association between sgk1 and ENaC is transient or only occurs between a minority of proteins. Sgk1 may compete with Nedd-4-2 to bind to ENaC and thus modulate ENaC surface expression.

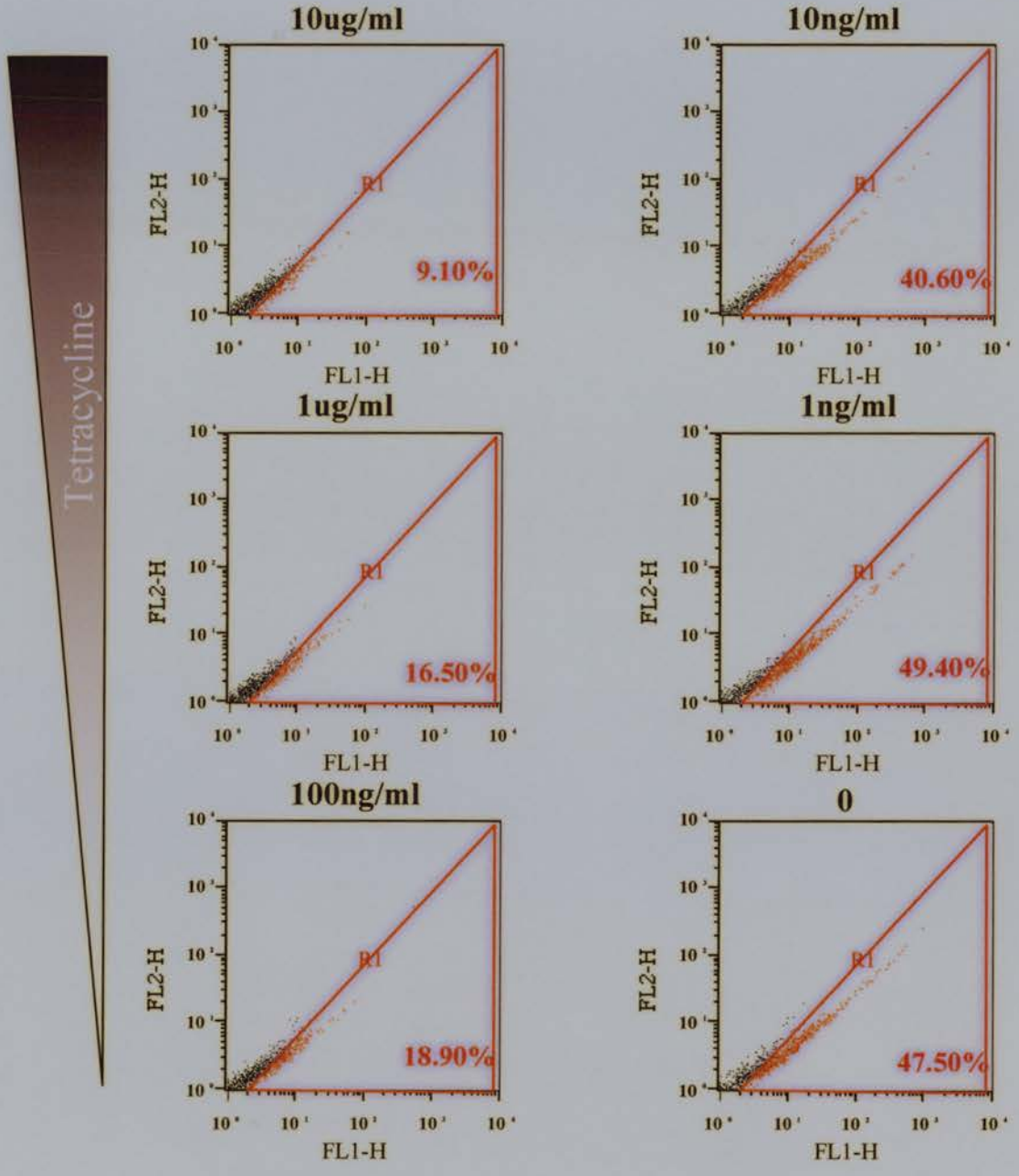

Figure 6.6. FACS analysis of the dose dependence of EYFP-sgk1 expression upon tetracycline. M-1 cells were treated for 24-h with a range of doses of tetracycline (Tet: 10ug/ml, 1ug/ml, 100ng/ml, 10ng/ml, 1ng/ml and 0). Note the percentage of EYFP expressing cells increases as tetracycline was progressively removed.

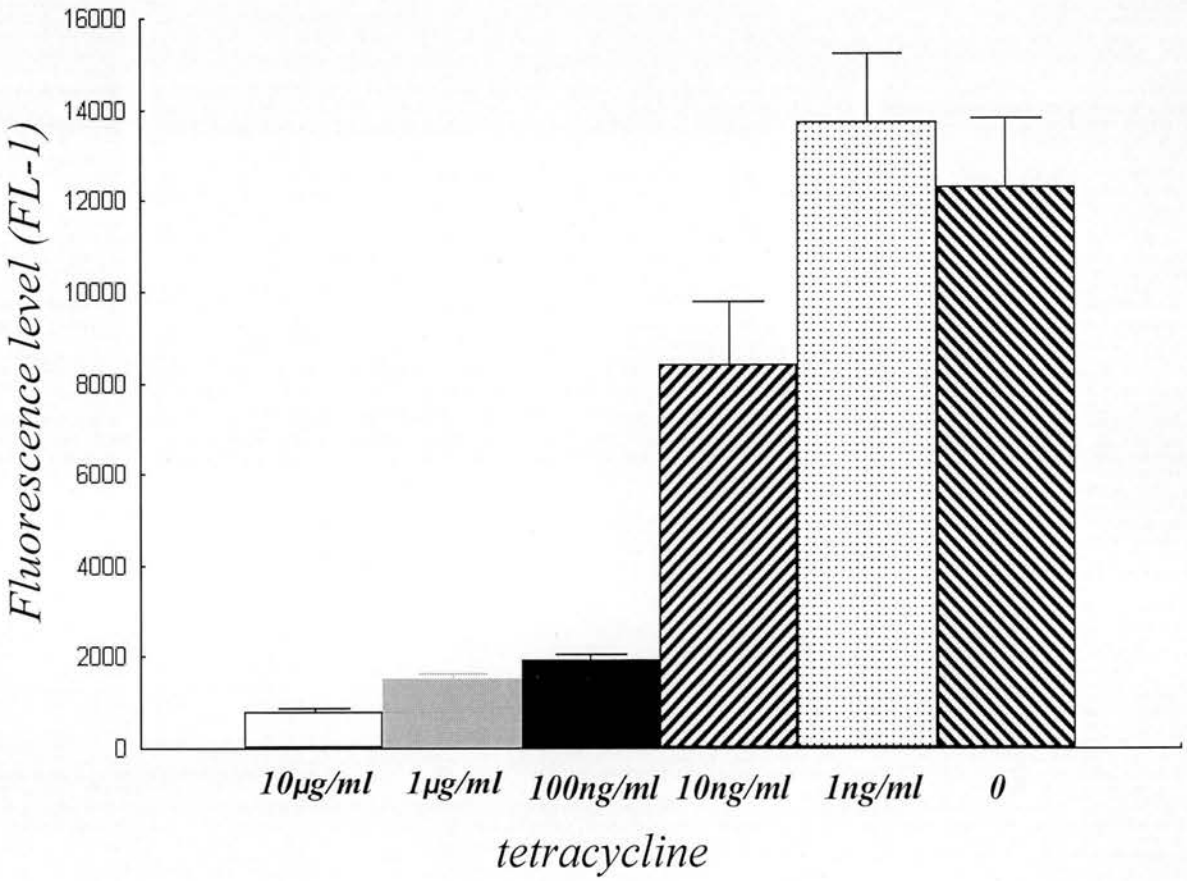

Figure 6.7. Quantification of EYFP-sgk1 expression in response to tetracycline. M-1 cells were treated for 24-h with a range of doses of tetracycline (Tet: 10µg/ml, 1µg/ml, 100ng/ml, 10ng/ml, 1ng/ml and 0). Note the induction of EYFP expression level when tetracycline is removed.

I have reported for the first time the generation of mouse collecting duct cell lines (M-1) that stably express sgk1 whose gene expression level is tightly controlled by the tetracycline-inducible system. In these cell lines, sgk1 gene has no 'leaky' expression and its gene induction is highly responsive to tetracycline. In addition, this cell line grows normally and forms high transepithelial resistance when becoming fully polarized. Sgk1 over-expression had no effect on transepithelial resistance of cells, suggesting sgk1 is not involved in modulating ion transport via the paracellular pathway (Zahraoui A et al 2000). My preliminary studies have also found no effects of sgk1 induction upon transepithelial potential difference (TPD) (2.483±0.079mV at 0 tetracycline compared to 2.540±0.312mV at 10μg/ml tetracycline, p=0.66, n=6). Theoretically, ionic equilibrium potentials (IEP) vary logarithmically with the ion concentration ratio between the apical side and the basal side (Boltzmann/Nernst equation). TPD is the sum of IEP of all ions present (including Na^+, K^+, Cl^-, Ca^{2+} et al) and in fact reflects the 'difference' of concentration of ions between the two sides, which is in turn determined by the conductivity of every ion transporter (including channels, Na^+/K^+-ATPase, co-transporters and exchangers). Ideally, if sgk1 only affects the transport of Na^+ via ENaC on the apical membrane of distal nephron, sodium concentration will increase in the basal medium at equilibrium, which will therefore elicit a change in TPD. Nevertheless, it has been found that sgk1 modulates the conductivity of a number of ion transporters [including ROMK (Kir1.1, a K^+ channel expressed on the apical surface of distal nephron: Yoo D et al 2003), Kv1 (a voltage gated K^+ channel in brain: Gamper N et al 2002), NHE3 (sodium hydrogen exchanger 3 in proximal tubules: Yun CC et al 2002) and NKCC2 ($Na^+/K^+/2Cl^-$ cotransporter 2 in thick ascending limbs: Lang F et al 2000)]. The complex effects of sgk1 on ion transport make it illicit to attribute TPD changes to changes in Na^+ transport alone. Thus further studies to elucidate the influences of sgk1 on sodium reabsorption may require a more sensitive and accurate approach of electrophysiology (for example, perfusing the cell monolayer with medium containing single cation in Ussing chambers and detecting short-circuit current or $^{22}Na^+$ current by adding an external electric field to offset TPD).

Potentially, this cell model can be used to elucidate the influences of sgk1 upon ENaC,

Na^+/K^+-ATPase, ROMK and others. Electrophysiological approach will provide functional data on transporter conductivity. The answer to how sgk1 modulates the trafficking of these ion transporters can be sought by approaches of cell biology. A modified protocol based upon Firsov D et al (1996) could be followed to develop a quantitative method to measure the surface expression level of transporter proteins, in which a hemagglutinin (HA) epitope is inserted into the extracellular loop of transporter. The level of HA expression detected by immunofluorescence reflects the amount of transporter proteins on the cell surface.

CHAPTER 7 DISCUSSION

Aldosterone is the primary hormone responsible for maintaining sodium reabsorption in the distal nephron of kidney. The Na^+ transport induced by aldosterone, is handled via the epithelial Na^+ channel (ENaC) (Rossier BC 1997; Horisberger JD 1998). The early phase of aldosterone action is often demarcated as the period when the pre-existing ENaC channels in the plasma membrane are activated; and the late phase (>3h) is when *de novo* synthesis of ENaC and its translocation to the plasma membrane take place (Verrey F et al 2000). Aldosterone influences expression of a broad pool of genes, the protein products of which transduce the actions of aldosterone in the nucleus out to the plasma membrane where its final effector ENaC is located. The first two aims of my PhD studies were to identify and characterize the genes that are transcriptionally regulated by aldosterone in the distal nephron. The strategy to achieve these aims involved: 1, systematically screening a large pool of candidate genes including those playing a pivotal role in the aldosterone pathway (MR and 11β-HSD2), those discovered by others and shown to be regulated by aldosterone (such as sgk1 and K-Ras) and those generated in the host laboratory; 2, focusing upon the gene sgk1 and its regulation by aldosterone in the distal nephron to elucidate whether regulation of sgk1 expression is consistent with its playing a role in transduction of aldosterone-driven sodium reabsorption.

The serine-threonine kinase sgk1 was first identified as a gene rapidly induced by aldosterone in the *Xenopus* A6 cell line, resulting in increased sodium transport *in vitro* (Chen SY et al. 1999). Others have confirmed the upregulation of sgk1 by aldosterone in the cell line derived from the distal nephron of rat, rabbit and mouse (Shigaev A et al 2000; Naray-Fejes-Toth A et al 1999). These *in vitro* findings identify sgk1 as a good candidate gene in hormonal regulation of sodium transport in cells of distal nephron. My research objective in achieving significant results was to determine the distribution of sgk1 in intact kidney and study its hormonal regulation *in vivo*. Although there have been some *in vivo* studies carried out previously, their research plans were limited to investigating the short-term (0.5hr-4hr) effect of aldosterone on sgk1 expression (Chen SY et al. 1999; Brennan FE and Fuller PJ 2000;

Bhargava A et al. 2001). In my thesis, I have determined the effect of aldosterone on sgk1 expression in both short term (acute) and long term (chronic) hyperaldosteronism. I have also examined the regulation of sgk1 by aldosterone in substantial detail including the dose response and cellular localization.

In kidney of control mice, I found an abundant expression of sgk1 in glomeruli and inner medullary collecting ducts, which was maintained independent of corticosteroids and thus persisted in adrenalectomized animals. I find in mice both acute and chronic aldosterone infusions induced sgk1 expression in the distal nephron (including the distal tubules through to the outer medullary collecting ducts). These regions have the potential to mediate amiloride-sensitive sodium transport, as they are the major sites of ENaC action. Most importantly, my work has shown for the first time an axial heterogeneity of prolonged upregulation of sgk1 mRNA, which correlates with the plasma level of aldosterone across groups on low-sodium diet to low-dose and high-dose aldosterone infusions. It appeared that mild aldosterone excess (0.03% sodium diet) induced sgk1 in the cortical portion of distal nephron whereas moderate (50μg/kg infusion) and more severe (150μg/kg and 750μg/kg infusions) excess affected the entire distal nephron. This heterogeneity of sgk1 expression would eventually translate to heterogeneity of sgk1 modulation of sodium transport along the distal nephron.

My study is so far the first to assess sgk1 regulation using *in situ* hybridization in mouse as well as the first to carefully quantify the degree of its induction in different parts of the nephron (distal tubules, glomeruli and inner medulla) using silver-grain counting. The upregulation of sgk1 mRNA exhibited dose dependence in individual renal tubules over a range of circulating aldosterone (2 to 75-fold elevation). The fact that the induction of sgk1 exhibited a ceiling (8-fold elevation) in animals with severe aldosterone excess suggests that the aldosterone-sgk1-ENaC pathway responses reach saturation at this level. It is possible that this is due to saturation of available MR sites. Potentially this mechanism may contribute to the 'escape' of kidney from aldosterone-induced Na retention (i.e. the reaching of the ceiling of sgk1 expression translates to the peaking of sodium reabsorption induced by sgk1 and its related pathway).

The next two aims of my PhD studies involve elucidation of the function of sgk1. Previous studies have shown that when co-injected with ENaC subunits into *Xenopus* oocytes, sgk1 significantly elevates the ENaC-mediated sodium transport and the surface expression of ENaC subunits (Chen SY et al. 1999; Alvarez de la Rosa D et al. 1999). It has long been thought that sgk1 links aldosterone to the hormone driven sodium reabsorption in distal nephron cells. The mechanism of sgk1 actions is largely elusive. A number of recent studies suggest that sgk1 mediates exocytosis (Alvarez de la Rosa D et al. 1999) or endocytosis (Debonneville C et al 2001; Snyder PM et al 2002) of ENaC in *Xenopus* oocytes. Thus it has attracted much attention to investigate ENaC trafficking in mammalian distal nephron cells and its modulation by hormones (primarily corticosteroids) and the key genes underpinning the corticosteroid driven pathway (especially sgk1).

To achieve my objectives of elucidating the role that sgk1 plays in ENaC-mediated sodium transport and ENaC trafficking, I, at the first step, have generated the mouse collecting duct M-1 cell lines stably expressing EGFP-tagged ENaCβ subunit and investigated its intracellular trafficking and the influences of epithelial polarity and corticosteroids. The second step involves investigating the effects of sgk1 on ENaC trafficking and generation of a cell model in which the expression of sgk1 is tightly regulated by the tetracycline inducible system. This model is valuable in determining whether upregulation of sgk1 by tetracycline influences ENaC-mediated sodium reabsorption in parallel to that by corticosteroids.

I have found that EGFP-fused ENaCβ proteins had a distribution restricted to the endoplasmic reticulum (ER) in M-1 cells as single unpolarized cells. This is consistent with previous studies conducted in *Xenopus* oocytes showing that ENaC maturation is inefficient (Valentijin JA et al. 1998). Treatments for 24-h with doses of dexamethasone ranging from 10nM to 1μM had no effect on the translocation of ENaC proteins in unpolarized M-1 cells. When cells were polarized, the EGFP-ENaC proteins exited the ER and the Golgi apparatus and accumulated in punctate structures (presumably in intracellular vesicles) in cytoplasm. Numerous studies have confirmed

that there exists a cytoplasmic pool of ENaC proteins (Morris RG et al. 1998; Hager H et al. 2001). Corticosteroids (100nM Dex) exert a profound impact upon the trafficking of ENaC by promoting its translocation to the apical plasma membrane. The accumulation of ENaC proteins did not occur on the basolateral membrane in response to corticosteroid stimulation.

The novelty and significance of my research on ENaC trafficking are that my study is so far the first to determine the effect of epithelial polarization upon the intracellular localization of ENaC proteins. ENaC localization and its regulation by corticosteroids are conspicuously dependent upon the state of cell polarization. Not only does this suggest that the pathway involved in cell polarization may cross-talk with that regulating ENaC trafficking, but also it contrasts with the more traditional view that trafficking of ENaC proteins is governed by a universal mechanism common to diverse cell types: from the non-epithelia (the *Xenopus* oocytes), less differentiated renal cells (the HEK-293 cells) and fully differentiated renal epithelial cells (the collecting duct cells) alike. I hypothesize a pathway of ENaC trafficking and its response to corticosteroids. Firstly, an early corticosteroid-independent stage may occur prior to polarization with ENaC exodus from the ER to vesicles, forming a potentially mobile intracellular pool of ENaC. Once cells become fully polarized, a second corticosteroid-dependent stage may then follow in which corticosteroids promote ENaC translocation to the apical membrane.

In unpolarized M-1 cells, I have found that sgk1 did not alter the intracellular localization of ENaC. This is consistent with my previous findings and hypothesis that polarization is a prerequisite for corticosteroid induced ENaC trafficking and indicates that polarization may have to be fulfilled so that sgk1 functions to link corticosteroids to stimulated ENaC trafficking.

Remaining questions that can now be addressed are how sgk1 influences ENaC trafficking or conductance in polarized M-1 cells. In this regard, the cell model I have generated is valuable, in which the expression of sgk1 is regulated by tetracycline (10 fold expression induction). A run of good experiments follows to elucidate: 1, the

substrate of sgk1; 2, the influences of sgk1 on ENaC conductance; 3, the influences of sgk1 on ENaC trafficking.

1, though Snyder P et al (2002) and Debonneville C et al (2001) have recently shown that sgk1 phosphorylated the ubiquitin ligase NEDD4–2 *in vitro*, it is worth testing whether sgk1 phosphorylates NEDD4-2 *in vivo* in the inducible cell model, providing the development of antibodies against phosphorylated NEDD4-2;

2, to examine the effects of sgk1 inducible expression on sodium transport [both the transepithelial sodium transport (using Ussing's principles and Ussing chambers) and the amiloride sensitive sodium transport across the apical plasma membrane (using patch clamping)] in M-1 cells is paramount and indispensable in regarding sgk1 as an essential step in corticosteroid signaling pathways;

3, to elucidate the influences of sgk1 on ENaC trafficking in polarized epithelia is an intriguing topic but is technically demanding. A quantitative method to measure the surface expression level of ENaC is required to show unequivocally the effects of sgk1. A modified protocol based upon Firsov D et al (1996) can be followed to solve this problem, in which a hemagglutinin (HA) epitope is inserted into the extracellular loop of EGFP-ENaCβ. The level of HA expression detected by immunofluorescence reflects the amount of ENaC proteins on the apical surface whereas the level of EGFP expression correlates to the amount of ENaC proteins in total.

In conclusion, the outcomes of my PhD studies have contributed to our understanding the signaling pathway of aldosterone and its influences on sodium transport in the distal nephron. It has also shed light on how transmembrane proteins such as sodium channels translocate to and from various intracellular organelles; and how this process is regulated by hormones and genes whose products mediate the transduction of hormonal signals to altered trafficking events.

REFERENCE

1 Abriel H, Loffing J, Rebhun JF, Pratt JH, Schild L, Horis-berger JD, Rotin D, and Staub O. Defective regulation of the epithelial Na channel by Nedd4 in Liddle's syndrome. *J Clin Invest* 103: 667–673, 1999.

2 Adams CM, Snyder PM, and Welsh MJ. Interactions between subunits of the human epithelial sodium channel. *J Biol Chem* 272: 27295–27300, 1997.

3 Adler V, Yin Z, Fuchs SY, Benezra M, Rosario L, Tew KD, Pincus MR, Sardana M, Henderson CJ, Wolf CR, Davis RJ and Ronai Z. Regulation of JNK signaling by GSTp. *EMBO J* 18: 1321-1334, 1999.

4 Aguilera G. Factors controlling steroid biosynthesis in the zona glomerulosa of the adrenal. *J Steroid Biochem Mol Biol* 45:147-151, 1993.

5 Al-Baldawi NF, Stockand JD, Al-Khalili OK, Yue G, and Eaton DC. Aldosterone induces Ras methylation in A6 epithelia. *Am J Physiol Cell Physiol* 279: C429–C439, 2000.

6 Albiston AL, Obeyesekere VR and Smith RE. Cloning and tissue distribution of the human 11 beta-hydroxysteroid dehydrogenase type 2 enzyme. *Mol Cell Endocrinol* 105:R11-17, 1994.

7 Alfaidy N, Blot-Chabaud M, Robic D, Kenouch S, Bourbouze R, Bonvalet JP, and Farman N. Characteristics and regulation of 11 beta-hydroxysteroid dehydrogenase of proximal and distal nephron. *Biochim Biophys Acta* 1243: 461–468, 1995.

8 Alliston TN, Gonzalez-Robayna IJ, Buse P, Firestone GL, and Richards JS. Expression and localization of serum/glucocorticoid-induced kinase in the rat ovary: relation to follicular growth and differentiation. *Endocrinology* 141: 385–395, 2000.

9 Alvarez de la Rosa D, Zhang P, Naray-Fejes-Toth A, Fejes-Toth G, and Canessa CM. The serum and glucocorticoid kinase sgk increases the abundance of epithelial sodium channels in the plasma membrane of *Xenopus* oocytes. *J Biol Chem* 274: 37834–37839, 1999.

10 Alvarez de la Rosa DA, Li H, and Canessa CM. Effects of aldosterone on biosynthesis, traffic, and functional expression of epithelial sodium channels in

A6 cells. *J Gen Physiol* 119:427-442, 2002.

11 Alvarez de la Rosa D and Canessa CM. Role of sgk in hormonal regulation of epithelial sodium channel in A6 cells. *Am J Physiol Cell Phyisol* 284:C404-414, 2003.

12 Ankenbauer W, Strahle U, and Schutz G. Synergistic action of glucocorticoid and estradiol responsive elements. *Proc Natl Acad Sci USA* 85: 7526–7530, 1988.

13 Ardaillou R, Chansel D. Synthesis and effects of active fragments of angiotensin II. *Kidney Int* 52:1458-1468, 1997.

14 Arystarkhova E, Wetzel RK, Asinovski NK, and Swead-ner KJ. The gamma subunit modulates Na and K affinity of the renal Na,K-ATPase. *J Biol Chem* 274: 33183–33185, 1999.

15 Asher C, Wald H, Rossier BC and Garty H. Aldosterone induced increase in the abundance of Na channel subunits. *Am J Physiol* 40: C605-611, 1996.

16 Attali B, Latter H, Rachamim N, and Garty H. A corticosteroid-induced gene expressing an "IsK-like" K channel activity in *Xenopus* oocytes. *Proc Natl Acad Sci USA* 92: 6092–6096, 1995.

17 Ausiello DA, Skorecki KL, Verkman AS and Bonventre JV. Vasopressin signaling in kidney cells. *Kidney Int* 31: 521-529, 1987.

18 Awayda MS, Ismailov II, Berdiev BK, Fuller CM and Benos DJ. Protein kinase regulation of a cloned epithelial sodium channel. *J. Gen. Physiol.* 108, 49-65, 1996.

19 Bamberger CM, Bamberger AM, Wald M, Chrousos GP, and Schulte HM. Inhibition of mineralocorticoid activity by the beta-isoform of the human glucocorticoid receptor. *J Steroid Biochem Mol Biol* 60: 43–50, 1997.

20 Bank N, Aynedjian HS: Failure of changes in intracapillary pressures to alter proximal fluid reabsorption. *Kidney Int* 26:275-282, 1984.

21 Barbry P and Hoffman P. Molecular biology of Na absorption. *Am. J. Physiol.* 273: G571-585, 1997.

22 Barker PM, Nguyen MS, Gatzy JT, Grubb B, Norman H, Hummler E, Rossier B, Boucher RC, and Koller B. Role of gamma-ENaC subunit in lung liquid clearance and electrolyte balance in newborn mice. Insights into perinatal adaptation and pseudohypoaldosteronism. *J Clin Invest* 102: 1634–1640, 1998.

23 Bar-Sagi D. A Ras by any other name. *Mol Cell Biol* 21: 1441–1443, 2001.

24 Bastl CP and Hayslett JP. The cellular action of aldosterone in target epithelia. *Kidney Int* 42: 250–264, 1992.

25 Baumann H, Jahreis GP, Morella KK, Won KA, Pruitt SC, Jones VE, and Prowse KR. Transcriptional regulation through cytokine and glucocorticoid response elements of rat acute phase plasma protein genes by C/EBP and JunB. *J Biol Chem* 266: 20390–20399, 1991.

26 Becchetti A, Kemendy AE, Stockand JD, Sariban-Sohraby S, and Eaton DC. Methylation increases the open probability of ENaC in A6 epithelia. *J Biol Chem* 275: 16550–16559, 2000.

27 Beers ET, Carroll RG, Young DB, et al: Effects of graded changes in reflex renal nerve activity on renal function. *Am J Physiol* 250:F559-F565, 1986.

28 Beguin P, Wang X, Firsov D, Puoti A, Claeys D, Horis-berger JD, and Geering K. The gamma subunit is a specific component of the Na,K-ATPase and modulates its transport function. *EMBO J* 16: 4250–4260, 1997.

29 Beguin P, Crambert G, Guennoun S, Garty H, Horis-berger JD, and Geering K. CHIF, a member of the FXYD protein family, is a regulator of Na,K-ATPase distinct from the gamma-subunit. *EMBO J* 20: 3993–4002, 2001.

30 Benos DJ, Saccomani G, Brenner BM and Sariban-Sohraby S. Purification and characterization of the amiloride-sensitive sodium channel from A6 cultured cells and bovine renal papilla. *Proc. Natl. Acad. Sci. USA.* 83: 8525-8529, 1986.

31 Bens M, Vallet V, Cluzeaud F, et al. Corticosteroid-dependent sodium transport in a novel immortalized mouse collecting duct principal cell line. *J Am Soc Nephrol* 10:923-934, 1999.

32 Berdiev BK, Prat AG, Cantiello HF, Ausiello DA, Fuller CM, Jovov B, Benos DJ, and Ismailov II. Regulation of epithelial sodium channels by short actin filaments. *J Biol Chem* 271: 17704–17710, 1996.

33 Berger S, Bleich M, Schmid W, Cole TJ, Peters J, Watanabe H, Kriz W, Warth R, Greger R, and Schutz G. Mineralocorticoid receptor knockout mice: pathophysiology of Na metabolism. *Proc Natl Acad Sci USA* 95: 9424–9429, 1998.

34 Berger S, Bleich M, Schmid W, Greger R, and Schutz G. Mineralocorticoid

receptor knockout mice: lessons on Na metabolism. *Kidney Int* 57: 1295–1298, 2000.

35 Bhargava A, Fullerton MJ, Myles K, Purdy TM, Funder JW, Pearce D, and Cole TJ. The serum- and glucocorticoid-induced kinase is a physiological mediator of aldosterone ac-tion. *Endocrinology* 142: 1587–1594, 2001.

36 Blantz RC, Konnen KS, Tucker BJ. Angiotensin II effects upon the glomerular microcirculation and ultrafiltration coefficient of the rat. *J Clin Invest* 57:419-434, 1976.

37 Blazer-Yost BL and Cox M. Insulin-like growth factor I stimulates renal epithelial Na transport. *Am J Physiol* 255:C413-417, 1988.

38 Blazer-Yost BL, Cox M and Furlanetto R. Insulin and IGF-1 receptor-mediated Na transport in toad urinary bladders. *Am J Physiol* 257: C612-620, 1989.

39 Blazer-Yost BL, Liu X, and Helman SI. Hormonal regulation of ENaCs: insulin and aldosterone. *Am J Physiol Cell Physiol* 274: C1373–C1379, 1998.

40 Blazer-Yost BL, Paunescu TG, Helman SI, Lee KD, and Vlahos CJ. Phosphoinositide 3-kinase is required for aldosterone-regulated sodium reabsorption. *Am J Physiol Cell Physiol* 277: C531–C536, 1999.

41 Blazer-Yost BL, Butterworth M, Hartman AD, Parker GE, Faletti CJ, Els WJ, and Rhodes SJ. Characterization and imaging of A6 epithelial cell clones expressing fluorescently labeled ENaC subunits. *Am J Physiol Cell Physiol* 281: C624–C632, 2001.

42 Bleich M, Warth R, Schmidt-Hieber M, Schulz-Baldes A, Hasselblatt P, Fisch D, Berger S, Kunzelmann K, Kriz W, Schutz G, and Greger R. Rescue of the mineralocorticoid receptor knock-out mouse. *Pflugers Arch* 438: 245–254, 1999.

43 Bloem LJ, Guo C, and Pratt JH. Identification of a splice variant of the rat and human mineralocorticoid receptor genes. *J Steroid Biochem Mol Biol* 55: 159–162, 1995.

44 Blot-Chabaud M, Wanstok F, Bonvalet JP and Farman N. Cell sodium induced recruitment of Na^+/K^+-ATPase pumps in rabbit cortical collecting tubules is aldosterone-dependent. *J Biol Chem* 265:11676-11681, 1990.

45 Blot-Chabaud M, Laplace M, Cluzeaud F, Capurro C, Cassingena R, Vandewalle A, Farman N and Bonvalet JP. Characteristics of a rat cortical collecting duct cell

line that maintains high transepithelial resistance. *Kidney Int.* 50:367-376, 1996.

46 Blot-Chabaud M, Djelidi S, Courtois-Coutry N, Fay M, Cluzeaud F, Hummler E, and Farman N. Coordinate control of Na,K-ATPase mRNA expression by aldosterone, vasopressin and cell sodium delivery in the cortical collecting duct. *Cell Mol Biol* 47: 247–253, 2001.

47 Bonventre JV, Leaf A: Sodium homeostasis: Steady states without a set point. Kidney Int 21:880-883, 1982.

48 Botero-Velez M, Curtis JJ, and Warnock DG. Brief report: Liddle's syndrome revisited-a disorder of sodium reabsorption in the distal tubule. *N Engl J Med* 330: 178–181, 1994.

49 Brennan FE and Fuller PJ. Acute regulation by corticosteroids of channel-inducing factor gene messenger ribonucleic acid in the distal colon. *Endocrinology* 140: 1213–1218, 1999.

50 Brennan FE and Fuller PJ. Rapid upregulation of serum and glucocorticoid-regulated kinase (sgk) gene expression by corti-costeroids in vivo. *Mol Cell Endocrinol* 166: 129–136, 2000.

51 Breyer MD and Ando Y. Hormonal signaling and regulation of salt and water transport in the collecting duct. *Annu. Rev. Physiol.* 56: 711-739, 1994.

52 Brown RW, Chapman KE, Murad P, Edwards CRW and Seckl JRS. Purification of 11β-hydroxysteroid dehydrogenase type 2 from human placenta utilizing a novel affinity labelling technique. *Biochem J* 313, 997-1005, 1996a.

53 Brown RW, Chapman KE, Kotelevtsev Y, Yau J, Lindsay RS, Brett L, Leckie C, Murad P, Lyods V, Mullins J, Edwards CRW and Seckl JR. Cloning and production of antisera to human placental 11β-hydroxysteroid dehydrogenase type 2. *Biochem J* 313, 1007-1017, 1996b.

54 Brunet A, Park J, Tran H, Hu LS, Hemmings BA, and Greenberg ME. Protein kinase SGK mediates survival signals by phosphorylating the forkhead transcription factor FKHRL1 (FOXO3a). *Mol Cell Biol* 21: 952–965, 2001.

55 Buller AL and White MM. Altered patterns of N-linked glycosylation of the *Torpedo* acetylcholine receptor expressed in *Xenopus* oocytes. *J Membr Biol* 115: 179–189, 1990.

56 Burg MB, Orloff J: Control of fluid absorption in the renal proximal tubule. *J*

Clin Invest 47:2016-2024, 1968.

57 BurgenerKairouz P, Corthesy-Theulaz I, Merillat AM. Polyadenylation of Na/K-APTase beta (1)-subunit during early development of *Xenopus laevis*. *Am J Physiol* 266:C157-164, 1994.

58 Burke ZD, Ho MY, Morgan H, Smith M, Murphy D, and Carter D. Repression of vasopressin gene expression by glucocorticoids in transgenic mice: evidence of a direct mechanism mediated by proximal 5-flanking sequence. *Neuroscience* 78: 1177–1185, 1997.

59 Buse P, Tran SH, Luther E, Phu PT, Aponte GW, and Firestone GL. Cell cycle and hormonal control of nuclear-cytoplasmic localization of the serum- and glucocorticoid-inducible protein kinase, Sgk, in mammary tumor cells. *J Biol Chem* 274: 7253–7263, 1999.

60 Canessa CM, Horisberger JD, and Rossier BC. Epithelial sodium channel related to proteins involved in neurodegeneration. *Nature* 361: 467–470, 1993.

61 Canessa CM, Schild L, Buell G, Thorens B, Gautschi I, Horisberger JD, and Rossier BC. Amiloride-sensitive epithelial Na channel is made of three homologous subunits. *Nature* 367: 463–467, 1994.

62 Canessa CM, Merillat AM, and Rossier BC. Membrane topology of the epithelial sodium channel in intact cells. *Am J Physiol Cell Physiol* 267: C1682–C1690, 1994(a).

63 Capurro C, Coutry N, Bonvalet JP, Escoubet B, Garty H, and Farman N. Cellular localization and regulation of CHIF in kidney and colon. *Am J Physiol Cell Physiol* 271: C753-C762, 1996.

64 Cha HH, Cram EJ, Wang EC, Huang AJ, Kasler HG, and Firestone GL. Glucocorticoids stimulate p21 gene expression by targeting multiple transcriptional elements within a steroid responsive region of the $p21^{waf1/cip1}$ promoter in rat hepatoma cells. *J Biol Chem* 273: 1998–2007, 1998.

65 Chalfant ML, Denton JS, Langloh AL, Karlson KH, Loffing J, Benos DJ, and Stanton BA. The NH_2 terminus of the epithelial sodium channel contains an endocytic motif. *J Biol Chem* 274: 32889–32896, 1999.

66 Chang SS, Grunder S, Hanukoglu A, Rosler A, Mathew PM, Hanukoglu I, Schild L, Lu Y, Shimkets RA, Nelson-Williams C, Rossier BC, and Lifton RP.

Mutations in subunits of the epithelial sodium channel cause salt wasting with hyperkalaemic acidosis, pseudohypoaldosteronism type 1. *Nat Genet* 12: 248–253, 1996.

67 Charron J and Drouin J. Glucocorticoid inhibition of transcription from episomal proopiomelanocortin gene promoter. *Proc Natl Acad Sci USA* 83: 8903–8907, 1986.

68 Chen S, Bhargava S, Mastroberardino L, Meijer OC, Wang J, Firestone P, Verrey F, and Pearce D. Epithelial sodium channel regualted by aldosterone-induced protein sgk. *Proc Nat Acad Sci USA* 96: 2514–2519, 1999.

69 Chen SY, Wang J, Liu W, and Pearce D. Aldosterone responsiveness of A6 cells is restored by cloned rat mineralocorticoid receptor. *Am J Physiol Cell Physiol* 274: C39–C46, 1998.

70 Cheng C, Prince LS, Snyder PM, and Welsh MJ. Assembly of the epithelial Na 1 channel evaluated using sucrose gradient sedimentation analysis. *J Biol Chem* 273: 22693–22700, 1998.

71 Chigaev A, Lu G, Shi H, Asher C, Xu R, Latter H, Seger R, Garty H, and Reuveny E. In vitro phosphorylation of COOH termini of the epithelial Na channel and its effects on channel activity in *Xenopus* oocytes. *Am J Physiol Renal Physiol* 280: F1030–F1036, 2001.

72 Cho JH, Musch MW, Bookstein CM, McSwine RL, Ra-benau K, and Chang EB. Aldosterone stimulates intestinal Na absorption in rats by increasing NHE3 expression of the proximal colon. *Am J Physiol Cell Physiol* 274: C586–C594, 1998.

73 Cho SG, Lee YH, Park HS, Ryoo K, Kang KW, Park J, Eom SJ, Kim MJ, Chang TS, Choi SY, Shim J, Kim Y, Dong MS, Lee MJ, Kim SG, Ichijo H and Choi EJ. Glutathione S-transferase mu modulates the stree-activated signals by suppressing apoptosis signal regulating kinase 1. *J Biol Chem* 276: 12749-12755, 2001.

74 Chou SY, Porush JG, Faubert PF. Renal medullary circulation: Hormonal control. *Kidney Int* 37:1-13, 1990.

75 Chraibi A and *et al.* Protease modulation of the activity of the epithelial sodium channel expressed in *Xenopus* oocytes. *J Gen Physiol.* 111:127-138, 1998.

76 Christy C, Ramage LE, Seckl JR and Brown RW. Expression of candidate aldosterone regulated genes and Ki-ras2 in adult kidney and during development. *Clin Sci* 98:26 (Suppl 42), 2000.

77 Civan MM, Peterson-Yantorno K and O'Brien TG. Insulin and phorbol ester stimulate conductive Na transport through a common pathway. *Proc Natl Acad Sci USA* 85:963-967, 1988.

78 Civan MM, Peterson-Yantorno K, George K and O'Brien TG. Interaction of TPA and insulin on Na transport across frog skin. *Am J Physiol* 256:C569-578, 1989.

79 Colarusso P and Spring KR. Reticulated Lipid Probe Fluorescence Reveals MDCK Cell Apical Membrane Topography. *Biophysical Journal* 82:752–761, 2002.

80 Cole TJ, Blendy JA, Monaghan AP, Krieglstein K, Schmid W, Aguzzi A, Fantuzzi G, Hummler E, Unsicker K, and Schutz G. Targeted disruption of the glucocorticoid receptor gene blocks adrenergic chromaffin cell development and severely retards lung maturation. *Genes Dev* 9: 1608–1621, 1995.

81 Coscoy S, Lingueglia E, Lazdunski M, and Barbry P. The Phe-Met-Arg-Phe-amide-activated sodium channel is a tetramer. *J Biol Chem* 273: 8317–8322, 1998.

82 Coutry N, Farman N, Bonvalet JP and Blot-Chabaud M. Role of cell volume variations in Na^+/K^+-ATPase recruitment and/or activation in cortical collecting duct. *Am J Physiol* 266:C1342-1349, 1994.

83 Coutry N, Farman N, Bonvalet JP and Blot-Chabaud M. Synergistic action of vasopressin and aldosterone on basolateral Na^+/K^+-ATPase in the cortical collecting duct. *J. Membr. Biol.* 145:99-106, 1995.

84 Cram EJ, Ramos RA, Wang EC, Cha HH, Nishio Y, and Firestone GL. Role of the CCAAT/enhancer binding protein-alpha transcription factor in the glucocorticoid stimulation of $p21^{waf1/cip1}$ gene promoter activity in growth-arrested rat hepatoma cells. *J Biol Chem* 273: 2008–2014, 1998.

85 Curtis JJ, Luke RG, Dustan HP, Kashgarian M, Welchel JD, Jones P, and Diethelm A. Remission of hypertension after renal transplantation. *N Engl J Med* 309, 1009-1015, 1983.

86 Dagenais A, Denis C, Vives MF, Girouard S, Masse C, Nguyen T, Yamagata T, Grygorczyk C, Kothary R, and Berthiaume Y. Modulation of α-ENaC and α1-

Na^+/K^+-ATPase by cAMP and dexamethasone in alveolar epithelial cells. *Am J Physiol Lung Cell Mol Physiol* 281: L217–L230, 2001.

87 Dai F, Yu L, He H, Zhao Y, Yang J, Zhang X and Zhao S. Cloning and mapping of a novel human serum/glucocorticoid regulated kinase-like gene, SGKL, to chromosome 8q12.3-q13.1. Genomics 62:95-7, 1999.

88 Debonneville C, Flores SY, Kamynina E, Plant PJ, Tauxe C, Thomas MA, Munster C, Chraibi A, Pratt JH, Horis-berger JD, Pearce D, Loffing J, and Staub O. Phosphorylation of Nedd4-2 by Sgk1 regulates epithelial Na channel cell surface expression. *EMBO J* 20: 7052–7059, 2001.

89 DeHart A, Schnell JD, Allen DA, and Hicke L. The conserved Pkh-Ypk kinase cascade is required for endocytosis in yeast. *J Cell Biol* 156:241-248, 2002.

90 De Kloet ER, Van Acker SA, Sibug RM, Oitzl MS, Meijer OC, Rahmouni K, and De Jong W. Brain mineralocorticoid receptors and centrally regulated functions. *Kidney Int* 57: 1329–1336, 2000.

91 De Kloet ER, Vreugdenhil E, Oitzl MS, and Joels M. Brain corticosteroid receptor balance in health and disease. *Endocr Rev* 19: 269–301, 1998.

92 Dijkink L, Hartog A, Deen PM, Van Os CH, and Bindels RJ. Time-dependent regulation by aldosterone of the amiloride-sensitive Na channel in rabbit kidney. *Pflugers Arch* 438: 354–360, 1999.

93 Djelidi S, Fay M, Cluzeaud F, Escoubet B, Eugene E, Capurro C, Bonvalet JP, Farman N, and Blot-Chabaud M. Transcriptional regulation of sodium transport by vasopressin in renal cells. *J Biol Chem* 272: 32919–32924, 1997.

94 Doucet A, Katz AI. Mineralocorticoid receptors along nephron. Tritiated-aldosterone binding in rabbit tubules. *Am J Physiol* 241: F605, 1981

95 Driscoll M and Chalfie M. The mec-4 gene is a member of a family of C. elegans genes that can mutate to induce neuronal degeneration. *Nature* 349:588-593, 1991.

96 Drouin J, Trifiro MA, Plante RK, Nemer M, Eriksson P, and Wrange O. Glucocorticoid receptor binding to a specific DNA sequence is required for hormone-dependent repression of pro-opiomelanocortin gene transcription. *Mol Cell Biol* 9: 5305–5314, 1989.

97 Drouin J, Sun YL, Chamberland M, Gauthier Y, De Lean A, Nemer M, and

Schmidt TJ. Novel glucocorticoid receptor complex with DNA element of the hormone-repressed POMC gene. *EMBO J* 12: 145–156, 1993.

98 Duc C, Farman N, Canessa CM, Bonvalet JP, and Rossier BC. Cell-specific expression of epithelial sodium channel alpha, beta, and gamma subunits in aldosterone-responsive epithelia from the rat: localization by in situ hybridization and immunocytochemistry. *J Cell Biol* 127: 1907–1921, 1994.

99 Eaton DC, Becchetti A, Ma H and Ling BN. Renal sodium channels: regulation and single channel properties. *Kidney Int.* 48: 941-949, 1995.

100 Ecelbarger CA, Kim GH, Terris J, Masilamani S, Mitchell C, Reyes I, Verbalis JG, and Knepper MA. Vasopressin-mediated regulation of epithelial sodium channel abundance in rat kidney. *Am J Physiol Renal Physiol* 279: F46–F53, 2000.

101 Edinger RS, Rokaw MD, and Johnson JP. Vasopressin stimulates sodium transport in A6 cells via a phosphatidylinositide 3 kinase dependent pathway. *Am J Physiol Renal Physiol* 277: F575–F579, 1999.

102 Erlij D, De Smet P and Van Driessche W. Effect of insulin on area and Na channel density of apical membrane of cultured toad kidney cells. *J Physiol* 481:533-542, 1994.

103 Erlij D, De Smet P, Mesotten D, and Van Driessche W. Forskolin increases apical sodium conductance in cultured toad kidney cells (A6) by stimulating membrane insertion. *Pflugers Arch* 438: 195–204, 1999.

104 Escoubet B, Coureau C, Blot-chabaud M, Bonvalet JP, Farman N: Corticosteroid receptor mRNA expression is unaffected by corticosteroids in rat kidney, heart and colon. *Am J Physiol* 270: C1343–C1353, 1996.

105 Escoubet B, Coureau C, Bonvalet JP, and Farman N. Noncoordinate regulation of epithelial Na channel and Na pump subunit mRNAs in kidney and colon by aldosterone. *Am J Physiol* 272: C1482-1491, 1997.

106 Estrada E, Liberona JL, Miranda M and Jaimovich E. Aldosterone and testosterone-mediated intracellular calcium response in skeletal muscle cell cultures. *Am J Physiol Endocrinol Metab* 279: E132–E139, 2000.

107 Faletti CJ, Perrotti N, Taylor SI, and Blazer-Yost BL. *sgk*: an essential convergence point for peptide and steroid hormone regulation of ENaC mediated

Na transport. *Am J Physiol Cell Physiol* 282: C494–C500, 2002.

108 Farman N: Steroid receptors: Distribution along the nephron. *Semin Nephrol* 12: 12–17, 1992.

109 Farman N, Talbot CR, Boucher R, Fay M, Canessa C, Rossier B, and Bonvalet JP. Noncoordinated expression of α-, β-, and γ-subunit mRNAs of epithelial Na channel along rat respiratory tract. *Am J Physiol Cell Physiol* 272: C131–C141, 1997.

110 Farman N and Rafestin-Oblin ME. Multiple aspects of mineralocorticoid selectivity. *Am J Physiol Renal Physiol* 280: F181–F192, 2001.

111 Farr TJ, Coddington-Lawson SJ, Snyder PM, and Mc-Donald FJ. Human Nedd4 interacts with the human epithelial Na channel: WW3 but not WW1 binds to Na-channel subunits. *Biochem J* 345: 503–509, 2000.

112 Feraille E and Doucet A. Sodium-potassium-adenosine-triphosphatase-dependent sodium transport in the kidney: hormonal control. *Physiol Rev* 81: 345–418, 2001.

113 Ferrari P and Krozowski Z. Role of the 11beta-hydroxysteroid dehydrogenase type 2 in blood pressure regulation. *Kidney Int* 57: 1374–1381, 2000.

114 Firsov D, Schild L, Gautschi I, Merillat AM, Schneeberger E, and Rossier BC. Cell surface expression of the epithelial Na channel and a mutant causing Liddle syndrome: a quantitative approach. *Proc Natl Acad Sci USA* 93: 15370–15375, 1996.

115 Firsov D, Gautschi I, Merillat AM, Rossier BC, and Schild L. The heterotetrameric architecture of the epithelial sodium channel (ENaC). *Embo J* 17: 344–352, 1998.

116 Fisher KA, Lee SH, Walker J, Dileto-Fang C, Ginsberg L, and Stapleton SR. Regulation of proximal tubule sodium/hydrogen antiporter with chronic volume contraction. *Am J Physiol Renal Physiol* 280: F922–F926, 2001.

117 Foschi M, Chari S, Dunn MJ, and Sorokin A. Biphasic activation of p21ras by endothelin-1 sequentially activates the ERK cascade and phosphatidylinositol 3-kinase. *EMBO J* 16: 6439–6451, 1997.

118 Foulkes NS and Sassonecorsi P. Transcription factors coupled to the cAMP-signaling pathway. *Biochim. Biophys. Acta* 1288: F101-121, 1996.

119 Friedrich B, Feng Y, Cohen P, Zimmermann S, Risler T, Vandevalle A, Pearce D,

Lang F. The serine/threonine kinases SGK2 and SGK3 are potent stimulators of the epithelial sodium channel. *Pflügers Arch* 445:693-696, 2003.

120 Frindt G, Masilamani S, Knepper MA, and Palmer LG. Activation of epithelial Na channels during short-term Na deprivation. *Am J Physiol Renal Physiol* 280: F112–F118, 2001.

121 Fuller PJ, Lim-Tio SS, and Brennan FE. Specificity in mineralocorticoid versus glucocorticoid action. *Kidney Int* 57: 1256–1264, 2000.

122 Funder JW, Pearce PT and Smith R. Mineralocorticoid action: target tissue specificity is enzyme, not receptor, mediated. *Science* 242: 583-585, 1988.

123 Funder JW. Glucocorticoid and mineralocorticoid receptors: biology and clinical relevance. *Annu Rev Med* 48: 231–240, 1997.

124 Gamper N, Fillon S, Feng Y, Friedrich B, Lang PA, Henke G, Huber SM, Kobayashi T, Cohen P and Lang F. K^+ channel activation by all three isoforms of serum- and glucocorticoid-dependent protein kinase SGK. *Eur J Physiol* 445:60–66, 2002.

125 Garty H and Edelman IS. Amiloride-sensitive trypsinization of apical sodium channels. Analysis of hormonal regulation of sodium transport in toad bladder. *J Gen Physiol* 81: 785–803, 1983.

126 Garty H and Palmer LG. Epithelial sodium channels: function, structure, and regulation. *Physiol Rev* 77: 359–396, 1997.

127 Geller, D.S., Rodriguez-Soriano, J., Vallo Boado, A., Schifter, S., Bayer, M., Chang, S.S., and Lifton, R.P. Mutations in the mineralocorticoid receptor gene cause autosomal dominant pseudohypoaldosteronism type I. Nat. Genet. *19*, 279–281, 1998.

128 Geller, D.S., Farhi, A., Pinkerton, N., Fradley, M., Moritz, M., Spitzer, A., Meinke, G., Tsai, F.T., Sigler, P.B., and Lifton, R.P. Activating mineralocorticoid receptor mutation in hypertension exacerbated by pregnancy. Science *289*, 119–123, 2000.

129 Ghosh S, Cox KH, and Cox JV. Chicken erythroid AE1 anion exchangers associate with the cytoskeleton during recycling to the Golgi. *Mol Biol Cell* 10: 455–469, 1999.

130 Goetz KL, Hermreck AS, Slick GL, et al: Atrial receptors and renal function in

conscious dogs. Am J Physiol 219:1417-1423, 1970.

131 Gonzalez-Robayna IJ, Alliston TN, Buse P, Firestone GL, and Richards JS. Functional and subcellular changes in the A-kinase-signaling pathway: relation to aromatase and Sgk expression during the transition of granulosa cells to luteal cells. *Mol Endocrinol* 13: 1318–1337, 1999.

132 Gossen M, and Bujard H. Tight control of gene expression in mammalian cells by tetracycline responsive promoters. *Proc. Natl. Acad. Sci. USA* 89: 5547–5551, 1992.

133 Goulet CC, Volk KA, Adams CM, Prince LS, Stokes JB, and Snyder PM. Inhibition of the epithelial Na channel by interaction of Nedd4 with a PY motif deleted in Liddle's syndrome. *J Biol Chem* 273: 30012–30017, 1998.

134 Gross R, Kirchheim H. Effects of bilateral carotid and auditory stimulation on renal blood flow and sympathetic nerve activity in the conscious dog. *Pflugers Arch* 383:233-239, 1980.

135 Grunder S, Firsov D, Chang SS, Jaeger NF, Gautschi I, Schild L, Lifton RP, and Rossier BC. A mutation causing pseudohypoaldosteronism type 1 identifies a conserved glycine that is involved in the gating of the epithelial sodium channel. *Embo J* 16: 899–907, 1997.

136 Guyton AC. The surprising kidney-fluid mechanism for pressure control—its infinite gain. *Hypertension* 16:725-730, 1990.

137 Guyton AC: Blood pressure control—special role of the kidneys and body fluids. *Science* 252:1813-1816, 1991.

138 Guyton AC and Hall JE. *Medical Physiology* 10th ed. p195-207, 2000.

139 Hager H, Kwon TH, Vinnikova AK, Masilamani S, Brooks HL, Frokiær J, Knepper MA, and Nielsen S. Immunocyto-chemical and immunoelectron microscopic localization of α-, β-, and γ-ENaC in rat kidney. *Am J Physiol Renal Physiol* 280: F1093–F1106, 2001.

140 Hai MA, Thomas S: The time-course of changes in renal composition during lysine vasopressin infusion in the rat. *Pflugers Arch* 310: 297, 1969.

141 Hall JE and *et al.* Role of renal hemodynamics and arterial pressure in aldosterone 'escape'. *Hypertension*, 6 (suppl I):I183-192, 1986(a).

142 Hall JE: Control of sodium excretion by angiotensin II: Intrarenal mechanisms

and blood pressure regulation. *Am J Physiol* 250:R960-R972, 1986(b).

143 Halperin ML, Skorecki KL: Interpretation of the urine electrolytes and osmolality in the regulation of body fluid tonicity. Am J Nephrol 6:241-245, 1986.

144 Handler JS, Steele RE, Sahib MK, et al. Toad urinary bladder epithelial cells in culture: maintenance of epithelial structure, sodium transport and response to hormones. *Proc Natl Acad Sci USA* 76:4151-4155, 1979.

145 Hansson JH, Nelson-Williams C, Suzuki H, Schild L, Shimkets R, Lu Y, Canessa C, Iwasaki T, Rossier B, and Lifton RP. Hypertension caused by a truncated epithelial sodium channel gamma subunit: genetic heterogeneity of Liddle syndrome. *Nat Genet* 11: 76–82, 1995(a).

146 Hansson JH, Schild L, Lu Y, Wilson TA, Gautschi I, Shimkets R, Nelson-Williams C, Rossier BC, and Lifton RP. A *de novo* missense mutation of the beta subunit of the epithelial sodium channel causes hypertension and Liddle syndrome, identifying a proline-rich segment critical for regulation of channel activity. *Proc Natl Acad Sci USA* 92: 11495–11499, 1995(b).

147 Hanwell D, Ishikawa T, Saleki R and Rotin D. Trafficking and Cell Surface stability of the Epithelial Na Channel Expressed in Epithelial Madin-Darby Canine Kidney Cells. *J Biol Chem* 277: 9772-9779, 2002.

148 Harvey BJ and Higgins M, Nongenomic effects of aldosterone on Ca^{2+} in M-1 cortical collecting duct cells. *Kidney Int* 57:1395-1403, 2000.

149 Harvey BJ, Condliffe S, and Doolan CM. Sex and salt hormones: rapid effects in epithelia. *News Physiol Sci* 16: 174–177, 2001.

150 Harvey KF, Dinudom A, Komwatana P, Jolliffe CN, Day ML, Parasivam G, Cook DI, and Kumar S. All three WW domains of murine Nedd4 are involved in the regulation of epithelial sodium channels by intracellular Na. *J Biol Chem* 274: 12525–12530, 1999.

151 Harvey KF and Kumar S. Nedd4-like proteins: An emerging family of ubiquitin-protein ligases implicated in diverse cellular functions. *Trends Cell Biol* 9:166–169, 1999.

152 Harvey KF, Dinudom A, Cook DI, and Kumar S. The Nedd4-like protein KIAA0439 is a potential regulator of the epithelial sodium channel. *J Biol Chem* 276: 8597–8601, 2001.

153 Haseroth K, Gerdes D, Berger S, Feuring M, Günther A, Herbst C, Christ M, and Wehling M. Rapid nongenomic effects of aldosterone in mineralocorticoid-receptor-knockout mice. *Biochem Biophys Res Commun* 266:257–261, 1999.

154 Hawk CT, Li L and Schafer JA. AVP and aldosterone at physiological concentration have synergistic effects on Na transport in rat CCD. *Kidney Int.* 50: S35-41, 1996.

155 Hayashi M, Tapping RI, Chao TH, Lo JF, King CC, Yang Y, and Lee JD. BMK1 mediates growth factor-induced cell proliferation through direct cellular activation of serum and glucocorticoid-inducible kinase. *J Biol Chem* 276: 8631–8634, 2001.

156 Heck S, Kullmann M, Gast A, Ponta H, Rahmsdorf HJ, Herrlich P, and Cato AC. A distinct modulating domain in glucocorticoid receptor monomers in the repression of activity of the transcription factor AP-1. *EMBO J* 13: 4087–4095, 1994.

157 Helman SI, Liu X, Baldwin K, Blazer-Yost BL, and Els WJ. Time-dependent stimulation by aldosterone of blocker-sensitive ENaCs in A6 epithelia. *Am J Physiol Cell Physiol* 274: C947– C957, 1998.

158 Helmberg A, Auphan N, Caelles C, and Karin M. Glucocorticoid-induced apoptosis of human leukemic cells is caused by the repressive function of the glucocorticoid receptor. *EMBO J* 14: 452–460, 1995.

159 Helms MN, Fejes-Toth G, and Naray-Fejes-Toth A. Hormone-regulated transepithelial Na transport in mammalian CCD cells requires sgk1 expression. *Am J Physiol Renal Physiol* 284:F480-487, 2003.

160 Hershko A and Ciechanover A. The ubiquitin system. *Annu Rev Biochem* 67: 425–479, 1998.

161 Hicke L. Ubiquitin-dependent internalization and down-regulation of plasma membrane proteins. *FASEB J* 11: 1215–1226, 1997.

162 Holmes MC, Kotelevtsev Y, Mullins JJ, and Seckl JR. Phenotypic analysis of mice bearing targeted deletions of 11beta-hydroxysteroid dehydrogenases 1 and 2 genes. *Mol Cell Endocrinol* 171: 15–20, 2001.

163 Hou J, Speirs HJL, Seckl JR, and Brown RW. Sgk1 gene expression in kidney and its regulation by aldosterone: spatio-temporal heterogeneity and quantitative

analysis. *J Am Soc Nephrol* 13: 1190–1198, 2002.

164 Hummler, E., Barker, P., Gatzy, J., Beermann, F., Verdumo, C., Schmidt, A., Boucher, R., and Rossier, B.C. Early death due to defective neonatal lung liquid clearance in alpha-ENaC-deficient mice. Nat. Genet. *12*, 325–328, 1996.

165 Hummler E, Barker P, Talbot C, Wang Q, Verdumo C, Grubb B, Gatzy J, Burnier M, Horisberger JD, Beermann F, Boucher R, and Rossier BC. A mouse model for the renal salt-wasting syndrome pseudohypoaldosteronism. *Proc Natl Acad Sci USA* 94: 11710–11715, 1997.

166 Hummler E and Horisberger JD. Genetic disorders of membrane transport. V. The epithelial sodium channel and its implication in human diseases. *Am J Physiol Gastrointest Liver Physiol* 276: G567–G571, 1999.

167 Inagami T, Mizuno K, Naruse K, et al. Intracellular formation and release of angiotensins from juxtaglomerular cells. *Kidney Int* 38(Suppl 30):S33-S37, 1990.

168 Inoue T, Okauchi Y, Matsuzaki Y, Kuwajima K, Kondo H, Horiuchi N, Nakao K, Iwata M, Yokogoshi Y, Shintani Y, Bando H, and Saito S. Identification of a single cytosine base insertion mutation at Arg-597 of the beta subunit of the human epithelial sodium channel in a family with Liddle's disease. *Eur J Endocrinol* 138: 691–697, 1998.

169 Ishikawa T, Marunaka Y, and Rotin D. Electrophysiological characterization of the rat epithelial Na channel (rENaC) expressed in MDCK cells. Effects of Na and Ca. *J Gen Physiol* 111: 825–846, 1998.

170 Jovov B, Tousson A, Ji HL, Keeton D, Shlyonsky V, Ripoll PJ, Fuller CM, and Benos DJ. Regulation of epithelial Na channels by actin in planar lipid bilayers and in the *Xenopus* oocyte expression system. *J Biol Chem* 274: 37845–37854, 1999.

171 Kalinyak JE, Dorin RI, Hoffman AR, Perlman AJ. Tissue-specific regulation of glucocorticoid receptor mRNA by dexamethasone. *J Biol Chem* 262: 10441-10444, 1987.

172 Kamynina E, Debonneville C, Bens M, Vandewalle A, and Staub O. A novel mouse Nedd4 protein suppresses the activity of the epithelial Na channel. *Faseb J* 15: 204–214, 2001.

173 Kanelis V, Rotin D, and Forman-Kay JD. Solution structure of a Nedd4 WW

domain-ENaC peptide complex. *Nat Struct Biol* 8: 407–412, 2001.

174 Karin M. New twists in gene regulation by glucocorticoid receptor: is DNA binding dispensable? *Cell* 93: 487–490, 1998.

175 Karin M and Chang L. AP-1-glucocorticoid receptor crosstalk taken to a higher level. *J Endocrinol* 169: 447–451, 2001.

176 Kemendy AE, Kleyman TR, and Eaton DC. Aldosterone alters the open probability of amiloride-blockable sodium channels in A6 epithelia. *Am J Physiol Cell Physiol* 263: C825– C837, 1992.

177 Kemppainen RJ and Behrend EN. Dexamethasone rapidly induces a novel ras superfamily member-related gene in AtT-20 cells. *J Biol Chem* 273: 3129–3131, 1998.

178 Kim GH, Masilamani S, Turner R, Mitchell C, Wade JB, and Knepper MA. The thiazide-sensitive Na-Cl cotransporter is an aldosterone-induced protein. *Proc Natl Acad Sci USA* 95:14552–14557, 1998.

179 Kleyman TR, Kraehenbuhl JP and Ernst SA. Charaterization and cellular localization of the epithelial Na channel. *J. Biol. Chem.* 266: 3907-3915, 1991.

180 Kleyman TR, Coupaye-Gerard B, and Ernst SA. Aldosterone does not alter apical cell-surface expression of epithelial Na channels in the amphibian cell line A6. *J Biol Chem* 267: 9622–9628, 1992.

181 Kleyman TR, Ernst SA, and Coupaye-Gerard B. Arginine vasopressin and forskolin regulate apical cell surface expression of epithelial Na channels in A6 cells. *Am J Physiol Renal Fluid Electrolyte Physiol* 266: F506–F511, 1994.

182 Kleyman TR, Zuckerman JB, Middleton P, McNulty KA, Hu B, Su X, An B, Eaton DC, and Smith PR. Cell surface expression and turnover of the α-subunit of the epithelial sodium channel. *Am J Physiol Renal Physiol* 281: F213–F221, 2001.

183 Kobayashi T and Cohen P. Activation of serum- and glucocorticoid-regulated protein kinase by agonists that activate phosphatidylinositide 3-kinase is mediated by 3-phosphoinositide- dependent protein kinase-1 (PDK1) and PDK2. *Biochem J* 339: 319–328, 1999(a).

184 Kobayashi T, Deak M, Morrice N, Cohen P. Characterization of the structure and regulation of two novel isoforms of serum- and glucocorticoid-induced protein

kinase. *Biochem J* 344:189-197, 1999(b).

185 Kohan DE and et al. Localization of the nephron sites responsible for mineralocorticoid escape in rats. *Am J Physiol* 239: F149-153, 1980.

186 Kolla V and Litwack G. Transcriptional regulation of the human Na^+/K^+-ATPase via the human mineralocorticoid receptor. *Mol Cell Biochem* 204: 35–40, 2000.

187 Kolla V, Robertson NM, and Litwack G. Identification of a mineralocorticoid/glucocorticoid response element in the human Na^+/K^+-ATPase alpha1 gene promoter. *Biochem Biophys Res Commun* 266: 5–14, 1999.

188 Kolla V and Litwack G. Inhibition of mineralocorticoid-me-diated transcription by NF-kappaB. *Arch Biochem Biophys* 383: 38–45, 2000.

189 Konstas A and Korbmacher C. The γ-subunit of ENaC is more important for channel surface expression than the β-subunit. *Am J Physiol Cell Physiol* 284: C447–C456, 2003.

190 Kosari F, Sheng S, Li J, Mak DO, Foskett JK, and Kleyman TR. Subunit stoichiometry of the epithelial sodium channel. *J Biol Chem* 273: 13469–13474, 1998.

191 Kotelevtsev Y, Brown RW, Fleming S, et al. Hypertension in mice lacking 11 beta-hydroxysteroid dehydrogenase type 2. *J Clin Invest* 1999; 103:683-689.

192 Kramer RE, Gallant S and Brownie AC. Actions of angiotensin II on aldosterone biosynthesis in the rat adrenal cortex. *J Biol Chem* 255: 3442-3447, 1980.

193 Kumar S, Tomooka Y, and Noda M. Identification of a set of genes with developmentally down-regulated expression in the mouse brain. *Biochem Biophys Res Commun* 185: 1155–1161, 1992.

194 Kunzelmann K, Kiser GL, Schreiber R and Riordan JR. Inhibition of epithelial sodium currents by intracellular domains of the cystic fibrosis transmembrane conductance regulator. *FEBS Lett.* 400:341-344, 1997.

195 Kwak SP, Patel PD, Thompson RC, Akil H, and Watson SJ. 5_-Heterogeneity of the mineralocorticoid receptor messenger ribonucleic acid: differential expression and regulation of splice variants within the rat hippocampus. *Endocrinology* 133: 2344–2350, 1993.

196 Lafont F, Lecat S, Verkade P, and Simons K. Annexin XIIIb associates with lipid microdomains to function in apical delivery. *J Cell Biol* 142: 1413–1427, 1998.

197 Lang F, Klingel K, Wagner CA, Stegen C, Broer S: Deranged transcriptional regulation of cell volume sensitive kinase hSGK in diabetic nephropathy. *Proc Natl Acad Sci USA* 97: 8157-8162, 2000.

198 Laplace JR, Husted RF, and Stokes JB. Cellular responses to steroids in the enhancement of Na1 transport by rat collecting duct cells in culture—differences between glucocorticoid and mineralocorticoid hormones. *J Clin Invest* 90: 1370-1378, 1992.

199 Laragh JH, Ulick S, Januszewicz V, Deming QB, Kelly WG, Lieberman S: Aldosterone secretion and primary and malignant hypertension. *J Clin Invest* 39: 1091, 1960.

200 Laverty G, Bjarnadottir S, Elbrond VS, and Arnason SS. Aldosterone suppresses expression of an avian colonic sodium-glucose cotransporter. *Am J Physiol Regulatory Integrative Comp Physiol* 281: R1041–R1050, 2001.

201 Lee JE, Beck TW, Wojnowski L, and Rapp UR. Regulation of A-raf expression. *Oncogene* 12: 1669–1677, 1996.

202 Lee JE, Beck TW, Brennscheidt U, DeGennaro LJ, and Rapp UR. The complete sequence and promoter activity of the human A-raf-1 gene (ARAF1). *Genomics* 20: 43–55, 1994.

203 Le Menuet D, Viengchareun S, Penfornis P, Walker F, Zennaro MC, and Lombes M. Targeted oncogenesis reveals a distinct tissue-specific utilization of alternative promoters of the human mineralocorticoid receptor gene in transgenic mice. *J Biol Chem* 275: 7878–7886, 2000.

204 Lester DS, Asher C and Garty H. Characterization of cAMP-induced activation of epithelial sodium channels. *Am. J. Physiol.* 254:C802-808, 1988.

205 Liebold KM, Reifarth FW, Clauss W and Weber WM. cAMP activation of amiloride-sensitive sodium channels from guinea-pig colon expressed in Xenopus oocytes. *Pfluegers Arch.* 431:913-922, 1996.

206 Li M, Ye X, Woodward RN, Zhu C, Nichols LA, and Holland LJ. Analysis of the DNA-binding site for *Xenopus* glucocorticoid receptor accessory factor. Critical nucleotides for binding specificity in vitro and for amplification of steroid-induced fibrinogen gene transcription. *J Biol Chem* 273: 9790– 9796, 1998.

207 Lifton, R.P., Dluhy, R.G., Powers, M., Rich, G.M., Cook, S., Ulick, S., and

Lalouel, J.M. A chimaeric 11 beta-hydroxylase/aldosterone synthase gene causes glucocorticoid-remediable aldosteronism and human hypertension. *Nature* 355, 262–265, 1992a.

208 Lifton, R.P., Dluhy, R.G., Powers, M., Rich, G.M., Gutkin, M., Fallo, F., Gill, J.R., Jr., Feld, L., Ganguly, A., Laidlaw, J.C., et al. Hereditary hypertension caused by chimaeric gene duplications and ectopic expression of aldosterone synthase. *Nat. Genet.* 2, 66–74, 1992b.

209 Linden RJ: Atrial reflexes and renal function. *Am J Cardiol* 44:879-883, 1979.

210 Lingueglia E, Voilley N, Waldmann R, Lazdunski M, and Barbry P. Expression cloning of an epithelial amiloride-sensitive Na channel. A new channel type with homologies to *Caenorhabditis elegans* degenerins. *FEBS Lett* 318: 95–99, 1993.

211 Liu D, Yang X and Songyang Z. Identification of CISK, a new member of the SGK kinase family that promotes IL-3-dependent survival. *Curr Biol* 10:1233-6, 2000.

212 Liu W, Wang J, Sauter NK, and Pearce D. Steroid receptor heterodimerization demonstrated in vitro and in vivo. *Proc Natl Acad Sci USA* 92: 12480–12484, 1995.

213 Lifton RP, Gharavi AG, and Geller DS. Molecular mechanisms of human hypertension. *Cell* 104: 545–556, 2001.

214 Lin HH, Zentner MD, Ho HL, Kim KJ, and Ann DK. The gene expression of the amiloride-sensitive epithelial sodium channel alpha-subunit is regulated by antagonistic effects between glucocorticoid hormone and ras pathways in salivary epithelial cells. *J Biol Chem* 274: 21544–21554, 1999.

215 Loffing J, Pietri L, Aregger F, Bloch-Faure M, Ziegler U, Meneton P, Rossier BC, and Kaissling B. Differential subcellular localization of ENaC subunits in mouse kidney in response to high- and low-Na diets. *Am J Physiol Renal Physiol* 279: F252–F258, 2000.

216 Loffing J, Zecevic M, Feraille E, Kaissling B, Asher C, Rossier BC, Firestone GL, Pearce D, and Verrey F. Aldosterone induces rapid apical translocation of ENaC in early portion of renal collecting system: possible role of SGK. *Am J Physiol Renal Physiol* 280: F675–F682, 2001.

217 Magnuson NS, Beck T, Vahidi H, Hahn H, Smola U, and Rapp UR. The Raf-1

serine/threonine protein kinase. *Semin Cancer Biol* 5: 247–253, 1994.

218 Maiyar AC, Phu PT, Huang AJ, and Firestone GL. Repression of glucocorticoid receptor transactivation and DNA binding of a glucocorticoid response element within the serum/glucocorticoid-inducible protein kinase (sgk) gene promoter by the p53 tumor suppressor protein. *Mol Endocrinol* 11: 312–329, 1997.

219 Malkoski SP and Dorin RI. Composite glucocorticoid regulation at a functionally defined negative glucocorticoid response element of the human corticotropin-releasing hormone gene. *Mol Endocrinol* 13: 1629–1644, 1999.

220 Malkoski SP, Handanos CM, and Dorin RI. Localization of a negative glucocorticoid response element of the human corti-cotropin releasing hormone gene. *Mol Cell Endocrinol* 127: 189–199, 1997.

221 Mall M, Hipper A, Greger R and Kunzelmann K. Wild type but not ΔF508 inhibits sodium conductace when coexpressed in *Xenopus* oocytes. *FEBS Lett.* 381:47-52, 1996.

222 Marunaka Y and Eaton DC. Effects of vasopressin and cAMP on single amiloride blockable Na channels. *Am. J. Physiol.* 260: C1071-1084, 1991.

223 Marunaka Y, Hagiwara N and Tohda H. Insulin activates single amiloride-blockable Na channel in a distal nephron cell line A6. Am J Physiol 263: F392-400, 1992.

224 Masilamani S, Kim GH, Mitchell C, Wade JB, and Knepper MA. Aldosterone-mediated regulation of ENaC alpha, beta, and gamma subunit proteins in rat kidney. *J Clin Invest* 104: R19–R23, 1999.

225 Mastroberardino L, Spindler B, Forster I, Loffing J, As-sandri R, May A, and Verrey F. Ras pathway activates epithelial Na channel and decreases its surface expression in *Xenopus* oocytes. *Mol Biol Cell* 9: 3417–3427, 1998.

226 May A, Puoti A, Gaeggeler HP, Horisberger JD, and Rossier BC. Early effect of aldosterone on the rate of synthesis of the epithelial sodium channel alpha subunit in A6 renal cells. *J Am Soc Nephrol* 8: 1813–1822, 1997.

227 MacDonald P, MacKenzie, Ramage LE, Seckl JR, Brown RW: Corticosteroid regulation of amiloride-sensitive sodium channel subunit mRNA expression in mouse kidney. *J Endocrinol.* 165: 25–37, 2000.

228 McDonald FJ, Snyder PM, McCray PB, and Welsh MJ. Cloning, expression, and

tissue distribution of a human amiloride- sensitive Na channel. *Am J Physiol Lung Cell Mol Physiol* 266: L728–L734, 1994.

229 McDonald FJ, Price MP, Snyder PM, and Welsh MJ. Cloning and expression of the beta- and gamma-subunits of the human epithelial sodium channel. *Am J Physiol Cell Physiol* 268: C1157–C1163, 1995.

230 McDonald FJ and Welsh MJ. The praline-rich region of the epithelial Na channel binds SH3 domains and associates with specific cellular proteins. *Biochem. J.* 312: 491-497, 1995.

231 McDonald FJ, Yang B, Hrstka RF, Drummond HA, Tarr DE, McCray PB, Stokes JB, Welsh MJ, and Williamson RA. Disruption of the beta subunit of the epithelial Na channel in mice: hyperkalemia and neonatal death associated with a pseudohypoaldosteronism phenotype. *Proc Natl Acad Sci USA* 96: 1727–1731, 1999.

232 McKay LI and Cidlowski JA. Cross-talk between nuclear factor-kappa B and the steroid hormone receptors: mechanisms of mutual antagonism. *Mol Endocrinol* 12: 45–56, 1998.

233 McKay LI and Cidlowski JA. Molecular control of immune/inflammatory responses: interactions between nuclear factor-kappa B and steroid receptor-signaling pathways. *Endocr Rev* 20: 435–459, 1999.

234 McKay LI and Cidlowski JA. CBP (CREB binding protein) integrates NF-kappa B (nuclear factor-kappa B) and glucocorticoid receptor physical interactions and antagonism. *Mol Endocrinol* 14: 1222–1234, 2000.

235 McKenna TJ, Island DP and Nicholson WE. The effects of potassium on early and late steps in aldosterone biosynthesis in cells of the zona glomerulosa. *Endocrinology* 103: 1411-1416, 1978.

236 McNew JA, Parlati F, Fukuda R, Johnston RJ, Paz K, Paumet F, Sollner TH and Rothman JE. Compartmental specificity of cellular membrane fusion encoded in SNARE proteins. *Nature* 407:153-159, 2000.

237 McNicholas CM and Canessa CM. Diversity of channels generated by different combinations of epithelial sodium channel subunits. *J. Gen. Physiol.* 109:681-692, 1997.

238 Mick VE, Itani OA, Loftus RW, Husted RF, Schmidt TJ, and Thomas CP. The

alpha-subunit of the epithelial sodium channel is an aldosterone-induced transcript in mammalian collecting ducts, and this transcriptional response is mediated via distinct *cis*-elements in the 5-flanking region of the gene. *Mol Endocrinol* 15: 575–588, 2001.

239 Mikosz CA, Brickley DR, Sharkey MS, Moran TW, and Conzen SD. Glucocorticoid receptor-mediated protection from apoptosis is associated with induction of the serine/threonine survival kinase gene, sgk-1. *J Biol Chem* 276: 16649–16654, 2001.

240 Mills JN: Aldosterone secretion in man. *Br Med Bull* 18: 170, 1962.

241 Mitsuuchi, Y., Kawamoto, T., Rosler, A., Naiki, Y., Miyahara, K., Toda, K., Kuribayashi, I., Orii, T., Yasuda, K., Miura, K., et al. Congenitally defective aldosterone biosynthesis in humans: the involvement of point mutations of the P-450(C18) gene (CYP11B2) in CMO II deficient patients. *Biochem. Biophys. Res. Commun.* 182, 974–979, 1992.

242 Morin B, Woodcock GR, Nichols LA, and Holland LJ. Heterodimerization between the glucocorticoid receptor and the unrelated DNA-binding protein, *Xenopus* glucocorticoid receptor accessory factor. *Mol Endocrinol* 15: 458–466, 2001.

243 Morin B, Zhu C, Woodcock GR, Li M, Woodward RN, Nichols LA, and Holland LJ. The binding site for *Xenopus* glucocorticoid receptor accessory factor and a single adjacent half-GRE form an independent glucocorticoid response unit. *Biochemistry* 39: 12234–12242, 2000.

244 Morris RG, Tousson A, Benos DJ and Schafer JA. Microtubule disruption inhibits an AVT-stimulated chloride secretion but not sodium reabsorption in A6 cells. *Am. J. Physiol.* 274:F300-314, 1998.

245 Mujais SK, Chekal MA, Hayslett JP and Katz AI. Regulation of renal Na^+/K^+-ATPase in the rat: role of the natural mineralo- glucocorticoid hormones. *J Clin Invest* 73:13-19, 1984.

246 Mune, T., Rogerson, F.M., Nikkila, H., Agarwal, A.K., and White, P.C. Human hypertension caused by mutations in the kidney isozyme of 11 beta-hydroxysteroid dehydrogenase. Nat. Genet. *10*, 394–399, 1995.

247 Nakhoul N and *et al.* Regulation of sodium transport in M-1 cells. *Am J Physiol.*

44:F998-1007, 1998.

248 Naray-Fejes-Toth A and Fejes-Toth G. Glucocorticoid receptors mediate mineralocorticoid-like effects in cultured collecting duct cells. *Am J Physiol Renal Fluid Electrolyte Physiol* 259: F672–F678, 1990.

249 Naray-Fejes-Toth A, Canessa C., Cleaveland ES, Aldrich G, and Fejes-Toth G. Sgk is an aldosterone-induced kinase in the renal collecting duct: effects on epithelial Na channels. *J Biol Chem* 274: 16973–16978, 2000.

250 Neades R, Betz NA, Sheng XY, and Pelling JC. Transient expression of the cloned mouse c-Ha-ras 5-upstream region in transfected primary SENCAR mouse keratinocytes demon-strates its power as a promoter element. *Mol Carcinog* 4: 369–375, 1991.

251 Olsen ME, Hall JE, Montani JP, et al: Mechanisms of angiotensin II natriuresis and antinatriuresis. *Am J Physiol* 249:F299-F307, 1985.

252 Oh Y, Smith PR, Bradford AL, Keeton D and Benos DJ. Regulation by phosphorylation of purified epithelial Na channels in planar lipid bilayers. *Am. J. Physiol.* 265: C85-91, 1993.

253 Pacha J, Frindt G, Antonian L, Silver RB, and Palmer LG. Regulation of Na channels of the rat cortical collecting tubule by aldosterone. *J Gen Physiol* 102: 25–42, 1993.

254 Paintal AS: Vagal sensory receptors and their reflex effects. *Physiol Rev* 53:159-227, 1973.

255 Parlati F, McNew JA, Fukuda R, Miller R, Sollner TH and Rothman JE. Topological restriction of SNARE-dependent membrane fusion. Nature 407:194-198, 2000.

256 Park J, Leong ML, Buse P, Maiyar AC, Firestone GL, and Hemmings BA. Serum and glucocorticoid-inducible kinase (SGK) is a target of the PI 3-kinase-stimulated signaling path-way. *EMBO J* 18: 3024–3033, 1999.

257 Pascoe, L., Curnow, K.M., Slutsker, L., Rosler, A., and White, P.C. Mutations in the human CYP11B2 (aldosterone synthase) gene causing corticosterone methyloxidase II deficiency. *Proc. Natl. Acad. Sci. USA* 89, 4996–5000, 1992.

258 Passo SS, Thornborough JR, Rothballer AB: Hepatic receptors in control of sodium excretion in anesthetized cats. *Am J Physiol* 224:373-375, 1973.

259 Paunescu TG, Blazer-Yost BL, Vlahos CJ, and Helman SI. LY-294002-inhibitable PI 3-kinase and regulation of baseline rates of Na transport in A6 epithelia. *Am J Physiol Cell Physiol* 279: C236–C247, 2000.

260 Pearce D. The role of SGK1 in hormone-regulated sodium transport. *Trends Endocrinol Metab* 12: 341–347, 2001.

261 Pethe V and Shekhar PV. Estrogen inducibility of c-Ha-ras transcription in breast cancer cells. Identification of functional estrogen-responsive transcriptional regulatory elements in exon 1/intron 1 of the c-Ha-ras gene. *J Biol Chem* 274: 30969–30978, 1999.

262 Pfeiffer R, Beron J, and Verrey F. Regulation of Na pump function by aldosterone is alpha-subunit isoform specific. *J Physiol (Lond)* 516: 647–655, 1999.

263 Plant PJ, Yeger H, Staub O, Howard P, and Rotin D. The C2 domain of the ubiquitin protein ligase Nedd4 mediates Ca-dependent plasma membrane localization. *J Biol Chem* 272: 32329–32336, 1997.

264 Plant PJ, Lafont F, Lecat S, Verkade P, Simons K, and Rotin D. Apical membrane targeting of Nedd4 is mediated by an association of its C2 domain with annexin XIIIb. *J Cell Biol* 149: 1473–1484, 2000.

265 Pradervand S, Barker P, Wang Q, et al. Salt restriction induces pseudohypoaldosteronism type I in mice expressing low levels of the beta-subunit of the amiloride-sensitive epithelial sodium channel. *Proc Natl Acad Sci USA* 96: 1732-1737, 1999a.

266 Pradervand S, Wang Q, Burnier M, et al. A mouse model for Liddle's syndrome. *J Am Soc Nephrol* 10: 2527-2533, 1999b.

267 Prat AG, Ausiello DA and Cantiello HF. Vasopressin and protein kinase A activate G protein-sensitive epithelial Na channels. *Am J Physiol.* 265:C218-223, 1993(a).

268 Prat AG, Bortorello AM, Ausiello DA and Cantiello HF. Activation of epithelial Na channels by protein kinase A requires actin filaments. *Am J Physiol.* 265:C224-233, 1993(b).

269 Prefontaine GG, Lemieux ME, Giffin W, Schild-Poulter C, Pope L, LaCasse E, Walker P, and Hache RJ. Recruitment of octamer transcription factors to DNA by

glucocorticoid receptor. *Mol Cell Biol* 18: 3416–3430, 1998.

270 Prince LS and Welsh MJ. Cell surface expression and biosynthesis of epithelial Na channels. *Biochem J* 336: 705–710, 1998.

271 Prince LS and Welsh MJ. Effect of subunit composition and Liddle's syndrome mutations on biosynthesis of ENaC. *Am J Physiol Cell Physiol* 276: C1346–C1351, 1999.

272 Qi J, Peters KW, Liu C, Wang JM, Edinger RS, Johnson JP, Watkins SC, and Frizzell RA. Regulation of the amiloride-sensitive epithelial sodium channel by syntaxin 1A. *J Biol Chem* 274: 30345–30348, 1999.

273 Quinn SJ and Williams GH. Regulation of aldosterone secretion. *Annu Rev Physiol* 50: 409-426, 1988.

274 Rayson BM and Lowther SO. Steroid regulation of Na^+/K^+-ATPase: differential sensitivities along the nephron. *Am J Physiol* 246: F656-662, 1984.

275 Record RD, Froelich LL, Vlahos CJ, and Blazer-Yost BL. Phosphatidylinositol 3-kinase activation is required for insulin-stimulated sodium transport in A6 cells. *Am J Physiol Endocrinol Metab* 274: E611–E617, 1998.

276 Rector FCJ, Glessen GV, Kiil F, et al: Influence of expansion of extracellular fluid volume on tubular reabsorption of sodium independent of changes in glomerular filtration rate and aldosterone activity. *J Clin Invest* 45:542, 1996.

277 Reichardt HM, Kaestner KH, Tuckermann J, Kretz O, Wessely O, Bock R, Gass P, Schmid W, Herrlich P, Angel P, and Schutz G. DNA binding of the glucocorticoid receptor is not essential for survival. *Cell* 93: 531–541, 1998.

278 Reif MC, Troutman SL and Schafer JA. Sodium transport by rat cortical collecting tubule. Effects of vasopressin and desoxycorticosterone. *J. Clin. Invest.* 77:1291-1298, 1986.

279 Renard S, Lingueglia E, Voilley N, Lazdunski M, and Barbry P. Biochemical analysis of the membrane topology of the amiloride-sensitive Na channel. *J Biol Chem* 269:12981–12986, 1994.

280 Renard S, Voilley N, Bassilana F, Lazdunski M, and Barbry P. Localization and regulation by steroids of the alpha, beta and gamma subunits of the amiloride sensitive Na channel in colon, lung and kidney. *Pfluegers Arch* 430: 299-307, 1995.

281 Roberts LR and Holland LJ. Coordinate transcriptional regulation of the three fibrinogen subunit genes by glucocorticoids in cultured primary liver cells from *Xenopus laevis*. *Endocrinology* 132: 2563–2570, 1993.

282 Robert-Nicoud M, Flahaut M, Elalouf JM, Nicod M, Sali-nas M, Bens M, Doucet A, Wincker P, Artiguenave F, Horisberger JD, Vandewalle A, Rossier BC, and Firsov D. Transcriptome of a mouse kidney cortical collecting duct cell line: effects of aldosterone and vasopressin. *Proc Natl Acad Sci USA* 98: 2712–2716, 2001.

283 Rogerson FM and Fuller PJ. Mineralocorticoid action. *Steroids* 65: 61–73, 2000.

284 Rommel C, Clarke BA, Zimmermann S, Nunez L, Ross-man R, Reid K, Moelling K, Yancopoulos GD, and Glass DJ. Differentiation stage-specific inhibition of the Raf-MEK-ERK pathway by Akt. *Science* 286: 1738–1741, 1999.

285 Rosewicz S, McDonald AR, Maddux BA, Goldfine ID, Miesfeld RL and Logsdon CD. Mechansim of glucocorticoid receptor down-regulated by glucocorticoids. *J Biol Chem* 263: 2581-2584, 1988.

286 Rotin D, Bar-Sagi D, O'Brodovich H, Merilainen J, Lehto VP, Canessa CM, Rossier BC, and Downey GP. An SH3 binding region in the epithelial Na channel (alpha rENaC) mediates its localization at the apical membrane. *Embo J* 13:4440–4450, 1994.

287 Rotin D, Staub O, and Haguenauer-Tsapis R. Ubiquitination and endocytosis of plasma membrane proteins: role of Nedd4/Rsp5p family of ubiquitin-protein ligases. *J Membr Biol* 176: 1–17, 2000.

288 Roudier-Pujol C, Rochat A, Escoubet B, Eugene E, Barrandon Y, Bonvalet JP and Farman N. Differential expression of epithelial sodium channel subunit mRNAs in rat skin. *J. Cell. Sci.* 109:379-385, 1996.

289 Sakai DD, Helms S, Carlstedt-Duke J, Gustafsson JA, Rottman FM, and Yamamoto KR. Hormone-mediated repression: a negative glucocorticoid response element from the bovine prolactin gene. *Genes Dev* 2: 1144–1154, 1988.

290 Santacruz-Toloza L, Huang Y, John SA, and Papazian DM. Glycosylation of Shaker potassium channel protein in insect cell culture and in *Xenopus* oocytes. *Biochemistry* 33: 5607–5613, 1994.

291 Sayegh R, Auerbach SD, Li X, Loftus RW, Husted RF, Stokes JB, and Thomas

CP. Glucocorticoid induction of epithelial sodium channel expression in lung and renal epithelia occurs via trans-activation of a hormone response element in the 5-flanking region of the human epithelial sodium channel alpha subunit gene. *J Biol Chem* 274: 12431–12437, 1999.

292 Saxena S, Quick MW, Tousson A, Oh Y, and Warnock DG. Interaction of syntaxins with the amiloride-sensitive epithelial sodium channel. *J Biol Chem* 274: 20812–20817, 1999.

293 Schafer JA and Hawk CT. Regulation of Na channels in the cortical collecting duct by AVP and mineralocorticoids. *Kidney Int* 41: 255-268, 1992.

294 Schafer JA. Salt and water homeostasis-is it just a matter of good bookkeeping? *J. Am. Soc. Nephrol.* 4:1933-1950, 1994.

295 Schild L, Canessa CM, Shimkets RA, Gautschi I, Lifton RP, and Rossier BC. A mutation in the epithelial sodium channel causing Liddle disease increases channel activity in the *Xenopus laevis* oocyte expression system. *Proc Natl Acad Sci USA* 92: 5699–5703, 1995.

296 Schild L, Lu Y, Gautschi I, Schneeberger E, Lifton RP, and Rossier BC. Identification of a PY motif in the epithelial Na channel subunits as a target sequence for mutations causing channel activation found in Liddle syndrome. *EMBO J* 15: 2381–2387, 1996.

297 Schmidt TJ, Husted RF, and Stokes JB. Steroid hormone stimulation of Na transport in A6 cells is mediated via glucocorticoid receptors. *Am J Physiol Cell Physiol* 264: C875–C884, 1993.

298 Schuster VL, Kokko JP, Jacobson HR. Angiotensin II directly stimulates sodium transport in rabbit proximal convoluted tubules. *J Clin Invest* 73:507-515, 1984.

299 Scott DK, Mitchell JA, and Granner DK. The orphan receptor COUP-TF binds to a third glucocorticoid accessory factor element within the phosphoenolpyruvate carboxykinase gene promoter. *J Biol Chem* 271: 31909–31914, 1996.

300 Sha Q, Lansbery KL, Distefano D, Mercer RW, and Ni-chols CG. Heterologous expression of the Na,K-ATPase gamma subunit in *Xenopus* oocytes induces an endogenous, voltage-gated large diameter pore. *J Physiol (Lond)* 535: 407-417, 2001.

301 Shapiro PS and Ahn NG. Feedback regulation of Raf-1 and mitogen-activated

protein kinase (MAP) kinase kinases 1 and 2 by MAP kinase phosphatase-1 (MKP-1). *J Biol Chem* 273: 1788–1793, 1998.

302 Sheehan D, Meade G, Foley VM and Dowd CA. Structure, function and evolution of glutathione transferase: implications for classification of non-mammalian members of an ancient enzyme superfamily. *Biochem J* 360:1-16, 2001.

303 Shi H, Levy-Holzman R, Cluzeaud F, Farman N, and Garty H. Membrane topology and immunolocalization of CHIF in kidney and intestine. *Am J Physiol Renal Physiol* 280: F505–F512, 2001.

304 Shigaev A, Asher C, Latter H, Garty H, and Reuveny E. Regulation of sgk by aldosterone and its effects on the epithelial Na channel. *Am J Physiol Renal Physiol* 278: F613–F619, 2000.

305 Shimkets RA, Lifton R, and Canessa CM. In vivo phosphorylation of the epithelial sodium channel. *Proc Natl Acad Sci USA* 95: 3301–3305, 1998.

306 Shimkets RA, Lifton RP, and Canessa CM. The activity of the epithelial sodium channel is regulated by clathrin-mediated endocytosis. *J Biol Chem* 272: 25537–25541, 1997.

307 Shimkets RA, Warnock DG, Bositis CM, Nelson-Williams C, Hansson JH, Schambelan M, Gill JR, Ulick S, Milora RV, Findling JW, Canessa CM, Rossier BC, and Lifton RP. Liddle's syndrome: heritable human hypertension caused by mutations in the beta subunit of the epithelial sodium channel. *Cell* 79: 407–414, 1994.

308 Simons K and Ikonen E. Functional rafts in cell membranes. *Nature* 387: 569–572, 1997.

309 Skott O, Briggs JP: Direct demonstration of macula densa-mediated renin secretion. *Science* 237:1618-1620, 1987.

310 Snyder PM, McDonald FJ, Stokes JB, and Welsh MJ. Membrane topology of the amiloride-sensitive epithelial sodium channel. *J Biol Chem* 269: 24379–24383, 1994.

311 Snyder PM, Price MP, McDonald FJ, Adams CM, Volk KA, Zeiher BG, Stokes JB, and Welsh MJ. Mechanism by which Liddle's syndrome mutations increase activity of a human epithelial Na channel. *Cell* 83: 969–978, 1995.

312 Snyder PM, Chen C, Prince LS, Rogers JC, and Welsh MJ. Electrophysiological and biochemical evidence that DEG/ENaC cation channels are composed of nine subunits. *J Biol Chem* 273:681–684, 1998.

313 Snyder PM. Liddle's syndrome mutations disrupt cAMP-mediated translocation of the epithelial Na+ channel to the cell surface. *J Clin Invest* 105:45–53, 2000.

314 Snyder PM, Olson DR, and Thomas BC. Serum and glucocorticoid-regulated kinase modulates Nedd4–2-mediated inhibition of ENaC. *J Biol Chem* 277: 5–8, 2002.

315 Speirs HJL, Hou J and Brown RW. Aldosterone excess downregulates a glutathione S-transferase isoform predominantly expressed in sodium transporting epithelia. *J. Am Soc Nephrol* 12: A2427, 2001

316 Spindler B, Mastroberardino L, Custer M, and Verrey F. Characterization of early aldosterone-induced RNAs identified in A6 kidney epithelia. *Pflugers Arch* 434: 323–331, 1997.

317 Spindler B and Verrey F. Aldosterone action: induction of p21(ras) and fra-2 and transcription-independent decrease in myc, jun, and fos. *Am J Physiol Cell Physiol* 276: C1154–C1161, 1999.

318 Staub O, Dho S, Henry P, Correa J, Ishikawa T, McGlade J, and Rotin D. WW domains of Nedd4 bind to the proline-rich PY motifs in the epithelial Na channel deleted in Liddle's syndrome. *Embo J* 15: 2371–2380, 1996.

319 Staub O, Gautschi I, Ishikawa T, Breitschopf K, Cie-chanover A, Schild L, and Rotin D. Regulation of stability and function of the epithelial Na channel (ENaC) by ubiquitination. *EMBO J* 16: 6325–6336, 1997.

320 Staub O, Yeger H, Plant PJ, Kim H, Ernst SA, and Rotin D. Immunolocalization of the ubiquitin-protein ligase Nedd4 in tissues expressing the epithelial Na channel (ENaC). *Am J Physiol Cell Physiol* 272: C1871–C1880, 1997(a).

321 Staub O, Abriel H, Plant P, Ishikawa T, Kanelis V, Saleki R, Horisberger JD, Schild L, and Rotin D. Regulation of the epithelial Na channel by Nedd4 and ubiquitination. *Kidney Int* 57: 809–815, 2000.

322 Stockand JD, Spier BJ, Worrell RT, Yue G, Al-Baldawi N, and Eaton DC. Regulation of Na reabsorption by the aldosterone-induced, small G protein K-Ras2A. *J Biol Chem* 274: 35449–35454, 1999.

323 Stockand JD, Bao HF, Schenck J, Malik B, Middleton P, Schlanger LE, and Eaton DC. Differential effects of protein kinase C on the levels of epithelial Na channel subunit proteins. *J Biol Chem* 275: 25760–25765, 2000.

324 Stockand JD, Johnson JP, and Edinger RS. Aldosterone signaling to the epithelial Na channel (Abstract). *J Am Soc Nephrol* 12: 40A, 2001.

325 Stockand JD, Zeltwanger S, Bao HF, Worrell R, and Eaton DC. S-adenosyl-L-homocysteine hydrolase is necessary for aldosterone-induced activity of epithelial Na channels. *Am J Physiol Cell Physiol* 281: C773–C785, 2001(a).

326 Stoecklin E, Wissler M, Moriggl R, and Groner B. Specific DNA binding of Stat5, but not of glucocorticoid receptor, is required for their functional cooperation in the regulation of gene transcription. *Mol Cell Biol* 17: 6708–6716, 1997.

327 Stoos BA, Naray-Fejes-Toth A, Carretero OA, et al. Characterization of a mouse cortical collecting duct cell line. *Kidney Int* 39:1168-1175, 1991.

328 Storm SM, Cleveland JL, and Rapp UR. Expression of raf family proto-oncogenes in normal mouse tissues. *Oncogene* 5: 345–351, 1990.

329 Strautnieks SS, Thompson RJ, Gardiner RM, and Chung E. A novel splice-site mutation in the gamma subunit of the epithelial sodium channel gene in three pseudohypoaldosteronism type 1 families. *Nat Genet* 13: 248–250, 1996.

330 Strawhecker JM, Betz NA, Neades RY, Houser W, and Pelling JC. Binding of the 97 kDa glucocorticoid receptor to the 5-upstream flanking region of the mouse c-Ha-ras onco-gene. *Oncogene* 4: 1317–1322, 1989.

331 Stewart, P.M., Wallace, A.M., Valentino, R., Burt, D., Shackleton, C.H., and Edwards, C.R. Mineralocorticoid activity of licorice: 11-beta-hydroxysteroid dehydrogenase deficiency comes of age. Lancet *2*, 821–824, 1987.

332 Sugiyama T, Scott DK, Wang JC, and Granner DK. Structural requirements of the glucocorticoid and retinoic acid response units in the phosphoenolpyruvate carboxykinase gene promoter. *Mol Endocrinol* 12: 1487–1498, 1998.

333 Sutherland, D.J., Ruse, J.L., and Laidlaw, J.C. Hypertension, increased aldosterone secretion and low plasma renin activity relieved by dexamethasone. *Can. Med. Assoc. J.* 95, 1109–1119, 1966.

334 Sweadner KJ and Rael E. The FXYD gene family of small ion transport regulators or channels: cDNA sequence, protein signature sequence, and

expression. *Genomics* 68: 41–56, 2000.

335 Synder PM, McDonald FJ, Stokes JB and Welsh MJ. Memebrane topology of the amiloride-sensitive epithelial sodium channel. *J. Biol. Chem.* 269: 24379-24383, 1994.

336 Tait JF, Tait SAS, Little B, Laumas KR: The disappearance of 7-H^3-D-aldosterone in the plasma of normal subjects. *J Clin Invest* 40: 72, 1961.

337 Terasaki M and Reese TS. Characterization of endoplasmic reticulum by co-localization of BiP and dicarbocyanine dyes. *J Cell Sci* 101:315-322, 1992.

338 Tomita K and *et al.* Control of sodiumand potassium transport in the cortical collecting duct of the rat. *J Clin Invest* 1985, 76: 132-136.

339 Tamura H, Schild L, Enomoto N, Matsui N, Marumo F, and Rossier BC. Liddle disease caused by a missense mutation of beta subunit of the epithelial sodium channel gene. *J Clin Invest* 97: 1780–1784, 1996.

340 Therien AG, Karlish SJ, and Blostein R. Expression and functional role of the gamma subunit of the Na, K-ATPase in mammalian cells. *J Biol Chem* 274: 12252–12256, 1999.

341 Tousson A, Alley CD, Sorscher EJ, Brinkley BR and Benos DJ. Immunochemical localization of amiloride sensitive sodium channels in sodium transporting epithelia. *J. Cell. Sci.* 93: 349-362, 1989.

342 Trapp T, Rupprecht R, Castren M, Reul JM, and Hols-boer F. Heterodimerization between mineralocorticoid and glucocorticoid receptor: a new principle of glucocorticoid action in the CNS. *Neuron* 13: 1457–1462, 1994.

343 Tu Y and Wu C. Cloning, expression and characterization of a novel human Ras-related protein that is regulated by glucocorticoid hormone. *Biochim Biophys Acta* 1489: 452–456, 1999.

344 Turnamian SG and Binder HJ. Aldosterone and glucocorticoid receptor-specific agonists regulate ion transport in rat proximal colon. *Am J Physiol Gastrointest Liver Physiol* 258: G492–G498, 1990.

345 Ulick, S., Levine, L.S., Gunczler, P., Zanconato, G., Ramirez, L.C., Rauh, W., Rosler, A., Bradlow, H.L., and New, M.I. A syndrome of apparent mineralocorticoid excess associated with defects in the peripheral metabolism of cortisol. J. Clin. Endocrinol. Metab. *49*, 757–764, 1979.

346 Valentijn JA, Fyfe GK, and Canessa CM. Biosynthesis and processing of epithelial sodium channels in *Xenopus* oocytes. *J Biol Chem* 273: 30344–30351, 1998.

347 Vallejo M. Transcriptional control of gene expression by cAMP-response element binding proteins. *J Neuroendocrinol.* 6:587-596, 1994.

348 Vallet V and *et al*: An epithelial serine protease activates the amiloride-sensitive sodium channel. *Nature* 389: 607-610, 1997

349 Vanhaesebroeck B and Alessi DR. The PI3K-PDK1 connection: more than just a road to PKB. *Biochem J* 346: 561–576, 2000.

350 Verrey F, Kraehenbuhl JP, Rossier BC. Aldosterone induces a rapid increase in the rate of Na^+/K^+-ATPase gene transcription in cultured kidney cells. *Mol Endocrinol* 3: 1369-1376, 1989.

351 Verrey F, Digicaylioglu M and Bolliger U. Polarized membrane movements in A6 kidney cells are regulated by aldosterone and vasopressin. *J. Membrane Biol.* 133: 213-226, 1993.

352 Verrey F, Groscurth P and Bolliger U. Cytoskeletal disruption in A6 kidney cells: Impact on endo/exocytosis and NaCl transport regulation by antidiuretic hormone. *J. Membr. Biol.* 145: 193-204, 1995.

353 Verrey F. Transcriptional control of sodium transport in tight epithelial by adrenal steroids. *J Membr Biol* 144: 93–110, 1995.

354 Verrey F. Early aldosterone action: toward filling the gap between transcription and transport. *Am J Physiol Renal Physiol* 277: F319–F327, 1999.

355 Verrey F, Pearce D, Pfeiffer R, Spindler B, Mastrober-ardino L, Summa V, and Zecevic M. Pleiotropic action of aldosterone in epithelia mediated by transcription and post-transcription mechanisms. *Kidney Int* 57: 1277–1282, 2000.

356 Voilley N, Bassilana F, Mignon C, Merscher S, Mattei MG, Carle GF, Lazdunski M, and Barbry P. Cloning, chromosomal localization, and physical linkage of the beta and gamma subunits (SCNN1B and SCNN1G) of the human epithelial amiloride-sensitive sodium channel. *Genomics* 28: 560–565, 1995.

357 Volk KA, Sigmund RD, Snyder PM, McDonald FJ, Welsh MJ and Stokes JB. rENaC is the predominant Na channel in the apical membrane of the rat renal inner medullary collecting duct. *J Clin Invest* 96: 2748-2757, 1995.

358 Wade JB, Stanton BA and Field MJ. Morphological and physiological response to aldosterone: time course and sodium dependence. *Am J Physiol* 259: F88-94, 1990.

359 Wald H, Goldstein O, Asher C, Yagil Y, and Garty H. Aldosterone induction and epithelial distribution of CHIF. *Am J Physiol Renal Fluid Electrolyte Physiol* 271: F322–F329, 1996.

360 Wald H, Popovtzer MM, and Garty H. Differential regulation of CHIF mRNA by potassium intake and aldosterone. *Am J Physiol Renal Physiol* 272: F617–F623, 1997.

361 Wald H, Garty H, Palmer LG, and Popovtzer MM. Differential regulation of ROMK expression in kidney cortex and medulla by aldosterone and potassium. *Am J Physiol Renal Physiol* 275: F239–F245, 1998.

362 Walser M: Phenomenological analysis of renal regulation of sodium and potassium balance. Kidney Int 27:837-841, 1985.

363 Wagner CA, Ott M, Klingel K, Beck S, Friedrich B, Wild KN, Broer S, Moschen I, Albers A, Waldegger S, Tummler B, Egan ME, Geibel JP, Kandolf R, and Lang F. Effects of the serine/threonine kinase sgk1 on the epithelial Na channel (ENaC) and CFTR: implications for cystic fibrosis. *Cell Physiol Biochem* 11: 209–218, 2001.

364 Waltner-Law M, Daniels MC, Sutherland C, and Granner DK. NF-kappa B inhibits glucocorticoid and cAMP-mediated expression of the phosphoenolpyruvate carboxykinase gene. *J Biol Chem* 275: 31847–31856, 2000.

365 Wang J, Barbry P, Maiyar AC, Rozansky DJ, Bhargava A, Leong M, Firestone GL, and Pearce D. SGK integrates insulin and mineralocorticoid regulation of epithelial sodium transport. *Am J Physiol Renal Physiol* 280: F303–F313, 2001.

366 Wang HC, Zentner MD, Deng HT, Kim KJ, Wu R, Yang PC, and Ann DK. Oxidative stress disrupts glucocorticoid hormone-dependent transcription of the amiloride-sensitive epithelial sodium channel alpha-subunit in lung epithelial cells through ERK-dependent and thioredoxin-sensitive pathways. *J Biol Chem* 275: 8600–8609, 2000.

367 Webster MK, Goya L, Ge Y, Maiyar AC, and Firestone GL. Characterization of sgk, a novel member of the serine/threonine protein kinase gene family which is

transcriptionally induced by glucocorticoids and serum. *Mol Cell Biol* 13: 2031–2040, 1993a.

368 Webster MK, Goya L, and Firestone GL. Immediate-early transcriptional regulation and rapid mRNA turnover of a putative serine/threonine protein kinase. *J Biol Chem* 268:11482–11485, 1993b.

369 Weisz OA, Wang JM, Edinger RS, and Johnson JP. Non-coordinate regulation of endogenous epithelial sodium channel (ENaC) subunit expression at the apical membrane of A6 cells in response to various transporting conditions. *J Biol Chem* 275: 39886–39893, 2000.

370 Wehling M, Kasmayr J and Theisen K, Rapid effects of mineralocorticoids on sodium-proton exchanger: genomic or nongenomic pathway? *Am J Physiol* 260: E719–E726, 1991.

371 Wehling M. Specific, nongenomic actions of steroid hormones. *Annu Rev Physiol* 59: 365–393, 1997.

372 Welling PA, Caplan M and Sutter M. Aldosterone-mediated Na^+/K^+-ATPase expression is alpha (1) isoform specific in the renal cortical collecting duct. *J Biol Chem* 268:23469-23476, 1993.

373 Wilce MCJ and Parker MW. Structure and function of glutathione S-transferase. *Biochim Biophy Acta* 1205:1-18, 1994.

374 Wilkinson DG: *In Situ Hybridization*. 2nd edition. Oxford, Oxford University Press, 1998.

375 Woo PL, Ching D, Guan Y, and Firestone GL. Requirement for ras and phosphatidylinositol 3-kinase signaling uncouples the glucocorticoid-induced junctional organization and transepithelial electrical resistance in mammary tumor cells. *J Biol Chem* 274: 32818-32828, 1999.

376 Woolfson RG and de Wardener JE. Primary renal abnormalities in hereditary hypertension. *Kidney Int* 50:717-731, 1996.

377 Wright FS and *et al.* Reduced sodium reabsorption by the proximal tubule of DOCA-escaped dogs. *Am J Physiol* 1969, 216:869-875.

378 Wulff P, Vallon V, Huang DY, Pfaff I, Klingel K, Kausel-mann D, Volkl H, Lang F, and Kuhl D. Deficient salt retention in the SGK1 knockout mouse (Abstract). *J Am Soc Nephrol* 12: 44A, 2001.

379 Yamashita Y, Koga M, Takeda Y, Enomoto N, Uchida S, Hashimoto K, Yamano S, Dohi K, Marumo F, and Sasaki S. Two sporadic cases of Liddle's syndrome caused by de novo ENaC mutations. *Am J Kidney Dis* 37: 499–504, 2001.

380 Yang-Yen HF, Chambard JC, Sun YL, Smeal T, Schmidt TJ, Drouin J, and Karin M. Transcriptional interference between c-Jun and the glucocorticoid receptor: mutual inhibition of DNA binding due to direct protein- protein interaction. *Cell* 62: 1205–1215, 1990.

381 Yan K, Kudo A, Hirano H, Watanabe T, Tasaka T, Kataoka S, Nakajima N, Nishibori Y, Shibata T, Kohsaka T, Higashihara E, Tahaka H, Watanabe H, Nagasawa T, Awa S: Subcellular localization of glucocorticoid receptor protein in the human kidney glomerulus. *Kidney Int* 56: 65, 1999.

382 Yan J, Roy S, Apolloni A, Lane A, and Hancock JF. Ras isoforms vary in their ability to activate Raf-1 and phosphoinositide 3-kinase. *J Biol Chem* 273: 24052–24056, 1998.

383 Yang L, Guan T and Gerace L. Integral membrane proteins of the nuclear envelope are dispersed throughout the endoplasmic reticulum during mitosis. *J Cell Biol* 137:1199-210, 1997.

384 Yeaman C, Grindstaff KK, and Nelson WJ. New perspectives on mechanisms involved in generating epithelial cell polarity. *Physiol Rev* 79: 73–98, 1999.

385 Yoo D, Kim BY, Campo C, Nance L, King A, Maouyo D, Welling PA. Cell Surface Expression of The ROMK (Kir 1.1) Channel Is Regulated by the Aldosterone-Induced Kinase, SGK-1, and PKA. *In press.*

386 Zahraoui A, Louvard D, and Galli T. Tight Junction, a Platform for Trafficking and Signaling Protein Complexes. *J Cell Biol* 151:5, F31–F36.

387 Zecevic M, Summa V, Bens M, Vandewalle A, Pearce D, and Verrey F. Does SGK mediate aldosterone action on both apical (ENaC) and basolateral (Na/K ATPase) Na transport proteins (Abstract)? *J Am Soc Nephrol* 12: 45A. 2001.

388 Zennaro MC, Souque A, Viengchareun S, Poisson E, and Lombes M. A new human mr splice variant is a ligand-independent transactivator modulating corticosteroid action. *Mol Endocrinol* 15: 1586–1598, 2001.

389 Zennaro MC, Farman N, Bonvalet JP, and Lombes M. Tissue-specific expression of alpha and beta messenger ribonucleic acid isoforms of the human

mineralocorticoid receptor in normal and pathological states. *J Clin Endocrinol Metab* 82:1345–1352, 1997.

390 Zentner MD, Lin HH, Wen X, Kim KJ, and Ann DK. The amiloride-sensitive epithelial sodium channel alpha-subunit is transcriptionally down-regulated in rat parotid cells by the extracellular signal-regulated protein kinase pathway. *J Biol Chem* 273: 30770–30776, 1998.

391 Zentner MD, Lin HH, Deng HT, Kim KJ, Shih HM, and Ann DK. Requirement for high mobility group protein HMGI-C interaction with STAT3 inhibitor PIAS3 in repression of alpha-subunit of epithelial Na channel (alpha-ENaC) transcription by Ras activation in salivary epithelial cells. *J Biol Chem* 276: 29805–29814, 2001.

392 Zhang BH, Tang ED, Zhu T, Greenberg ME, Vojtek AB, and Guan KL. Serum- and glucocorticoid-inducible kinase SGK phosphorylates and negatively regulates B-Raf. *J Biol Chem* 276: 31620–31626, 2001.

393 Zhang Z, Jones S, Hagood JS, Fuentes NL, and Fuller GM. STAT3 acts as a coactivator of glucocorticoid receptor signaling. *J Biol Chem* 272: 30607–30610, 1997.

394 Zhou MY, Gomez-Sanchez CE, and Gomez-Sanchez EP. An alternatively spliced rat mineralocorticoid receptor mRNA causing truncation of the steroid binding domain. *Mol Cell Endocrinol* 159: 125–131, 2000.

395 Zuckerman JB, Chen X, Jacobs JD, Hu B, Kleyman TR, and Smith PR. Association of the epithelial sodium channel with Apx and alpha-spectrin in A6 renal epithelial cells. *J Biol Chem* 274: 23286–23295, 1999.